Roles of GSK-3beta and PYK2 signaling pathways in synaptic plasticity

by

Honor Hsin

B.A. Biochemical Sciences
Harvard University, 2005

SUBMITTED TO THE DEPARTMENT OF BIOLOGY IN PARTIAL FULFILLMENT OF THE REQUIREMENTS FOR THE DEGREE OF

DOCTOR OF PHILOSOPHY
at the
MASSACHUSETTS INSTITUTE OF TECHNOLOGY

JUNE 2010

Signature of Author: _____
Department of Biology
May 20, 2010

Certified by: _____
Dr. Morgan Sheng
Professor of Biology, and Brain and Cognitive Sciences
Thesis Supervisor

Accepted by: _____
Dr. Stephen P. Bell
Professor of Biology
Chair, Committee for Graduate Students

Roles of GSK-3beta and PYK2 signaling pathways in synaptic plasticity

by

Honor Hsin

Submitted to the Department of Biology
on May 20, 2010 in Partial Fulfillment of the Requirements
for the Degree of Doctor of Philosophy in Biology

Abstract

Activity-dependent modification of synapses, as in long term potentiation (LTP) or long term depression (LTD), is widely believed to be a crucial mechanism for learning and memory. Molecular perturbations in these processes may underlie certain neuropsychiatric conditions. This thesis examines the role of two signaling pathways, glycogen synthase kinase 3 beta (GSK-3beta) and proline-rich tyrosine kinase 2 (PYK2), in LTD at rat hippocampal synapses.

GSK-3beta, a serine/threonine kinase implicated in the pathophysiology of schizophrenia, mood disorders, and Alzheimer's disease, is known to play a critical role in LTD. Here we report that GSK-3beta phosphorylates the postsynaptic scaffold protein PSD-95, a major determinant of synaptic strength, at the Thr-19 residue. In hippocampal neurons, this promotes the activity-dependent dispersal of synaptic PSD-95 clusters. We found that overexpression of a phospho-null mutant (T19A-PSD-95), but not a phospho-mimic mutant, blocks LTD without affecting basal synaptic function relative to wild type PSD-95 overexpression. Thus PSD-95 phosphorylation by GSK-3beta is a necessary step in LTD. [This project is a collaboration with Myung Jong Kim, and I am second author of the manuscript.]

PYK2 is a calcium-dependent tyrosine kinase that is activated in cerebral ischemia and seizures. PYK2 is also known to bind PSD-95 at a region implicated in LTD signaling. Here we report a novel role for PYK2 in LTD. Chemical LTD treatment induces PYK2 phosphorylation at Tyr-402, and small hairpin RNA-mediated knockdown of PYK2 blocks LTD, but not LTP. We identify both enzymatic and non-enzymatic (scaffolding) roles for PYK2 in LTD, and find that PYK2 is required to suppress activity-dependent phosphorylation of the mitogen activated protein kinase ERK. ERK activity is believed to promote glutamate receptor insertion at synapses. Overexpression of WT-PYK2 further depresses activity-dependent ERK phosphorylation, and inhibits LTP, but not LTD. Our studies support a model whereby PYK2 antagonizes ERK signaling to promote LTD, at the expense of LTP, in hippocampal neurons. [This project is a collaboration with Myung Jong Kim and Chi-Fong Wang, and I am first author of the manuscript.]

Thesis Supervisor: Morgan Sheng
Title: Professor of Biology, and Brain and Cognitive Sciences

Acknowledgements

My deepest thanks extend to …

… Morgan Sheng, for introducing me to the most fascinating area of molecular neuroscience today and to the smartest group of scientists studying it; for his encouragement and optimism throughout my term in the lab; and for his exemplary model of scientific excellence and efficiency;

… Troy Littleton and David Sabatini, my thesis committee members, for their perceptive comments and advice; and Elly Nedivi and Bernardo Sabatini, my defense committee members, for generously sharing their time with me;

… Li-Huei Tsai for her helpful feedback on my projects, and for graciously "adopting" me into her lab community;

… Yasunori Hayashi, for first introducing me to neuroscience at MIT;

… Kensuke Futai, Myung Jong Kim, Kelly Foster, Daniel Seeburg, Chi-Fong Wang, Dieter Edbauer, and Nelly Khidekel, my tutors and best critics in the lab – to MJ and Chi-Fong especially, who as my dedicated collaborators have helped make this work possible;

… The Sheng lab, the Tsai lab, the Hayashi lab, and members of the Stanley Center at the Broad Institute for enriching discussions and meetings;

… Betsey Walsh and the staff and Graduate Committee of the Biology Department for ensuring that my student experience proceeded smoothly and without any hitches;

… My mom, my dad, and my sisters, Heart and Happy, for their continued support;

… My family and my coaches and teammates at MIT Masters, for keeping my life balanced and healthy throughout graduate school;

… My husband, Ben, for his lasting inspiration, encouragement, and strength.

TABLE OF CONTENTS

List of Figures

CHAPTER 1:

Introduction

A fundamental problem in neuroscience is to understand how the brain encodes and modifies information acquired through experience. This capacity, which underlies learning and memory and may be impaired in certain neuropsychiatric diseases, is believed to require the activity-dependent modification of synapses, or sites of communication between neurons. Here we review current knowledge on the functional plasticity of synaptic strength in the hippocampus, a structure implicated in memory formation, and discuss the molecular mechanisms thought to mediate major forms of synaptic plasticity. *In vivo* physiological and pathophysiological implications of these processes will also be presented, as well as the possible activity-dependent roles that GSK3beta and PYK2 signaling pathways could play at synapses.

I. Functional plasticity of synapses

Early lesion studies demonstrated a critical role for the hippocampus in the formation of long-term memories (Kandel et al., 2000). Information synthesized at cortical association areas—such as perceptual and emotional knowledge—is transmitted to superficial layer neurons of the entorhinal cortex, which in turn project to defined circuits within the hippocampus (Nakazawa et al., 2004). These circuits are believed to help process and bind information, which is eventually sent back to the association areas, where memories are stored (Kandel et al., 2000). One example of a processing circuit in the hippocampus is the excitatory trisynaptic pathway, where inputs from entorhinal cortex project to the dentate gyrus (via perforant path axons), from dentate gyrus to CA3 (via the mossy fiber path), from CA3 to CA1 (via Schaffer collaterals), and finally from CA1 to the entorhinal deep layer neurons (Kandel et al., 2000; Figure 1A). In transgenic mice with specific ablation of CA3 synaptic output (Schaffer as well as recurrent CA3-CA3 collaterals), the rapid formation of contextual memories is significantly impaired, demonstrating the importance and dissociability of particular synaptic connections within this circuit (Nakashiba et al., 2008).

The hippocampus also plays a role in encoding spatial information. About 30-50% of pyramidal CA1 neurons are 'place cells,' because their firing rates depend on the animal's location within a particular environment (O'Keefe and Dostrovsky, 1971; Nakazawa et al., 2004). Each place cell possesses a unique place field, or a physical area of space to which it responds (O'Keefe and Dostrovsky, 1971). The spatial tuning of place cells (or the 'resolution'

of place field maps) is also regulated by synaptic connections within the trisynaptic circuit (Nakashiba et al., 2008).

The idea that learning may involve changes in synaptic strength was first proposed by Hebb (1949), who suggested that coincident activation of presynaptic and postsynaptic neurons could induce modifications that increase overall synaptic efficacy. In 1973, Bliss and Lømo provided the first experimental demonstration of this concept, by showing that high frequency stimulation of perforant path fibers in the hippocampus led to a persistent enhancement of synaptic strength in the dentate gyrus, a process termed long term potentiation (LTP). Since this discovery, many additional forms of long-term synaptic plasticity have been described at other brain regions, including the heavily studied Schaffer collateral-CA1 synapses of the hippocampus.

Long term potentiation in CA1

LTP at this synapse is commonly triggered by a short burst of high frequency stimulation of presynaptic Schaffer collateral fibers (tetanic protocol), and can be measured as an increase in the slope of CA1 excitatory postsynaptic potentials (EPSPs). This plasticity exhibits properties suggestive of a putative role in learning and memory: the resulting potentiation is generated rapidly (within minutes) and is long-lasting (hours to days). LTP is also cooperative (simultaneous activation of multiple presynaptic fibers can induce LTP), associative (LTP can be induced in neighboring synapses if they are also activated by weak stimuli), and input-specific (non-activated synapses do not exhibit LTP). These features can provide a cellular basis for understanding certain characteristics of learning—associativity in LTP, for example, could be one mechanism underlying associative learning in the brain (Citri and Malenka, 2008).

Does learning actually induce LTP in CA1? A recent study showed that inhibitory avoidance training, in which animals learned to avoid a dark chamber that delivers foot shocks, increased the slope of field EPSPs at selective CA1 sites for several hours (Whitlock et al., 2006). This enhancement occluded subsequent LTP induced by tetanic stimulation, suggesting that both phenomena share common mechanisms (Whitlock et al., 2006). There is similar evidence for experience-dependent synaptic potentiation in non-hippocampal areas, such as the amygdala after fear conditioning (McKernan and Shinnick-Gallagher, 1997; Rogan et al., 1997)

and the ventral tegmental area after a single exposure to cocaine (Ungless et al., 2001). In early postnatal experience, LTP mechanisms may also contribute to developmental plasticity, as described in the somatosensory barrel cortex (Takahashi et al., 2003).

Long term depression in CA1

A circuit that exhibited only Hebbian LTP would theoretically become unstable unless a mechanism for synaptic weakening also existed. In 1982, Bienenstock, Cooper, and Munro proposed that postsynaptic activity below a critical threshold (Θ_m) could lead to depression of overall synaptic efficacy, while postsynaptic activity above Θ_m would increase it (as in Hebbian LTP). Furthermore, Θ_m could be modified by the history of synaptic activity (Bienenstock et al., 1982). In this model (now known as BCM theory), the depression of synaptic connections could arise from uncorrelated pre- and postsynaptic activity, and this depression could be necessary for the refinement of stimulus selectivity in the developing visual cortex.

It was not until 1992 that Dudek and Bear described the first form of activity-dependent synaptic depression in CA1 hippocampus. In contrast to tetanic stimulation, prolonged low frequency stimulation of Schaffer collaterals resulted in long term depression (LTD) of synaptic strength that was input-specific (Dudek and Bear, 1992). Unfortunately, direct evidence for CA1 LTD in animals undergoing a cognitive task has not yet been shown; however, LTD mechanisms have been described in the experience-dependent plasticity of sensory cortices (see Malenka and Bear, 2004). Monocular deprivation, for example, induces molecular changes in visual cortex that mimic the effect of LTD, and this depression occludes subsequent LTD induced by low frequency stimulation (Heynan et al., 2003). Likewise, whisker trimming decreases synaptic responses in specific barrel cortex layers, and occludes LTD (Allen et al., 2003). In addition, LTD has been described in non-cortical areas, such as the nucleus accumbens after chronic cocaine administration (Thomas et al., 2001).

CA1 LTD could contribute to the pathophysiology of neuropsychiatric disorders. In Alzheimer's disease, which is characterized by learning deficits and memory loss, beta-amyloid (Abeta) peptides accumulate and promote synaptic dysfunction (Selkoe, 2002). Overexpression of Abeta peptide in CA1 neurons depresses synaptic strength in a manner that occludes subsequent LTD (Kamenetz et al., 2003; Hsieh et al., 2006). A recent study found that

application of Abeta oligomers isolated directly from the brains of human Alzheimer's patients could block LTP and enhance LTD in hippocampal slices (Shankar et al., 2008; Li et al., 2009). In bipolar disorder, lithium is commonly used to stabilize mood symptoms, and exposure of hippocampal slices to lithium blocks CA1 LTD (Peineau et al., 2007). Thus impaired hippocampal synaptic plasticity may play an important role in neuropsychiatric conditions. Additional support for the involvement of LTP and LTD in memory and disease has come from studies using genetic or pharmacological manipulation of the molecular pathways of plasticity, which we detail in Part II.

Structural correlates of synaptic plasticity

Synapses can be identified under electron microscopy by the presence of (1) a presynaptic membrane specialization for vesicle exocytosis (active zone) surrounded by synaptic vesicles (~40 nm diameter), (2) a synaptic cleft (~20-30 nm wide), and (3) a postsynaptic density (PSD) (Sheng and Hoogenraad, 2007). The PSD is a segment of thickened postsynaptic membrane (~200-800 nm wide and ~30-50 nm thick) that contains an organized lattice of receptors, channels, adhesion molecules, signaling enzymes, scaffolds, cytoskeletal elements, and other proteins (Sheng and Hoogenraad, 2007). Most excitatory postsynaptic compartments in the brain are housed in dendritic spines, small protrusions that can appear thin, stubby, or mushroom-shaped (Tada and Sheng, 2006; Alvarez and Sabatini, 2007). In hippocampal pyramidal neurons, there is roughly a one-to-one correlation between the numbers of spines and synapses (Harris et al., 1992). Furthermore, each individual spine head size tends to correlate with synaptic strength, suggesting that changes in synaptic function may correlate with changes in spine morphology (Matsuzaki et al., 2001; Kasai et al., 2003).

Advances in two-photon microscopy have revealed the dynamic nature of spines in brain slices and *in vivo*. Although the majority of cortical spines (~55%-90%, depending on cortical area and age) persist for months in an animal, some spines can appear and disappear over the course of days (Grutzendler et al., 2002; Trachtenberg et al., 2002; Majewska and Sur, 2003; Holtmaat et al., 2005; Zuo et al., 2005). As animals age, spine turnover and spine motility decreases (Trachtenberg et al., 2002; Holtmaat et al., 2005; Zuo et al., 2005). In hippocampal slices, chemical and electrical stimuli also cause significant alterations in spine morphology.

LTP induction is associated with the formation of new spines and the persistent growth of existing spines (Engert and Bonhoeffer, 1999; Maletic-Savatic et al., 1999; Matsuzaki et al., 2004; Okamoto et al., 2004; Kopec et al., 2006), whereas LTD induction causes spine shrinkage (Okamoto et al., 2004; Zhou et al., 2004). Interestingly, LTP-associated spine growth occurs preferentially at smaller spines, presumably due to the limited diffusion of signaling factors (such as calcium, as detailed below) from the spine head (Noguchi et al., 2005). Thus spine geometry has important implications for the functional compartmentalization of synaptic molecules.

Changes in spine morphology have also been reported to occur in experience-dependent plasticity (see Alvarez and Sabatini, 2007; Holtmaat and Svoboda, 2009). Monocular deprivation, for example, increases spine density in the binocular zone of visual cortex (Hofer et al., 2009), and whisker trimming increases the stability of new spines in somatosensory barrel cortex (Holtmaat et al., 2006). Recent studies have also shown that motor learning increases the formation of new spines in motor cortex (from ~5% to ~10%), and although subsequent pruning eventually restores spine density to its original level, these new spines are selectively stabilized in later training sessions (Xu et al., 2009; Yang et al., 2009). Thus the morphological plasticity of spines appears to accompany changes in the functional connectivity of neuronal circuits.

II. Molecular mechanisms of synaptic plasticity in CA1 hippocampus

Some progress has been made toward understanding the molecular pathways of LTP and LTD. In CA1 neurons, the most commonly studied forms of synaptic plasticity involve the postsynaptic N-methyl-D-aspartate (NMDA) receptor, a tetrameric complex consisting of four subunits – typically two NR1 and two NR2 monomers (NR2A and/or NR2B; see Lau and Zukin, 2007; Citri and Malenka, 2008). Other forms of plasticity also exist and have important implications for synaptic physiology and behavior (such as metabotropic glutamate receptor-dependent LTD), but the focus of this thesis will be on NMDAR-dependent mechanisms of synaptic plasticity.

NMDARs are permeable to Na^+ and Ca^{2+}, and are normally closed at resting membrane potential because channel conduction is blocked by extracellular Mg^{2+} ions (Mayer et al., 1983; Nowak et al., 1984). NMDARs open only in the presence of glutamate, co-agonist glycine, and sufficient membrane depolarization to relieve the Mg^{2+} block. These molecular properties

suggest that NMDARs are ideally suited to serve as "coincidence detectors" of presynaptic firing and postsynaptic depolarization, as occurs in Hebbian plasticity. Postsynaptic depolarization of CA1 synapses is mediated chiefly by activation of α-amino-3-hydroxy-5-methyl-4-isoxazolepropionate (AMPA) receptors, which are permeable to Na^+ and K^+ ions and open rapidly upon glutamate binding. At resting membrane potential, basal synaptic responses consist primarily of cationic influx through AMPARs. NMDAR antagonists, therefore, block LTP and LTD without significantly affecting basal synaptic function (Collingridge et al., 1983; Harris et al., 1984; Dudek and Bear, 1992).

It is not surprising, therefore, that a variety of experimental methods exist to elicit NMDAR-dependent LTP in CA1, all of which are consistent with a pattern of presynaptic firing synchronized with postsynaptic depolarization (see Citri and Malenka, 2008):

(1) The traditional tetanic protocol mentioned above, where activation of postsynaptic AMPARs sufficiently depolarizes the membrane to enable NMDAR opening;

(2) A pairing protocol, where lower frequency afferent stimulation is paired with direct depolarization of the postsynaptic cell (Figure 1B);

(3) A spike-timing dependent plasticity protocol, where the firing of pre- and postsynaptic action potentials is coordinated within a specific time window;

(4) A more recently developed single-spine LTP protocol, where synaptic stimulation by 2-photon-mediated uncaging of glutamate is paired with direct depolarization of the postsynaptic cell, or with application of 0 Mg^{2+} bath solution (see Alvarez and Sabatini, 2007).

Similarly, CA1 LTD has been studied using the equivalent of methods (1) through (3), though typically at lower frequency and longer duration of presynaptic stimulation, with lower magnitudes of postsynaptic depolarization (Figure 1B).

Are NMDARs required for the behavioral effects of hippocampal function? An early study found that intracerebroventricular infusion of NMDAR antagonists into rat brains blocked LTP, and impaired spatial learning in a water maze task (Morris et al., 1986). Likewise, CA1-specific disruption of the NR1 subunit blocks LTP, impairs spatial learning, and reduces the spatial specificity of place fields (Tsien et al., 1996; McHugh et al., 1996). Thus NMDAR-dependent mechanisms of synaptic plasticity likely play an important role in hippocampal-dependent learning tasks.

Calcium signaling in LTP and LTD

It is well known that calcium influx through NMDARs is critical for LTP and LTD (see Malenka and Nicoll, 1993). In early studies, tetanus-induced LTP was found to cause an NMDAR-dependent rise in postsynaptic calcium (Regehr and Tank, 1990), and a critical threshold of this Ca^{2+} elevation (lasting less than 2-2.5 seconds) is required for LTP (Malenka, 1991; Malenka et al., 1992). Similarly, NMDAR-dependent LTD requires a rise in postsynaptic calcium (Mulkey and Malenka, 1992). Compared to the calcium elevation achieved during LTP, however, the calcium rise during LTD is thought to be modest in magnitude, since partial blockade of NMDARs can convert an LTP-inducing stimulus to an LTD-inducing one (Cummings et al., 1996; Nishiyama et al., 2000). Additionally, the temporal kinetics of calcium elevation may differ between LTP and LTD: altering the time window between pre- and postsynaptic activation by just tens of milliseconds can reverse the direction of synaptic modification in spike-timing dependent plasticity (Bi and Poo, 2001). LTD also requires a more prolonged duration of postsynaptic calcium elevation, as low frequency stimulation must last several minutes or more to elicit LTD (Dudek and Bear, 1992). Lastly, the mode of cytosolic calcium entry could affect calcium dynamics in a manner that favors one form of plasticity over another: blockade of the IP_3 receptor pathway for calcium release, for example, has been reported to convert LTD to LTP (Nishiyama et al., 2000).

Experiments with photolabile calcium chelators suggest that postsynaptic calcium elevations of ~1 μM for ~ 1 minute are sufficient for LTD, whereas calcium elevations on the order of 10 μM for a few seconds are sufficient for LTP (Yang et al., 1999). Interestingly, chemical stimulation of NMDARs (~20 μM NMDA on the order of minutes) can induce a form of LTD that occludes subsequent homosynaptic LTD (Lee et al., 1998). Chemical LTD, therefore, shares some mechanisms with regular LTD – perhaps the spatiotemporal characteristics of calcium influx from bath NMDAR stimulation promote recruitment of shared downstream effectors. Additionally, bath NMDA application can activate both extrasynaptic and synaptic NMDARs, which likely couple to distinct pathways: activation of extrasynaptic NMDARs promotes synaptic depression and cell death, whereas synaptic NMDAR activation promotes synaptic potentiation and cell survival (Lu et al., 2001; Hardingham et al., 2002). Consistent with the idea, LTP can be induced chemically by stimulation of NMDARs with co-agonist glycine (~200 μM on the order of minutes, or chemical LTP), which presumably

activates only those NMDARs that are bound to synaptically-released glutamate (Musleh et al., 1997; Lu et al., 2001). Thus the localization of activated NMDARs may contribute to the differential induction of LTP versus LTD (see Sheng and Kim, 2002; Collingridge et al., 2004).

NR2B-containing and NR2A-containing NMDARs tend to be extrasynaptically and synaptically localized, respectively (Stocca and Vicini, 1998). It has been suggested that differential activation of these distinct NMDAR subtypes may also influence the direction of plasticity changes (with NR2B influx favoring LTD, and NR2A influx favoring LTP; Liu et al., 2004; Massey et al., 2004), although there is considerable controversy surrounding this model (Barria and Malinow, 2005; Bartlett et al., 2007; Morishita et al., 2007). In addition to their ion-conducting properties as channels, however, NMDAR subunits also function as protein scaffolds, and different subunit types may recruit distinct signaling proteins to promote LTP or LTD induction (see below; Bayer et al., 2001; Barria and Malinow, 2005; Foster et al., 2010).

What are the signaling pathways downstream of calcium influx? The involvement of calcium/calmodulin-dependent protein kinase II (CaMKII) in LTP has been well established (see Lisman et al., 2002). CaMKII exists as a dodecamer complex in synapses, and is highly abundant in the postsynaptic density (Cheng et al., 2006). Upon binding to calcium-calmodulin complexes, CaMKII undergoes autophosphorylation at T286, which renders it constitutively active and calcium-independent (Miller and Kennedy, 1986; Yang and Schulman, 1999). This property could be an important molecular mechanism for the persistence of LTP (Lisman, 1989). Indeed, CaMKII is autophosphorylated after LTP induction (Fukunaga et al., 1995; Barria et al., 1997), and translocates to stimulated spines (Shen and Meyer, 1999; Lee et al., 2009). At the PSD, CaMKII associates with the NMDAR subunit NR2B, an interaction that promotes autonomous CaMKII activity independent of T286 phosphorylation (Bayer et al., 2001). Thus CaMKII is dynamically regulated by synaptic activity.

CaMKII also fulfills the classic criteria for being a "mediator" of LTP (Citri and Malenka, 2008). Inhibition of postsynaptic CaMKII activity by interfering peptides blocks LTP (Malenka et al., 1989; Malinow et al., 1989), whereas acute administration of constitutively-active CaMKII subunits enhances basal synaptic strength and occludes LTP (Pettit et al., 1994; Lledo et al., 1995). LTP is also reduced in CaMKII knockouts (Silva et al., 1992) and in knock-in mice expressing the non-autophosphorylatable form of CaMKII (T286A; Giese et al., 1998).

T286A mice also show significant deficits in spatial learning and place cell stability, lending further support to the idea that LTP is important for hippocampal function (Giese et al., 1998; Cho et al., 1998).

Calcium-calmodulin complexes also activate adenylyl cyclases, triggering a cyclic AMP (cAMP) cascade that leads to the activation of protein kinase A (PKA; see Xia and Storm, 2005). PKA phosphorylation of the transcription factor cAMP responsive element (CRE)-binding protein (CREB) is believed to promote gene expression events necessary for longer-lasting forms of LTP (late-LTP, induced by multiple trains of LTP-inducing stimuli; Impey et al., 1996; Abel et al., 1997). Mice lacking one subtype of calcium-dependent adenylyl cyclase (AC1) display reduced CA1 LTP, suggesting that cAMP-dependent pathways are also important for LTP signaling (Wu et al., 1995; Otmakhova et al., 2000). In fact, LTP can be induced chemically by forskolin, an adenylyl cyclase activator, and rolipram, a cAMP phosphodiesterase inhibitor, in the absence of extracellular magnesium (Otmakhov, 2004; Kim et al., 2007). On a molecular level, the cAMP pathway is believed to promote LTP in part by decreasing phosphatase activity, and thereby enhancing CaMKII autophosphorylation: PKA-mediated phosphorylation of inhibitor-1 protein, an endogenous phosphatase blocker, decreases the activity of protein phosphatase 1 (PP1; Blitzer et al., 1998; Makhinson et al., 1999).

With CaMKII/PKA signaling playing a critical role in LTP, one attractive hypothesis for LTD signaling is that calcium-dependent phosphatases are important (Lisman, 1989). Calcineurin (PP2B) is also stimulated by calcium-calmodulin binding, and can dephosphorylate inhibitor-1 to promote PP1 activity (Xia and Storm, 2005). In CA1, postsynaptic inhibition of PP1, calcineurin, or the related protein phosphatase 2A (PP2A) blocks LTD, whereas infusion of PP1 enhances LTD (Morishita et al., 2001; Mulkey et al., 1993, 1994). Neither inhibition nor infusion of PP1 affects basal synaptic transmission, suggesting that phosphatase action is gated by NMDAR stimulation (Morishita et al., 2001). The differential activation of calcineurin versus CaMKII/adenylyl cyclase in NMDAR-dependent plasticity could arise from the greater calcium sensitivity of calcineurin, which would ensure that CaMKII/adenylyl cyclase signaling is active only when calcium levels have reached the threshold for inducing LTP (Lisman, 1989; Xia and Storm, 2005).

The role of phosphatases in synaptic plasticity provided a molecular foothold toward understanding the physiological role of LTD. Forebrain-specific knockout of calcineurin function, for example, abolishes LTD and causes schizophrenia-like behavioral deficits in working memory and social interaction (Zeng et al., 2001; Miyakawa et al., 2003). Interestingly, these animals also display a shift in the LTD/LTP modification threshold that promotes LTP at intermediate stimulation frequencies (Zeng et al., 2001). Additionally, inhibition of PP2A activity *in vivo* by expression of a known protein blocker (small t antigen) eliminates LTD without affecting LTP (Nicholls et al., 2008). While these PP2A-inhibited mice are able to locate a hidden platform in a water maze (Morris water maze task) as well as their uninhibited counterparts, they have difficulties re-learning the platform location once it has been moved (Nicholls et al., 2008). Thus CA1 LTD appears to be important for behavioral flexibility, or the ability of an animal to "weaken" previous memory traces when acquiring new information.

It is interesting to note that these calcium-dependent proteins also contribute to the structural plasticity of synapses. CaMKII promotes the maintenance of mature spine structures in a kinase-independent manner (Okamoto et al., 2007). This regulation likely arises from CaMKII's ability to bundle filamentous actin; the equilibrium between filamentous and globular actin is bidirectionally modulated by synaptic stimulation (Okamoto et al., 2004, 2007). Conversely, calcineurin (but not PP1) is required for spine shrinkage induced by LTD (Zhou et al., 2004).

How does postsynaptic calcium signaling downstream of NMDAR activation increase or decrease synaptic strength? For many years, there was a great debate as to whether LTP at Schaffer collateral-CA1 synapses is expressed presynaptically (e.g., by an increase in the probability of transmitter release) via a retrograde signal, or postsynaptically (e.g., by an increase in the number of postsynaptic glutamate receptors). As reviewed by Nicoll (2003), several early studies provided pivotal evidence in support of a postsynaptic, not presynaptic, mechanism of LTP expression:

(1) LTP selectively enhanced the AMPAR component of excitatory postsynaptic currents (EPSCs) over the NMDAR component, arguing against an increase in overall glutamate release (Kauer et al., 1988; Muller et al., 1988).

(2) LTP was *not* accompanied by changes in paired pulse facilitation (PPF – where the second response to two closely-delivered stimuli is increased), by changes in the rate of glutamate receptor blockade by use-dependent antagonists, nor by changes in the rate of presynaptic vesicle dye (FM1-43) destaining (all measures of changes in the presynaptic release probability; Manabe et al., 1993; Manabe and Nicoll, 1994; Zakharenko et al., 2001).

(3) LTP increased the magnitude of responses to exogenous (bath) AMPA exposure, as well as the number of AMPA binding sites assayed by quantitative autoradiography (Montgomery et al., 2001; Maren et al., 1993).

(4) LTP was accompanied by an increase in quantal size (the unitary postsynaptic response to a single presynaptic vesicle release), as estimated by miniature EPSC measurements and minimal stimulation methods (potency measurements; Oliet et al., 1996; Isaac et al., 1996).

(5) LTP was associated with an increase in the single-channel conductance of AMPARs (Benke et al., 1998).

(6) LTP switched on "silent synapses" – synapses that exhibited NMDAR-mediated responses but no AMPAR response (Isaac et al., 1995; Liao et al., 1995). These synapses are thus functionally silent until "unsilenced" by LTP, presumably by the introduction of new postsynaptic AMPARs.

The discovery of silent synapses provided an alternative explanation for one of the leading arguments in *support* of a presynaptic LTP mechanism – namely, the increase in quantal content (the total presynaptic output, equal to the number of release sites multiplied by the probability of release per site) and the decrease in number of failures (events where presynaptic stimulation failed to elicit a response) observed after LTP induction (Malinow and Tsien, 1990; Bekkers and Stevens, 1990). While these changes could have been due to an increase in the number of presynaptic release sites, they could also have been caused by an increase in the number of postsynaptic sites *capable* of responding to transmitter release. Indeed, two groups showed that under weak stimulation conditions just below the threshold for inducing AMPAR EPSCs, a clear NMDAR response could still be identified; after LTP induction, the same stimulation conditions then yielded persistent AMPAR responses (Isaac et al., 1995; Liao et al., 1995). Thus previously silent synapses were functionally activated by LTP. This discovery launched the study of AMPAR trafficking as a key mechanism in synaptic plasticity (see Sheng

and Kim, 2002; Collingridge et al., 2004; Derkach et al., 2007; Shepherd and Huganir, 2007; Citri and Malenka, 2008; Kessels and Malinow, 2009).

Glutamate receptor trafficking in LTP and LTD

Four genes encoding AMPAR subunits have been identified in mammals, GluR1-GluR4 (or GluRA-D). Mature CA1 hippocampal neurons primarily express the subunits GluR1, -2, and -3 (Zhu et al., 2000). In the postsynaptic membrane, AMPAR channels exist as tetrameric complexes thought to be composed of two identical heterodimers, GluR1/2 or GluR2/3 (Wenthold et al., 1996; Mansour et al., 2001; Lu et al., 2009). GluR1, GluR4, and a long splice form of GluR2 (GluR2L) possess long cytoplasmic C-terminal tails, whereas GluR2, GluR3, and a short form of GluR4 (GluR4c) possess short tails. The intracellular proteins that bind these C-terminal tails are believed to impart specific trafficking properties to each subunit type. Studies where a subunit type was visually or electrophysiologically "tagged" and expressed in hippocampal neurons have shown that surface insertion of GluR1/2 channels is increased by LTP or NMDAR stimulation, depending on the presence of the GluR1 C-terminal tail (Shi et al., 2001; Passafaro et al., 2001). GluR2/3 channels, on the other hand, are incorporated into the synapse on a continuous and more rapid time scale, a process requiring the intact GluR2 C-terminal tail (Shi et al., 2001; Passafaro et al., 2001). Overexpression of a GluR1 C-terminal fragment, therefore, blocks AMPAR trafficking in LTP and experience-dependent synaptic potentiation in the barrel cortex (Shi et al., 2001; Takahashi et al., 2003). GluR1 knockout mice, by contrast, fail to exhibit LTP (although spatial learning is intact in these animals; Zamanillo et al., 1999).

GluR1 can be regulated by phosphorylation of C-terminal tail residues. CaMKII directly phosphorylates Ser-831, which increases single-channel conductance, but only in homomeric receptors (Barria et al., 1997; Mammen et al., 1997). PKA directly phosphorylates Ser-845, which increases channel open-probability (Banke et al., 2000) and is necessary for synaptic insertion of GluR1 during LTP (Esteban et al., 2003). During LTD, Ser-845 is dephosphorylated, consistent with previous findings that PKA inhibition is required for LTD (Kameyama et al., 1998; Lee et al., 1998; Lee et al., 2000). Interestingly, bidirectional changes in GluR1 phosphorylation depend on previous synaptic history: When potentiated synapses are

depressed (a process called depotentiation), Ser-831 is preferentially dephosphorylated; when depressed synapses are potentiated (called de-depression), Ser-845 is preferentially phosphorylated (Lee et al., 2000).

Knock-in mice have been generated where Ser-831 and Ser-845 of GluR1 have been substituted with alanine residues to prevent phosphorylation. In the double knock-in mice, LTD is blocked and LTP is significantly reduced, yet basal synaptic transmission is normal (Lee et al., 2003). These animals also display severe deficits in retention of spatial memory (Lee et al., 2003). More recently, single knock-in mutants have been generated, and while both S831A and S845A hippocampal slices can support LTP, only S845A mutants show a deficit in LTD (Lee et al., 2010). Thus, either Ser-831 or Ser-845 can sustain LTP, but only Ser-845 is critical for LTD (Lee et al., 2010).

LTD requires clathrin-dependent endocytosis of AMPARs (Man et al., 2000), and GluR2 internalization is also believed to play a key role in this process. After internalization, AMPARs are sorted to recycling endosomes for reinsertion, or to lysosomes for degradation, depending on the nature of stimulation (AMPA versus NMDA) and the previous history of synaptic activity (Ehlers et al., 2000; Lee et al., 2004). GluR2 interacts with both the membrane fusion ATPase N-ethylmaleimide-sensitive factor (NSF) and the clathrin adaptor complex AP-2 at an overlapping site; interaction of GluR2 with one or the other of these proteins is believed to determine the basal versus activity-dependent trafficking patterns of GluR2/3 AMPARs (Lee et al., 2002). Another region in the GluR2 C-terminal tail binds the tethering protein glutamate receptor-interaction protein (GRIP), and phosphorylation of GluR2 Ser-880 or Tyr-876 residues decreases this interaction, thereby favoring GluR2 internalization (Chung et al., 2000; Hayashi and Huganir, 2004). Phosphorylation of either residue is also required for LTD, but not for the basal synaptic delivery of GluR2-containing AMPARs (Seidenman et al., 2003; Ahmadian et al., 2004). In cerebellar neurons, Ser-880 is phosphorylated by protein kinase C (PKC), but the responsible kinase in hippocampal neurons has not yet been identified (Kim et al., 2001). GluR2 phosphorylation at C-terminal tyrosine residues is likely mediated by Src family kinases (Hayashi and Huganir, 2004).

Is GluR2 internalization important for LTD *in vivo*? Hippocampal slices from GluR2 knockout mice display normal LTD, but reduced AMPAR EPSCs and enhanced LTP (Jia et al.,

1996). To eliminate the possibility of compensation from GluR3 receptors, a double knockout mouse was made lacking GluR2 and GluR3; these animals also show normal LTD, impaired basal synaptic transmission, and enhanced LTP (Meng et al., 2003). Thus either GluR2/3 is not required for LTD, or additional compensation occurs in the GluR2/3 double knockout (such as GluR1 dephosphorylation) to enable LTD. Indeed, LTD observed in the double knockout is only partially blocked by an endocytosis inhibitor (which normally abolishes LTD completely), suggesting that additional LTD mechanisms may be recruited in the double knockout mice (Meng et al., 2003). Interestingly, acute disruption of the GluR2-AP2 interaction blocks LTD and inhibits synaptic depression in the visual cortex after monocular deprivation (Yoon et al., 2009).

Although the subunit "rules" governing AMPAR insertion and removal have important implications for synaptic function, more recent work suggests a useful role in the regulation of synaptic structure as well. GluR1 insertion is necessary, though not sufficient, for the LTP-induced increase in spine size, and this process requires the C-terminal tail of GluR1 (Kopec et al., 2007). GluR2 overexpression increases spine size and density, an effect dependent on interactions between the extracellular N-terminal domain and the cell adhesion molecule N-cadherin (Passafaro et al., 2003; Saglietti et al., 2007). Thus changes in the functional strength of synapses can be correlated with structural modifications through the regulation of AMPAR trafficking.

Since the discovery of NMDAR-dependent synaptic plasticity and the earliest studies linking calcium-dependent serine/threonine kinases and phosphatases to AMPAR trafficking pathways, a plethora of additional signaling cascades have been described for LTP and LTD at hippocampal synapses. Many of these additional players and/or their regulators are found in the PSD (see Sheng and Hoogenraad, 2007). The remainder of this chapter will provide an overview of the other major signaling pathways in synaptic plasticity, and discuss the putative roles of two particular pathways that will be examined further in this thesis.

Small GTPase/MAPK signaling is required for LTP and LTD

Mitogen activated kinases (MAPKs) are signaling proteins integral to the regulation of cell proliferation, differentiation, and stress responses in many cell types. They are also highly expressed in post-mitotic, differentiated neurons, and play important roles in synaptic plasticity and behavior (see Thomas and Huganir, 2004). Early studies showed that tetanic stimulation in hippocampal slices activated the MAPK extracellular signal-regulated kinase (ERK), and inhibition of ERK activation blocked LTP and spatial learning (English and Sweatt 1996; 1997). Interestingly, ERK activity is required for the enhancement of AMPAR transmission in LTP (Zhu et al., 2002). This effect involves the upstream Ras protein, a member of the Ras superfamily of small GTPases that triggers MAPK signaling when bound to GTP (Figure 2). In hippocampal neurons, expression of constitutively-active Ras enhances basal synaptic strength in an ERK-dependent manner and occludes LTP, whereas dominant-negative Ras decreases basal transmission and blocks LTP (Zhu et al., 2002). ERK activity is also required for the elevation of basal synaptic strength by constitutively-active CaMKII (Zhu et al., 2002).

Direct targets of ERK in LTP, however, remain elusive. Although ERK is required for maintaining phosphorylation of the transcription factor CREB, the rapid effect of ERK pathway inhibitors on LTP suggests that additional synaptic targets are likely at play (Wu et al., 2001). Elevated Ras-ERK signaling increases GluR1 phosphorylation at Ser-845, though perhaps indirectly (Qin et al., 2005).

It is important to note that overexpression of ERK is not sufficient to enhance basal synaptic responses, implying that other Ras targets must account for the ability of active Ras to occlude LTP (Thomas and Huganir, 2004). In most cell types, active Ras can directly bind and stimulate activity of phosphatidylinositol 3-kinase (PI3K), which in turn catalyzes phosphorylation of the membrane lipid phosphatidylinositol-4,5-bisphosphate [PI(4,5)P2] to phosphatidylinositol-3,4,5-trisphosphate [PI(3,4,5)P3] (see Cantley, 2002; Figure 2). PI(3,4,5)P3 recruits the serine-threonine kinases Akt (also known as protein kinase B) and phosphoinositide-dependent kinase 1 (PDK1; Cantley, 2002); PDK1 phosphorylates Akt at Thr-308, which enhances Akt activity (Lawlor and Alessi, 2001). In hippocampal neurons, PI3K is required for chem-LTP (glycine)-induced potentiation of synaptic function, but not for chem-LTD (NMDA)-induced synaptic depression (Man et al., 2003). Overexpression of PI3K enhances basal AMPAR transmission and occludes chem-LTP (Man et al., 2003). Ras-PI3K signaling is

believed to enhance GluR1 phosphorylation at Ser-831 (Qin et al., 2005), and PI3K activation promotes the surface insertion of AMPARs (Man et al., 2003). Hence Ras pathways regulate AMPAR function on multiple levels.

How is Ras signaling triggered by calcium influx? In most cell types, small GTPase activity is determined by a balance between the positive regulatory effects of guanine nucleotide exchange factors (GEFs), and the negative regulatory effects of GTPase activating proteins (GAPs). Ras-guanine nucleotide-releasing factors (RasGRFs) are calcium-calmodulin-activated RasGEFs abundant in the brain (Farnsworth et al., 1995; Figure 2). The RasGRF1 subtype binds directly to the NMDAR subunit NR2B (Krapivinsky et al., 2003). RasGRF1 knockouts exhibit defective LTD, whereas animals lacking the RasGRF2 subtype display defective LTP; double RasGRF1/RasGRF2 knockouts show impaired LTD and LTP (Li et al., 2006). NMDAR-dependent ERK activation is also abolished in hippocampal slices from double knockout mice (Li et al., 2006). Thus RasGRF function links NMDAR calcium influx to Ras-ERK signaling.

Consistent with the finding that RasGRFs affect LTD, small GTPase/MAPK signaling pathways have been linked to LTD as well. Expression of constitutively-active Rap GTPase, a different member of the Ras superfamily, depresses basal synaptic strength and occludes LTD, whereas dominant-negative Rap enhances basal transmission and blocks LTD (Zhu et al., 2002). In this study, the effect of Rap in LTD required activity of the MAPK p38, leading the authors to speculate that activation of distinct MAPK subtypes could determine the induction of LTD versus LTP at synapses (Zhu et al., 2002). While attractive, this model is probably incomplete: the requirement for p38 MAPK in LTD has not been found by all groups (e.g., Peineau et al., 2009), and Rap can control activation of ERK signaling in neurons (Thomas and Huganir, 2004).

Another model has emerged for how MAPK signaling can influence the direction of plasticity change. In many cell types, the magnitude and time course of ERK activation can signal distinct outcomes: modest, transient elevation of ERK activity induced by epidermal growth factor (EGF) in pheochromocytoma cells (PC12), for example, promotes proliferation, whereas sustained ERK activity induced by nerve growth factor (NGF) promotes differentiation (Marshall, 1995). These functional effects are determined by the integrative output of the collective cellular ERK interactome (Von Kriegsheim et al., 2009). Interestingly, LTD induces transient ERK activation in hippocampal slices, while LTP induces prolonged ERK activation

(Thiels et al., 2002; Coba et al., 2008). Inhibition of ERK blocks LTP and *in vivo* hippocampal LTD, suggesting that ERK is absolutely required for both LTP and LTD (English and Sweatt 1996; Thiels et al., 2002). The distinct *dynamics* of ERK signaling, therefore, could potentially specify one form of plasticity over the other, much like the dynamics of calcium signaling: modest or transient ERK activation may be critical for LTD, and elevated or sustained ERK activation may be important for LTP. This hypothesis remains untested, however, as no simple molecular manipulation exists to covert one NMDAR-induced pattern of ERK activation to another.

What are the mechanisms for shutting down Ras/Rap signaling? Synaptic GAP (SynGAP) is a Ras and Rap GAP that interacts with the NR2B subunit (Kim et al., 2003; Krapivinsky et al., 2003; Kim et al., 2005; Figure 2). It is also one of the most abundant proteins in the PSD (Cheng et al., 2006). Hippocampal neurons cultured from SynGAP knockout mice show enhanced AMPAR transmission and elevated basal ERK activity (Rumbaugh et al., 2006). ERK activation does not increase further upon chem-LTP stimulation, an effect consistent with the reduced LTP observed in SynGAP heterozygote mice (Rumbaugh et al., 2006; Kim et al., 2003). Other studies, however, have found that SynGAP knockdown abnormally elevates NMDA-induced (but not basal) ERK activation, consistent with impaired chem-LTD in SynGAP heterozygote mice (Kim et al., 2005; Carlisle et al., 2008). Thus SynGAP is an important regulator of synaptic strength and ERK signaling, although it remains unclear precisely how SynGAP action is gated by NMDAR stimulation. SynGAP is also phosphorylated by CaMKII, which may increase overall GAP activity (Oh et al., 2004).

Spine-associated RapGAP (SPAR) is also found at synapses. Knockdown of SPAR enhances Rap signaling, and reduces synaptic function (Seeburg et al., 2008). Degradation of SPAR during periods of chronic synaptic activity is a critical mechanism for homeostatic plasticity in hippocampal neurons (Pak and Sheng, 2003; Seeburg et al., 2008).

Many small GTPases in neurons have significant effects on spine morphology (see Tada and Sheng, 2006). Ras promotes spine development; SynGAP mutants thus display accelerated spine morphogenesis and larger spine size (Vazquez et al., 2004). In contrast, Rap decreases spine density, and loss of SPAR reduces the number of mature spines (Pak and Sheng, 2003). Lastly, members of the Rho GTPase family (e.g., RhoA, Rac1) are known to regulate actin

dynamics in many cell types, and also influence spine growth and/or stability in neurons (Tada and Sheng, 2006).

SFK and PKC signaling regulate NMDAR trafficking and promote LTP

Like MAPKs, Src family tyrosine kinases (SFKs) are important regulators of proliferation and differentiation in many cell types, and are highly expressed in neurons (see Kalia et a., 2004). SFK inhibitors block CA1 LTP, and mice lacking the SFK subtype Fyn show impairments in LTP and spatial learning (Grant et al., 1992; Lu et al., 1998). Infusion of a Src activating peptide increases basal synaptic strength and occludes LTP (Lu et al., 1998). On a molecular level, SFKs phosphorylate NMDAR subunits, suppressing NMDAR internalization from the membrane surface (Prybylowski et al., 2005). This enhancement of NMDAR accumulation and function is required for SFK's role in LTP, although the mechanism by which NMDAR potentiation increases AMPAR transmission in LTP remains unknown (Lu et al., 1998; Huang et al., 2001). Interestingly, LTP and LTD of NMDAR EPSCs have been described in the hippocampus, although primarily in older animals (Grosshans et al., 2001), and with distinct mechanistic underpinnings than AMPAR synaptic plasticity (Selig et al., 1995).

Protein kinase C (PKC) has similarly been linked to NMDAR trafficking and LTP. PKC is an auto-inhibited enzyme that is activated by intracellular calcium, and promotes NMDAR insertion at synapses (Lan et al., 2001). Active PKC can be converted to a constitutively-active form of the kinase called PKM, and the zeta isoform of PKM is essential for LTP maintenance and the persistence of spatial memory (Pastalkova et al., 2006).

GSK-3beta signaling is required for LTD

Glycogen synthase kinase 3 (GSK-3) is a serine/threonine kinase implicated in numerous cellular processes, from glycogen metabolism to proliferation, migration, and cell death (see Frame and Cohen, 2001; Doble and Woodgett, 2003; Jope and Johnson, 2004; Forde and Dale, 2007). Two isoforms, alpha and beta, have been found in mammals, with GSK-3beta being the predominant isoform in the brain (Kaytor and Orr, 2002). Since its discovery as a target of the mood stabilizer lithium, GSK-3beta has been aggressively studied for its potential role in the pathophysiology of psychiatric and neurological diseases (see Jope and Roh, 2006).

Haploinsufficiency of GSK-3beta, for example, has antidepressant-like effects on mouse behavior, and GSK-3beta inhibitors rescue neuronal proliferation and behavioral phenotypes in a mouse model of schizophrenia (O'Brien et al., 2004; Mao et al., 2009). Overexpression of GSK-3beta enhances neurodegeneration and causes Alzheimer's disease-like pathology in the brain (Lucas et al., 2001). Thus GSK-3beta function in neurons has important implications for the study of neuropsychiatric disorders.

GSK-3beta participates in the Wnt/beta-catenin signaling pathway, which plays critical roles in embryonic development, stem cell fate determination, and synaptogenesis. Beta-catenin is a transcription factor and adhesion protein, and contributes to the activity-dependent remodeling of spine structure through its association with N-cadherin proteins at the synapse (Tai et al., 2007). In the canonical Wnt signaling pathway, beta-catenin is phosphorylated under basal conditions by casein kinase 1 (CK1) and then GSK-3beta, both components of a multi-protein complex that includes the scaffold protein Axin and the tumor suppressor *adenomatous polyposis coli* gene product (APC; GSK-3beta is also capable of phosphorylating Axin and APC; MacDonald et al., 2009). Beta-catenin phosphorylation results in its ubiquitination and subsequent degradation (MacDonald et al., 2009). Wnt ligand binding to the Frizzled receptor and low-density lipoprotein receptor-related protein 6 (LRP6) co-receptor leads to Axin recruitment and disruption of beta-catenin phosphorylation/degradation, thereby allowing beta-catenin levels to stabilize (MacDonald et al., 2009). In mature hippocampal neurons, expression of stabilized beta-catenin (carrying mutations in CK1 and GSK-3beta phosphorylation sites) increases total dendritic branch length, which induces homeostatic decreases in miniature EPSC amplitude and AMPAR transmission in mature hippocampal neurons (Peng et al., 2009). Loss-of-function experiments suggest that beta-catenin is required for the bidirectional scaling of synaptic strength in response to manipulation of chronic activity (Okuda et al., 2007).

In other cellular pathways such as insulin signaling, GSK-3beta is regulated through a distinct mechanism. Phosphorylation of the Ser-9 residue of GSK-3beta creates an intramolecular pseudo-substrate that binds and auto-inhibits GSK-3beta kinase activity (Doble and Woodgett, 2003). Examples of enzymes known to phosphorylate Ser-9 include Akt, PKA, $p90^{RSK}$ and $p70^{S6K}$ (Ford and Dale, 2007). Activation of GSK-3beta, therefore, occurs through phosphatase-mediated dephosphorylation of Ser-9 (McManus et al., 2005). Targets of GSK-3beta in these pathways include transcription factors (e.g., c-Jun, c-Myc), metabolic enzymes

(e.g., glycogen synthase, ATP citrate lyase), and microtubule-associated proteins (e.g., Tau; Frame and Cohen, 2001). Knock-in mice expressing constitutively-active GSK-3beta (with alanine substitution of the Ser-9 residue) show decreased insulin-dependent activation of glycogen synthase; however, overall glucose levels remain unchanged and the animals appear largely normal (although nervous system function and behaviors have yet to be examined; McManus et al., 2005). Importantly, Wnt signaling is intact in these knock-in mice, a finding consistent with previous studies showing functional separation between GSK-3beta's roles in Wnt and non-Wnt pathways (Ding et al., 2000). This separation could arise from the sequestration of GSK-3beta into distinct signaling complexes, although the precise mechanism remains unclear (Doble and Woodgett, 2003).

Recent studies have uncovered a critical role for GSK-3beta in synaptic plasticity. GSK-3 inhibitors block LTD, but not LTP or basal synaptic transmission, at CA1 hippocampal synapses (Peineau et al., 2007). LTD induction causes a decrease in Ser-9 phosphorylation of GSK-3beta, a decrease in Thr-308 phosphorylation of Akt, and an increase in GSK-3beta kinase activity; conversely, LTP induction increases phospho-S9 levels of GSK-3beta (Peineau et al., 2007). The involvement of a Ras-PI3K pathway in LTP (Man et al., 2003) suggests that Akt regulation of GSK-3beta could be a mechanism for cross-talk between LTP and LTD pathways (Figure 2). Indeed, application of an LTP stimulus immediately before LTD induction can inhibit LTD, and this inhibition requires PI3K activity and Akt activation (Peineau et al., 2007). Thus GSK-3beta is required for LTD, and regulation of GSK-3beta through PI3K-Akt signaling could be important for LTD inhibition.

GSK-3beta is an intriguing candidate for an LTD "mediator," since it has been shown to phosphorylate PP1 and protein phosphatase inhibitor-2 protein, events that both enhance overall phosphatase activity (Kockeritz et al., 2006). This could promote activation of additional GSK-3beta molecules through Ser-9 dephosphorylation, thereby providing a "feed-forward" mechanism for maintaining LTD. The effects of constitutively-active GSK-3beta on basal synaptic transmission have not yet been identified, however. More importantly, no synaptic targets of GSK-3beta have yet been linked to LTD signaling. These targets could have interesting therapeutic applications, as GSK-3beta activity is also required for LTD enhancement by Abeta oligomers, suggesting that Abeta could recruit GSK-3beta signaling mechanisms to pathologically increase activity-dependent synaptic depression (Li et al., 2009).

PSD-95 promotes synaptic strength and is required for LTD

In addition to protein kinases and phosphatases, non-enzymatic scaffold proteins have also been implicated in synaptic plasticity. Early studies postulated the presence of "slot" molecules at the PSD that capture exocytosed AMPA receptors and control AMPAR number in a manner that regulates overall synaptic strength (Sheng and Kim, 2002; Citri and Malenka, 2008). Possible candidates for these "slot" molecules include members of the membrane-associated guanylate kinase (MAGUK) superfamily – multimodular scaffold proteins consisting of several protein interaction domains: (1) one to three peptide binding domains named for the proteins in which they were originally identified (postsynaptic density-95, discs large, and zona occludens 1), or PDZ, (2) a Src homology 3 (SH3) domain, and (3) a catalytically-inactive guanylate kinase-like (GK) domain (see Kim and Sheng, 2004; Elias and Nicoll, 2007; Keith and El-Husseini, 2008; Figure 3). The most well-characterized MAGUK is postsynaptic density-95 (PSD-95), a highly abundant component of the PSD that has been implicated in multiple aspects of synaptic function, plasticity, and maturation (Kim and Sheng, 2004; Elias and Nicoll, 2007).

In hippocampal neurons, overexpression of PSD-95 enhances AMPAR transmission and occludes LTP, without changing (or with smaller changes to) NMDAR transmission (Stein et al., 2003; Ehrlich and Malinow, 2004; Futai et al., 2007). While consistent with the idea of an AMPAR "slot" function for PSD-95 at synapses, this finding initially conflicted with reports of direct association of PSD-95 with NMDAR NR2 subunits (through PDZ domain-binding motif interactions Kornau et al., 1995), but not with AMPAR subunits. The discovery of transmembrane AMPAR regulatory proteins (TARPs) provided a mechanistic basis for PSD-95 modulation of AMPAR function (Elias and Nicoll, 2007). TARPs are calcium channel homologs that interact directly with AMPARs and PSD-95 PDZ domains, and are required for AMPAR delivery to the membrane surface (Chen et al., 2000; Tomita et al., 2003). TARP association also promotes AMPAR assembly and biosynthesis, and regulates the biophysical and pharmacological properties of AMPARs (Nicoll et al., 2006). More importantly, TARP interaction with PSD-95 is required for synaptic localization of AMPARs (Schnell et al., 2003). CaMKII phosphorylation of TARPs promotes synaptic AMPAR delivery during LTP (Tomita et al., 2005). As expected, hippocampal TARP knockouts display severely reduced basal synaptic

transmission, decreased synaptic and extrasynaptic AMPARs, and reduced LTP, although LTD is intact (Rouach et al., 2005).

In contrast to the effects of PSD-95 overexpression, knockdown of PSD-95 levels decreases surface AMPARs and synaptic strength (Schluter et al., 2006; Ehrlich et al., 2007; Futai et al., 2007). Interestingly, PSD-95 knockdown does not affect LTP, but completely abolishes LTD, suggesting that PSD-95 is required for LTD but not LTP (Ehrlich et al., 2007). In PSD-95 knockouts, LTP is even enhanced while LTD is blocked, and the mice exhibit severe deficits in spatial learning (Migaud et al., 1998). This shift in the LTP/LTD modification threshold is similar to what has been reported in forebrain-specific calcineurin knockouts (Zeng et al., 2001), suggesting a possible shared mechanism in the induction of LTD.

Does PSD-95 play a role in LTP? The LTP observed in PSD-95 knockdown or knockout experiments may be due to the function of other synaptic MAGUKs that compensate for loss of PSD-95 (Elias et al., 2006). Indeed, PSD-95 is required for LTP-induced spine growth (Ehrlich et al., 2007; Steiner et al., 2008), and PSD-95 contributes to the experience-dependent potentiation of AMPAR transmission in the barrel cortex (Ehrlich and Malinow, 2004). PSD-95 also promotes synapse maturation in neurons, a process that may share similar signaling mechanisms with LTP (El-Husseini et al., 2000). Thus PSD-95 and/or related MAGUKs are likely important for LTP.

PSD-95 is dynamically regulated in neurons – at least four different modes of protein regulation have been identified (multimerization, palmitoylation, degradation, and phosphorylation), many of which are important for basal and/or activity-dependent functions of PSD-95.

Multimerization. PSD-95 can multimerize through N-terminal or C-terminal domain interactions. Head-to-head multimerization through disulfide linkage of N-terminal cysteine residues (Cys-3, Cys-5) has been described, and this interaction is required for PSD-95's ability to cluster ion channels that bind to PDZ domains (Hsueh et al., 1997; Figure 3). Expression of multimerization-deficient N-terminal PSD-95 mutants does not enhance basal AMPAR transmission in hippocampal neurons, suggesting that multimerization may be important for synaptic targeting of PSD-95 (Xu et al., 2008).

In the C-terminal region of PSD-95, SH3 and GK domains interact in an intra- or intermolecular fashion, although the former predominates *in vivo* (McGee and Bredt, 1999; Shin et al., 2000). Proteins that bind the linker region between both domains, such as calcium-bound calmodulin, may structurally constrain the area to promote intermolecular SH3-GK assembly (Masuko et al., 1999; McGee et al., 2001), or to promote interaction with other signaling scaffold proteins at the synapse (see below).

Palmitoylation. The PSD-95 N-terminal cysteines identified above are also important for conjugation of the fatty acid palmitate, which provides a mechanism for synaptic targeting and lipid-mediated multimerization of PSD-95 (Craven et al., 1999; Christopherson et al., 2003; Figure 3). Palmitoylation is required for synaptic clustering of PSD-95 and AMPARs, while depalmitoylation has been reported to be required for glutamate-induced AMPAR internalization (El-Husseini et al., 2002). Depalmitoylation is not required for LTD, however, suggesting that other mechanisms may explain PSD-95's role in LTD (Xu et al., 2008).

Degradation. In the vicinity of the palmitoylation cysteines of PSD-95 lies a putative PEST (Pro-, Glu-, Ser-, Thr-rich) degradation sequence (amino acids 13-23; Colledge et al., 2003; Figure 3). Chemical LTD appears to cause ubiquitination of PSD-95 in a PEST sequence-dependent manner, and promotes subsequent degradation by proteasome activity (Colledge et al., 2003). The PEST motif is important for basal synaptic targeting of PSD-95, although mutations in the PEST region also affect PSD-95 multimerization (Xu et al., 2008).

Phosphorylation. Many putative phosphorylation sites have been found in PSD-95; this discussion will focus on those where the functional effects of such phosphorylation events have been identified (Figure 3).

(1) N-terminal Thr-19, Ser-25, and Ser-35 residues of PSD-95 are reported substrates of cyclin-dependent kinase 5 (Cdk5), a serine/threonine kinase important in neurogenesis and neurodegeneration (Morabito et al., 2004). In heterologous cells, co-expression of Cdk5 and PSD-95 decreases PSD-95 multimerization, and expression of a triple phospho-null mutant (T19A-S25A-S35A PSD-95) in hippocampal neurons increases PSD-95 cluster size (Morabito et al., 2004). Phosphorylation at these N-terminal sites, therefore, regulates PSD-95 multimerization.

(2) Ser-73 lies in the first PDZ domain of PSD-95. CaMKII phosphorylation of Ser-73 decreases NR2A association with PSD-95 (Gardoni et al., 2006), and promotes PSD-95

trafficking out of spines (Steiner et al., 2008). Ser-73 phosphorylation inhibits LTP, suggesting that CaMKII regulation of PSD-95 at this residue constitutes a negative feedback mechanism for limiting LTP-induced changes at spines (Steiner et al., 2008).

(3) Phosphorylation of Ser-295 by the MAPK JNK enhances synaptic accumulation of PSD-95 (Kim et al., 2007). Chemical LTD induces Ser-295 dephosphorylation by PP1 and/or PP2A phosphatases, and expression of a phospho-mimic mutant (S295D) blocks NMDA-induced AMPAR internalization and LTD (Kim et al., 2007). Ser-295 lies between the second and third PDZ domains, so it is unlikely that head-to-head multimerization is regulated by this residue. The precise mechanism underlying Ser-295 function remains unknown.

(4) c-Abl tyrosine kinase phosphorylates Tyr-533, which lies between the SH3 and GK domains of PSD-95 (De Arce et al., 2010). Phosphorylation promotes PSD-95 clustering at synapses, perhaps by regulating SH3-GK domain interactions (De Arce et al., 2010).

Recent studies using two-photon time-lapse imaging of proteins tagged with photo-activatable markers have revealed new insights into the molecular dynamics of PSD-95, which may reflect a cumulative outcome of the above modes of PSD-95 regulation. Under basal conditions, PSD-95 molecules are highly stable in spines (Sturgill et al., 2009). SH3-GK domains are strictly required for the formation of a stable, synaptic lattice of PSD-95 molecules, but are not required for the incorporation of PSD-95 into a pre-formed lattice (Sturgill et al., 2009; also confirmed by electrophysiological studies in Xu et al., 2008). N-terminal PDZ domains, on the other hand, are required for PSD-95 insertion into a pre-formed lattice (Sturgill et al., 2009). Interestingly, LTP does not enhance PSD-95 clustering (Steiner et al., 2008). Rather, PSD-95 molecules are transiently lost from spines after LTP induction, and then replaced with new PSD-95 molecules within 5 minutes, such that total PSD-95 levels are unchanged from baseline (Steiner et al., 2008). In contrast, chemical LTD promotes rapid removal of PSD-95 from spines, an effect *independent* of calcineurin and PP1 (Sturgill et al., 2009). Thus PSD-95 is dynamically regulated during periods of synaptic plasticity.

Is it possible to dissociate PSD-95's roles in basal synaptic transmission and LTD? Although increased levels of wild-type PSD-95 enhance AMPAR EPSCs without affecting LTD (or with lowering the threshold for LTD; Stein et al., 2003), Xu et al. (2008) reported that mutations in the N-terminal (E17R, Q15A) or SH3-GK (L460P) regions enhanced AMPAR

EPSCs but blocked LTD (Figure 3). This raises the possibility that synaptic proteins associated with either region could play important and specific roles in LTD signaling. The potential identities of these proteins are of major interest, therefore, in improving our understanding of LTD, and inspire the major research questions of this thesis.

N-terminal region. The N-terminal mutations (Q15A, E17R) that selectively block LTD lie near the multimerization and PEST regions of PSD-95. PEST mutations in PSD-95 also affect multimerization (Xu et al., 2008), and Gln-15/Glu-17 reside in the vicinity of Cdk5 phosphorylation sites that regulate PSD-95 clustering (Morabito et al., 2004). One hypothesis, therefore, is that these N-terminal residues could be important for the activity-dependent de-multimerization of PSD-95, and consequent de-clustering and/or removal of PSD-95 from spines in LTD. Because neither Q15A nor E17R mutations affect the basal synaptic targeting of PSD-95, this de-multimerization step must be gated by NMDAR activation, or must be regulated by a protein whose function is activity-dependent.

Interestingly, the nearby residue Thr-19 does not strictly conform to a Cdk5 phosphorylation site (Songyang et al., 1996), and Morabito et al. (2004) preferentially examined Ser-25 as a putative Cdk5 target. The possibility remains that Thr-19 is phosphorylated by a novel LTD mediator (see Conclusions).

SH3-GK region. Replacement of wild type PSD-95 with L460P-PSD-95 selectively blocks LTD (Xu et al., 2008). The Leu-460 residue lies within the SH3 domain, and L460P mutations block intramolecular SH3-GK interactions without affecting N-terminal multimerization (McGee and Bredt, 1999; Shin et al., 2000). At synapses containing only L460P-PSD-95 molecules, therefore, it is possible that altered recruitment of signaling proteins normally associated with the SH3-GK region leads to deficits in LTD (Xu et al., 2008).

Many signaling proteins, particularly large molecular scaffolds, have been shown to bind the SH3-GK region of PSD-95 (Kim and Sheng, 2004). Guanylate kinase-associated protein (GKAP) is one example that preferentially interacts with the GK domain (Naisbitt et al., 1997). GKAP binding to PSD-95 regulates targeting of the scaffold protein Shank, and Shank is required for maintaining proper spine and PSD structure (Romorini et al., 2004; Hung et al., 2008). Similarly, SPAR has been shown to interact with the GK region of PSD-95, and changes in SPAR levels have significant impacts on basal synaptic function and spine morphology (Pak and Sheng, 2003; Seeburg et al., 2008). Because GK interactions appear intact in L460P-PSD-

95 mutants, however, it is unlikely that GKAP or SPAR recruitment in spines is altered by the L460P mutation (McGee and Bredt, 1999; Shin et al., 2000).

Two other scaffold proteins that bind PSD-95 SH3-GK are the A-kinase-anchoring protein 79/150 (AKAP; Colledge et al., 2000) and proline-rich tyrosine kinase 2 (PYK2; Seabold et al., 2003). AKAP interacts with PKA, calcineurin, and PKC at the synapse, and AKAP knockouts exhibit severe deficits in spatial memory and motor coordination (Tunquist et al., 2008). The mice also show reduced basal levels of phospho-Ser-845 GluR1, and decreased basal AMPAR transmission that occludes LTD, consistent with a role for AKAP in targeting PKA to synapses (Tunquist et al., 2008; Colledge et al., 2000). Selective inhibition of the AKAP-PKA interaction decreases AMPAR EPSCs and blocks both LTP and LTD (Tavalin et al., 2002; Lu et al., 2007, Lu et al., 2008). In contrast, expression of mutant AKAP lacking the calcineurin binding site increases basal AMPAR delivery and blocks NMDA-induced AMPAR internalization (Bhattacharyya et al., 2009). Thus AKAP is critical for basal and activity-dependent pathways of AMPAR trafficking, and selective perturbations in AKAP function may specifically block LTD.

PYK2 binds PSD-95, and plays a role in synaptic plasticity

PYK2, also known as cell adhesion kinase beta (CAKbeta) or protein tyrosine kinase 2b (PTK2B), is a calcium-dependent tyrosine kinase found in the PSD (Huang et al., 2001; Collins et al., 2006). PYK2 is closely related to the focal adhesion kinase (FAK; 48% identity, 65% similarity), but whereas FAK is expressed ubiquitously, PYK2 is expressed predominantly in postnatal hematopoietic lineages and in the forebrain (Girault et al., 1999; Menegon et al., 1999; Avraham et al., 2000). In the hematopoietic lineage, PYK2 is required for integrin-dependent osteoclast function (Gil-Henn et al., 2007) and chemokine-activated macrophage migration (Okigaki et al., 2003). In HeLa cells, PYK2 is involved in focal adhesion disassembly in response to calcium transients (Hashido et al., 2006). Thus in various peripheral cell types, PYK2 is a component of an inducible cell migration pathway, usually in response to a rise in intracellular calcium (although PYK2 activation by other signals such as osmolarity stress or T cell receptor activation have been reported; Avraham et al., 2000).

PYK2 consists of a band4.1/ezrin/radixin/moesin homology (FERM) domain, a kinase domain, a focal adhesion targeting (FAT) domain, and several proline-rich interaction regions (Girault et al., 1999; Avraham et al., 2000; Figure 4). A rise in intracellular calcium is believed to induce dimerization of PYK2 and trans-autophosphorylation at Y402, a residue located between the FERM and kinase domains (Lev et al., 1995; Park et al., 2004, Kohno et al., 2008; Bartos et al., 2010). In hematopoietic cells, phospho-Y402 PYK2 subsequently recruits downstream signaling proteins, including Src family kinases and MAPK (JNK, ERK) pathway regulators (Girault et al., 1999; Park et al., 2004).

Several mechanisms for PYK2 activation by calcium have been proposed (see Chapter 3). Direct binding of calcium-calmodulin complexes to the PYK2 FERM domain has been reported to induce dimerization and transphosphorylation at Y402 (Kohno et al., 2008). Second, in pheochromocytoma cells (PC12), calcineurin enhances PYK2 Y402 phosphorylation through an unknown mechanism involving direct dephosphorylation of several PYK2 serine/threonine residues (Faure et al., 2007). A similar mechanism has been proposed for FAK activation by PP1 (Bianchi et al., 2005). Thirdly, calcium-calmodulin binding to PSD-95 may inhibit intramolecular SH3-GK interactions, and enable PYK2 binding to the SH3 region (Bartos et al., 2010). Recruitment of PYK2 to the PSD could cluster PYK2 molecules and promote transphosphorylation at Y402 (Bartos et al., 2010). Consistent with the idea, PYK2 has been reported to bind PSD-95 in the presence of calcium, or in the absence of the GK domain (Seabold et al., 2003; Bartos et al., 2010). This functional relationship between PYK2 and PSD-95 suggests that altered PYK2 activity may occur in neurons expressing PSD-95 molecules with mutations in the SH3 domain.

Not much is known about PYK2's role at synapses. One study was published using infusion experiments of recombinant PYK2 protein into hippocampal neurons (Huang et al., 2001). This study found that PYK2 played a role in the Src pathway of LTP signaling: infusion of wild type PYK2 enhanced basal synaptic strength in an NMDAR- and Src-dependent manner and occluded LTP, whereas infusion of a kinase-dead PYK2 mutant blocked LTP (Huang et al., 2001). For a protein as large as PYK2, however, the post-translational modification, assembly, and trafficking of injected recombinant protein versus transfected cDNA of PYK2 could differ, and to our knowledge, no other infusion experiments have been published for a protein of PYK2's size (116 Kd). Additionally, the role of PYK2 in LTD has not yet been examined – an

intriguing hypothesis given PYK2's unique properties of calcium-dependence and PSD-95-association.

FAK, on the other hand, has been well studied in focal adhesion and spine dynamics. The FERM domain of FAK interacts with various receptor tyrosine kinases (RTKs, e.g., epidermal growth factor and platelet-derived growth factor receptors); Pro-rich regions bind SH3-containing adaptors and GTPase regulators (e.g., p130Cas protein and GAP regulators of Rho and Arf GTPases); and the FAT domain interacts with p190 RhoGEF, the Grb2 adaptor in Ras signaling, and various integrin-associated proteins (e.g., paxilin, talin; Mitra et al., 2005; Figure 4). Phosphorylation of FAK at Tyr-397, the functional equivalent of Tyr-402 in PYK2, has been associated with the recruitment and activation of a host of signaling proteins: Src kinase, the Shc adaptor in Ras signaling, p120 RasGAP, and the PI3K p85 subunit, among others (Mitra et al., 2005). FAK thus appears to be a signaling nexus between integrins, RTKs, Rho, Ras, and Src pathways in motile cells.

FAK knockouts die at early embryonic stages, an effect likely arising from impaired migration of embryonic precursor cells (Ilic et al., 1995). FAK-deficient cells show increased number of focal adhesion contacts, suggesting that FAK plays an important role in focal adhesion turnover (Ilic et al., 1995). FAK also promotes "maturation" of focal adhesions into larger, more stable complexes connected with actin stress fibers (Sieg et al., 1999). Similarly, FAK is a negative regulator of neurite outgrowth and axonal branching in developing hippocampal neurons (Rico et al., 2004). In mature neurons, FAK promotes spine stability as a component of the ephrin B receptor signaling pathway (Shi et al., 2009), and FAK is required for dentate gyrus LTP (Yang et al., 2003).

It remains unclear how many of FAK's cellular functions are shared with PYK2. The proteins are similar enough for one to functionally compensate for the other in genetic knockout experiments (Lim et al., 2008); however, they can also have opposing roles, as in cell cycle regulation, cell survival, and cell rounding (Xiong and Parsons, 1997; Zhao et al., 2000; Du et al., 2001). Some signaling partners may be shared between FAK and PYK2 pathways, but the extent of such overlap is unknown, and targets of PYK2 signaling at synapses remain unidentified.

Conclusions

N-terminal mutations in PSD-95 selectively block LTD (Xu et al., 2008) and can affect PSD-95 multimerization (Morabito et al., 2004). The Thr-19 residue of PSD-95 resides near these mutations, and appears to be a site for phosphorylation in neurons (Morabito et al., 2004). We hypothesize that Thr-19-dependent N-terminal multimerization of PSD-95 plays a role in LTD. To address this, we would need to examine the following questions:

(1) Do Thr-19 mutations affect PSD-95 multimerization and stability at spines?

(2) Do Thr-19 mutations affect LTD (but not basal synaptic function), in a manner that correlates with the effects on PSD-95 multimerization/stability?

(3) What is the kinase responsible for phosphorylating Thr-19?

(4) Does this kinase affect PSD-95 multimerization/stability?

(5) Does this kinase play a role in LTD? And is it regulated in an activity-dependent manner?

Mutation of the SH3-GK region in PSD-95 also selectively blocks LTD (Xu et al., 2008). PYK2 is a large multimodular protein that reportedly associates with the SH3 domain (Seabold et al., 2003), and PSD-95 may contribute to the NMDA-dependent recruitment of PYK2 to synapses (Bartos et al., 2010). PYK2 is also known to be calcium-dependent, and is important for the activity-induced reorganization of specialized adhesion sites (Girault et al., 1999; Avraham et al., 2000). We hypothesize that PYK2 could play a role in LTD, and this thesis investigates the following questions:

(1) Does NMDAR activation alter PYK2 activity?

(2) Is PYK2 necessary for LTD? Are scaffold and/or kinase functions of PYK2 important for LTD?

(3) Is overexpression of PYK2 sufficient to enhance basal or activity-dependent depression of synaptic function?

(4) If PYK2 is critical for LTD, what downstream effects of PYK2 could explain its role in LTD?

Together, these studies will improve our understanding of LTD mechanisms. Given the significance of LTD and LTP in memory and neuropsychiatric disorders, novel insights into the molecular pathways of synaptic plasticity will be invaluable.

III. Figure Legends and Figures

Figure 1. Synaptic plasticity in CA1 hippocampus. (**A**) Schematic representation of the neural circuitry of a rodent hippocampal slice (coronal section). Position of stimulus (Stim) and recording (Rec) electrodes for electrophysiological recording of synaptic plasticity at Schaffer collateral-CA1 synapses is indicated. DG, dentate gyrus; MF, mossy fiber pathway; SC, Schaffer collateral pathway. (**B**) Long term potentiation (LTP) and long term depression (LTD) at Schaffer collateral-CA1 synapses. LTP and LTD were first described using field recording measurements of excitatory postsynaptic potentials (EPSPs); the data shown here was obtained using whole-cell recording measurements of excitatory postsynaptic currents (EPSCs). Sample EPSC traces before and after LTP/LTD induction are shown (scale bar, 50 pA/50 msec), and averaged EPSC responses of 6 (left) or 10 (right) neurons are plotted below (normalized to baseline EPSC amplitude). Baseline measurements were obtained while holding the postsynaptic CA1 cell at -70 mV (stimulated at 0.2 Hz, left; or 0.033 Hz, right). LTP was induced by pairing 3 Hz presynaptic stimulation (200 pulses) with postsynaptic depolarization to 0 mV (indicated by the arrow, left); LTD was induced by pairing 1 Hz presynaptic stimulation (200 pulses) with postsynaptic depolarization to -40 mV (indicated by the bar, right). For details on LTP and LTD protocols, see Chapter 2 or 3, Materials and Methods section.

Figure 2. Schematic diagram of Ras signaling in synaptic plasticity. Ras cycles between active, GTP-bound (yellow) and inactive, GDP-bound (blue) forms. RasGRFs and SynGAP are the most abundant Ras regulators at synapses. Ras activation of ERK signaling is critical for LTP, and Ras inhibition of GSK-3beta (via PI3K-Akt signaling) may be important for inhibition of LTD by LTP stimuli (see text).

Figure 3. Domain organization and protein-protein interactions of PSD-95. Schematic diagram of PSD-95 (rat), showing major domains (PSD-95/Discs large/Zona occludens [PDZ], Src homology 3 [SH3], guanylate kinase [GK], putative Pro-/Glu-/Ser-/Thr-rich [PEST] degradation motif), and locations of key amino acids (e.g., phosphorylation sites) discussed in the text. PSD-95-associated proteins discussed in the text are listed in boxes below the appropriate PSD-95 interaction domain.

Figure 4. Domain organization of PYK2 and FAK. Schematic diagram of PYK2 and FAK proteins, showing major domains (band 4.1/ezrin/radixin/moesin homology [FERM], tyrosine kinase, focal adhesion targeting [FAT], and proline rich [PR]). The Tyr-402 site of PYK2, and functionally equivalent Tyr-397 site in FAK, are also indicated. Sequence similarities between PYK2 and FAK are shown for N-terminal, kinase, and C-terminal regions (~40%, ~60%, ~40%, respectively), and key FAK-associated proteins mentioned in the text are listed in boxes below the appropriate FAK interaction domain (proteins that bind Tyr-397 only associate with the phosphorylated form of this residue).

Figure 1

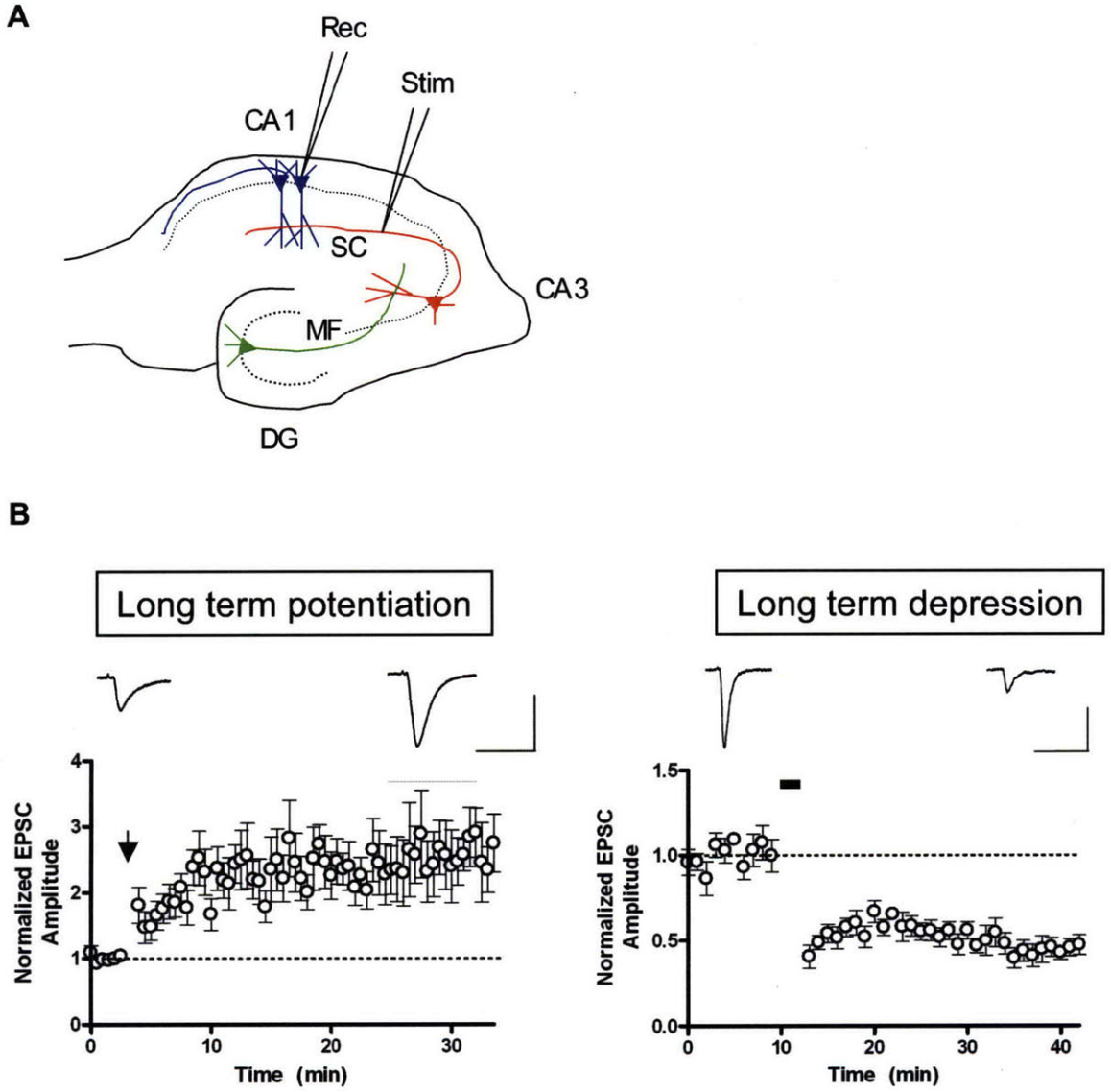
A
Rec
Stim
CA1
SC
CA3
MF
DG
B
Long term potentiation
Long term depression
Normalized EPSC Amplitude
Time (min)
Normalized EPSC Amplitude
Time (min)

Figure 2

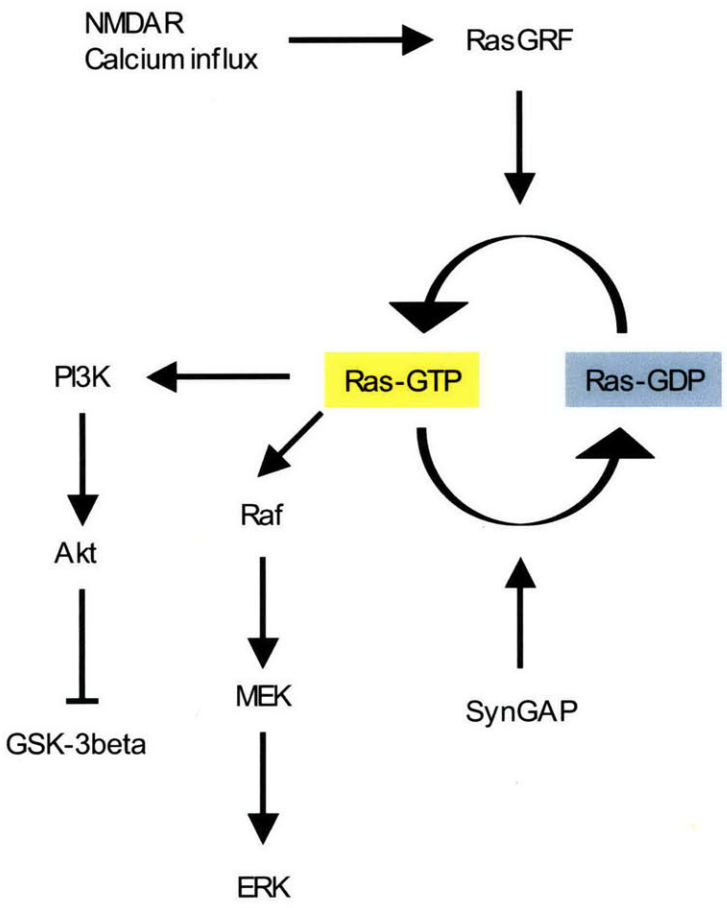
NMDAR
Calcium influx
RasGRF
PI3K
Ras-GTP
Ras-GDP
Raf
Akt
MEK
SynGAP
GSK-3beta
ERK

Figure 3

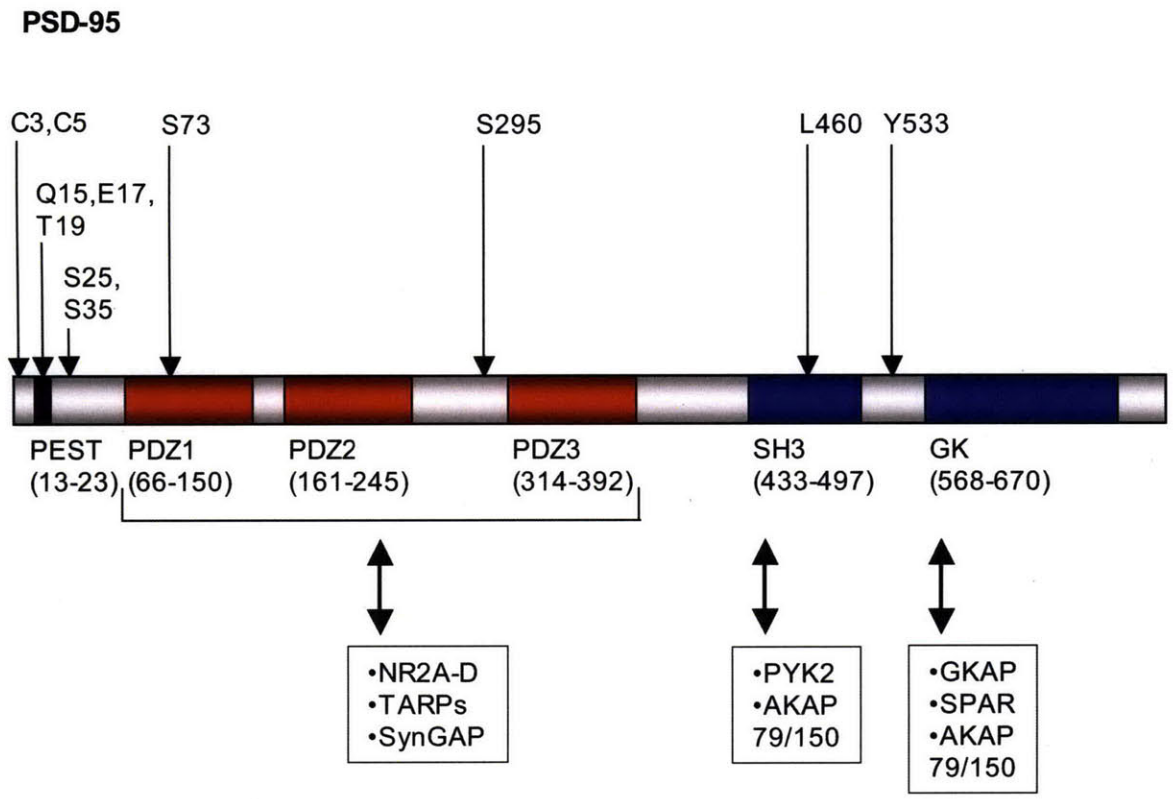
PSD-95
C3,C5
S73
S295
L460
Y533
Q15,E17,
T19
S25,
S35
PEST
(13-23)
PDZ1
(66-150)
PDZ2
(161-245)
PDZ3
(314-392)
SH3
(433-497)
GK
(568-670)
•NR2A-D
•TARPs
•SynGAP
•PYK2
•AKAP
79/150
•GKAP
•SPAR
•AKAP
79/150

Figure 4

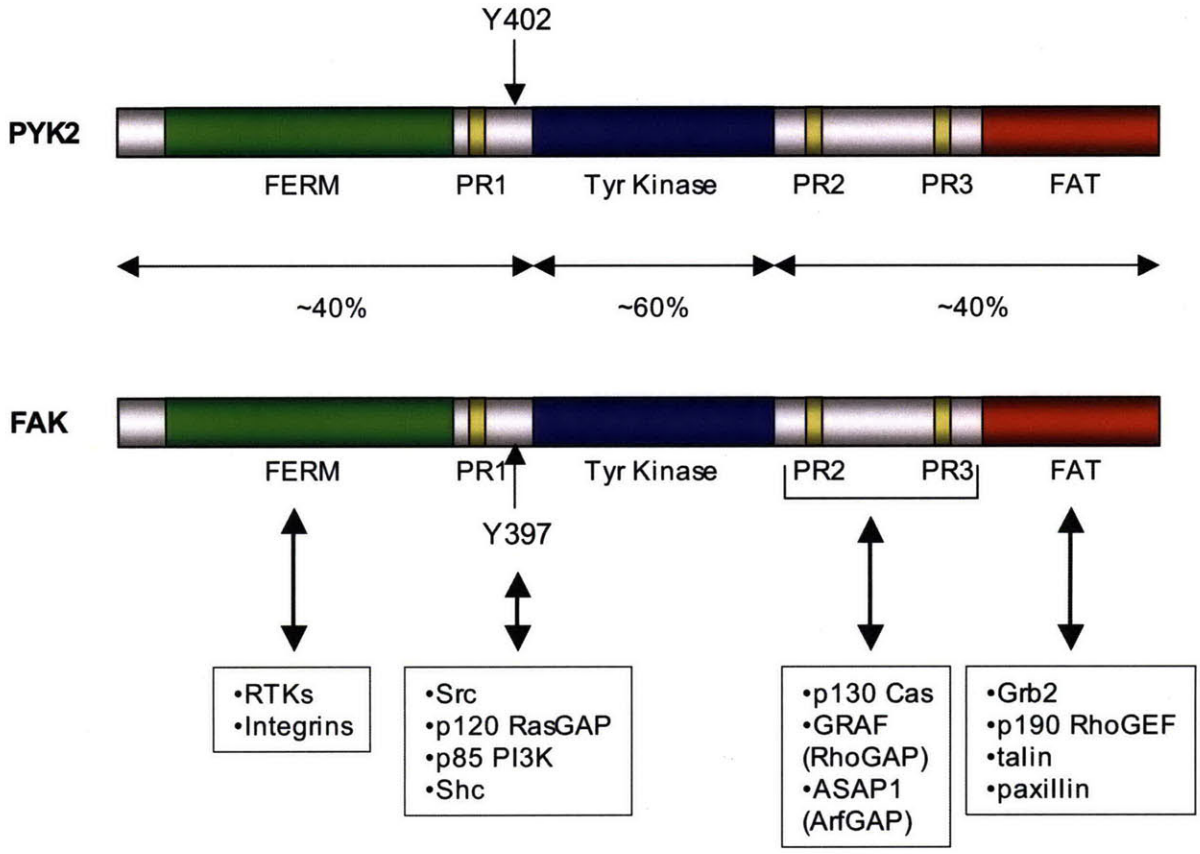
Y402
PYK2
FERM
PR1
Tyr Kinase
PR2
PR3
FAT
~40%
~60%
~40%
FAK
FERM
PR1
Tyr Kinase
PR2
PR3
FAT
Y397
•RTKs
•Integrins
•Src
•p120 RasGAP
•p85 PI3K
•Shc
•p130 Cas
•GRAF (RhoGAP)
•ASAP1 (ArfGAP)
•Grb2
•p190 RhoGEF
•talin
•paxillin

IV. References

Abel T, Nguyen P, Barad M, Deuel T, Kandel E, Bourtchouladze R (1997) Genetic demonstration of a role for PKA in the late phase of LTP and in hippocampus-based long-term memory. Cell 88:615-626.

Ahmadian G, Ju W, Liu L, Wyszynski M, Lee S, Dunah A, Taghibiglou C, Wang Y, Lu J, Wong T, Sheng M, and Wang Y (2004) Tyrosine phosphorylation of GluR2 is required for insulin-stimulated AMPA receptor endocytosis and LTD. EMBO J 23:1040-1050.

Allen CB, Celikel T, and Feldman DE (2003) Long-term depression induced by sensory deprivation during cortical map plasticity in vivo. Nat. Neurosci. 6:291-299.

Alvarez VA and Sabatini BL (2007) Anatomical and physiological plasticity of dendritic spines. Ann. Rev. Neurosci. 30:79-97.

Avraham H, Park S, Schinkmann K, and Avraham S (2000) RAFTK/Pyk2-mediated cellular signaling. Cell Signal 12:123-133.

Banke T, Bowie D, Lee H, Huganir R, Schousboe A, and Traynelis S (2000) Control of GluR1 AMPA receptor function by cAMP-dependent protein kinase. J Neurosci 20:89-102.

Barria A, Muller D, Derkach V, Griffith L, and Soderling T (1997) Regulatory phosphorylation of AMPA-type glutamate receptors in CaM-KII during long-term potentiation. Science 276:2042-2045.

Barria A and Malinow R (2005) NMDA receptor subunit composition controls synaptic plasticity by regulating binding to CaMKII. Neuron 48:289-301.

Bartlett T, Bannister N, Collett V, Dargan S, Massey P, Bortolotto Z, Fitzjohn S, Bashir Z, Collingridge G, and Lodge D (2007) Differential roles of NR2A and NR2B-containing NMDA receptors in LTP and LTD in the CA1 region of two-week old rat hippocampus. Neuropharmacol 52:60-70.

Bartos J, Ulrich J, Li H, Beazely M, Chen Y, MacDonald J, and Hell J (2010) Postsynaptic clustering and activation of Pyk2 by PSD-95. J Neurosci 30:449-463.

Bayer K, De Koninck P, Leonard A, Hell J, and Schulman H (2001) Interaction with the NMDA receptor locks CaMKII in an active conformation. Nature 411:801-805.

Bekkers J and Stevens C (1990) Presynaptic mechanism for long-term potentiation in the hippocampus. Nature 346:724-729.

Benke T, Luthi A, Isaac J, and Collingridge G (1998) Modulation of AMPA receptor unitary conductance by synaptic activity. Nature 393:793-797.

Bhattacharyya S, Biou V, Xu W, Schluter O, and Malenka R (2009) A critical role for PSD-95/AKAP interactions in endocytosis of synaptic AMPA receptors. Nat Neurosci 12:172-181.

Bi G and Poo M (2001) Synaptic modification by correlated activity: Hebb's postulate revisited. Annu Rev Neurosci 24:139-166.

Bianchi M, De Lucchini S, Marin O, Turner D, Hanks S, and Villa-Moruzzi E (2005) Regulation of FAK Ser-722 phosphorylation and kinase activity by GSK3 and PP1 during cell spreading and migration. Biochem J 391:359-370.

Bienenstock EL, Cooper LN, and Munro PW (1982) Theory for the development of neuron selectivity: orientation specificity and binocular interaction in visual cortex. J Neurosci 2:32-48.

Bliss TV and Lømo T (1973) Long-lasting potentiation of synaptic transmission in the dentate area of the anaesthetized rabbit following stimulation of the perforant path. J Physiol (London) 232:331-356.

Blitzer R, Connor J, Brown G, Wong T, Shenolikar S, Iyengar R, and Landau E (1998) Gating of CaMKII by cAMP-regulated protein phosphatase activity during LTP. Science 280:1940-1942.

Cantley L (2002) The phosphoinositide 3-kinase pathway. Science 296:1655-1657.

Carlisle H, Manzerra P, Marcora E, and Kennedy M (2008) SynGAP regulates steady-state and activity-dependent phosphorylation of cofilin. J Neurosci 28:13673-13683.

Chen L, Chetkovich D, Petralia R, Sweeney N, Kawasaki Y, Wenthold R, Bredt D, and Nicoll R (2000) Stargazin regulates synaptic targeting of AMPA receptors by two distinct mechanisms. Nature 408:936-943.

Cheng D, Hoogenraad C, Rush J, Ramm E, Schlager M, Duong D, Xu P, Wijayawardana S, Hanfelt J, Nakagawa T, Sheng M, and Peng J (2006) Relative and absolute quantification of postsynaptic density proteome isolated from rat forebrain and cerebellum. Mol Cell Proteomics 5:1158-1170.

Cho Y, Giese K, Tanila H, Silva A, and Eichenbaum H (1998) Abnormal hippocampal spatial representations in alphaCaMKIIT286A and CREBalphaDelta- mice. Science 279:867-869.

Christopherson K, Sweeney N, Craven S, Kang R, El-Husseini A, and Bredt D (2003) Lipid- and protein-mediated multimerization of PSD-95: implications for receptor clustering and assembly of synaptic protein networks. J Cell Sci 116:3213-3219.

Chung H, Xia J, Scannevin R, Zhang X, and Huganir R (2000) Phosphorylation of the AMPA receptor subunit GluR2 differentially regulates its interaction with PDZ domain-containing proteins. J Neurosci 20:7258-7267.

Citri A and Malenka RC (2008) Synaptic plasticity: multiple forms, functions, and mechanisms. Neuropsychopharm 33:18-41.

Coba M, Valor L, Kopanitsa M, Afinowi N, and Grant S (2008) Kinase networks integrate profiles of N-methyl-D-aspartate receptor-mediated gene expression in hippocampus. J Biol Chem 283:34101-34107.

Colledge M, Dean R, Scott G, Langeberg L, Huganir R, and Scott J (2000) Targeting of PKA to glutamate receptors through a MAGUK-AKAP complex. Neuron 27:107-119.

Colledge M, Snyder E, Crozier R, Soderling J, Jin Y, Langeberg L, Lu H, Bear M, and Scott J (2003) Ubiquitination regulates PSD-95 degradation and AMPA receptor surface expression. Neuron 40:595-607.

Collingridge G, Kehl S, and McLennan H (1983) Excitatory amino acids in synaptic transmission in the Schaffer collateral-commissural pathway of the rat hippocampus. J Physiol 334:33-46.

Collingridge G, Isaac J, and Wang Y (2004) Receptor trafficking and synaptic plasticity. Nature Rev Neurosci 5:952-962.

Collins M, Husi H, Yu L, Brandon J, Anderson C, Blackstock W, Choudhary J, and Grant S (2006) Molecular characterization and comparison of the components and multiprotein complexes in the postsynaptic proteome. J Neurochem 97 Supp 1:16-23.

Craven S, El-Husseini A, and Bredt D (1999) Synaptic targeting of the postsynaptic density protein PSD-95 mediated by lipid and protein motifs. Neuron 22:497-509.

Cummings J, Mulkey R, Nicoll R, and Malenka R (1996) Ca2+ signaling requirements for long-term depression in the hippocampus. Neuron 16:825-833.
De Arce K, Varela-Nallar L, Farias O, Cifuentes A, Bull P, Couch B, Koleske A, Inestrosa N, and Alvarez A (2010) Synaptic clustering of PSD-95 is regulated by c-Abl through tyrosine phosphorylation. J Neurosci 30:3728-3738.
Derkach V, Oh M, Guire E, and Soderling T (2007) Regulatory mechanisms of AMPA receptors in synaptic plasticity. Nat Rev Neurosci 8:101-113.
Ding V, Chen R, and McCormick F (2000) Differential regulation of glycogen synthase kinase 3beta by insulin and Wnt signaling. J Biol Chem 275:32475-32481.
Doble B and Woodgett J (2003) GSK-3: tricks of the trade for a multi-tasking kinase. J Cell Sci 116:1175-1186.
Du Q, Ren X, Xie Y, Wang Q, Mei L, and Xiong W (2001) Inhibition of PYK2-induced actin cytoskeleton reorganization, PYK2 autophosphorylation and focal adhesion targeting by FAK. J Cell Sci 114:2977-2987.
Dudek SM and Bear MF (1992) Homosynaptic long-term depression in area CA1 of hippocampus and effects of N-methyl-D-aspartate receptor blockade. Proc Natl Acad Sci USA 89:4363-4367.
Ehlers M (2000) Reinsertion or degradation of AMPA receptors determined by activity-dependent endocytic sorting. Neuron 28:511-525.
Ehrlich I and Malinow R (2004) Postsynaptic density 95 controls AMPA receptor incorporation during long-term potentiation and experience-driven synaptic plasticity. J Neurosci 24:916-927.
Ehrlich I, Klein M, Rumpel S, and Malinow R (2007) PSD-95 is required for activity-driven synapse stabilization. Proc Natl Acad Sci USA 104:4176-4181.
El-Husseini A, Schnell E, Chetkovich D, Nicoll R, and Bredt D (2000) PSD-95 involvement in maturation of excitatory synapses. Science 290:1364-1368.
El-Husseini A, Schnell E, Dakoji S, Sweeney N, Zhou Q, Prange O, Gauthier-Campbell C, Aguilera-Moreno A, Nicoll R, and Bredt D (2002) Synaptic strength regulated by palmitate cycling on PSD-95. Cell 108:849-863.
Elias G, Funke L, Stein V, Grant S, Bredt D, and Nicoll R (2006) Synapse-specific and developmentally regulated targeting of AMPA receptors by a family of MAGUK scaffolding proteins. Neuron 52:307-320.
Elias G and Nicoll R (2007) Synaptic trafficking of glutamate receptors by MAGUK scaffolding proteins. Trends Cell Biol 17:343-352.
Engert F and Bonhoeffer T (1999) Dendritic spine changes associated with hippocampal long-term synaptic plasticity. Nature 399:66-70.
English J and Sweatt J (1996) Activation of p42 mitogen-activated protein kinase in hippocampal long term potentiation. J Biol Chem 271:24329-24332.
English J and Sweatt J (1997) A requirement for the mitogen-activated protein kinase cascade in hippocampal long term potentiation. J Biol Chem 272:19103-19106.
Esteban J, Shi S, Wilson C, Nuriya M, Huganir R, and Malinow R (2003) PKA phosphorylation of AMPA receptor subunits controls synaptic trafficking underlying plasticity. Nat Neurosci 6:136-143.
Farnsworth C, Freshney N, Rosen L, Ghosh A, Greenberg M, and Feig L (1995) Calcium activation of Ras mediated by neuronal exchange factor Ras-GRF. Nature 376:524-527.

Faure C, Corvol J, Toutant M, Valjent E, Hvalby O, Jensen V, Messari S, Corsi J, Kadare G, and Girault J (2007) Calcineurin is essential for depolarization-induced nuclear translocation and tyrosine phosphorylation of PYK2 in neurons. J Cell Sci 120:3034-3044.

Forde J and Dale T (2007) Glycogen synthase kinase 3: a key regulator of cellular fate. Cell Mol Life Sci 64:1930-1944.

Foster K, McLaughlin N, Edbauer D, Phillips M, Bolton A, Constantine-Paton M, and Sheng M (2010) Distinct roles of NR2A and NR2B cytoplasmic tails in long-term potentiation. J Neurosci 30:2676-2685.

Frame S and Cohen P (2001) GSK3 takes centre stage more than 20 years after its discovery. Biochem J 359:1-16.

Fukunaga K, Muller D, and Miyamoto E (1995) Increased phosphorylation of Ca2+/calmodulin-dependent protein kinase II and its endogenous substrates in the induction of long-term potentiation. J Biol Chem 270:6119-6124.

Futai K, Kim M, Hashikawa T, Scheiffele P, Sheng M, and Hayashi Y (2007) Retrograde modulation of presynaptic release probability through signaling mediated by PSD-95-neuroligin. Nat Neurosci 10:186-195.

Gardoni F, Polli F, Cattabeni F, and Di Luca M (2006) Calcium-calmodulin-dependent protein kinase II phosphorylation modulates PSD-95 binding to NMDA receptors. Eur J Neurosci 24:2694-2704.

Giese K, Fedorov N, Filipkowski R, and Silva A (1998) Autophosphorylation at Thr286 of the alpha calcium-calmodulin kinase II in LTP and learning. Science 279:870-873.

Gil-Henn H, Destaing O, Sims N, Aoki K, Alles N, Neff L, Sanjay A, Bruzzaniti A, De Camili P, Baron R, and Schlessinger J (2007) Defective microtubule-dependent podosome organization in osteoclasts lead to increased bone density in Pyk2 (-/-) mice. J Cell Biol 178:1053-1064.

Girault J, Costa A, Derkinderen P, Studler J, and Toutant M (1999) FAK and PYK2/CAKbeta in the nervous system: a link between neuronal activity, plasticity, and survival? Trends Neurosci 22:257-263.

Grant S, O'Dell T, Karl K, Stein P, Soriano P, and Kandel E (1992) Impaired long-term potentiation, spatial learning, and hippocampal development in Fyn mutant mice. Science 258:1903-1910.

Grosshans D, Clayton D, Coultrap S, and Browning M (2001) LTP leads to rapid surface expression of NMDA but not AMPA receptors in adult rat CA1. Nat Neurosci 5:27-33.

Grutzendler J, Kasthuri N, and Gan W-B (2002) Long-term dendritic spine stability in the adult cortex. Nature 420:812-816.

Hardingham G, Fukunaga Y, and Bading H (2002) Extrasynaptic NMDARs oppose synaptic NMDARs by triggering CREB shut-off and cell death pathways. Nat Neurosci 5:405-414.

Harris F, Ganong A, and Cotman C (1984) Long-term potentiation in the hippocampus involves activation of N-methyl-D-aspartate receptors. Brain Res 323:132-137.

Hashido M, Hayashi K, Hirose K, and Iino M (2006) Ca2+ lightning conveys cell-cell contact information inside cells. EMBO Reports 7:1117-1123.

Hayashi T and Huganir R (2004) Tyrosine phosphorylation and regulation of the AMPA receptor by SRC family tyrosine kinases. J Neurosci 24:6152-6160.

Hebb DO (1949) The organization of behavior: a neuropsychological theory. New York: John Wiley.

Heynen AJ, Yoon BJ, Liu CH, Chung HJ, Huganir RL, and Bear MF (2003) Molecular mechanism for loss of visual cortical responsiveness following brief monocular deprivation. Nat. Neurosci. 6:854-862.

Hofer S, Mrsic-Flogel T, Bonhoeffer T and Hubener M (2009) Experience leaves a lasting structural trace in cortical circuits. Nature 457:313-317.

Holtmaat A, Trachtenberg J, Wilbrecht L, Shepherd G, Zhang X, et al. (2005) Transient and persistent dendritic spines in the neocortex in vivo. Neuron 45:279-291.

Holtmaat A, Wilbrecht L, Knott G, Welker E, and Svoboda L (2006) Experience-dependent and cell-type-specific spine growth in the neocortex. Nature 441:979-983.

Holtmaat A and Svoboda K (2009) Experience-dependent structural synaptic plasticity in the mammalian brain. Nat. Rev. Neurosci. 10:647-658.

Hsieh H, Boehm J, Sato C, Iwatsubo T, Tomita T, Sisodia S, and Malinow, R (2006) AMPAR removal underlies Abeta-induced synaptic depression and dendritic spine loss. Neuron 52:831-843.

Hsueh Y, Kim E, and Sheng M (1997) Disulfide-linked head-to-head multimerization in the mechanism of ion channel clustering by PSD-95. Neuron 18:803-814.

Huang Y, Lu W, Ali D, Pelkey K, Pitcher G, Lu Y, Aoto H, Roder J, Sasaki T, Salter M, and MacDonald J (2001) CAKbeta/Pyk2 kinase is a signaling link for induction of long-term potentiation in CA1 hippocampus. Neuron 29:485-496.

Hung A, Futai K, Sala C, Valtschanoff J, Ryu J, Woodworth M, Kidd F, Sung C, Miyakawa T, Bear M, Weinberg R, and Sheng M (2008) Smaller dendritic spines, weaker synaptic transmission, but enhanced spatial learning in mice lacking Shank1. J Neurosci 28:1697-1708.

Ilic D, Furuta Y, Kanazawa S, Takeda N, Sobue K, Nakatsuji N, Nomura S, Fujimoto J, Okada M, and Yamamoto T (1995) Reduced cell motility and enhanced focal adhesion contact formation in cells from FAK-deficient mice. Nature 377:539-544.

Impey S, Mark M, Villacres E, Poser S, Chavkin C, and Storm D (1996) Induction of CRE-mediated gene expression by stimuli that generate long-lasting LTP in area CA1 of the hippocampus. Neuron 16:973-982.

Isaac J, Nicoll R, and Malenka R (1995) Evidence for silent synapses: implications for the expression of LTP. Neuron 15:427-434.

Isaac J, Hjelmstad G, Nicoll R, and Malenka R (1996) Long-term potentiation at single fiber inputs to hippocampal CA1 pyramidal cells. Proc Natl Acad Sci USA 93:8710-8715.

Jia Z, Agopyan N, Miu P, Xiong Z, Henderson J, Gerlai R, Taverna F, Velumian A, MacDonald J, Carlen P, Abramow-Newerly W, and Roder J (1996) Enhanced LTP in mice deficient in the AMPA receptor GluR2. Neuron 17:945-956.

Jope R and Johnson G (2004) The glamour and gloom of glycogen synthase kinase -3. Trends Biochem Sci 29:95-102.

Jope R and Roh M (2006) Glycogen synthase kinase-3 (GSK3) in psychiatric diseases and therapeutic interventions. Curr Drug Targets 7:1421-1434.

Kalia L, Gingrich J, and Salter M (2004) Src in synaptic transmission and plasticity. Oncogene 23:8007-8016.

Kamenetz F, Tomita T, Hsieh H, Seabrook G, Borchelt D, Iwatsubo T, Sisodia S, and Malinow R (2003) APP processing and synaptic function. Neuron 37:925-937.

Kameyama K, Lee H, Bear M, and Huganir R (1998) Involvement of a postsynaptic protein kinase A substrate in the expression of homosynaptic long-term depression. Neuron 21:1163-1175.
Kandel ER, Kupfermann I, Iversen S (2000) Learning and memory. In: Principles of neural science (Kandel ER, Schwartz JH, Jessell TM, ed), pp1227-1246. New York: McGraw-Hill.
Kasai H, Matsuzaki M, Noguchi J, Yasumatsu N, and Nakahara H (2003) Structure-stability-function relationships of dendritic spines. Trends Neurosci. 26:360-368.
Kauer J, Malenka R, and Nicoll R (1988) A persistent postsynaptic modification mediates long-term potentiation in the hippocampus. Neuron 1:911-917.
Kaytor M and Orr H (2002) The GSK3beta signaling cascade and neurodegenerative disease. Curr Opin Neurobiol 12:275-278.
Keith D and El-Husseini A (2008) Excitation control: balancing PSD-95 function at the synapse. Front Mol Neurosci 1:1-12.
Kessels H and Malinow R (2009) Synaptic AMPA receptor plasticity and behavior. Neuron 61:340-350.
Kohno T, Matsuda E, Sasaki H, and Sasaki T (2008) Protein-tyrosine kinase CAKbeta/PYK2 is activated by binding Ca2+/calmodulin to FERM F2 alpha2 helix and thus forming its dimer. Biochem J 410:513-523.
Kim C, Chung H, Lee H, and Huganir R (2001) Interaction of the AMPA receptor subunit GluR2/3 with PDZ domains regulates hippocampal long-term depression. Proc Natl Acad Sci USA 98:11725-11730.
Kim E and Sheng M (2004) PDZ domain proteins of synapses. Nat Rev Neurosci 5:771-781.
Kim J, Lee H, Takamiya K, and Huganir R (2003) The role of synaptic GTPase-activating protein in neuronal development and synaptic plasticity. J Neurosci 23:1119-1124.
Kim M, Dunah A, Wang Y, and Sheng M (2005) Differential roles of NR2A- and NR2B-containing NMDA receptors in Ras-ERK signaling and AMPA receptor trafficking. Neuron 46:745-760.
Kim M, Futai K, Jo J, Hayashi Y, Cho K, and Sheng M (2007) Synaptic accumulation of PSD-95 and synaptic function regulated by phosphorylation of serine-295 of PSD-95. Neuron 56:488-502.
Kockeritz L, Doble B, Patel S, and Woodgett J (2006) Glycogen synthase kinase-3 – an overview of an over-achieving protein kinase. Curr Drug Targets 7:1377-1388.
Kopec C, Li B, Boehm J, and Malinow R (2006) Glutamate receptor exocytosis and spine enlargement during chemically induced long-term potentiation. J Neurosci 26:2000-2009.
Kopec C, Real E, Kessels H, and Malinow R (2007) GluR1 links structural and functional plasticity at excitatory synapses. J Neurosci 27:13706-13718.
Kornau H, Schenker L, Kennedy M, and Seeburg P (1995) Domain interaction between NMDA receptor subunits and the postsynaptic density protein PSD-95. Science 269:1737-1740.
Krapivinsky G, Krapivinsky L, Manasian Y, Ivanov A, Tyzio R, Pellegrino C, Ben-Ari Y, Clapham D, and Medina I (2003) The NMDA receptor is coupled to the ERK pathway by a direct interaction between NR2B and RasGRF1. Neuron 40:775-784.
Lau C and Zukin R (2007) NMDA receptor trafficking in synaptic plasticity and neuropsychiatric disorders. Nat Rev Neurosci 8:413-425.
Lawlor M and Alessi D (2001) PKB/Akt: a key mediator of cell proliferation, survival, and insulin responses? J Cell Sci 114:2903-2910.

Lee H, Kameyama K, Huganir R, and Bear M (1998) NMDA induces long-term synaptic depression and dephosphorylation of the GluR1 subunit of AMPA receptors in hippocampus. Neuron 21:1151-1162.

Lee H, Barbarosie M, Kameyama K, Bear M, and Huganir R (2000) Regulation of distinct AMPA receptor phosphorylation sites during bidirectional synaptic plasticity. Nature 405:955-959.

Lee H, Takamiya K, Han J, Man H, Kim C, Rumbaugh G, Yu S, Ding L, He C, Petralia R, Wenthold R, Gallagher M, and Huganir R (2003) Phosphorylation of the AMPA receptor GluR1 subunit is required for synaptic plasticity and retention of spatial memory. Cell 112:631-643.

Lee H, Takamiya K, He K, Song L, and Huganir R (2010) Specific roles of AMPA receptor subunit GluR1 (GluA1) phosphorylation sites in regulating synaptic plasticity in the CA1 region of hippocampus. J Neurophysiol 103:479-489.

Lee S, Liu L, Wang Y, and Sheng M (2002) Clathrin adaptor AP2 and NSF interact with overlapping sites of GluR2 and play distinct roles in AMPA receptor trafficking and hippocampal LTD. Neuron 36:661-674.

Lee S, Simonetta A, and Sheng M (2004) Subunit rules governing the sorting of internalized AMPA receptors in hippocampal neurons. Neuron 43:221-236.

Lee S, Escobedo-Lozoya Y, Szatmari E, and Yasuda R (2009) Activation of CaMKII in single dendritic spines during long-term potentiation. Nature 458:299-304.

Lev S, Moreno H, Martinez R, Canoll P, Peles E, Musachhio J, Plowman G, Rudy B, and Schlessinger J (1995) Protein tyrosine kinase PYK2 involved in Ca2+-induced regulation of ion channel and MAP kinase functions. Nature 376:737-745.

Li S, Tian X, Hartley D, and Feig L (2006) Distinct roles for Ras-guanine nucleotide-releasing factor 1 (Ras-GRF1) and Ras-GRF2 in the induction of long-term potentiation and long-term depression. J Neurosci 26:1721-1729.

Li S, Hong S, Shepardson N, Walsh D, Shankar G, and Selkoe D (2009) Soluble oligomers of amyloid beta protein facilitate hippocampal long-term depression by disrupting neuronal glutamate uptake. Neuron 62:788-801.

Liao D, Hessler N, and Malinow R (1995) Activation of postsynaptically silent synapses during pairing-induced LTP in CA1 region of hippocampal slice. Nature 375:400-404.

Lim Y, Lim S, Tomar A, Gardel M, Bernard-Trifilo J, Chen X, Uryu S, Canete-Soler R, Zhai J, Lin J, Schlaepfer W, Nalbant P, Bokock G, Ilic D, Waterman-Storer C, and Schlaepfer D (2008) Pyk2 and FAK connections to p190Rho guanine nucleotide exchange factor regulate RhoA activity, focal adhesion formation, and cell motility. J Cell Biol 180:187-203.

Lisman J (1989) A mechanism for the Hebb and the anti-Hebb processes underlying learning and memory. Proc Natl Acad Sci USA 86:9574-9578.

Lisman J, Schulman H, and Cline H (2002) The molecular basis of CaMKII function in synaptic and behavioural memory. Nat Rev Neurosci 3:175-190.

Liu L, Wong T, Pozza M, Lingenhoehl K, Wang Y, Sheng M, Auberson Y, and Wang Y (2004) Role of NMDA receptor subtypes in governing the direction of hippocampal synaptic plasticity. Science 304:1021-1024.

Lledo P, Hjelmstad G, Mukherji S, Soderling T, Malenka R, and Nicoll R (1995) Calcium/calmodulin-dependent kinase II and long-term potentiation enhance synaptic transmission by the same mechanism. Proc Natl Acad Sci USA 92:11175-11179.

Lu W, Man H, Ju W, Trimble W, MacDonald J, and Wang Y (2001) Activation of synaptic NMDA receptors induces membrane insertion of new AMPA receptors and LTP in cultured hippocampal neurons. Neuron 29:243-254.

Lu W, Shi Y, Jackson A, Bjorgan K, During M, Sprengel R, Seeburg P, and Nicoll R (2009) Subunit composition of synaptic AMPA receptors revealed by a single-cell genetic approach. Neuron 62:254-268.

Lu Y, Roder J, Davidow J, and Salter M (1998) Src activation in the induction of long-term potentiation in CA1 hippocampal neurons. Science 279:1363-1367.

Lu Y, Allen M, Halt A, Weisenhaus M, Dallapiazza R, Hall D, Usachev Y, McKnight G, and Hell J (2007) Age-dependent requirement of AKAP150-anchored PKA and GluR2-lacking AMPA receptors in LTP. EMBO J 26:4879-4890.

Lu Y, Zhang M, Lim I, Hall D, Allen M, Medvedeva Y, McKnight G, Usachev Y, and Hell J (2008) AKAP150-anchored PKA activity is important for LTD during its induction phase. J Physiol 586:4155-4164.

Lucas J, Hernandez F, Gomez-Ramos P, Morgan M, Hen R, and Avila J (2001) Decreased nuclear beta-catenin, tau hyperphosphorylation and neurodegeneration in GSK-3beta conditional transgenic mice. EMBO J 20:27-39.

MacDonald B, Tamai K, and He X (2009) Wnt/beta-catenin signaling: components, mechanisms, and diseases. Dev Cell 17:9-26.

Majewska A and Sur M (2003) Motility of dendritic spines in visual cortex in vivo: changes during the critical period and effects of visual deprivation. Proc Natl Acad Sci USA 100:16024-16029.

Makhinson M, Chotiner J, Watson J, and O'Dell T (1999) Adenylyl cyclase activation modulates activity-dependent changes in synaptic strength and Ca2+/calmodulin-dependent kinase II autophosphorylation. J Neurosci 19:2500-2510.

Malenka R, Kauer J, Perkel D, Mauk M, Kelly P, Nicoll R, and Waxham M (1989) An essential role for postsynaptic calmodulin and protein kinase activity in long-term potentiation. Nature 340:554-557.

Malenka RC (1991) Postsynaptic factors control the duration of synaptic enhancement in area CA1 of the hippocampus. Neuron 6:53-60.

Malenka R, Lancaster B, and Zucker R (1992) Temporal limits on the rise in postsynaptic calcium required for the induction of long-term potentiation. Neuron 9:121-128.

Malenka RC and Bear MF (2004) LTP and LTD: an embarrassment of riches. Neuron 44:5-21.

Maletic-Savatic M, Malinow R, and Svoboda K (1999) Rapid dendritic morphogenesis in CA1 hippocampal dendrites induced by synaptic activity. Science 283:1923-1927.

Malinow R, Schulman H, and Tsien R (1989) Inhibition of postsynaptic PKC or CaMKII blocks induction but not expression of LTP. Science 245:862-866.

Malinow R and Tsien R (1990) Presynaptic enhancement shown by whole-cell recordings of long-term potentiation in hippocampal slices. Nature 346:177-180.

Mammen A, Kameyama K, Roche K, and Huganir R (1997) Phosphorylation of the alpha-amino-3-hydroxy-5-methylisoxazole-4-proprionic acid receptor GluR1 subunit by calcium/calmodulin-dependent kinase II. J Biol Chem 272:32528-32533.

Man H, Lin J, Ju W, Ahmadian G, Liu L, Becker L, Sheng M, and Wang Y (2000) Regulation of AMPA receptor-mediated synaptic transmission by clathrin-dependent receptor internalization. Neuron 25:649-662.

Man H, Wang Q, Lu W, Ju W, Ahmadian G, Liu L, D'Souza S, Wong T, Taghibiglou C, Lu J, Becker L, Pei L, Liu F, Wymann M, MacDonald J, and Wang Y (2003) Activation of PI3-kinase is required for AMPA receptor insertion during LTP of mEPSCs in cultured hippocampal neurons. Neuron 38:611-624.

Manabe T, Wyllie D, Perkel D, and Nicoll R (1993) Modulation of synaptic transmission and long-term potentiation: effects on paired pulse facilitation and EPSC variance in the CA1 region of the hippocampus. J Neurophysiol 70:1451-1459.

Manabe T and Nicoll R (1994) Long-term potentiation: evidence against an increase in transmitter release probability in the CA1 region of the hippocampus. Science 265:1888-1892.

Mansour M, Nagarajan N, Nehring R, Clements J, and Rosenmund C (2001) Heteromeric AMPA receptors assemble with a preferred subunit stoichiometry and spatial arrangement. Neuron 32:841-853.

Mao Y, Ge X, Frank C, Madison J, Koehler A, Doud M, Tassa C, Berry E, Soda T, Singh K, Biechele T, Petryshen T, Moon R, Haggarty S, and Tsai L (2009) Disrupted in schizophrenia 1 regulates neuronal progenitor proliferation via modulation of GSK3beta/beta-catenin signaling. Cell 136:1017-1031.

Maren S, Tocco G, Standley S, Baudry M, and Thompson R (1993) Postsynaptic factors in the expression of long-term potentiation (LTP): increased glutamate receptor binding following LTP induction in vivo. Proc Natl Acad Sci USA 90:9654-9658.

Marshall C (1995) Specificity of receptor tyrosine kinase signaling: transient versus sustained extracellular signal-regulated kinase activation. Cell 80:179-185.

Massey P, Johnson B, Moult P, Auberson Y, Brown M, Molnar E, Collingridge G, and Bashir Z (2004) Differential roles of NR2A and NR2B-containing NMDA receptors in cortical long-term potentiation and long-term depression. J Neurosci 24:7821-7828.

Masuko N, Makino K, Kuwahara H, Fukunaga K, Sudo T, Araki N, Yamamoto H, Yamada Y, Miyamoto E, and Saya H (1999) Interaction of NE-dlg/SAP102, a neuronal and endocrine tissue-specific membrane-associated guanylate kinase protein, with calmodulin and PSD-95/SAP90: a possible regulatory role in molecular clustering at synaptic sites. J Biol Chem 274:5782-5790.

Matsuzaki M, Ellis-Davies G, Nemoto T, Miyashita Y, Iino M, and Kasai H (2001) Dendritic spine geometry is critical for AMPA receptor expression in hippocampal CA1 pyramidal neurons. Nat Neurosci 4:1086-1092.

Matsuzaki M, Honkura N, Ellis-Davies G, and Kasai H (2004) Structural basis of long-term potentiation in single dendritic spines. Nature 429:761-766.

Mayer M, Westbrook G, and Guthrie P (1984) Voltage-dependent block by Mg2+ of NMDA responses in spinal cord neurons. Nature 309:261-263.

McGee A and Bredt D (1999) Identification of an intramolecular interaction between the SH3 and guanylate kinase domains of PSD-95. J Biol Chem 274:17431-17436.

McGee A, Dakoji S, Olsen O, Bredt D, Lim W, and Prehoda K (2001) Structure of the SH3-guanylate kinase module from PSD-95 suggests a mechanism for regulated assembly of MAGUK scaffolding proteins. Mol Cell 8:1291-1301.

McHugh T, Blum K, Tsien J, Tonegawa S, and Wilson M (1996) Impaired hippocampal representation of space in CA1-specific NMDAR1 knockout mice. Cell 87:1339-1349.

McKernan MG and Shinnick-Gallagher P (1997) Fear conditioning induces a lasting potentiation of synaptic currents in vitro. Nature 390:607-611.

McManus E, Sakamoto K, Armit L, Ronaldson L, Shpiro N, Marquez R, and Alessi D (2005) Role that phosphorylation of GSK3 plays in insulin and Wnt signaling defined by knockin analysis. EMBO J 24:1571-1583.

Menegon A, Burgaya F, Baudot P, Dunlap D, Girault J, and Valtorta F (1999) FAK+ and PYK2/CAKbeta, two related tyrosine kinases highly expressed in the central nervous system: similarities and differences in the expression pattern. Eur J Neurosci 11:3777-3788.

Meng Y, Zhang Y, and Jia Z (2003) Synaptic transmission and plasticity in the absence of AMPA glutamate receptor GluR2 and GluR3. Neuron 39:163-176.

Migaud M, Charlesworth P, Dempster M, Webster L, Watabe A, Makhinson M, He Y, Ramsay M, Morris R, Morrison J, O'Dell T, and Grant S (1998) Enhanced long-term potentiation and impaired learning in mice with mutant postsynaptic density-95 protein. Nature 396:433-439.

Miller S and Kennedy M (1986) Regulation of brain type II Ca2+/calmodulin-dependent protein kinase by autophosphorylation: a Ca2+-triggered molecular switch. Cell 44:861-870.

Mitra S, Hanson D, and Schlaepfer D (2005) Focal adhesion kinase: in command and control of cell motility. Nat Rev Mol Cell Biol 6:56-68.

Miyakawa T, Leiter L, Gerber D, Gainetdinov R, Sotnikova T, Zeng H, Caron M, and Tonegawa S (2003) Conditional calcineurin knockout mice exhibit multiple abnormal behaviors related to schizophrenia. Proc Natl Acad Sci USA 100:8987-8992.

Montgomery J, Pavlidis P, and Madison D (2001) Pair recordings reveal all-silent synaptic connections and the postsynaptic expression of long-term potentiation. Neuron 29:691-701.

Morabito M, Sheng M, and Tsai L (2004) Cyclin-dependent kinase 5 phosphorylates the N-terminal domain of the postsynaptic density protein PSD-95 in neurons. J Neurosci 24:865-876.

Morishita W, Connor J, Xia H, Quinlan E, Shenolikar S, and Malenka R (2001) Regulation of synaptic strength by protein phosphatase 1. Neuron 32:1133-1148.

Morishita W, Lu W, Smith G, Nicoll R, Bear M, and Malenka R (2007) Activation of NR2B-containing NMDA receptors is not required for NMDA receptor-dependent long-term depression. Neuropharmacol 52:71-76.

Morris R, Anderson E, Lynch G, and Baudry M (1986) Selective impairment of learning and blockade of long-term potentiation by an N-methyl-D-aspartate receptor antagonist, AP5. Nature 319:774-776.

Mulkey R and Malenka R (1992) Mechanisms underlying induction of homosynaptic long-term depression in area CA1 of the hippocampus. Neuron 9:967-975.

Mulkey R, Herron C, and Malenka R (1993) An essential role for protein phosphatases in hippocampal long-term depression. Science 261:1051-1055.

Mulkey R, Endo S, Shenolikar S, and Malenka R (1994) Involvement of a calcineurin/inhibitor-1 phosphatase cascade in hippocampal long-term depression. Nature 369:486-488.

Muller D, Joly M, and Lynch G (1988) Contributions of quisqualate and NMDA receptors to the induction and expression of LTP. Science 242:1694-1697.

Musleh W, Bi X, Tocco G, Yaghoubi S, and Baudry M (1997) Glycine-induced long-term potentiation is associated with structural and functional modifications of alpha-amino-3-hydroxyl-5-methyl-4-isoxazolepropionic acid receptors. Proc Natl Acad Sci USA 94:9451-9456.

Naisbitt S, Kim E, Weinberg R, Rao A, Yang F, Craig A, and Sheng M (1997) Characterization of guanylate kinase-associated protein, a postsynaptic density protein at excitatory synapses that interacts directly with postsynaptic density-95/synapse-associated protein 90. J Neurosci 17:5687-5696.

Nakashiba T, Young JZ, McHugh TJ, Buhl DL, and Tonegawa S (2008) Transgenic inhibition of synaptic transmission reveals role of CA3 output in hippocampal learning. Science 319:1260-1264.

Nakazawa K, McHugh TJ, Wilson MA, and Tonegawa S (2004) NMDA receptors, places cells and hippocampal spatial memory. Nat Rev Neurosci 5:361-372.

Nicholls R, Alarcon J, Malleret G, Carroll R, Grody M, Vronskaya S, and Kandel E (2008) Transgenic mice lacking NMDAR-dependent LTD exhibit deficits in behavioral flexibility. Neuron 58:104-117.

Nicoll R (2003) Expression mechanisms underlying long-term potentiation: a postsynaptic view. Phil Trans R Soc Lond B 358:721-726.

Nicoll R and Malenka R (1993) NMDA-receptor-dependent synaptic plasticity: multiple forms and mechanisms. Trends Neurosci 16:521-527.

Nicoll R, Tomita S, and Bredt S (2006) Auxiliary subunits assist AMPA-type glutamate receptors. Science 311:1253-1256.

Nishiyama M, Hong K, Mikoshiba K, Poo M, Kato K (2000) Calcium stores regulate the polarity and input specificity of synaptic modification. Nature 408:584-588.

Noguchi J, Matsuzaki M, Ellis-Davies G, and Kasai H (2005) Spine-neck geometry determines NMDA receptor-dependent Ca2+ signaling in dendrites. Neuron 46:609-622.

Nowak L, Bregestovski P, Ascher P, Herbet A, and Prochiantz A (1984) Magnesium gates glutamate-activated channels in mouse central neurons. Nature 307:462-465.

O'Brien W, Harper A, Jove F, Woodgett J, Maretto S, Piccolo S, and Klein P (2004) Glycogen synthase kinase-3beta haploinsufficiency mimics the behavioral and molecular effects of lithium. J Neurosci 24:6791-6798.

Oh J, Manzerra P, and Kennedy M (2004) Regulation of the neuron-specific Ras GTPase-activating protein, SynGAP, by Ca2+/calmodulin-dependent protein kinase II. J Biol Chem 279:17980-17988.

Okamoto K, Narayanan R, Lee S, Murata K, and Hayashi Y (2007) The role of CaMKII as an F-actin-bundling protein crucial for maintenance of dendritic spine structure. Proc Natl Acad Sci USA 104:6418-6423.

O'Keefe J and Dostrovsky J (1971) The hippocampus as a spatial map: preliminary evidence from unit activity in the freely-moving rat. Brain Res 34:171-175.

Okigaki M, Davis C, Falasca M, Harroch S, Felsenfeld D, Sheetz M, and Schlessinger J (2003) Pyk2 regulates multiple signaling events crucial for macrophage morphology and migration. Proc Natl Acad Sci USA 100:10740-10745.

Okuda T, Yu L, Cingolani L, Kemler R, and Goda Y (2007) Beta-catenin regulates excitatory postsynaptic strength at hippocampal synapses. Proc Natl Acad Sci USA 104:13479-13484.

Oliet S, Malenka R, and Nicoll R (1996) Bidirectional control of quantal size by synaptic activity in the hippocampus. Science 271:1294-1297.

Otmakhov N, Khibnik L, Otmakhovaa N, Carpenter S, Riahi S, Asrican B, and Lisman J (2004) Forskolin-induced LTP in the CA1 hippocampal region is NMDA receptor dependent. J Neurophysiol 91:1955-1962.

Otmakhova N, Otmakhov N, Mortenson L, and Lisman J (2000) Inhibition of the cAMP pathway decreases early long-term potentiation at CA1 hippocampal synapses. J Neurosci 20:4446-4451.

Okamoto K, Nagai T, Miyawaki A, and Hayashi Y (2004) Rapid and persistent modulation of actin dynamics regulates postsynaptic reorganization underlying bidirectional plasticity. Nat Neurosci 7:1103-1112.

Pak D and Sheng M (2003) Targeted protein degradation and synapse remodeling by an inducible protein kinase. Science 302:1368-1373.

Park S, Avraham H, and Avraham S (2004) RAFTK/Pyk2 activation is mediated by trans-acting autophosphorylation in a Src-dependent manner. J Biol Chem 279:33315-33322.

Passafaro M, Piech V, and Sheng M (2001) Subunit-specific temporal and spatial patterns of AMPA receptor endocytosis in hippocampal neurons. Nat Neurosci 4:917-926.

Passafaro M, Nakagawa T, Sala C, and Sheng M (2003) Induction of dendritic spines by an extracellular domain of AMPA receptor subunit GluR2. Nature 424:677-681.

Pastalkova E, Serrano P, Pinkhasova D, Wallace E, Fenton A, and Sacktor T (2006) Storage of spatial information by the maintenance mechanism of LTP. Science 313:1141-1144.

Peineau S, Taghibiglou C, Bradley C, Wong TP, Liu L, Lu J, Lo E, Wu D, Saule E, Bouschet T, Matthews P, Isaac JT, Bortolotto ZA, Wang YT, and Collingridge GL (2007) LTP inhibits LTD in the hippocampus via regulation of GSK3beta. Neuron 53:703-717.

Peineau S, Nicolas C, Bortolotto Z, Bhat R, Ryves W, Harwood A, Dournaud P, Fitzjohn S, and Collingridge G (2009) A systematic investigation of the protein kinases involved in NMDA receptor-dependent LTD: evidence for a role of GSK-3 but not other serine/threonine kinases. Mol Brain 2:22-32.

Peng Y, He S, Marie H, Zeng S, Ma J, Tan Z, Lee S, Malenka R, and Yu X (2009) Coordinated changes in dendritic arborization and synaptic strength during neural circuit development. Neuron 61:71-84.

Pettit D, Perlman S, and Malinow R (1994) Potentiated transmission and prevention of further LTP by increased CaMKII activity in postsynaptic hippocampal slice neurons. Science 266:1881-1885.

Prybylowski K, Chang K, Sans N, Kan L, Vicini S, and Wenthold R (2005) The synaptic localization of NR2B-containing NMDA receptors is controlled by interactions with PDZ proteins and AP-2. Neurons 47:845-857.

Qin Y, Zhu Y, Baumgart J, Stornetta R, Seidenman K, Mack V, Van Aelst L, and Zhu J (2005) State-dependent Ras signaling and AMPA receptor trafficking. Genes Dev 19:2000-2015.

Regehr W and Tank D (1990) Postsynaptic NMDA receptor-mediated calcium accumulation in hippocampal CA1 pyramidal cell dendrites. Nature 345:807-810.

Rico B, Beggs H, Schahin-Reed D, Kimes N, Schmidt A, and Reichardt L (2004) Control of axonal branching and synapse formation by focal adhesion kinase. Nat Neurosci 7:1059-1069.

Rogan MT, Staubli UV, LeDoux JE (1997) Fear conditioning induces associative long-term potentiation in the amygdala. Nature 390:604-607.

Romorini S, Piccoli G, Jiang M, Grossano P, Tonna N, Passafaro M, Zhang M, and Sala C (2004) A functional role of postsynaptic density-95-guanylate kinase-associated protein complex in regulating Shank assembly and stability to synapses. J Neurosci 24:9391-9404.

Rouach N, Byrd K, Petralia R, Elias G, Adesnik H, Tomita S, Karimzadegan S, Kealey C, Bredt D, and Nicoll R (2005) TARP gamma-8 controls hippocampal AMPA receptor number, distribution and synaptic plasticity. Nat Neurosci 8:1525-1533.

Rumbaugh G, Adams J, Kim J, and Huganir R (2006) SynGAP regulates synaptic strength and mitogen-activated protein kinases in cultured neurons. Proc Natl Acad Sci USA 103:4344-4351.

Saglietti L, Dequidt C, Kamieniarz K, Rousset M, Valnegri P, Thoumine O, Beretta F, Fagni L, Choquet D, Sala C, Sheng M, and Passafaro M (2007) Extracellular interactions between GluR2 and N-cadherin in spine regulation. Neuron 54:461-477.

Schluter O, Xu W, and Malenka R (2006) Alternative N-terminal domains of PSD-95 and SAP97 govern activity-dependent regulation of synaptic AMPA receptor function. Neuron 51:99-111.

Schnell E, Sizemore M, Karimzadegan S, Chen L, Bredt D, and Nicoll R (2002) Direct interactions between PSD-95 and Stargazin control synaptic AMPA receptor number. Proc Natl Acad Sci USA 99:13902-13907.

Seabold G, Burette A, Lim I, Weinberg R, and Hell J (2003) Interaction of the tyrosine kinase Pyk2 with the N-methyl-D-aspartate receptor complex via the Src homology 3 domains of PSD-95 and SAP102. J Biol Chem 278:15040-15048.

Seeburg D, Feliu-Mojer M, Gaiottino J, Pak D, and Sheng M (2008) Critical role of CDK5 and Polo-like kinase 2 in homeostatic synaptic plasticity during elevated activity. Neuron 58:571-583.

Seidenman K, Steinberg J, Huganir R, and Malinow R (2003) Glutamate receptor subunit 2 serine 880 phosphorylation modulates synaptic transmission and mediates plasticity in CA1 pyramidal cells. J Neuorsci 23:9220-9228.

Selkoe DJ (2002) Alzheimer's disease is a synaptic failure. Science 298:789-791.

Selig D, Hjelmstad G, Herron C, Nicoll R, and Malenka R (1995) Independent mechanisms for long-term depression of AMPA and NMDA responses. Neuron 15:417-426.

Shankar GM, Li S, Mehta TH, Garcia-Munoz A, Shepardson NE, Smith I, Brett FM, Farrell MA, Rowan MJ, Lemere CA, Regan CM, Walsh DM, Sabatini BL, and Selkoe DJ (2008) Amyloid-beta protein dimers isolated directly from Alzheimer's brains impair synaptic plasticity and memory. Nat. Med. 14:837-842.

Shen K and Meyer T (1999) Dynamic control of CaMKII translocation and localization in hippocampal neurons by NMDA receptor stimulation. Science 284:162-166.

Sheng M and Kim M (2002) Postsynaptic signaling and plasticity mechanisms. Science 298:776-780.

Sheng M and Hoogenraad CC (2007) The postsynaptic architecture of excitatory synapses: a more quantitative view. Ann. Rev. Biochem. 76:823-847.

Shepherd J and Huganir R (2007) The cell biology of synaptic plasticity: AMPA receptor trafficking. Ann Rev Cell Dev Biol 23:613-643.

Shi S, Hayashi Y, Esteban J, and Malinow R (2001) Subunit-specific rules governing AMPA receptor trafficking to synapses in hippocampal pyramidal neurons. Cell 105:331-343.

Shi Y, Pontrello C, DeFea K, Reichardt L, and Ethell I (2009) Focal adhesion kinase acts downstream of EphB receptors to maintain mature dendritic spines by regulating cofilin activity. J Neurosci 29:8129-8142.

Shin H, Hsueh Y, Yang F, Kim E, and Sheng M (2000) An intramolecular interaction between Src homology 3 domain and guanylate kinase-like domain required for channel clustering by postsynaptic density-9/SAP90. J Neurosci 20:3580-3587.

Sieg D, Hauck C, and Schlaepfer D (1999) Required role of focal adhesion kinase (FAK) for integrin-stimulated cell migration. J Cell Sci 112:2677-2691.

Silva A, Paylor R, Wehner J, and Tonegawa S (1992) Impaired spatial learning in alpha-calcium-calmodulin kinase II mutant mice. Science 257:206-211.

Songyang Z, Lu K, Kwon Y, Tsai L, Filhol O, Cochet C, Brickey D, Soderling T, Bartleson C, Graves D, DeMaggio A, Hoekstra M, Blenis J, Hunter T, and Cantley L (1996) A structural basis for substrate specificities of protein Ser/Thr kinases: primary sequence preference of casein kinases I and II, NIMA, phosphorylase kinase, calmodulin-dependent kinase II, CDK5, and Erk1. Mol Cell Biol 16:6486-6493.

Stein V, House D, Bredt D, and Nicoll R (2003) Postsynaptic density-95 mimics and occludes hippocampal long-term potentiation and enhances long-term depression. J Neurosci 23:5503-5506.

Steiner P, Higley M, Xu W, Czervionke B, Malenka R, and Sabatini B (2008) Destabilization of the postsynaptic density by PSD-95 serine 73 phosphorylation inhibits spine growth and synaptic plasticity. Neuron 60:788-802.

Stocca G and Vicini S (1998) Increased contribution of NR2A subunit to synaptic NMDA receptors in developing rat cortical neurons. J Physiol 507:13-24.

Sturgill J, Steiner P, Czervionke B, and Sabatini B (2009) Distinct domains within PSD-95 mediate synaptic incorporation, stabilization, and activity-dependent trafficking. J Neurosci 29:12845-12854.

Tada T and Sheng M (2006) Molecular mechanisms of dendritic spine morphogenesis. Curr Opin Neurobiol 16:95-101.

Tai C, Mysore S, Chiu C, and Schuman E (2007) Activity-regulated N-cadherin endocytosis. Neuron 54:771-785.

Takahashi T, Svoboda K, and Malinow R (2003) Experience strengthening transmission by driving AMPA receptors into synapses. Science 299:1585-1588.

Tavalin S, Colledge M, Hell J, Langeberg L, Huganir R, and Scott J (2002) Regulation of GluR1 by the A-kinase anchoring protein 79 (AKAP79) signaling complex shares properties with long-term depression. J Neurosci 22:3044-3051.

Thiels E, Kanterewicz B, Norman E, Trzaskos J, and Klann E (2002) Long-term depression in the adult hippocampus in vivo involves activation of extracellular signal-regulated kinase and phosphorylation of Elk-1. J Neurosci 22:2054-2062.

Thomas G and Huganir R (2004) MAPK cascade signaling and synaptic plasticity. Nat Rev Neurosci 5:173-183.

Thomas MJ, Beurrier C, Bonci A, and Malenka RC (2001) Long-term depression in the nucleus accumbens: a neural correlate of behavioral sensitization to cocaine. Nat. Neurosci. 4:1217-1223.

Tomita S, Chen L, Kawasaki Y, Petralia R, Wenthold R, Nicoll R, and Bredt D (2003) Functional studies and distribution define a family of transmembrane AMPA receptor regulatory proteins. J Cell Biol 161:805-816.

Tomita S, Stein V, Stocker T, Nicoll R, and Bredt D (2005) Bidirectional synaptic plasticity regulated by phosphorylation of stargazin-like TARPs. Neuron 45:269-277.

Trachtenberg JT, Chen BE, Knott GW, Feng G, Sanes JR, Welker E, and Svoboda K (2002) Long-term in vivo imaging of experience-dependent synaptic plasticity in adult cortex. Nature 420:788-794.
Tsien J, Huerta P, and Tonegawa S (1996) The essential role of hippocampal CA1 NMDA receptor-dependent synaptic plasticity in spatial memory. Cell 87:1327-1338.
Tunquist B, Hoshi N, Guire E, Zhang F, Mullendorff K, Langeberg L, Raber J, and Scott J (2008) Loss of AKAP150 perturbs distinct neuronal processes in mice. Proc Natl Acad Sci USA 105:12557-12562.
Ungless MA, Whistler JL, Malenka RC, and Bonci A (2001) Single cocaine exposure in vivo induces long-term potentiation in dopamine neurons. Nature 411:583-587.
Vazquez L, Chen H, Sokolova I, Knuesel I, and Kennedy M (2004) SynGAP regulates spine formation. J Neurosci 24:8862-8872.
Von Kriegsheim, Baiocchi D, Birtwistle M, Sumpton D, Bienvenut W, Morrice N, Yamada K, Lamond A, Kalna G, Orton R, Gilbert D, and Kolch W (2009) Cell fate decisions are specified by the dynamic ERK interactome. Nat Cell Biol 11:1458-1464.
Wenthold R, Petralia R, Blahos J, and Niedzielski A (1996) Evidence for multiple AMPA receptor complexes in hippocampal CA1/CA2 neurons. J Neurosci 16:1982-1989.
Whitlock JR, Heynen AJ, Shuler MG, and Bear MF (2006) Learning induces long-term potentiation in the hippocampus. Science 313:1084-1097.
Wu G, Deisseroth K, and Tsien R (2001) Activity-dependent CREB phosphorylation: convergence of a fast calmodulin kinase pathway and a slow, less-sensitive mitogen-activated protein kinase pathway. Proc Natl Acad Sci USA 98:2808-2813.
Wu Z, Thomas S, Villacres E, Xia Z, Simmons M, Chavkin C, Palmiter R, and Storm D (1995) Altered behavior and long-term potentiation in type I adenylyl cyclase mutant mice. Proc Natl Acad Sci USA 92:220-224.
Xia Z and Storm D (2005) The role of calmodulin as a signal integrator for synaptic plasticity. Nat Rev Neurosci 6:267-276.
Xiong W and Parsons J (1997) Induction of apoptosis after expression of PYK2, a tyrosine kinase structurally related to focal adhesion kinase. J Cell Biol 139:529-539.
Xu T, Yu X, Perlik A, Tobin W, Zweig J, Tennant K, Jones T, and Zuo Y (2009) Rapid formation and selective stabilization of synapses for enduring motor memories. Nature 462:915-919.
Xu W, Schluter O, Steiner P, Czervionke B, Sabatini B, and Malenka R (2008) Molecular dissociation of the role of PSD-95 in regulating synaptic strength and LTD. Neuron 57:248-262.
Yang E and Schulman H (1999) Structural examination of autoregulation of multifunctional calcium/calmodulin-dependent protein kinase II. J Biol Chem 274:26199-26208.
Yang G, Pan F, and Gan W (2009) Stably maintained dendritic spines are associated with lifelong memories. Nature 462:920-924.
Yang S, Tang Y, and Zucker R (1999) Selective induction of LTP and LTD by postsynaptic [Ca2+]i elevation. J Neurophysiol 81:781-787.
Yang Y, Ma Y, Chen S, Wang C, and Lee E (2003) Focal adhesion kinase is required, but not sufficient, for the induction of long-term potentiation in dentate gyrus neurons in vivo. J Neurosci 23:4072-4080.

Yoon B, Smith G, Heynen A, Neve R, and Bear M (2009) Essential role for a long-term depression mechanism in ocular dominance plasticity. Proc Natl Acad Sci USA 106:9860-9865.

Zakharenko S, Zablow L, and Siegelbaum S (2001) Visualization of changes in presynaptic function during long-term synaptic plasticity. Nat Neurosci 4:711-717.

Zamanillo D, Sprengel R, Hvalby O, Jensen V, Burnashev N, Rozov A, Kaiser K, Koster H, Borchardt T, Worley P, Lubke J, Frotscher M, Kelly P, Sommer B, Andersen P, Seeburg P, and Sakmann B (1999) Importance of AMPA receptors for hippocampal synaptic plasticity but not for spatial learning. Science 284:1805-1811.

Zeng H, Chatterji S, Barbarosie M, Rondi-Reig L, Philpot B, Miyakawa T, Bear M, and Tonegawa S (2001) Forebrain-specific calcineurin knockout selectively impairs bidirectional synaptic plasticity and working/episodic-like memory. Cell 107:617-629.

Zhao J, Zheng C, and Guan J (2000) Pyk2 and FAK differentially regulate progression of the cell cycle. J Cell Sci 113:3064-3072.

Zhou Q, Homma K, and Poo M (2004) Shrinkage of dendritic spines associated with long-term depression of hippocampal synapses. Neuron 44:749-757.

Zhu J, Esteban J, Hayashi Y, and Malinow R (2000) Postnatal synaptic potentiation: delivery of GluR4-containing AMPA receptors by spontaneous activity. Nat Neurosci 3:1098-1106.

Zhu J, Qin Y, Zhao M, Van Aelst L, and Malinow R (2002) Ras and Rap control AMPA receptor trafficking during synaptic plasticity. Cell 110:443-455.

Zuo Y, Lin A, Chang P, Gan W-B (2005) Development of long-term dendritic spine stability in diverse regions of cerebral cortex. Neuron 46:181-189.

CHAPTER 2:

Phosphorylation of PSD-95 by GSK-3beta is required for long term depression

Myung Jong Kim, Honor Hsin, and Morgan Sheng

MJK performed biochemical and imaging experiments in Figures 1, 2, and 3. HH performed electrophysiology experiments in Figures 1 and 4. This chapter is adapted from a manuscript under consideration at *Neuron.*

Abstract

PSD-95 is a major scaffold protein of the postsynaptic density (PSD) that promotes synaptic strength. Activity of Glycogen Synthase Kinase-3beta (GSK-3beta) is required for long-term depression (LTD). Here we report that PSD-95 is phosphorylated on a specific N-terminal residue (Thr-19) by GSK-3beta. GSK-3beta phosphorylation of Thr-19 increases rapidly with chemical LTD and blocks head-to-head multimerization of PSD-95. In hippocampal neurons, the non-phosphorylatable mutant T19A-PSD-95 formed larger, more stable synaptic clusters than wildtype PSD-95. The NMDA-induced dispersal of synaptic PSD-95 clusters was inhibited by GSK-3 antagonists (including LiCl) and by RNAi knockdown of endogenous GSK-3beta. Overexpression of the T19A-PSD-95 mutant inhibited the induction of LTD in cultured hippocampal slices. These data indicate that phosphorylation of PSD-95 on Thr-19 by GSK-3beta is a critical step in the molecular mechanisms underlying LTD.

Introduction

PSD-95 is an abundant scaffold protein of the PSD of excitatory synapses. Through its three PDZ domains, an SH3 domain, and a guanylate kinase-like domain, PSD-95 mediates a host of interactions with intracellular signaling molecules, cell surface adhesion molecules, ion channels, and receptors, including NMDA receptors and AMPA receptor/TARP complexes (Funke et al., 2004; Kim and Sheng, 2004; Peng et al., 2004; Scannevin and Huganir, 2000; Sheng and Hoogenraad, 2007). PSD-95 promotes synapse maturation and exerts a strong positive influence on synaptic strength (Ehrlich and Malinow, 2004; El-Husseini et al., 2000; Elias et al., 2006; Futai et al., 2007; Kim et al., 2007; Nakagawa et al., 2004; Schnell et al., 2002; Stein et al., 2003; Xu et al., 2008).

Synaptic accumulation (or synaptic "targeting") of PSD-95, which is crucial for its ability to recruit postsynaptic AMPA receptors and to potentiate excitatory synaptic transmission, depends on two factors – transport of the protein to the synapse and stability of the protein at the synapse. Synaptic accumulation of PSD-95 is enhanced by palmitoylation of two cysteine residues in the N-terminal region of PSD-95 (Craven et al., 1999; El-Husseini Ael et al., 2002), which is also important for multimerization of PSD-95 (Christopherson et al., 2003; Hsueh et al., 1997; Hsueh and Sheng, 1999).

Recently, synaptic accumulation of PSD-95 was also found to depend on Rac1/JNK1-mediated phosphorylation of a specific residue (ser-295) lying between PDZ2 and PDZ3 domains of PSD-95 (Kim et al., 2007). Dephosphorylation of ser-295, probably mediated by PP1/PP2A phosphatases, is required for AMPA receptor internalization and long-term depression (LTD) in the hippocampus, and is induced by LTD-like stimulation (Kim et al., 2007). There is compelling evidence that the postsynaptic abundance of PSD-95 determines synaptic strength by controlling AMPA receptor trafficking (Ehrlich and Malinow, 2004; El-Husseini et al., 2000; Elias et al., 2006; Futai et al., 2007; Kim et al., 2007; Nakagawa et al., 2004; Schnell et al., 2002; Stein et al., 2003; Xu et al., 2008) and that post-translational modification of PSD-95 is critically involved in AMPA receptor mobilization and induction of LTD.

Activity of the protein kinase GSK-3beta has been shown recently to be essential for LTD; moreover, GSK-3beta activity is suppressed during long term potentiation (LTP) (Peineau et al., 2007). However, the molecular basis of GSK-3beta's key role in the balance of LTP and LTD is unknown. Given that GSK-3 is a major target of Li^+, a mainstay treatment of bipolar disorder, any synaptic action of GSK-3beta might be highly relevant to the understanding of this mental illness.

We report here that GSK-3beta phosphorylates PSD-95 on residue Thr-19, which lies within the putative PEST sequence in the N-terminal region of PSD-95. The phosphorylation of Thr-19, which is bi-directionally modulated by chemical LTP and chemical LTD in neurons, prevents multimerization of PSD-95 and promotes PSD-95 dispersal from synapses. We present evidence that phosphorylation of Thr-19 is essential for LTD. These findings reveal the first synaptic mechanism of action of GSK-3beta and a critical molecular step in the induction of LTD.

Materials and Methods

Antibodies and chemicals

The following antibodies were used in this study: rabbit anti-GSK-3beta Ab (Cell Signaling), rabbit anti-phospho-S9-GSK-3beta Ab (Cell Signaling), rabbit anti-GSK-3alpha Ab (Cell Signaling), rabbit anti-pT19-PSD-95 Ab (Abcam), rabbit anti-GST Ab (Santa Cruz), rabbit

anti-HA (Y11, Santa Cruz), rabbit anti-beta-gal (ICN), mouse anti-beta-gal (Promega), mouse anti-PSD-95 Ab (clone K28/43, NeuroMab), rabbit anti-GluR1-N Ab (EMD), mouse anti-GluR2-N Ab (Chemicon), rabbit anti-pS-133 CREB Ab (Cell Signaling), mouse anti-pS-396 Tau (Cell Signaling), rabbit anti-Myc-Ab agarose (Sigma), mouse anti-HA Ab (Covance), mouse anti-tubulin Ab (Sigma), Alexa-conjugated secondary antibody (Invitrogen). pS-295-PSD-95 antibody was previously described (Kim et al., 2007). Roscovitine and SB216763 were from Tocris. All other chemicals were purchased from Sigma unless otherwise stated.

Cell culture and transfection

Hippocampal neurons were prepared from E19 rats as described (Kim et al., 2007). Hippocampal neurons were transfected at 15 DIV ~ 17 DIV with 1.8 μg DNA per 1 ml Neurobasal media in a 12-well plate using 3.3 μl of Lipofectamine 2000 (Invitrogen). COS-7 cells were maintained in DMEM supplemented with 10% fetal calf serum and transiently transfected with indicated plasmid constructs using Lipofectamine 2000 (Invitrogen) according to the manufacturer's instructions.

DNA constructs

WT-PSD-95 expression vector in pGW1 vector and WT-PSD-95-EGFP construct are previously described (Kim et al., 2007). pGW1-Myc-N-PDZ1 construct is previously described (Hsueh and Sheng, 1999). T19A PSD-95 mutant constructs were generated with site-directed mutagenesis kit from Stratagene. For electrophysiology experiments, PSD-95 constructs were subcloned into pCAG vector (expression of PSD-95 constructs driven by chicken beta-actin promoter with CMV-enhancer). Rat GSK-3beta cDNA was cloned from rat brain Match-Maker Yeast-two hybrid library (Clonetech) with PCR amplification, and sub-cloned into pGW1-HA vector. Kinase-dead (K85M/K86I)-GSK-3beta, constitutively active (S9A)-GSK-3beta, and R96A-GSK-3beta were generated with Site-Directed Mutagenesis Kit from Stratagene. For the construction of GST-tagged fusion protein of PSD-95, the following two oligonucleotides were annealed and sub-cloned into BamH1 / EcoR1 site of pGEX-4T1 vector (Pharmacia).
5'GATCCCGCTACCAAGATGAAGACACGCCCCCTCTGGAACACAGCCCGGCCCACCT
CTGA-3'

5'AATTTCAGAGGTGGGCCGGGCTGTGTTCCAGAGGGGGCGTGTCTTCATCTTGGTAG CGG-3'

For pSUPER-GSK-3beta-RNAi construct, the following oligonucleotides were annealed and inserted into the HindIII / BglII sites of pSUPER vector (Brummelkamp et al., 2002).

GSK-3beta-RNAi:

5'GATCCCCGCTAGATCACTGTAACATATTCAAGAGATATGTTACAGTGATCTAGCTT TTTA-3'

5'AGCTTAAAAAGCTAGATCACTGTAACATATCTCTTGAATATGTTACAGTGATCTAG CGGG-3'

pSUPER-Luciferase-RNAi construct was generous gift from Dr. Huaye Zhang (Zhang and Macara, 2006). Target sequence of pSUPER-Luciferase-RNAi construct is 5'CGTACGCGGAATACTTCGA-3'.

RNAi-Lentivirus

Lentiviral transfer vector constructs were modified from the original FUGW vector backbone (Lois et al., 2002). H1 promoter cassettes from pSuper constructs (pSUPER-Luciferase RNAi and pSUPER-GSK-3beta-RNAi) were cloned between the HIV-flap and synapsin promoter. For the production of lentiviral vectors, the transfer vector, the packaging vector Δ8.9 and the VSVG envelope vector were cotransfected into HEK293-FT cells (Invitrogen). Supernatants of culture media were collected 48 hours after transfection, and centrifuged at 50,000 x g to concentrate the lentivirus. Dissociated hippocampal neurons were infected with RNAi-lentivirus at DIV 25, and analyzed 5 days later.

Immunoblotting and drug treatment

All biochemical studies using hippocampal neurons were done with mature hippocampal neurons grown in 12-well plates at DIV 24-30. After indicated drug treatments, hippocampal neurons were washed with ice-cold PBS twice, and lysed with 120 μl of DTT-containing 2X SDS sample buffer per single well. Protein samples were separated in 7.5% SDS-PAGE gels and analyzed with immunoblotting using indicated antibodies. For chemical LTP induction, cultured hippocampal neurons were incubated in ACSF (ACSF in mM: NaCl 168, KCl 2.6, HEPES 10, D-Glucose 10, $CaCl_2$ 2, $MgCl_2$ 2, Strychnine 0.001; pH 7.2) for 20 min at room

temperature. Neurons were then incubated in ACSF without $MgCl_2$ and with 200 μM glycine for 5 min (Lu et al., 2001; Man et al., 2003). After Gly/ 0 Mg^{2+} stimulation, neurons were incubated in ACSF containing 2 mM $MgCl_2$, and lysed with DTT-containing 2 x SDS sample buffer at indicated time points.

Co-immunoprecipitation Assay

COS-7 cells grown in 35 mm culture dish were transfected with indicated DNAs by using Lipofectamine 2000 (invitrogen). ~48hrs after transfection, COS-7 were washed with cold PBS and lysed with cold RIPA buffer (50 mM Tris [pH 7.4], 150 mM NaCl, 10 mM NaF, 1% NP40, 0.5% deoxycholate, and 0.1% SDS) containing protease inhibitors (PMSF, aprotinin and leupeptin). After centrifugation at 4 °C, cleared cell lysates were incubated with 25 μl of rabbit anti-Myc-Ab agarose (Sigma) for 2hrs in cold room and washed four times with cold RIPA buffer. Immunoprecipitates were separated in 4-15% gradient SDS–PAGE gel (Bio-Rad), and analyzed by immunoblotting using mouse anti-PSD-95 antibody, mouse anti-Myc antibody or mouse anti-HA-antibody.

Immunostaining

For endogenous PSD-95 staining, hippocampal neurons were fixed in methanol in 20°C for 15 min. After washing with 1XPBS, hippocampal neurons were incubated with indicated antibodies in GDB buffer (30 mM phosphate buffer, pH 7.4, containing 0.1% gelatin, 0.3% Triton X-100, and 0.45 M NaCl). Alexa-488 and Alexa-568 secondary antibody (Invitrogen) were used for the visualization of target proteins. Surface GluR1 labeling and NMDA-induced surface GluR2-internalization assay were performed as previously described (Kim et al., 2007). COS-7 cells grown on glass coverslips were fixed in 4% formaldehyde / 1X PBS for 10 min at room temperature followed by permeabilization with 0.1% Triton X-100 and 10% BSA in PBS for 5 min. Primary mouse anti-PSD-95 antibody (clone K28/43) and Alexa-488-conjugated secondary antibody were diluted in Tris-buffered saline (10 mM Tris, pH 7.4, 150 mM NaCl) containing 3% normal goat serum and 0.1% BSA.

Image acquisition and quantification

Confocal images were obtained using a Zeiss 63x (NA 1.4) objective. The confocal microscope settings were kept the same for all scans when fluorescence intensity was compared. All measurements were performed using ImageJ (NIH) software. All values in figures and text refer to mean ± SEM unless otherwise stated. N refers to number of cells unless otherwise indicated. Statistical analysis was performed with Student's t test unless otherwise indicated.

PA-GFP imaging

PA-GFP was tagged at the C-terminus of PSD-95. Protein expression was driven by chicken beta-actin promoter with CMV enhancer (pCAG vector). Hippocampal neurons grown on 35 mm glass bottom culture dish (MatTeck) were transfected at DIV 16-17 either with WT-PSD-95-PA-GFP plus pCAG-mCherry or T19A-PSD-95-PA-GFP plus pCAG-mCherry (4:1 ratio in favor of PA-GFP plasmid). Four days later, time-lapse imaging was performed with Zeiss inverted LSM 510 confocal microscope using a 63 X 1.2 numerical aperture (NA) oil-immersion objective with 4X zoom. Before imaging, neurons were adapted in imaging buffer (in mM: NaCl, 140; $CaCl_2$, $MgCl_2$, 2; 1.3; KCl, 5.0; HEPES, 25; glucose, 33; at pH 7.4 and osmolarity 325–335 $mosmol^{-1}$) for at least 45 min at 37 °C. Photo-activation of PA-GFP was done with 405 nm laser, and time-lapse images were taken with multi-track setting for GFP / mCherry. Images were taken every 1 min for 35 min at 37 °C. Decay of photo-activated GFP was analyzed with ImageJ software (NIH).

In vitro GSK-3beta kinase assay

GST-tagged fusion protein of PSD-95 N-terminal region (a.a 13– 29 of rat PSD-95) was expressed in E. coli BL21(DE3), and purified with GSH-agarose (Invitrogen). Purified GST-PSD-95 substrates (~50 ng in 50 μl of kinase reaction volume) were incubated with 10 ng of purified GSK-3beta from Upstate Biotech in kinase buffer (25 mM Tris-HCl (pH 7.5), 5 mM beta-glycerophosphate, 2 mM dithiothreitol (DTT), 0.1 mM Na_3VO_4, 10 mM $MgCl_2$, 200 μM ATP) for 20 min at 30°C. After in vitro kinase reaction, proteins samples were separated in 4-15% gradient SDS-PAGE gels (Bio-Rad) and analyzed with immunoblotting. Phosphorylation of Thr-19 of PSD-95 was detected with immunoblotting with p-T19 PSD-95 antibody. After stripping the blot, GST-tagged fusion protein of PSD-95 were detected with GST antibody (Santa Cruz). GSK-3beta kinase was detected with anti-GSK-3beta antibody (Cell signaling).

Electrophysiology

Electrophysiological recordings were performed on organotypic slices cultures dissected from postnatal day-7 rat hippocampus as described (Kim et al., 2007; Nakagawa et al., 2004). Neurons were transfected by biolistic gene gun at DIV 3-5 (total 100 μg DNA; 45% of the test construct in pCAG; 45% empty pCAG vector; 10% 16pl-EGFP marker [driven by beta-actin promotor]) and recorded 3 days after transfection. Recordings were carried out in solution containing (in mM): NaCl (119), KCl (2.5), CaCl2 (4), MgCl2 (4), NaHCO3 (26), NaH2PO4 (1), glucose (11), picrotoxin (0.1), and 2-chloroadenosine (0.002-0.008), and bubbled continuously with 5% CO2/ 95% O2. Patch recording pipettes (2-4 M ohms) were filled with internal solution containing (in mM): cesium methanesulfonate (115), CsCl (20), HEPES (10), $MgCl_2$ (2.5), ATP disodium salt (4), GTP trisodium salt (0.4), sodium phosphocreatine (10), and EGTA (0.6), at pH 7.25. Simultaneous whole-cell recordings were obtained from a pair of transfected and neighboring untransfected CA1 pyramidal neurons during stimulation of presynaptic Schaffer collaterals. For basal synaptic transmission experiments, presynaptic fibers were stimulated at 0.2 Hz. AMPA receptor EPSCs were recorded at -70 mV, and NMDA receptor EPSCs at +40 mV in the presence of 0.01 mM NBQX. Each data point represents an average of 60 consecutive synaptic responses. For LTD experiments, presynaptic fibers were stimulated at 0.033 Hz during baseline recordings, and synaptic responses were obtained at -70 mV. After at least 10 minutes of stable baseline, LTD was induced by 1 Hz stimulation (200 pulses) at -40 mV. Synaptic responses were then obtained under baseline conditions for another 30 minutes. Results are expressed as mean ± SEM, and statistical significance was assessed by paired t-test on mean EPSC amplitude for basal transmission experiments, or by two-tailed t-test on mean normalized EPSC (averaged over the last 10 minutes of post-induction recordings) for LTD experiments.

Results

T19A-PSD-95 mutant forms bigger synaptic clusters in neurons

An earlier study showed that CDK5 can phosphorylate Ser-25, and to a lesser extent Thr-19, in the N-terminal region of PSD-95 in vitro; moreover, phosphorylation of one or both these residues occurs in the brain, based on immunoblotting with a phosphoantibody raised against a

peptide dually phosphorylated on Thr-19 and Ser-25 (Morabito et al., 2004). Because Thr-19 does not conform to an optimal CDK5 phosphorylation sequence (Songyang et al., 1996), we wondered whether other kinases might mediate Thr-19 phosphorylation of PSD-95 in neurons. It is notable that Thr-19 is located inside a putative PEST motif, which is suggested to be important for PSD-95 ubiquitination and subsequent proteasome-mediated degradation (Colledge et al., 2003), and it lies close to Cys-3 and Cys-5, which are important for palmitoylation and head-to-head multimerization of PSD-95 (Christopherson et al., 2003; Craven et al., 1999; El-Husseini Ael et al., 2002; Hsueh et al., 1997; Hsueh and Sheng, 1999).

What might be the functional role of Thr-19 phosphorylation of PSD-95 in neurons? As a first step, we looked at localization of the phospho-null mutant T19A-PSD-95-EGFP when transfected in cultured hippocampal neurons. The wildtype PSD-95-EGFP localized in clusters at presumptive postsynaptic sites in the dendritic spines of transfected neurons. In comparison, we found that T19A-PSD-95-EGFP formed bigger and brighter clusters (Figure 1A).

PSD-95 promotes surface expression of AMPA receptors (El-Husseini et al., 2000; Kim et al., 2007; Regalado et al., 2006). To further investigate the functional significance of PSD-95 Thr-19 phosphorylation, we examined the effect of overexpression of WT-PSD-95 and T19A-PSD-95 on excitatory synaptic transmission in CA1 pyramidal neurons in hippocampal slice cultures (Figure 1B). Neurons in hippocampal slice cultures were transfected with WT-PSD-95 plus GFP or T19A-PSD-95 plus GFP by biolistic gene gun at DIV 3-5 and recorded 3 days after transfection. Simultaneous recording of EPSCs was performed from neighboring untransfected and transfected CA1 pyramidal neurons (the latter identified by GFP fluorescence). WT-PSD-95 strongly enhanced AMPAR-EPSCs (4.2 ± 0.41 fold relative to untransfected cells, $p < 0.0001$, $n = 33$ pairs), as previously reported (Ehrlich and Malinow, 2004; Elias et al., 2006; Futai et al., 2007; Kim et al., 2007; Nakagawa et al., 2004; Schnell et al., 2002; Stein et al., 2003; Xu et al., 2008). Overexpression of the phospho-null mutant T19A-PSD-95 caused a similarly large increase in AMPAR-EPSC (4.4 ± 0.47 fold, $p < 0.0001$, $n = 24$ pairs; Figure 1B, 1C), as did overexpression of the phospho-mimic T19D-PSD-95 mutant (4.0 ± 0.48 fold, $p < 0.0001$, $n = 23$ pairs; Figure 1B, 1C). Overexpression of WT-PSD-95, T19A-PSD-95, or T19D-PSD-95 also enhanced NMDAR-EPSCs, as reported by Futai et al. (2007) (1.4 ± 0.14 fold, $p = 0.012$, $n = 33$; 1.9 ± 0.18 fold, $p < 0.0001$, $n = 22$; 1.5 ± 0.16 fold, $p = 0.018$, $n = 22$; respectively; Figure 1).

Together, these data suggest that Thr-19 phospho-mutants are targeted to synapses like WT-PSD-95, and that Thr-19 phosphorylation does not affect basal AMPAR transmission.

GSK-3 kinase activity mediates Thr-19 phosphorylation of PSD-95

To determine which kinases might be responsible for Thr-19 phosphorylation of PSD-95 in neurons, we treated cultured hippocampal neurons (DIV24-28) with a panel of kinase inhibitors: 5 μM H89 (PKA inhibitor), 1 μM calphostin (PKC inhibitor), 5 μM Y27632 (ROCK inhibitor), 10 μM KN-93 (CaMKII inhibitor), 10 μM roscovitine (CDK5 inhibitor), 10 μM LY294002 (PI-3K pathway inhibitor), 10 μM SB216763 (GSK-3 inhibitor) for ~16 hrs and assayed Thr-19 phosphorylation by a phospho-specific antibody (Kim and Sheng, data not shown). Among the tested drugs, SB216763 most strongly reduced phospho-T19 PSD-95 levels in cultured hippocampal neurons (Figure 2A and Kim and Sheng, data not shown), suggesting that GSK-3 activity is required for phosphorylation of Thr-19 in neurons. To confirm this conclusion, we tested LiCl, which is also known to inhibit GSK-3. Treatment of cultured hippocampal neurons with 10 mM LiCl for ~16 hrs greatly reduced phospho-T19 levels without altering total PSD-95 levels significantly (Figure 2A). As expected, SB216763 and LiCl also suppressed phosphorylation of Tau on ser-396 (Figure 2A).

Since Thr-19 of PSD-95 was originally suggested to be phosphorylated by CDK5 based on in vitro kinase reactions (Morabito et al., 2004), we tested the effect of CDK5 inhibitor (roscovitine) on PSD-95 Thr-19 phosphorylation. Treatment with roscovitine (5-10 μM; ~16 hrs) did not affect phospho-T19-levels of PSD-95 in cultured hippocampal neurons (Figure 2A). Together, these data imply that GSK-3, rather than CDK5, is the important protein kinase involved in the phosphorylation of PSD-95 Thr-19 in hippocampal neurons.

To corroborate the pharmacological findings from cultured hippocampal neurons, we co-expressed various GSK-3beta constructs with PSD-95 in COS-7, and examined effects on Thr-19 phosphorylation of PSD-95. Overexpression of wild type (wt)-GSK-3beta and constitutively active GSK-3beta (S9A GSK-3beta) strongly increased phospho-T19 PSD-95 levels in COS-7 cells, as judged by immunoblot analysis using phospho-T19 PSD-95 antibody (Figure 2B). A kinase-dead mutant of GSK-3beta (K85M/K86I GSK-3beta) did not affect phospho-T19 PSD-95 levels (Figure 2B). Since GSK-3beta phosphorylation often requires prior "priming phosphorylation" of the substrate at the +4 position relative to the phosphoacceptor serine or

threonine, we tested R96A-GSK-3beta, a point mutant of GSK-3beta which cannot phosphorylate substrates requiring prior priming phosphorylation at the +4 position (Doble and Woodgett, 2003). In heterologous cells, R96A GSK-3beta was able to phosphorylate PSD-95 Thr-19 as efficiently as wt-GSK-3beta and S9A GSK-3beta (Figure 2B). Co-expression of WT-GSK-3beta, S9A-GSK-3beta or R96A-GSK3beta did not affect total PSD-95 protein levels in COS-7 cells, compared with co-expression of kinase-dead GSK-3beta. These results show that PSD-95 can be phosphorylated at Thr-19 by GSK-3beta in a cellular context, and does not require prior priming phosphorylation by other kinases. It also implies that GSK-3beta-mediated Thr-19 phosphorylation of PSD-95 does not affect PSD-95 protein stability in heterologous cells. We also found that GSK-3beta can phosphorylate PSD-95 on Thr-19 directly, by incubating a purified GST-fusion protein of the N-terminus of PSD-95 with recombinant human GSK-3beta, and detecting Thr-19 phosphorylation in an in vitro kinase reaction (Kim and Sheng, data not shown).

Bi-directional regulation of Thr-19 phosphorylation in chemical LTD and chemical LTP

How is Thr-19 phosphorylation of PSD-95 regulated in neurons by activity? Bath application of NMDA (75 μM), which is often used to induce "chemical LTD," increased pThr-19 levels of PSD-95 over the time course of 10 min, without affecting total PSD-95 levels (Figure 2C). We next tested a "chemical LTP" protocol (200 μM glycine / 0 Mg2+), which is known to increase synaptic strength and drive AMPA receptors to the surface (Lu et al., 2001; Man et al., 2003). In contrast to the rapid increase induced by NMDA treatment, Thr-19 phosphorylation of PSD-95 was decreased by the chemical LTP protocol, over a time frame of ~ 30 min (Figure 2C). Strikingly, this bidirectional regulation of Thr-19 phosphorylation by LTP and LTD is opposite to that seen for Ser-295 phosphorylation: Chemical LTD induces rapid dephosphorylation of Ser-295 (Kim et al., 2007) in contrast to rapid phosphorylation of Thr-19, whereas chemical LTP induces phosphorylation of Ser-295 (Kim et al., 2007) versus dephosphorylation of Thr-19. It has been reported that GSK-3beta activity is stimulated by LTD stimuli and inhibited by LTP induction in hippocampal slices (Peineau et al., 2007). We confirmed here that NMDA treatment of mature cultured hippocampal neurons also results in the activation of GSK-3beta, as judged by immunoblotting with phospho-S9-GSK-3beta antibody

(Kim and Sheng, data not shown). These findings are consistent with the idea that activation of GSK-3beta is responsible for the increased phosphorylation of PSD-95 on Thr-19 during LTD.

Pharmacological inhibition of GSK-3 activity or lentiviral knockdown of endogenous GSK-3beta in cultured neurons reduces NMDA-induced Thr-19 phosphorylation of PSD-95

NMDA treatment increases GSK-3 activity and phospho-Thr-19 levels of PSD-95 in neurons. To test whether the NMDA-induced Thr-19 phosphorylation of PSD-95 is mediated by GSK-3 in neurons, we treated cultured neurons with GSK-3 inhibitors (LiCl and SB216763), and examined NMDA-induced Thr-19 phosphorylation of PSD-95. Treatment of cultured neurons (DIV25) with 10 mM LiCl or 10 μM SB216763 for ~16 hrs reduced basal phosphorylation of PSD-95 on Thr-19 (Figure 2D; see also Figure 2A). These GSK-3 inhibitors also strongly impaired the NMDA-induced increase in phospho-Thr-19 levels (Figure 2D). These data suggest that GSK-3 activity is important for both the basal and stimulated phosphorylation of PSD-95 Thr-19. In addition, both LiCl and SB216763 were effective in reducing phosphorylation of Tau on Ser-396, which is believed to be a GSK-3 regulated site. Curiously, we noted that LiCl increased the level of phosphorylation of the inhibitory Ser-9 site of GSK-3 (Figure 2D), suggesting LiCl may have a complex mechanism of inhibition of GSK-3 (Beaulieu et al., 2008).

To confirm genetically the importance of GSK-3 in Thr-19 phosphorylation, we turned to lentiviral RNAi system to knockdown endogenous GSK-3 in cultured neurons. Although both isoforms of GSK-3 (GSK-3alpha and GSK-3beta) are present in the brain, we focused on GSK-3beta because it is more highly expressed (Leroy and Brion, 1999), and because GSK-3beta was found in the postsynaptic density fraction (Hirabayashi et al., 2004). Cultured hippocampal neurons were infected at DIV 25 with luciferase-RNAi lentivirus or GSK-3beta-RNAi lentivirus, and five days later, were treated with 75 μM NMDA for 10 min (Figure 2E). Infection with GSK-3beta-RNAi lentivirus in cultured neurons reduced protein levels of GSK-3beta, without altering GSK-3alpha or total PSD-95 protein levels. The NMDA-induced increase in phospho-Thr-19 was strongly inhibited by GSK-3beta knockdown (Figure 2E arrow), confirming that GSK-3beta is essential for NMDA-induced phosphorylation of Thr-19 in neurons. RNAi

knockdown of GSK-3beta did not affect NMDA-induced dephosphorylation of Ser-295 of PSD-95 or NMDA-induced dephosphorylation of CREB on Ser-133 (Figure 2E) (Sala et al., 2000).

LiCl and GSK-3beta knockdown inhibit NMDA-induced PSD-95 loss from synapses

Next, to investigate functional roles of GSK-3beta in synaptic level of PSD-95, we generated a pSUPER plasmid-based RNAi construct that targets the GSK-3beta. In COS-7 cells, the GSK-3beta-RNAi construct, but not a control RNAi construct against luciferase, suppressed expression of co-transfected rat GSK-3beta (Kim and Sheng, data not shown). In cultured rat hippocampal neurons, transfection of the GSK-3beta-RNAi, but not luciferase-RNAi, construct for 3 days (DIV15+3) reduced levels of endogenous GSK-3β protein by ~70%, as measured by immunostaining with a GSK-3beta antibody (Kim and Sheng, data not shown).

In neurons (DIV 16) transfected for 3 days with GSK-3beta-RNAi and beta-gal marker (final age DIV16 + 3), there was little effect on mean intensity of dendritic PSD-95 staining in basal conditions, as compared with luciferase-RNAi-transfected neurons in the same culture. Treatment with 75 μM NMDA for 10 min resulted in ~35 % reduction in mean immunofluorescence staining intensity of dendritic PSD-95 in control neurons transfected with Luciferase-RNAi (Figure 3). Because total PSD-95 protein levels by immunoblot analysis were unaffected by the same NMDA treatment (see Figure 2C), we interpret the diminution of dendritic PSD-95 staining as NMDA-induced partial dispersal of PSD-95 from synaptic clusters. In neurons transfected with GSK-3beta-RNAi, however, the NMDA-induced reduction of dendritic PSD-95 staining intensity was largely prevented (Figure 3). These results suggest that GSK-3beta is critical for loss of PSD-95 from synapses following NMDA stimulation.

To corroborate this idea by a pharmacological approach, we pre-treated cultured hippocampal neurons with the GSK-3beta inhibitors 10 mM LiCl or 10 μM SB216763 for ~16 hr, and then treated neurons with 75 μM NMDA for 10 min. Pre-treatment with LiCl resulted in a slight but significant increase in the average "basal" size of PSD-95 clusters, compared to DMSO alone (Figure 3). The inhibitor SB216763 had no significant effect on basal PSD-95 cluster size. In control neurons pre-treated with DMSO, 75 μM NMDA for 10 min resulted in ~ 30 % reduction in mean size of PSD-95 clusters (similar in degree to the reduction in mean dendritic PSD-95 staining intensity measured above). In neurons pre-treated with 10 mM LiCl,

the NMDA effect on PSD-95 cluster size was almost completely abrogated (Figure 3). SB216763 also significantly impaired the shrinkage of PSD-95 clusters induced by NMDA, as compared with DMSO control neurons (Figure 3). These data support the idea that GSK-3beta activity is important for NMDA-induced PSD-95 loss from synapses.

What could be the mechanism behind GSK-3beta's effect on PSD-95 dispersal? Sturgill et al. (2009) found that NMDA treatment decreased PSD-95 stability in spines. We therefore wondered if T19A-PSD-95 exhibited enhanced stability in spines. Indeed, we found that T19A-PSD-95 tagged with photoactivatable GFP (PA-GFP) diffused much less out of spines after photoactivation than tagged WT-PSD-95 (fluorescence of T19A-PSD-95-PA-GFP and WT-PSD-95-PA-GFP required ~25 min and ~17 min, respectively, to fall to ~70% of original spine intensity; Kim and Sheng, data not shown). We next hypothesized that phosphorylation of Thr-19 impedes multimerization mediated by the N-terminal domain, thereby favoring the mobilization of PSD-95 from the PSD. In fact, Morabito et al. (2004) found that phosphorylation of N-terminal residues in PSD-95 enhanced head-to-head multimerization. Consistent with this result, we observed that transfection of COS cells with wild type GSK-3beta reduced the coimmunoprecipitation of WT-PSD-95 with a Myc-tagged N-PDZ1 fragment of PSD-95, compared to kinase-dead GSK-3beta (K85M/K86I-GSK-3beta; Kim and Sheng, data not shown). The mutant T19A-PSD-95 retained its ability to co-immunoprecipitate with Myc-N-PDZ1, and the association between T19A-PSD-95 and Myc-N-PDZ1 was less affected by expression of WT-GSK-3beta, compared with that of WT-PSD-95 and the Myc-N-PDZ1 fragment (Kim and Sheng, data not shown).

Overexpression of T19A-PSD-95 mutant inhibits LTD

Is there a functional role for Thr-19 phosphorylation in synaptic plasticity? NMDA bath application is well known to stimulate AMPA receptor internalization and give rise to depression of synaptic transmission (chemical LTD) (Brown et al., 2005; Lee et al., 1998; Malenka and Bear, 2004). PSD-95 is a scaffold protein that is important for immobilizing AMPA receptors at postsynaptic sites (Bats et al., 2007). Since NMDA treatment stimulates phosphorylation of PSD-95 on Thr-19-PSD-95 (see Figure 2), we hypothesized that Thr-19 phosphorylation is mechanistically involved in NMDA-induced AMPA receptor internalization and LTD.

We investigated the role of Thr-19 phosphorylation in LTD, using cultured hippocampal slices where we can measure EPSCs in neighboring transfected and untransfected cells in the same slice. Overexpression of WT-PSD-95 (with EGFP marker) in CA1 neurons increased basal synaptic strength (see Figure 1); however, LTD could be robustly induced at these Schaffer collateral-CA1 synapses by a pairing protocol (53% ± 3% (SEM), n = 8, p = 0.076 compared with untransfected neurons). The normalized magnitude of LTD in WT-PSD-95 expressing cells was not significantly different from that obtained in neighboring untransfected neurons (Figure 4B), which is consistent with a recent study (Xu et al., 2008). In contrast, LTD was impaired in cells overexpressing the mutant T19A-PSD-95 (which produced an increase in basal synaptic transmission similar to WT-PSD-95 (see Figure 1) (Figure 4A). T19A-PSD-95 expressing cells showed LTD of 79% ± 9% (SEM), compared with 47% ± 5% (SEM) in neighboring untransfected neurons (n = 10, p = 0.0058). Expression of the phospho-mimic T19D-PSD-95 mutant had no effect on basal synaptic transmission (see Figure 1) or LTD (48% ± 6% (SEM), n = 9, p = 0.49 compared with untransfected neurons; Figure 4C), suggesting that blockade of LTD by Thr-19 mutants of PSD-95 is specific to the phospho-null mutation (additionally, it is possible that T19D in PSD-95 does not function as a true phospho-mimic). We did not study LTP because overexpression of PSD-95 results already in greatly strengthened synapses that occludes LTP (Ehrlich and Malinow, 2004; Futai et al., 2007; Stein et al., 2003; Xu et al., 2008). Taken together, these results indicate that Thr-19 phosphorylation of PSD-95 is required for AMPA receptor internalization and critical for the induction of LTD.

Discussion

Thr-19 phosphorylation regulates PSD-95 multimerization and dynamics and is required for LTD

The abundance of PSD-95 in the PSD determines the number of AMPA receptors gathered in the postsynaptic membrane and thus controls synaptic strength (Bats et al., 2007; Ehrlich and Malinow, 2004; El-Husseini et al., 2000; El-Husseini Ael et al., 2002; Elias et al., 2006; Futai et al., 2007; Kim et al., 2007; Schnell et al., 2002; Stein et al., 2003; Xu et al., 2008). Previously, phosphorylation of Ser-295 was shown to promote the accumulation of PSD-95 in synapses, thereby enhancing synaptic strength (Kim et al., 2007). We demonstrate here that

PSD-95 is also phosphorylated on Thr-19, and that this phosphorylation disrupts the multimerization of PSD-95 that is mediated by the N-terminal region. Mutant PSD-95 (T19A) that cannot be phosphorylated on Thr-19 forms dynamically more stable clusters in dendritic spines. It is plausible that dissociation of PSD-95 multimers due to Thr-19 phosphorylation is the cause of PSD-95 destabilization in the PSD; alternatively, Thr-19 phosphorylation could enhance PSD-95 mobility by affecting palmitoylation of PSD-95, which occurs nearby on N-terminal cysteines Cys-3 and Cys-5 (Craven et al., 1999; El-Husseini Ael et al., 2002).

Thr-19 phosphorylation appears to be important for LTD, because overexpression of the phospho-null T19A-PSD-95 mutant results in the impairment of LTD. We hypothesize that the de-multimerization of PSD-95 and/or mobilization of PSD-95 from the PSD – which is triggered by Thr-19 phosphorylation – is a critical step that allows AMPA receptor/TARP complexes to "escape" more easily from the PSD. The uncorralled AMPA receptors can then diffuse from the synapse to endocytic zones lateral to the PSD (Blanpied et al., 2002).

Is PSD-95 phosphorylation on Thr-19 merely permissive for LTD, or could it be instructive? Several lines of evidence argue for a more active role. First, Thr-19 phosphorylation is induced by LTD stimuli, on a similarly rapid time scale (within minutes) as synaptic depression. Second, we show that the protein kinase responsible for Thr-19 phosphorylation is GSK-3beta, an enzyme that is required for LTD (Peineau et al., 2007) and that is activated during LTD (Peineau et al., 2007). Third, activated GSK-3beta inhibits the multimerization of PSD-95 and promotes its dissociation from synapses, a plausible mechanism for stimulating AMPA receptor mobilization and internalization. Our findings provide the first molecular explanation for GSK-3beta involvement in LTD: namely, Thr-19 of PSD-95 is a critical substrate of GSK-3beta in LTD signaling.

A previous study showed that overexpression of a PSD-95 mutant lacking the N-terminal PEST motif impaired NMDA-induced AMPA receptor internalization (Colledge et al., 2003). This result was interpreted as the PEST sequence being important for ubiquitination and degradation of PSD-95 (however, see Bingol and Schuman, 2004). Because Thr-19 lies within the deleted PEST motif, the Colledge et al. (2003) result is also concordant with our conclusion that Thr-19 phosphorylation is required for mobilization of PSD-95 from synapses, and consequently, AMPA receptor internalization. We did not find significant loss of total endogenous PSD-95 protein following bath NMDA application by immunoblot analysis (see

Figure 2C), making it unlikely that degradation of PSD-95 is important for AMPA receptor endocytosis and LTD.

An elegant recent study showed that PSD-95 mutants with small deletions or substitutions in the N-terminal region were able to potentiate synaptic transmission but block LTD (Xu et al., 2008), a behavior similar to our PSD-95 T19A mutant. It is possible that at least some of the N-terminal mutations of Xu et al. (2008) could also be affecting Thr-19 phosphorylation.

Thr-19 and Ser-25 residues of PSD-95 were previously suggested to be CDK5 phosphorylation sites based on in vitro kinase reactions with purified CDK5 and from phospho-antibody studies (Morabito et al., 2004). However, Morabito et al. (2004) used a phospho-antibody that was raised against a diphospho-peptide containing both phospho-Thr-19 and phospho-Ser-25. Indeed, from the published data (Morabito et al., 2004), it seems likely that phospho-antibody preferentially recognizes phospho-Ser-25. We found that phosphorylation of Thr-19 was unaffected by roscovitine, a CDK5 inhibitor. Thus it is conceivable that Ser-25 is specifically targeted by CDK5, whereas Thr-19 is phosphorylated by GSK-3beta. Potential interactions between these two phosphorylation events would be interesting to study. It seems unlikely that Ser-25 needs to be phosphorylated before Thr-19 can be phosphorylated by GSK-3beta, because "priming" phosphorylation for GSK-3beta usually occurs on the +4 residue relative to the phosphosite (Doble and Woodgett, 2003), and because the R96A-GSK-3beta mutant can phosphorylate Thr-19 (see Results). We note that the +4 amino acid (Glu-23) is already negatively charged, which might mimic a constitutive "priming" phosphorylation. Consistent with our results with the T19 point mutant, Morabito et al. (2004) found that expression of the triple alanine mutant of PSD-95 (T19A, S25A, S35A) in hippocampal neurons induced larger PSD-95 clusters (Morabito et al., 2004).

How does Thr-19 phosphorylation affect PSD-95 function? We found that GSK-3beta-mediated Thr-19 phosphorylation reduces head-to-head multimerization of PSD-95. Phosphorylation of the N-terminal region by overexpressed CDK5/p35 has also been reported to inhibit PSD-95 multimerization in heterologous cells (Morabito et al., 2004). Impaired multimerization of the N-terminal region could arise from electrostatic interference introduced by the phosphate groups. Alternatively, Thr-19 phosphorylation might interfere with, or counteract the effects of, palmitoylation of nearby residues Cys-3 and Cys-5, which are known to

be important for head-to-head multimerization, as well as plasma membrane association and synaptic localization of PSD-95 (Christopherson et al., 2003; Craven et al., 1999; El-Husseini Ael et al., 2002; Hsueh et al., 1997; Hsueh and Sheng, 1999). The potential influence of Thr-19 phosphorylation on PSD-95 palmitoylation remains to be examined.

By preventing Thr-19 phosphorylation, the T19A mutant of PSD-95 should exhibit more stable N-terminus-mediated multimerization and hence greater stability in the PSD. We hypothesize that this property hinders an activity-dependent mobilization of PSD-95 that is needed to loosen up AMPA receptors in the postsynaptic membrane, thereby impairing the induction of LTD. Consistent with this mechanism, Sturgill et al. (2009) reported that NMDA treatment destabilizes PSD-95 at spines, although they found that this process required N-terminal PDZ1/2 domains. It would be intriguing to investigate the precise molecular relationship between PSD-95 stability, multimerization, and PDZ domain interactions.

PSD-95 Thr-19 phosphorylation and Ser-295 dephosphorylation as a molecular coincidence detector in LTD

Recently, we reported that phosphorylation of PSD-95 Ser-295 by Rac1/JNK1 promotes the synaptic accumulation of PSD-95 (Kim et al., 2007), suggesting that this phosphorylation event also regulates PSD-95 stability. NMDA treatment induces rapid dephosphorylation of Ser-295 (probably mediated by PP1/PP2A phosphatase(s)), and the phospho-mimic mutant S295D-PSD-95 blocks AMPA receptor internalization and LTD. The direction of regulation of Ser-295 phosphorylation (Kim et al., 2007) is essentially "opposite" to that of Thr-19 (this study). Our findings indicate that PSD-95 needs to be both dephosphorylated at Ser-295 and phosphorylated on Thr-19 to allow for AMPA receptor internalization and LTD. The simplest model is that the dual modification is required to mobilize PSD-95 from the PSD, thereby facilitating AMPA receptor diffusion to extrasynaptic sites where they are endocytosed (Bats et al., 2007; Newpher and Ehlers, 2008). Thus PSD-95 acts as molecular coincidence detector for PP1/PP2A and GSK-3beta activation, both of which are essential for LTD.

We note that GSK-3beta activation is triggered by dephosphorylation of Ser-9 by PP1/PP2A (Lin et al., 2007; Welsh and Proud, 1993; Zhang et al., 2003). Thus, both molecular events leading to destabilization of postsynaptic PSD-95 (phosphorylation of Thr-19 and

dephosphorylation of Ser-295 of PSD-95) seem to depend on PP1/PP2A, the activation of which correlates with LTD-like stimuli (Kim et al., 2007). It is widely accepted that PP1 activation and recruitment to stimulated synapses is required for LTD (Morishita et al., 2001; Mulkey et al., 1994), although the mechanism of phosphatase action in LTD has been quite unclear. Our findings highlight PSD-95 as a critical convergent target of PP1/PP2A signaling in LTD.

Although this study focuses on the role of PSD-95 in LTD, we do not suggest that PSD-95 phosphorylation/dephosphorylation is the only factor in the induction of LTD. Rather, the control of AMPA receptor number in the postsynaptic membrane is likely to result from an interplay between activity-dependent regulation of PSD-95 and activity-dependent regulation of AMPA receptors – the latter via phosphorylation of cytoplasmic tails of GluR subunits and interacting proteins (Elias and Nicoll, 2007; Lee et al., 2003; Malenka and Bear, 2004; Newpher and Ehlers, 2008; Shepherd and Huganir, 2007). Phosphorylation of AMPA receptors and TARPs could additionally affect the association of AMPA receptors with PSD-95 and hence the propensity for internalization and LTD.

PSD-95 – a synaptic target of GSK-3beta

It is increasingly recognized that dysfunction of synapses might contribute to the cognitive defects of neurodegeneration and psychiatric illness (Bourgeron, 2007; Gray and Roth, 2007; Javitt, 2004; Kauer and Malenka, 2007; Knobloch and Mansuy, 2008; Lau and Zukin, 2007). The precise molecular mechanisms of synaptic dysfunction in neuropsychiatric disorders has not been worked out. Excessive activity of GSK-3 (particularly GSK-3beta, which is highly enriched in the brain and most studied) and/or elevated GSK-3 protein levels have been implicated in common mental illnesses (e.g. bipolar disorder) and neurodegenerative diseases (e.g. Alzheimer's disease) (Anderton, 1999; Bhat et al., 2004; Eldar-Finkelman, 2002; Grimes and Jope, 2001; Pei et al., 1997). Currently LiCl, a GSK-3 inhibitor, is used as mainstay treatment of bipolar disorder, suggesting that aberrant GSK-3 signaling may play a role in this disease (Bachmann et al., 2005; Eldar-Finkelman, 2002; Scolnick, 2006). Our report links GSK-3beta directly with synaptic function by identifying PSD-95 as a critical synaptic substrate of GSK-3beta.

PSD-95 is a major scaffold protein of the PSD that promotes maturation and strengthening of excitatory synapses and which is highly relevant for synaptic plasticity. According to our findings, GSK-3beta phosphorylation of PSD-95 would lead to weakened synapses and altered plasticity. Thus regulation of PSD-95 by GSK-3beta has major implications for the pathogenesis and treatment of CNS disorders such as bipolar disorder and Alzheimer's, in which altered GSK-3 function is invoked.

Acknowledgments

MS was Investigator of Howard Hughes Medical Institute. We thank Dr. Huaye Zhang for providing pSUPER Luciferase-RNAi construct.

Figure Legends and Figures

Figure 1. Effects of PSD-95 Thr-19 mutants on synaptic localization of PSD-95 and synaptic transmission. (**A**) Localization of EGFP-tagged T19A-PSD-95, or wildtype PSD-95 in hippocampal neurons. Cultured hippocampal neurons were transfected at DIV15, and three days later, fixed with 4% formaldehyde/ 4% sucrose / 1X PBS for 10 min. Representative images are shown. (**B**) Effect of PSD-95 Thr-19 mutants on synaptic transmission in cultured hippocampal slices. Synaptic AMPA receptor EPSCs are recorded from T19A-PSD-95, WT-PSD-95, and T19D-PSD-95 transfected neurons versus untransfected controls (n = 24 pairs, 33 pairs, 23 pairs, respectively). Synaptic NMDA receptor EPSCs are also from T19A-PSD-95, WT-PSD-95, and T19D-PSD-95 transfected neurons versus untransfected controls (n = 22 pairs, 33 pairs, 22 pairs, respectively). Sample traces of AMPA-R-EPSCs (downward trace), overlaid with NMDA-R-EPSCs (upward trace) are shown. Scale bars, 100 pA/100 msec. (**C**) Summary of PSD-95 Thr-19 mutant overexpression on AMPA-R-EPSCs and NMDA-R-EPSCs, as indicated by the ratio of EPSC amplitudes between transfected and neighboring untransfected cells.

Figure 2. GSK-3 regulates phosphorylation of Thr-19 of PSD-95. (**A**) Effects of pharmacological GSK-3 kinase inhibitors on phospho-Thr-19 levels of PSD-95. Cultured hippocampal neurons at DIV 25-28 were treated with DMSO, SB216763 (10 μM), LiCl (10 μM), or roscovitine (5 or 10 μM) for ~16 hrs, and then immunoblotted with pT-19 antibody. After stripping, the blot was re-probed with mouse PSD-95 antibody and pS-396 Tau antibody. Graph shows pT-19 immunoblot intensity (divided by total PSD-95 intensity) normalized to DMSO control (mean ± SEM of three independent experiments). Statistical analysis was performed by one-way ANOVA, followed by the Dunnett's test. ** $p < 0.01$ compared with DMSO control. (**B**) Phosphorylation of PSD-95 on Thr-19 by GSK-3beta in COS-7 cells. Wild-type PSD-95 was transfected with vector control (pGW1), HA-WT-GSK-3beta, Kinase dead HA-KD-GSK-3beta, or HA-R96A-GSK-3beta. 30 hrs later, transfected COS-7 cell lysates were immunoblotted with pT-19 antibody or HA antibody. After stripping, the blot was re-probed with mouse PSD-95 antibody. (**C**) Bi-directional regulation of phospho-Thr-19 levels by NMDA treatment and chemical LTP induction. Cultured hippocampal neurons at DIV 24 ~ 28

were stimulated with NMDA (75 μM) or 200 μM glycine in ACSF lacking $MgCl_2$ (and returned to ACSF; see Materials and Methods) for indicated times, and immunoblotted with pT-19 antibody. After stripping, the blot was re-probed with mouse PSD-95 antibody. Graphs show time course of pT-19 band intensity (divided by total PSD-95) after stimulation ($n = 3$ for each experiment; normalized to untreated control). Statistical analysis was performed by one-way ANOVA, followed by the Dunnett's test. ** $p < 0.01$, compared to untreated control; * $p < 0.05$, compared to untreated control. (**D, E**) Pharmacological inhibition of GSK-3 activity (D) or RNAi knockdown of endogenous GSK-3beta (E) in cultured neurons reduces NMDA-induced Thr-19 phosphorylation of PSD-95. Cultured hippocampal neurons at DIV 25 were treated with DMSO, LiCl (10 mM), or SB216763 (10 μM) for ~16 hrs; or infected with RNAi lentivirus for 5 days. Cells were either untreated or treated with 75 μM NMDA for 10 min. Cell lysates were immunoblotted with pT-19 PSD-95, PSD-95, pS-9-GSK-3beta, GSK-3beta, pS-396 Tau, pS-295-PSD-95, pS-133 CREB, GSK-3alpha, or tubulin antibody.

Figure 3. Effects of RNAi knockdown of endogenous GSK-3beta and pharmacological inhibition of GSK-3 activities on NMDA-induced loss of synaptic PSD-95 levels. (**A, B**) Knockdown of endogenous GSK-3beta inhibits NMDA-induced loss of postsynaptic PSD-95. Cultured hippocampal neurons at DIV15-16 were cotransfected with luciferase-RNAi, or GSK-3beta-RNAi, plus beta-gal. Three days later, transfected neurons were either untreated or treated with 75 μM NMDA for 10 min, and then double labeled for beta-gal and PSD-95. Bar graph shows mean ± SEM of dendritic staining intensity of PSD-95, normalized to untransfected cells. Statistical analysis was performed by one-way ANOVA. $n = 11$ neurons for each. ** $p < 0.01$, *** $p < 0.001$ (**C**) Effect of pharmacological GSK-3 inhibitors on size of PSD-95 clusters. Cultured hippocampal neurons were pre- treated with DMSO, 10 mM LiCl or 10 μM SB216763 for ~16 hrs, then stimulated or not with 75 μM NMDA for 10 min. Neurons were fixed with cold methanol and stained for PSD-95. Bar graph shows mean ± SEM of PSD-95 puncta size, normalized to untreated cells. $n = 23, 29, 23, 26, 20$, and 24 from left to right. Statistical analysis was performed by one-way ANOVA. ** $p < 0.01$, *** $p < 0.001$.

Figure 4. Overexpression of T19A-PSD-95 inhibits LTD in CA1 neurons of organotypic hippocampal slice cultures. CA1 neurons were biolistically transfected with T19A-PSD-95,

WT-PSD-95, or T19D-PSD-95 (transfected cells identified by cotransfected GFP) and recorded together with untransfected neighboring cells in double whole-cell patch-clamp mode. LTD was induced by a pairing protocol (see Materials and Methods). Sample traces are shown above each experiment (thick line: average 10 minutes of EPSC recordings pre-LTD induction; thin line: average 10 minutes of EPSC recordings post-LTD induction). (**A**) LTD in T19A-PSD-95-transfected neurons compared with untransfected controls in the same slice (average LTD in transfected 79% ± 9%; untransfected control 47% ± 5%; $p = 0.0058$; $n = 10$ pairs). Scale bars: 100 pA/20 msec (transfected), 50 pA/20 msec (untransfected). (**B**) LTD in WT-PSD-95-transfected neurons and untransfected controls (average LTD in transfected 53% ± 3%; untransfected control 40% ± 6%; $p = 0.076$; $n = 8$ pairs). Scale bars: 100 pA/20 msec (transfected), 50 pA/20 msec (untransfected). (**C**) LTD in T19D-PSD-95-transfected neurons and untransfected controls (average LTD in transfected 48% ± 6%; untransfected control 43% ± 4%; $p = 0.49$; $n = 9$ pairs). Scale bars: 50 pA/20 msec (transfected), 40 pA/20 msec (untransfected).

Figure 1

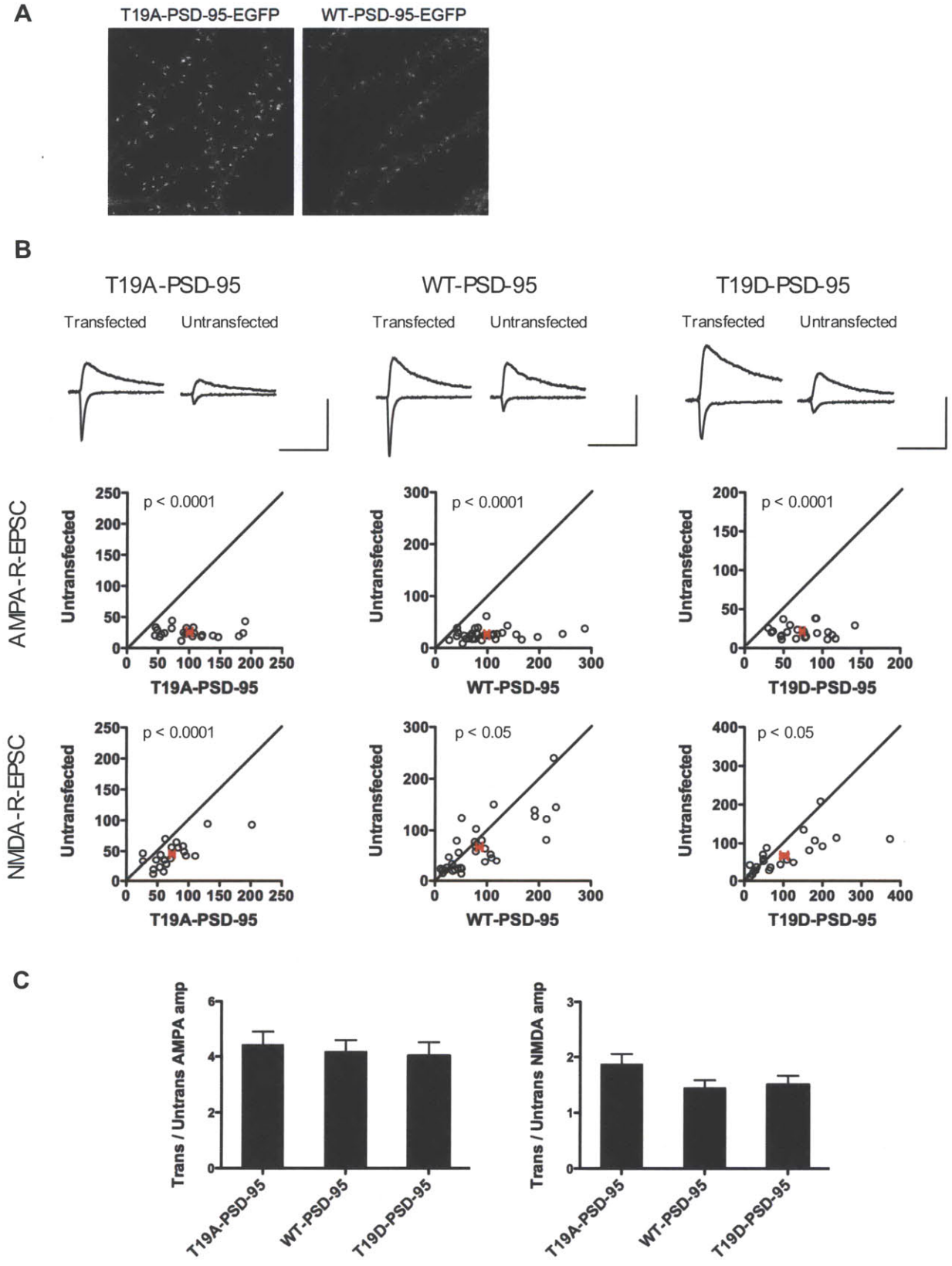
A
T19A-PSD-95-EGFP
WT-PSD-95-EGFP
B
T19A-PSD-95
WT-PSD-95
T19D-PSD-95
Transfected
Untransfected
AMPA-R-EPSC
NMDA-R-EPSC
Untransfected
T19A-PSD-95
WT-PSD-95
T19D-PSD-95
p < 0.0001
p < 0.05
C
Trans / Untrans AMPA amp
Trans / Untrans NMDA amp
T19A-PSD-95
WT-PSD-95
T19D-PSD-95

Figure 2

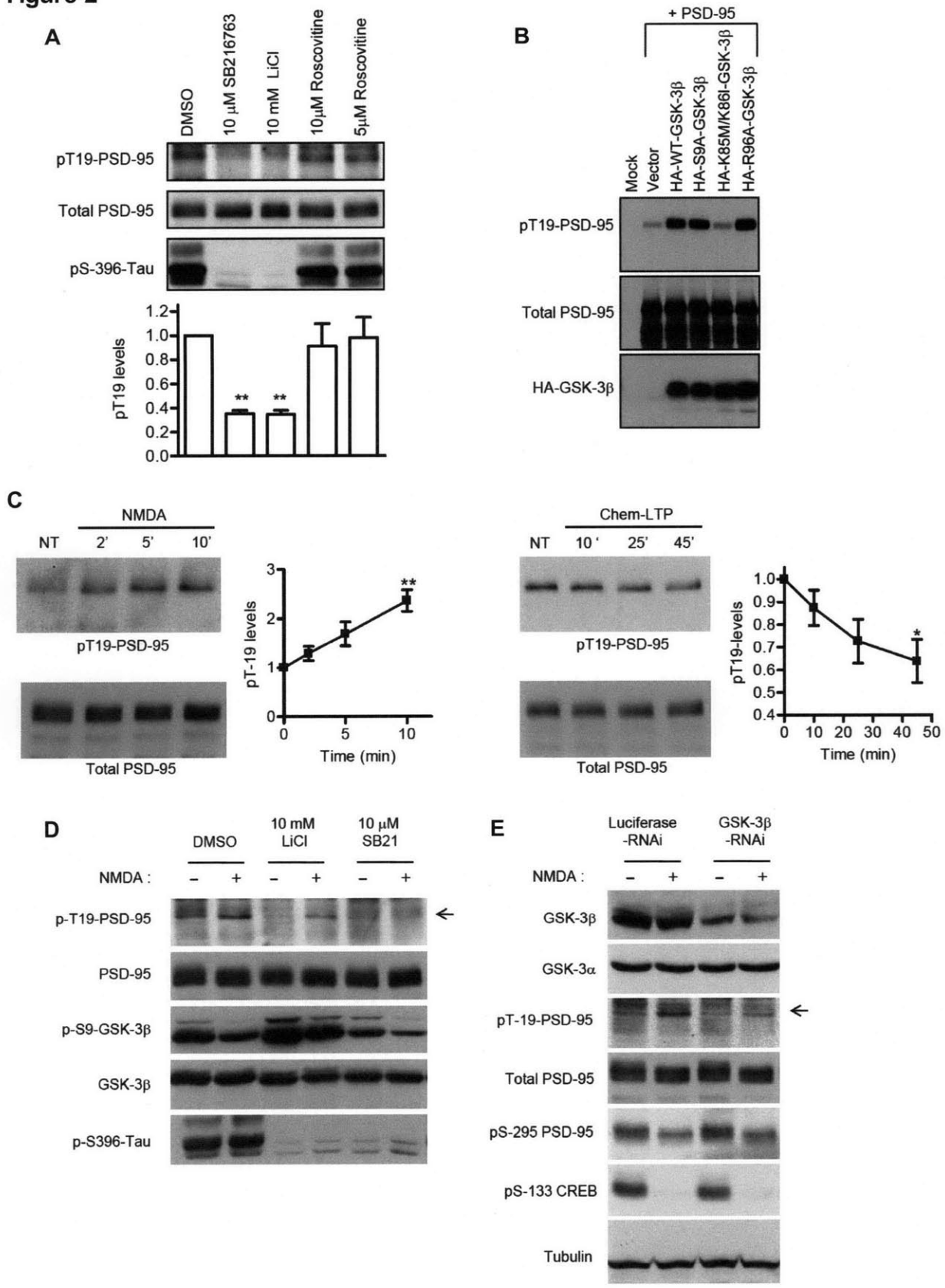
A
DMSO
10 μM SB216763
10 mM LiCl
10μM Roscovitine
5μM Roscovitine
pT19-PSD-95
Total PSD-95
pS-396-Tau
pT19 levels
1.2
1.0
0.8
0.6
0.4
0.2
0.0
**
**
B
+ PSD-95
Mock
Vector
HA-WT-GSK-3β
HA-S9A-GSK-3β
HA-K85M/K86I-GSK-3β
HA-R96A-GSK-3β
pT19-PSD-95
Total PSD-95
HA-GSK-3β
C
NMDA
NT
2'
5'
10'
pT19-PSD-95
Total PSD-95
pT-19 levels
3
2
1
0
0
5
10
Time (min)
**
Chem-LTP
NT
10 '
25'
45'
pT19-PSD-95
Total PSD-95
pT19-levels
1.0
0.9
0.8
0.7
0.6
0.5
0.4
0
10
20
30
40
50
Time (min)
*
D
DMSO
10 mM LiCl
10 μM SB21
NMDA :
– + – + – +
p-T19-PSD-95
PSD-95
p-S9-GSK-3β
GSK-3β
p-S396-Tau
E
Luciferase -RNAi
GSK-3β -RNAi
NMDA :
– + – +
GSK-3β
GSK-3α
pT-19-PSD-95
Total PSD-95
pS-295 PSD-95
pS-133 CREB
Tubulin

Figure 3

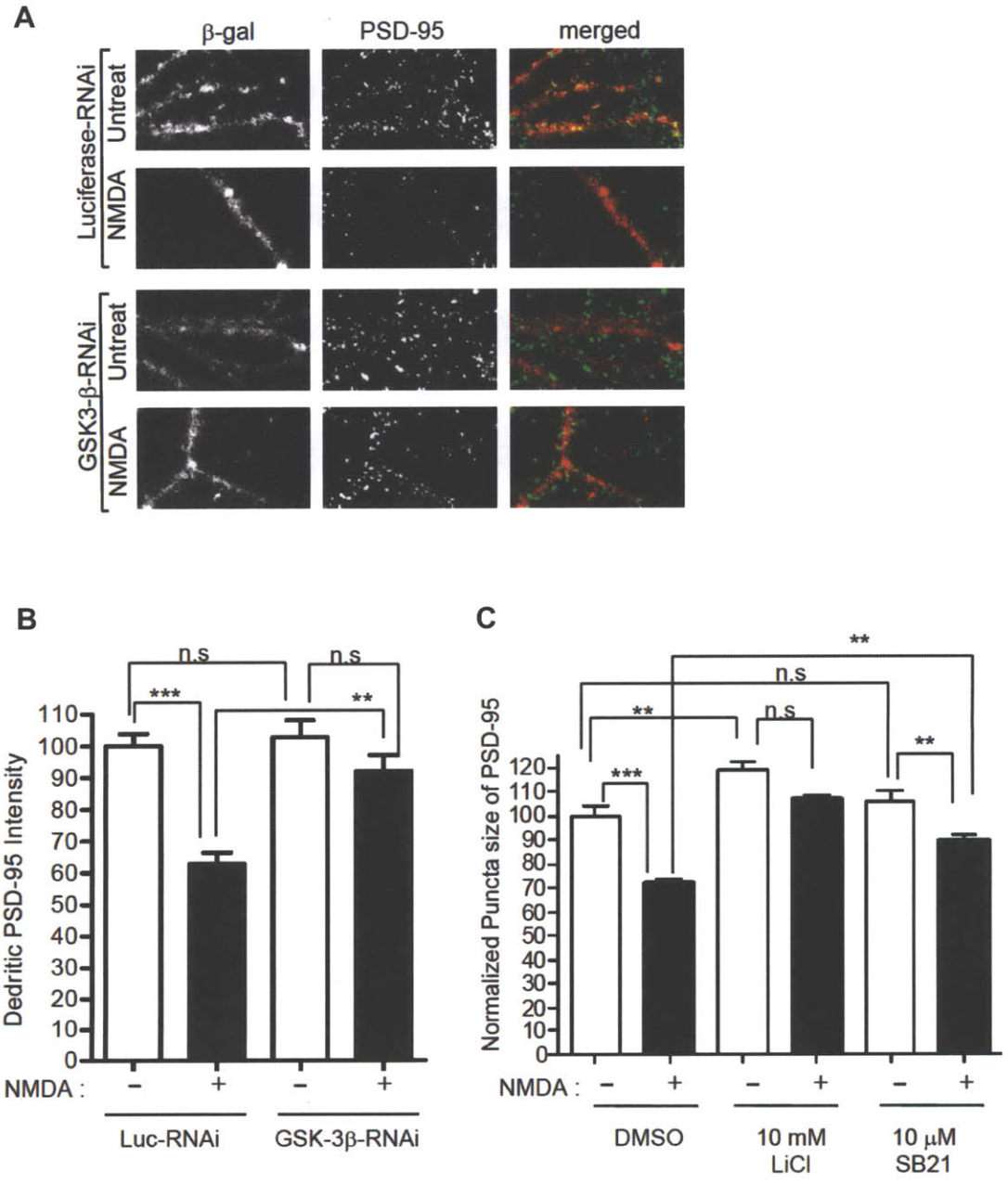
A
β-gal
PSD-95
merged
Luciferase-RNAi
Untreat
NMDA
GSK3-β-RNAi
Untreat
NMDA
B
n.s
n.s
***
**
Dedritic PSD-95 Intensity
110
100
90
80
70
60
50
40
30
20
10
0
NMDA : – + – +
Luc-RNAi
GSK-3β-RNAi
C
**
n.s
**
n.s
***
**
Normalized Puncta size of PSD-95
120
110
100
90
80
70
60
50
40
30
20
10
0
NMDA : – + – + – +
DMSO
10 mM LiCl
10 μM SB21

Figure 4

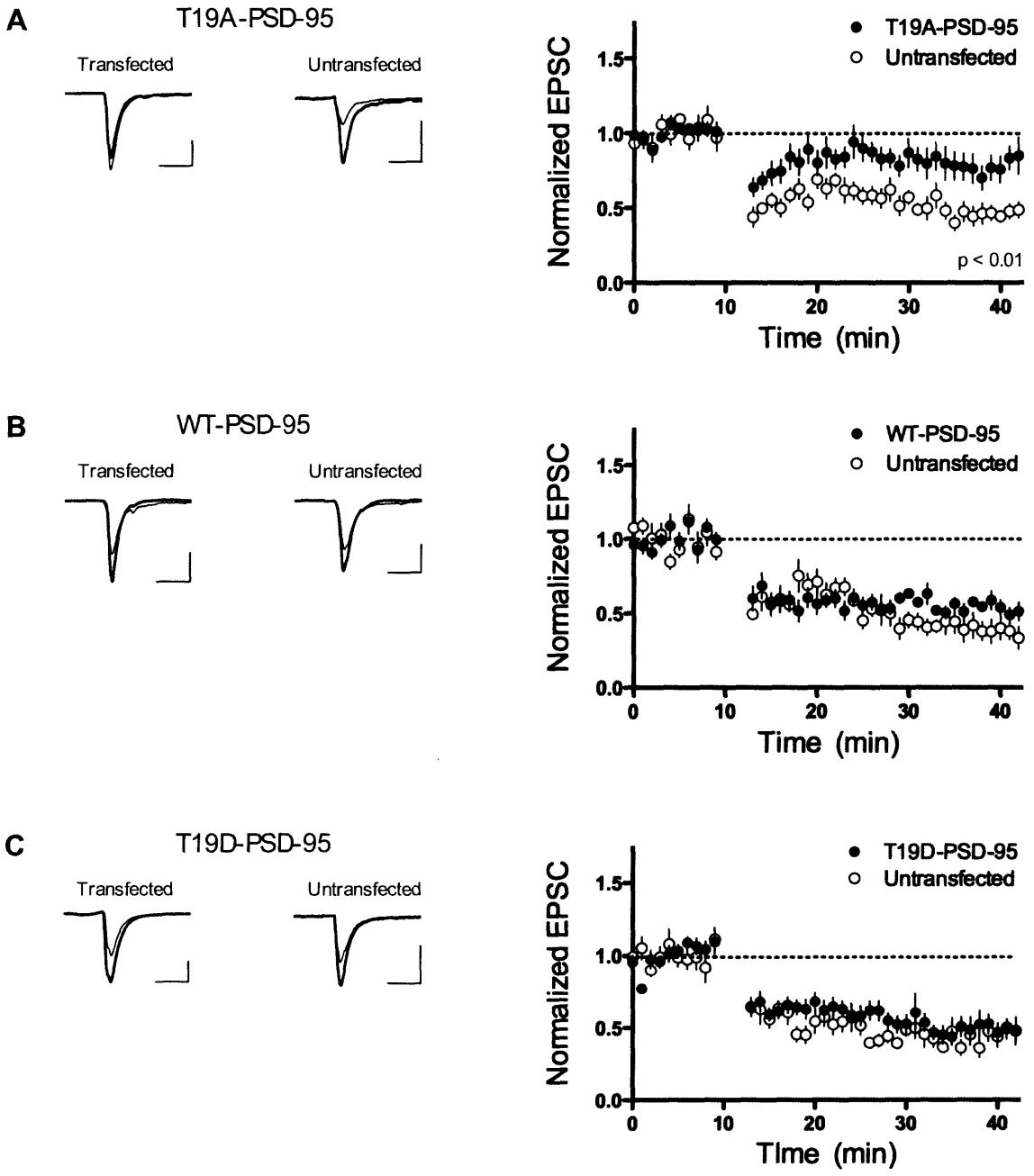
A
T19A-PSD-95
Transfected
Untransfected
Normalized EPSC
T19A-PSD-95
Untransfected
p < 0.01
Time (min)
B
WT-PSD-95
Transfected
Untransfected
Normalized EPSC
WT-PSD-95
Untransfected
Time (min)
C
T19D-PSD-95
Transfected
Untransfected
Normalized EPSC
T19D-PSD-95
Untransfected
Tlme (min)

References

Anderton, B.H. (1999). Alzheimer's disease: clues from flies and worms. Curr Biol 9, R106-109.

Bachmann, R.F., Schloesser, R.J., Gould, T.D., and Manji, H.K. (2005). Mood stabilizers target cellular plasticity and resilience cascades: implications for the development of novel therapeutics. Mol Neurobiol 32, 173-202.

Bats, C., Groc, L., and Choquet, D. (2007). The interaction between Stargazin and PSD-95 regulates AMPA receptor surface trafficking. Neuron 53, 719-734.

Beaulieu, J.M., Marion, S., Rodriguiz, R.M., Medvedev, I.O., Sotnikova, T.D., Ghisi, V., Wetsel, W.C., Lefkowitz, R.J., Gainetdinov, R.R., and Caron, M.G. (2008). A beta-arrestin 2 signaling complex mediates lithium action on behavior. Cell 132, 125-136.

Bhat, R.V., Budd Haeberlein, S.L., and Avila, J. (2004). Glycogen synthase kinase 3: a drug target for CNS therapies. J Neurochem 89, 1313-1317.

Bingol, B., and Schuman, E.M. (2004). A proteasome-sensitive connection between PSD-95 and GluR1 endocytosis. Neuropharmacology 47, 755-763.

Blanpied, T.A., Scott, D.B., and Ehlers, M.D. (2002). Dynamics and regulation of clathrin coats at specialized endocytic zones of dendrites and spines. Neuron 36, 435-449.

Bourgeron, T. (2007). The possible interplay of synaptic and clock genes in autism spectrum disorders. Cold Spring Harb Symp Quant Biol 72, 645-654.

Brown, T.C., Tran, I.C., Backos, D.S., and Esteban, J.A. (2005). NMDA receptor-dependent activation of the small GTPase Rab5 drives the removal of synaptic AMPA receptors during hippocampal LTD. Neuron 45, 81-94.

Christopherson, K.S., Sweeney, N.T., Craven, S.E., Kang, R., El-Husseini Ael, D., and Bredt, D.S. (2003). Lipid- and protein-mediated multimerization of PSD-95: implications for receptor clustering and assembly of synaptic protein networks. J Cell Sci 116, 3213-3219.

Colledge, M., Snyder, E.M., Crozier, R.A., Soderling, J.A., Jin, Y., Langeberg, L.K., Lu, H., Bear, M.F., and Scott, J.D. (2003). Ubiquitination regulates PSD-95 degradation and AMPA receptor surface expression. Neuron 40, 595-607.

Craven, S.E., El-Husseini, A.E., and Bredt, D.S. (1999). Synaptic targeting of the postsynaptic density protein PSD-95 mediated by lipid and protein motifs. Neuron 22, 497-509.

Doble, B.W., and Woodgett, J.R. (2003). GSK-3: tricks of the trade for a multi-tasking kinase. J Cell Sci 116, 1175-1186.

Ehrlich, I., and Malinow, R. (2004). Postsynaptic density 95 controls AMPA receptor incorporation during long-term potentiation and experience-driven synaptic plasticity. J Neurosci 24, 916-927.

El-Husseini, A.E., Schnell, E., Chetkovich, D.M., Nicoll, R.A., and Bredt, D.S. (2000). PSD-95 involvement in maturation of excitatory synapses. Science 290, 1364-1368.

El-Husseini Ael, D., Schnell, E., Dakoji, S., Sweeney, N., Zhou, Q., Prange, O., Gauthier-Campbell, C., Aguilera-Moreno, A., Nicoll, R.A., and Bredt, D.S. (2002). Synaptic strength regulated by palmitate cycling on PSD-95. Cell 108, 849-863.

Eldar-Finkelman, H. (2002). Glycogen synthase kinase 3: an emerging therapeutic target. Trends Mol Med 8, 126-132.

Elias, G.M., Funke, L., Stein, V., Grant, S.G., Bredt, D.S., and Nicoll, R.A. (2006). Synapse-specific and developmentally regulated targeting of AMPA receptors by a family of MAGUK scaffolding proteins. Neuron 52, 307-320.

Elias, G.M., and Nicoll, R.A. (2007). Synaptic trafficking of glutamate receptors by MAGUK scaffolding proteins. Trends Cell Biol 17, 343-352.
Funke, L., Dakoji, S., and Bredt, D.S. (2004). Membrane-Associated Guanylate Kinases Regulate Adhesion and Plasticity at Cell Junctions. Annu Rev Biochem.
Futai, K., Kim, M.J., Hashikawa, T., Scheiffele, P., Sheng, M., and Hayashi, Y. (2007). Retrograde modulation of presynaptic release probability through signaling mediated by PSD-95-neuroligin. Nat Neurosci 10, 186-195.
Gray, J.A., and Roth, B.L. (2007). The pipeline and future of drug development in schizophrenia. Mol Psychiatry 12, 904-922.
Grimes, C.A., and Jope, R.S. (2001). The multifaceted roles of glycogen synthase kinase 3beta in cellular signaling. Prog Neurobiol 65, 391-426.
Hirabayashi, S., Nishimura, W., Iida, J., Kansaku, A., Kishida, S., Kikuchi, A., Tanaka, N., and Hata, Y. (2004). Synaptic scaffolding molecule interacts with axin. J Neurochem 90, 332-339.
Hsueh, Y.P., Kim, E., and Sheng, M. (1997). Disulfide-linked head-to-head multimerization in the mechanism of ion channel clustering by PSD-95. Neuron 18, 803-814.
Hsueh, Y.P., and Sheng, M. (1999). Requirement of N-terminal cysteines of PSD-95 for PSD-95 multimerization and ternary complex formation, but not for binding to potassium channel Kv1.4. J Biol Chem 274, 532-536.
Javitt, D.C. (2004). Glutamate as a therapeutic target in psychiatric disorders. Mol Psychiatry 9, 984-997, 979.
Kauer, J.A., and Malenka, R.C. (2007). Synaptic plasticity and addiction. Nat Rev Neurosci 8, 844-858.
Kim, E., and Sheng, M. (2004). PDZ domain proteins of synapses. Nat Rev Neurosci 5, 771-781.
Kim, M.J., Futai, K., Jo, J., Hayashi, Y., Cho, K., and Sheng, M. (2007). Synaptic accumulation of PSD-95 and synaptic function regulated by phosphorylation of serine-295 of PSD-95. Neuron 56, 488-502.
Knobloch, M., and Mansuy, I.M. (2008). Dendritic spine loss and synaptic alterations in Alzheimer's disease. Mol Neurobiol 37, 73-82.
Lau, C.G., and Zukin, R.S. (2007). NMDA receptor trafficking in synaptic plasticity and neuropsychiatric disorders. Nat Rev Neurosci 8, 413-426.
Lee, H.K., Kameyama, K., Huganir, R.L., and Bear, M.F. (1998). NMDA induces long-term synaptic depression and dephosphorylation of the GluR1 subunit of AMPA receptors in hippocampus. Neuron 21, 1151-1162.
Lee, H.K., Takamiya, K., Han, J.S., Man, H., Kim, C.H., Rumbaugh, G., Yu, S., Ding, L., He, C., Petralia, R.S., et al. (2003). Phosphorylation of the AMPA receptor GluR1 subunit is required for synaptic plasticity and retention of spatial memory. Cell 112, 631-643.
Lee, S.H., Liu, L., Wang, Y.T., and Sheng, M. (2002). Clathrin adaptor AP2 and NSF interact with overlapping sites of GluR2 and play distinct roles in AMPA receptor trafficking and hippocampal LTD. Neuron 36, 661-674.
Leroy, K., and Brion, J.P. (1999). Developmental expression and localization of glycogen synthase kinase-3beta in rat brain. J Chem Neuroanat 16, 279-293.
Lin, C.F., Chen, C.L., Chiang, C.W., Jan, M.S., Huang, W.C., and Lin, Y.S. (2007). GSK-3beta acts downstream of PP2A and the PI 3-kinase-Akt pathway, and upstream of caspase-2 in ceramide-induced mitochondrial apoptosis. J Cell Sci 120, 2935-2943.

Lu, W., Man, H., Ju, W., Trimble, W.S., MacDonald, J.F., and Wang, Y.T. (2001). Activation of synaptic NMDA receptors induces membrane insertion of new AMPA receptors and LTP in cultured hippocampal neurons. Neuron 29, 243-254.

Malenka, R.C., and Bear, M.F. (2004). LTP and LTD: an embarrassment of riches. Neuron 44, 5-21.

Man, H.Y., Wang, Q., Lu, W.Y., Ju, W., Ahmadian, G., Liu, L., D'Souza, S., Wong, T.P., Taghibiglou, C., Lu, J., et al. (2003). Activation of PI3-kinase is required for AMPA receptor insertion during LTP of mEPSCs in cultured hippocampal neurons. Neuron 38, 611-624.

Morabito, M.A., Sheng, M., and Tsai, L.H. (2004). Cyclin-dependent kinase 5 phosphorylates the N-terminal domain of the postsynaptic density protein PSD-95 in neurons. J Neurosci 24, 865-876.

Morishita, W., Connor, J.H., Xia, H., Quinlan, E.M., Shenolikar, S., and Malenka, R.C. (2001). Regulation of synaptic strength by protein phosphatase 1. Neuron 32, 1133-1148.

Mulkey, R.M., Endo, S., Shenolikar, S., and Malenka, R.C. (1994). Involvement of a calcineurin/inhibitor-1 phosphatase cascade in hippocampal long-term depression. Nature 369, 486-488.

Nakagawa, T., Futai, K., Lashuel, H.A., Lo, I., Okamoto, K., Walz, T., Hayashi, Y., and Sheng, M. (2004). Quaternary structure, protein dynamics, and synaptic function of SAP97 controlled by L27 domain interactions. Neuron 44, 453-467.

Newpher, T.M., and Ehlers, M.D. (2008). Glutamate receptor dynamics in dendritic microdomains. Neuron 58, 472-497.

Pei, J.J., Tanaka, T., Tung, Y.C., Braak, E., Iqbal, K., and Grundke-Iqbal, I. (1997). Distribution, levels, and activity of glycogen synthase kinase-3 in the Alzheimer disease brain. J Neuropathol Exp Neurol 56, 70-78.

Peineau, S., Taghibiglou, C., Bradley, C., Wong, T.P., Liu, L., Lu, J., Lo, E., Wu, D., Saule, E., Bouschet, T., et al. (2007). LTP inhibits LTD in the hippocampus via regulation of GSK3beta. Neuron 53, 703-717.

Peng, J., Kim, M.J., Cheng, D., Duong, D.M., Gygi, S.P., and Sheng, M. (2004). Semiquantitative proteomic analysis of rat forebrain postsynaptic density fractions by mass spectrometry. J Biol Chem 279, 21003-21011.

Regalado, M.P., Terry-Lorenzo, R.T., Waites, C.L., Garner, C.C., and Malenka, R.C. (2006). Transsynaptic signaling by postsynaptic synapse-associated protein 97. J Neurosci 26, 2343-2357.

Sala, C., Rudolph-Correia, S., and Sheng, M. (2000). Developmentally regulated NMDA receptor-dependent dephosphorylation of cAMP response element-binding protein (CREB) in hippocampal neurons. J Neurosci 20, 3529-3536.

Scannevin, R.H., and Huganir, R.L. (2000). Postsynaptic organization and regulation of excitatory synapses. Nat Rev Neurosci 1, 133-141.

Schnell, E., Sizemore, M., Karimzadegan, S., Chen, L., Bredt, D.S., and Nicoll, R.A. (2002). Direct interactions between PSD-95 and stargazin control synaptic AMPA receptor number. Proc Natl Acad Sci U S A 99, 13902-13907.

Scolnick, E.M. (2006). Mechanisms of action of medicines for schizophrenia and bipolar illness: status and limitations. Biol Psychiatry 59, 1039-1045.

Sheng, M., and Hoogenraad, C.C. (2007). The postsynaptic architecture of excitatory synapses: a more quantitative view. Annu Rev Biochem 76, 823-847.

Shepherd, J.D., and Huganir, R.L. (2007). The cell biology of synaptic plasticity: AMPA receptor trafficking. Annu Rev Cell Dev Biol 23, 613-643.

Songyang, Z., Lu, K.P., Kwon, Y.T., Tsai, L.H., Filhol, O., Cochet, C., Brickey, D.A., Soderling, T.R., Bartleson, C., Graves, D.J., et al. (1996). A structural basis for substrate specificities of protein Ser/Thr kinases: primary sequence preference of casein kinases I and II, NIMA, phosphorylase kinase, calmodulin-dependent kinase II, CDK5, and Erk1. Mol Cell Biol 16, 6486-6493.

Stein, V., House, D.R., Bredt, D.S., and Nicoll, R.A. (2003). Postsynaptic density-95 mimics and occludes hippocampal long-term potentiation and enhances long-term depression. J Neurosci 23, 5503-5506.

Sturgill, J.F., Steiner P., Czervionke B.L., and Sabatini B.L. (2009) Distinct domains within PSD-95 mediate synaptic incorporation, stabilization, and activity-dependent trafficking. J Neurosci 29:12845-12854.

Welsh, G.I., and Proud, C.G. (1993). Glycogen synthase kinase-3 is rapidly inactivated in response to insulin and phosphorylates eukaryotic initiation factor eIF-2B. Biochem J 294 (Pt 3), 625-629.

Xu, W., Schluter, O.M., Steiner, P., Czervionke, B.L., Sabatini, B., and Malenka, R.C. (2008). Molecular dissociation of the role of PSD-95 in regulating synaptic strength and LTD. Neuron 57, 248-262.

Zhang, F., Phiel, C.J., Spece, L., Gurvich, N., and Klein, P.S. (2003). Inhibitory phosphorylation of glycogen synthase kinase-3 (GSK-3) in response to lithium. Evidence for autoregulation of GSK-3. J Biol Chem 278, 33067-33077.

CHAPTER 3:

PYK2 is required for long term depression and regulates ERK signaling

Honor Hsin, Myung Jong Kim, Chi-Fong Wang, and Morgan Sheng

HH performed electrophysiology experiments in Figures 2, 3, 4, 7. MJK performed early foundational work for this study, including lentiviral construction in Figure S2A, and contributed intellectually to the study. HH contributed and supervised CFW in performing imaging and biochemical experiments in Figures 1, 5, 6, S1, S2B, and S3-5. This chapter is adapted from a manuscript under consideration at *Journal of Neuroscience.*

Abstract

Proline-rich tyrosine kinase 2 (PYK2), also known as cell adhesion kinase beta (CAKbeta) or protein tyrosine kinase 2b (PTK2B), is a calcium-dependent signaling protein involved in cell migration. Phosphorylation of residue Y402 is associated with activation of PYK2, and leads to the recruitment of downstream signaling molecules. PYK2 was previously implicated in long term potentiation (LTP); however, the role of PYK2 in long term depression (LTD) is unknown. Here we report that PYK2 is activated by NMDA receptor stimulation (chemical LTD) in cultured neurons. Small hairpin RNA (shRNA)-mediated knockdown of PYK2 blocks LTD, but not LTP, in hippocampal slice cultures. Both the Y402 residue and PYK2 kinase activity contribute to PYK2's role in LTD. Knockdown experiments indicate that PYK2 is required to suppress NMDA-induced ERK phosphorylation. Overexpression of PYK2 depresses NMDA-induced ERK phosphorylation, and inhibits LTP, but not LTD. Our studies support a mechanism whereby PYK2 antagonizes ERK signaling to promote LTD, at the expense of LTP, in hippocampal neurons.

Introduction

Activity-dependent modification of synapses is widely considered to be a mechanism for learning and memory. In the commonly studied forms of hippocampal synaptic plasticity – NMDA receptor (NMDAR)-dependent LTP and LTD – different levels and/or kinetics of NMDAR-mediated calcium influx are believed to activate distinct signaling pathways. Calcium elevation during LTP promotes activity of calcium/calmodulin-dependent kinase II and AMPA receptor (AMPAR) insertion into the postsynaptic membrane (Malenka et al., 1989; Malinow et al., 1989; Silva et al., 1992), whereas calcium influx during LTD promotes AMPAR endocytosis depending on activity of serine/threonine phosphatases like calcineurin (Mulkey et al., 1993, 1994; Morishita et al., 2001). Src family kinases can contribute to LTP through the phosphorylation and functional enhancement of NMDARs (Grant et al., 1992; Lu et al., 1998). Differential activation of Ras family GTPases and downstream mitogen activated protein kinase (MAPK) pathways may determine the direction of activity-dependent synaptic modification during LTP or LTD (Zhu et al., 2002; Kim et al., 2005; Zhu et al., 2005). Sustained activation of the MAPK ERK, for example, is believed to promote LTP (English and Sweatt, 1997; Zhu et al,

2002). These signaling mechanisms help explain how NMDAR activation can lead to distinct functional outcomes in neurons.

PYK2 is a calcium-dependent tyrosine kinase found in the postsynaptic density (PSD) of central neurons (Huang et al., 2001; Collins et al., 2006; reviewed in Sheng and Hoogenraad, 2007). In non-neuronal cells, PYK2 is involved in osteoclast function (Gil-Henn et al., 2007), macrophage migration (Okigaki et al., 2003), and focal adhesion disassembly (Hashido et al., 2006). While the precise mechanism of PYK2 activation remains unclear, it is believed that a rise in intracellular calcium can directly or indirectly induce dimerization of PYK2 and trans-autophosphorylation at Y402, a residue located N-terminal to the kinase domain (Lev et al., 1995; Park et al., 2004; Kohno et al., 2008, Bartos et al., 2010). In hematopoietic cells, the phosphorylated Y402 and surrounding residues mediate association with and activation of Src family kinases, which in turn phosphorylate additional tyrosine residues in the PYK2 kinase domain to enhance PYK2 kinase activity (Park et al., 2004). Thus Y402 phosphorylation is commonly used as a marker of activated PYK2. Tyrosine phosphorylation of PYK2 also leads to changes in MAPK activity, although the direction of change and the subtype of MAPK affected vary across different cell types (Girault et al., 1999; Zhao et al., 2000).

Using recombinant PYK2 proteins, Huang et al. (2001) found that PYK2 is involved in LTP and the Src-dependent pathway of NMDAR potentiation. The role of PYK2 in synaptic plasticity, however, has not been examined by a molecular genetic approach. Interestingly, PYK2 is reported to bind PSD-95 (Seabold et al., 2003), an abundant scaffold protein of the PSD that promotes synaptic strength and that is required for LTD (Migaud et al., 1998; Stein et al., 2003; Ehrlich and Malinow, 2004; Kim et al., 2007; Xu et al., 2008). Because PYK2 is calcium-regulated, associates with PSD-95, and functions in reorganizing specialized adhesion sites, we hypothesized that PYK2 may play a role in LTD at neuronal synapses. We report here that PYK2 phosphorylation at Y402 is enhanced by stimulation of NMDARs that mimics LTD (chem-LTD) and that PYK2 is required for LTD. PYK2 dampens NMDAR-dependent activation of ERK MAPKs, a function consistent with PYK2's critical role in LTD.

Materials and Methods

Antibodies and chemicals

The following antibodies were used in this study (purchased from Cell Signaling Technology, unless indicated otherwise): rabbit anti-GluR1 (Millipore), rabbit anti-phospho S845 GluR1 (Chemicon), rabbit anti-phospho Y402 PYK2 (Invitrogen), mouse anti-PYK2 (BD Biosciences), rabbit anti-phospho Y416 Src, rabbit anti-Src, mouse anti-phospho T202/Y204 ERK, rabbit anti-ERK, rabbit anti-phospho S9 GSK3beta, rabbit anti-GSK3beta, rabbit anti-phospho T308 Akt, rabbit anti-Akt, rabbit anti-phospho T183/Y185 JNK, rabbit anti-JNK, mouse anti-tubulin (Sigma), anti-NR2A (Covance), anti-NR2B (NeuroMab), anti-PSD95 (NeuroMab), mouse anti-myc (Santa Cruz Biotechnology). The following chemicals were used (purchased from Sigma unless indicated otherwise): NMDA, tetrodotoxin (Tocris), NBQX (Tocris), nimodipine, picrotoxin, chlor-adenosine.

DNA constructs and Lentivirus shRNA

WT-PYK2 construct (myc-tagged in pCMV vector) was a gift from Dr. Wen-Cheng Xiong, Medical College of Georgia (Xiong and Parsons, 1997). For PYK2 shRNA, the following oligonucleotides were annealed and inserted into the *Hin*dIII/*Bgl*II sites of pSuper vector (Brummelkamp et al., 2002): 5'-GAT CCC CGC TGT AGC ATA GAG TCA GAT TCA AGA GAT CTG ACT CTA TGC TAC AGC TTT TTA-3'; 5'-AGC TTA AAA AGC TGT AGC ATA GAG TCA GAT CTC TTG AAT CTG ACT CTA TGC TAC AGC GGG-3'. The final target sequence of PYK2 shRNA is 5'-GCT GTA GCA TAG AGT CAG A-3'. Luciferase shRNA (in pSuper vector) was a gift from Dr. Huaye Zhang, University of Virginia (Zhang and Macara, 2006). The target sequence of luciferase shRNA is 5'-CGT ACG CGG AAT ACT TCG A-3'.

Lentiviral transfer vector constructs were modified from the original FUGW vector backbone (Lois et al., 2002). H1 promoter cassettes from pSuper constructs (PYK2 shRNA and luciferase shRNA) were cloned between the HIV-flap and synapsin promoter. For the production of lentiviral vectors, the transfer vector, packaging vector Δ8.2 and VSVG envelope vector were cotransfected into HEK293 cells. Supernatants of culture media were collected 48 hours after transfection, and centrifuged at 50,000 x g to concentrate the lentivirus.
PYK2 mutants were constructed by site-directed mutagenesis (Stratagene Quikchange kit). The following primers were used: (1) For Y402F-PYK2, 5'-GCA TAG AGT CAG ACA TCT TTG CAG AGA TTC CTG ATG AG-3' (2) For K457A-PYK2, 5'-GAA AAA ATT AAT GTG GCC

GTC GCG ACC TGT AAG AAA GAT TGT ACC-3' (3) For WT-PYK2* or K457A-PYK2*, two sequential reactions were performed to introduce 9 point mutations spread throughout the target region (final shRNA-resistant target region: 5'-GCT GCT CTA TTG AAA GCG A-3'). Primer set 1, 5'-CGG TCC CAC CTC TCA GAA AGC TGC TCT ATA GAG TCA GAC ATC TAT GCA GAG-3'; Primer set 2, 5'-CCC ACC TCT CAG AAA GCT GCT CTA TTG AAA GCG ACA TCT ATG CAG AGA TTC C-3'.

Cell culture and chem-LTD

HEK293 cells were maintained in DMEM (Gibco), supplemented with 10% fetal bovine serum (Gibco) and penicillin/streptomycin (Gibco), and transiently transfected with plasmids using Lipofectamine 2000 (Invitrogen). Cells were harvested after 24-48 hours. Hippocampal neurons were cultured as described (Kim et al., 2007), and infected with lentivirus in the media at DIV15 for 7 days in vitro. Mature cultured neurons (DIV 21-26) in 12-well plates were treated for 10 minutes with 20 μM NBQX, 2 μM tetrodotoxin, and 5 μM nimodipine before treatment with 70 μM NMDA for 2.5, 5, or 15 minutes (or untreated). Plates were then placed on ice, and each well was washed with ice-cold PBS before lysing in 2X sample buffer (containing beta-mercaptoethanol). For experiments with calcineurin inhibitors, FK506 (1 μM) or cyclosporine A (1 μM) were added to neurons for 10 minutes-1 hour prior to NMDA treatment.

Hippocampal slice culture

Organotypic slice cultures were prepared from postnatal day-7 rat hippocampus as described (Sala et al., 2003; Seeburg and Sheng, 2008). Rat brains were dissected in ice-cold buffer containing (in mM): sucrose (238), KCl (2.5), NaHCO3 (26), NaH2PO4 (1), glucose (11), MgCl2 (5) and CaCl2 (1). Hippocampi were cut into 350 mm-thick slices with a McIlwain tissue chopper, and plated on tissue inserts (Millipore) in wells with MEM (Cellgro) culture media containing (in mM): glucose (26), NaHCO3 (5.8), HEPES (30), CaCl2 (2), MgSO4 (2), and supplemented with horse serum (20%), insulin (1 μg/μl), and ascorbic acid (0.0012%). Slices were incubated in 5% CO2 at 35°C.

Electrophysiology

Electrophysiological recordings were performed as described (Kim et al., 2007; Seeburg and Sheng, 2008). Neurons were transfected by biolistic gene gun at DIV 3-5 (total 100 μg DNA; 90% test DNA construct; 10% eGFP marker) and recorded 3 days after transfection. Recordings were carried out in solution containing (in mM): NaCl (119), KCl (2.5), CaCl2 (4), MgCl2 (4), NaHCO3 (26), NaH2PO4 (1), glucose (11), picrotoxin (0.1), and 2-chloroadenosine (0.002-0.004), and bubbled continuously with 5% CO2/95% O2. Patch recording pipettes (2.5-5 M ohms) were filled with internal solution containing (in mM): cesium methanesulfonate (115), CsCl (20), HEPES (10), MgCl2 (2.5), ATP disodium salt (4), GTP trisodium salt (0.4), sodium phosphocreatine (10), and EGTA (0.6), at pH 7.25. Simultaneous whole-cell recordings were obtained from a pair of transfected and neighboring untransfected CA1 pyramidal neurons during stimulation of presynaptic Schaffer collaterals. For basal synaptic transmission experiments, presynaptic fibers were stimulated at 0.2 Hz. AMPAR EPSCs were recorded at -70 mV, and NMDAR EPSCs at +40 mV in the presence of 0.01 mM NBQX. Each data point represents an average of 60 consecutive synaptic responses. For LTD experiments, presynaptic fibers were stimulated at 0.033 Hz during baseline recordings, and synaptic responses were obtained at -70 mV. After at least 10 minutes of baseline recording, LTD was induced by pairing 1 Hz stimulation (200 pulses) with depolarization of the postsynaptic cell to -40 mV. Synaptic responses were then obtained under baseline conditions. For LTP experiments, presynaptic fibers were stimulated at 0.2 Hz during baseline recordings, and synaptic responses obtained at -70 mV. After at least 3 minutes of baseline recording, LTP was induced by pairing 3 Hz stimulation (200 pulses) with postsynaptic depolarization to 0 mV. Synaptic responses were then obtained under baseline conditions. For plasticity experiments, data was collected only if the untransfected cell in a paired recording displayed LTD or LTP.

All recordings were made using a Multiclamp 700A amplifier (Molecular Devices), and data was digitized at 20 kHz with Digidata 1322A (Molecular Devices). Analysis of recordings was performed using Clampfit software (Molecular Devices) for basal transmission experiments, or Igor Pro software (Wavemetrics) for plasticity experiments. Results are expressed as mean ± SEM, and statistical significance was assessed by paired Student's t-test on mean EPSC amplitude for basal transmission experiments, or on mean normalized EPSC (averaged over the last 10 minutes of post-induction recordings) for plasticity experiments.

Immunostaining

Hippocampal cultured neurons were transiently transfected at DIV16-19 with a mix of test DNA construct (80%) and marker (20%; eGFP or beta-galactosidase) using Lipofectamine 2000 (Invitrogen). The control construct used was an empty myc-tag vector. For dendritic spine morphology studies, neurons were fixed three days later in 4% PFA/4% sucrose/PBS, immunostained for eGFP (rabbit anti-GFP from MBL, goat anti-rabbit IgG Alexa 488 conjugate secondary antibody from Invitrogen, all in GDB buffer [30 mM phosphate buffer pH 7.4, 0.1% gelatin, 0.3% Triton-X100, 0.45 M NaCl]), and imaged by confocal microscopy on an LSM510 microscope (Zeiss) as described previously (Tada et al, 2007). Analysis of neuron morphology was performed with Metamorph software (Molecular Devices). For phospho-ERK studies, neurons were pre-treated three days after transfection with 1 μM TTX (1 hr), 20 μM NBQX (10 minutes), and 5 μM nimodipine (10 minutes), followed by exposure to 70 μM NMDA for 2.5 or 5 minutes. Neurons were immediately fixed in 4% PFA/4% sucrose/TBS (made immediately prior to fixation), and immunostained for phospho-ERK (rabbit anti-phospho ERK from Cell Signaling Technologies, goat anti-rabbit IgG Alexa 488 conjugate secondary antibody from Invitrogen) and beta-galactosidase (mouse anti-beta-galactosidase from Promega, goat anti-mouse IgG Alexa 568 conjugate secondary antibody from Invitrogen). The confocal microscope settings were kept the same for all scans within the experiment, and average fluorescence intensity measurements were obtained from cell somas with Metamorph software. Results were all normalized to the untreated empty-vector control, and expressed as mean ± SEM. Analysis was by two-tailed Student's t-test, between experimental and control neurons for each time point.

Western blot

Protein samples were separated on 6% (for PYK2 or GluR1 blotting) or 10% (all others) SDS-PAGE gels in running buffer (25 mM Tris, 200 mM Glycine, 0.1% SDS). Gels were transferred to PVDF membranes (BioRad) in running buffer without SDS. Membranes were blocked with 5% skim milk powder in Tris-buffered saline (TBS, pH 7.6) with 0.1% Tween-20, and probed overnight at 4°C with primary antibodies in TBS-Tween-20 with 5% BSA and 0.01% sodium azide. Membranes were then washed in TBS with 0.2% Triton X-100, and probed with sheep anti-mouse or donkey anti-rabbit HRP-linked secondary antibodies (GE Healthcare) in 5% milk TBS-Tween-20. After a second set of washes in TBS-Triton X-100, membranes were

exposed to ECL chemiluminescence reagent (Perkin-Elmer Life Sciences), and developed on an X-OMAT processor (Kodak). For phospho-antibody blots, membranes were subsequently washed in stripping buffer (Thermo Scientific), re-blocked, and then re-probed with antibody against total protein. Quantification was performed using Scion Image software (Scion Corp), and results are expressed as mean normalized ratio (ratio of phospho-signal to total protein, normalized to an untreated control) ± SEM.

Subcellular and biochemical fractionation

PSD fractionation was performed on bilateral hippocampi dissected from a postnatal day 17 male rat, using a procedure modified from Han et al. (2009). Briefly, tissues were homogenized in 0.32 M sucrose, 4 mM HEPES pH 7.4 (homogenate) and spun at 1,000 x g for 10 minutes for supernatant (S1) and pellet (P1) fractions. S1 was spun at 10,000 x g for 15 minutes to obtain supernatant (S2) and the crude synaptosomal pellet (P2). P2 was washed once in homogenate buffer, lysed by hypo-osmotic shock in water, homogenized, and agitated for 30 minutes in 4 mM HEPES 7.4. This lysate was then spun at 25,000 x g for 20 minutes to obtain the synaptosomal cytosolic fraction (LS1) and synaptosomal membrane fraction (LP1). LP1 was resuspended in 50 mM HEPES pH 7.4, 2 mM EDTA, 0.5% Triton X-100, agitated for 15 minutes, and spun at 32,000 x g for 20 minutes to obtain PSD I pellet. PSD I was resuspended in 50 mM HEPES pH 7.4, 2 mM EDTA, 0.5% Triton X-100, agitated for 15 minutes, and spun at 200,000 x g for 20 minutes, to obtain PSD II pellet. All fractions were quantified by Pierce BCA Protein Assay (Thermo Scientific). All steps were performed at 4 degrees, with cocktail protease inhibitors, Ser/Thr phosphatase inhibitors, and Tyr phosphatase inhibitors (Calbiochem).

For Triton X-100 solubility experiments, cultured neurons in 6 well-plates (DIV 22) were pre-treated for 10 minutes with 20 μM NBQX, 2 μM tetrodotoxin, and 5 μM nimodipine before treatment with 70 μM NMDA for 5 minutes (or untreated), and then placed immediately on ice and homogenized in buffer containing 50 mM HEPES 7.4, 2 mM EDTA, 0.5% Triton X-100, 0.1 mM PMSF, with cocktail protease inhibitors, tyrosine phosphatase inhibitors, and serine/threonine phosphatase inhibitors (Calbiochem). Homogenates were agitated for 20 minutes, then spun at 20,000 g for 20 minutes. Pellet fractions were solubilized in the same buffer with 1% SDS, and boiled for 5 minutes. Homogenate, supernatant, and pellet fractions

were quantified by Pierce BCA Protein Assay (Thermo Scientific) prior to loading on SDS-PAGE gels (10 μg protein per well).

Results

Chem-LTD regulates PYK2 phosphorylation at Y402

PYK2 is detected in the PSD of adult rat hippocampus (Figure 1A), as described previously (Huang et al., 2001; Collins et al., 2006). We first examined whether NMDAR activation regulates PYK2 activity using Y402 phosphorylation as a marker. In cultured hippocampal neurons (DIV 21-26), bath application of NMDA (70 μM for 2.5 or 5 minutes) results in endocytosis of AMPARs, which is associated with dephosphorylation of GluR1 at Ser-845 (Lee et al., 1998; Figure 1B). This chem-LTD protocol also induced a rapid and transient increase in PYK2 Y402 phosphorylation, peaking at ~1.5-2-fold above basal levels within 5 minutes of NMDAR stimulation (Figure 1C). Incidentally, the immunoblots also revealed a persistent shift in the migration of total PYK2 after chem-LTD treatment that is opposite of what would be expected with an increase in tyrosine phosphorylation (Figure 1C). This finding is consistent, however, with previous reports suggesting that PYK2 Y402 phosphorylation occurs simultaneously with calcineurin-mediated dephosphorylation of multiple PYK2 Ser/Thr residues, resulting in a net downward shift in PYK2 mobility by SDS-PAGE (Faure et al., 2007). In fact, the NMDA-dependent shift in PYK2 mobility was partially blocked by chemical inhibitors of calcineurin (Figure S1A).

At 2.5 and 5 minutes treatment, chem-LTD additionally caused a redistribution of total PYK2 protein from Triton-soluble to Triton-insoluble fractions of cultured neurons (Figure S1B), although we did not discern any change in PYK2 localization, as assayed by immunostaining (data not shown). PYK2 phosphorylated on Y402 was not specifically enriched in the insoluble fraction after chem-LTD (Figure S1B), implying that Y402 phosphorylation and subcellular redistribution are not directly linked. Together, our data indicate that NMDAR activation results in enhanced activity, as well as altered biochemical distribution, of PYK2 in hippocampal neurons.

PYK2 knockdown blocks LTD

Because PYK2 is activated during chem-LTD, we asked whether PYK2 activity is required for LTD. We designed a small hairpin RNA (shRNA) expression construct targeting rat PYK2 (PYK2 shRNA). Expressed via a lentiviral vector, PYK2 shRNA strongly reduced the level of endogenous PYK2 protein in hippocampal cultures, compared to a control shRNA against firefly luciferase (Figure S2). Expression of PSD-95 and other synaptic components were unaffected by either shRNA (Figure S2A), and a "rescue" experiment with an shRNA-resistant PYK2 confirmed on-target specificity of PYK2 shRNA (see below).

PYK2 shRNA was introduced by biolistic transfection into CA1 pyramidal neurons of hippocampal slice cultures, a useful preparation for acute manipulation of protein levels and in-slice comparison with untransfected neighboring neurons (Stein et al., 2003; Seeburg and Sheng, 2008; Xu et al., 2008). LTD – induced by a pairing protocol (see Materials and Methods) – was strongly suppressed in neurons transfected with PYK2 shRNA, as compared with nearby untransfected cells in the same slice (average normalized EPSC during the last 10 minutes of recording: PYK2 shRNA 0.91 ± 0.13 of baseline, untransfected control 0.60 ± 0.052, $p = 0.031$; Figure 2A). As a further control, neurons transfected with luciferase shRNA showed LTD indistinguishable from untransfected neighboring cells (luciferase shRNA 0.71 ± 0.079, untransfected control 0.65 ± 0.053, $p = 0.56$; Figure 2B). Notably, neither PYK2 shRNA nor control luciferase shRNA had a significant effect on LTP (average normalized EPSC during the last 10 minutes of recording: PYK2 shRNA 2.08 ± 0.17, untransfected control 1.86 ± 0.25, $p = 0.48$; Figure 2C; luciferase shRNA 1.66 ± 0.32, untransfected control 1.81 ± 0.18, $p = 0.64$; Figure 2D). Thus PYK2 is specifically necessary for LTD signaling.

We also examined baseline synaptic transmission, and found that neither PYK2 nor luciferase shRNA transfection affected basal AMPAR excitatory postsynaptic currents (AMPAR EPSCs; average transfected/untransfected EPSC ratio ± SEM: PYK2 shRNA 1.00 ± 0.18, $p = 0.55$ vs. untransfected control; luciferase shRNA 1.11 ± 0.15, $p = 0.50$ vs. untransfected control; Figure 2E). Basal NMDAR EPSCs were slightly reduced by PYK2 shRNA, but this effect was small and indistinguishable from that of control luciferase shRNA (PYK2 shRNA 0.80 ± 0.065, $p = 0.024$ vs. untransfected control; luciferase shRNA 0.82 ± 0.085, $p = 0.015$ vs. untransfected control; Figure 2F). These results suggest that although PYK2 is required for LTD, it is not critical for the maintenance of basal synaptic function.

Y402F-PYK2 blocks LTD

Overexpression of mutant PYK2 with a phospho-null Y402F substitution has commonly been used to inhibit PYK2 function in a dominant negative manner (Lakkakorpi et al., 2003; Park et al., 2004). In CA1 neurons transfected with Y402F-PYK2, LTD was also completely blocked (Y402F-PYK2 0.96 ± 0.11, untransfected control 0.65 ± 0.055, $p = 0.0057$; Figure 3A). This result corroborates our earlier loss-of-function result with PYK2 shRNA (see Figure 2A) showing a necessary role for PYK2 in LTD. Overexpression of wild type (WT)-PYK2, on the other hand, had no effect on LTD (WT-PYK2 0.59 ± 0.042, untransfected control 0.54 ± 0.032, $p = 0.43$; Figure 3B).

In terms of baseline synaptic transmission, neurons overexpressing WT-PYK2 displayed a ~30% reduction in AMPAR EPSCs (WT-PYK2 0.69 ± 0.11, $p = 0.049$ vs. untransfected control; Figure 3C), but normal NMDAR EPSCs (WT-PYK2 1.09 ± 0.25; $p = 0.52$ vs. untransfected control; Figure 3D). Overexpression of Y402F-PYK2, on the other hand, failed to cause synaptic depression. In fact, baseline AMPAR EPSCs were slightly increased by overexpression of Y402F-PYK2, supporting a possible dominant negative effect, although this trend did not reach statistical significance (Y402F-PYK2 1.35 ± 0.30; $p = 0.45$ vs. untransfected control). These results suggest that under basal conditions, PYK2 overexpression is sufficient to decrease synaptic function in a manner dependent on Y402. This depression did not occlude LTD, however (Figure 3B), suggesting that additional molecular mechanisms are at work during LTD (see Discussion).

Like WT-PYK2 overexpression, Y402F-PYK2 overexpression did not affect NMDAR EPSCs, implying that PYK2 is not required for NMDAR function (Y402F-PYK2 1.10 ± 0.14; $p = 0.83$ vs. untransfected control; Figure 3D). Unfortunately, there is no available constitutively active PYK2 mutant that can be tested, as the putative phospho-mimic Y402 PYK2 mutant has been found to inhibit PYK2 function like the phospho-null mutant (Li et al., 1999). Together, our results suggest that PYK2 overexpression selectively affects AMPAR, but not NMDAR, transmission.

Changes in synaptic structure often correlate with changes in synaptic function (reviewed in Tada and Sheng, 2006; Alvarez and Sabatini, 2007); however, none of the above

modifications we introduced (PYK2 knockdown, WT-PYK2 overexpression, or Y402F-PYK2 overexpression) significantly affected dendritic spine morphology or dendritic branching in mature cultured neurons (Figure S3). Thus PYK2 does not play a major role in determining basal-state neuronal morphology.

PYK2 kinase activity contributes to LTD

Is the kinase activity of PYK2 required for LTD? Alanine substitution at K457 in PYK2 abolishes kinase activity (Li et al., 1999; Lakkakorpi et al., 2003; Park et al., 2004). If PYK2 kinase activity were important, we would expect overexpression of K457A-PYK2 in neurons to have effects similar to overexpression of Y402F-PYK2. When we examined basal synaptic transmission, however, we found that K457A-PYK2 overexpression significantly depressed baseline AMPAR EPSCs, to the same extent seen with WT-PYK2 overexpression (K457A-PYK2 0.75 ± 0.11; $p = 0.036$ vs. untransfected control; Figure 4A). Because kinase-dead PYK2 proteins could still be trans-autophosphorylated by endogenous wild-type PYK2 (as occurs in osteoclasts; Lakkakorpi et al., 2003), we turned to a "molecular replacement" approach in which endogenous PYK2 is suppressed by PYK2 shRNA while kinase-dead PYK2 is overexpressed by co-transfection of shRNA-resistant K457A-PYK2. We altered nine nucleotides in the shRNA target region of K457A- and WT-PYK2 to render these constructs resistant to suppression by PYK2 shRNA, without changing the amino acid sequence (Figure S4). Transfection of shRNA-resistant WT-PYK2 (WT-PYK2*) together with PYK2 shRNA resulted in significantly decreased baseline AMPAR EPSCs (WT-PYK2* + shRNA 0.76 ± 0.14; $p = 0.036$ vs. untransfected control; Figure 4B), which is, as expected, similar to overexpression of WT-PYK2 in the absence of PYK2 shRNA. Overexpression of shRNA-resistant kinase-dead K457A-PYK2 (K457A-PYK2*) in conjunction with PYK2 shRNA also reduced basal AMPAR EPSC amplitude (K457A-PYK2* + shRNA 0.73 ± 0.15; $p = 0.026$ vs. untransfected control; Figure 4B), similar to overexpression of the K457A-PYK2 mutant alone. Thus overexpression of PYK2 reduces basal synaptic strength, independent of its kinase activity. These data are consistent with a scaffold function of PYK2 that inhibits synaptic strength.

Although unimportant for the regulation of *basal* synaptic strength, could PYK2 kinase activity play a role in LTD? We tested LTD in CA1 neurons that had undergone "molecular

replacement" with WT or kinase-dead PYK2. WT-PYK2* fully rescued the LTD defect caused by PYK2 shRNA expression (WT-PYK2* + shRNA 0.61 ± 0.054, untransfected control 0.60 ± 0.043; p = 0.91; Figure 4C), a result that also confirms the on-target specificity of the shRNA effect. K457A-PYK2*, however, only partially rescued LTD in neurons cotransfected with PYK2 shRNA (K457A-PYK2* + shRNA 0.73 ± 0.079, untransfected control 0.50 ± 0.041; p = 0.031; Figure 4D). These data imply that PYK2 kinase activity is important for PYK2's function in LTD; however, kinase-independent functions also seem to contribute.

PYK2 is required for inhibition of ERK phosphorylation in chem-LTD

PYK2 is a large scaffold protein (~116 kDa) as well as a kinase, and it is likely that PYK2 recruits and modulates multiple signaling proteins at the synapse. To gain an understanding of how PYK2 influences postsynaptic signaling during LTD, we screened the activation profile of several signaling proteins after chem-LTD stimulation in cultured neurons where PYK2 expression had been suppressed by PYK2 shRNA lentivirus. Compared to luciferase shRNA control, PYK2 knockdown significantly enhanced the phosphorylation of ERK T202/Y204 at 5 minutes following chem-LTD, which corresponds to the peak of PYK2 phosphorylation at Y402 (Figure 5A, quantified in 5B). There was also a slight, but not significant, enhancement of basal ERK phosphorylation with PYK2 knockdown. We did not find significant alteration in the phosphorylation-activation time course of Src (Y416), GSK3beta (S9), Akt (T308), or JNK (T183/Y185) (Figure 5). These data suggest that PYK2 is required for dampening ERK activation in response to NMDAR stimulation.

LTD is associated with dephosphorylation of GluR1 S845, and elevated Ras-ERK signaling promotes GluR1 S845 phosphorylation in hippocampal slice cultures (Qin et al., 2005). Control neurons virally infected with luciferase shRNA showed rapid increasing dephosphorylation of GluR1 S845, reaching significance at 5 min after NMDAR stimulation (Figure S5A). In contrast, neurons infected with PYK2 shRNA showed no significant loss of S845 phosphorylation till 15 minutes (Figure S5A). The delay in S845 GluR1 dephosphorylation was similar to the effect of calcineurin inhibitors, which are known to block LTD (Figure S5B, C). Thus PYK2's effect on GluR1 dephosphorylation is consistent with its effects on ERK signaling and LTD.

Does overexpression of WT-PYK2 further decrease activity-dependent ERK activation? We immunostained for phospho-ERK in neurons transfected with plasmids expressing WT-PYK2 or Y402F-PYK2, and measured fluorescence intensities in cells at 2.5 and 5 minutes chem-LTD treatment, as described previously (Kim et al., 2005). Consistent with the PYK2-knockdown experiments above, overexpression of Y402F-PYK2 enhanced NMDA-induced ERK phosphorylation, relative to control neurons transfected with an empty vector (Figure 6). This enhancement was significant in unstimulated neurons and at 2.5 minutes post-chem-LTD treatment (Figure 6). Overexpression of WT-PYK2, on the other hand, significantly suppressed NMDA-induced ERK phosphorylation at 5 minutes chem-LTD treatment (Figure 6). Thus overexpression of PYK2 is sufficient to dampen NMDA-induced ERK activation, just as PYK2 knockdown enhances it.

Overexpression of PYK2 blocks LTP

Because it further inhibited NMDA-dependent ERK activation, we hypothesized that WT-PYK2 overexpression would inhibit LTP or even enhance LTD. While there was no effect of WT-PYK2 overexpression on LTD (Figure 3B), we did observe that WT-PYK2 significantly reduced LTP relative to untransfected controls (WT-PYK2 1.53 ± 0.10, untransfected control 2.56 ± 0.29, $p = 0.011$; Figure 7A). In contrast, overexpression of Y402F-PYK2 did not affect LTP (Y402F-PYK2 2.13 ± 0.28, untransfected control 1.93 ± 0.19, $p = 0.64$; Figure 7B). Thus PYK2 supports LTD at the expense of LTP, in a manner dependent on Y402 and consistent with effects on ERK phosphorylation.

Discussion

We report here that PYK2 plays a critical role in LTD. PYK2 is phosphorylated at Y402 by chem-LTD activation of NMDARs, and shRNA and dominant negative experiments show that it is required for LTD in hippocampal slice cultures. We find that both kinase and non-kinase (presumably scaffold) functions of PYK2 contribute to LTD. We propose the following model: Following NMDAR stimulation, the rise in postsynaptic calcium activates PYK2, resulting in phosphorylation at Y402. Y402 is autophosphorylated primarily by the PYK2 kinase domain, as proposed previously (Lev et al., 1995; Park et al., 2004; Kohno et al., 2008; Bartos et

al., 2010), but other tyrosine kinases — perhaps a member of the Src family or a receptor tyrosine kinase — could also contribute to Y402 phosphorylation (Lakkakorpi et al., 2003). Phospho-Y402 PYK2 then recruits additional signaling proteins to mediate downstream effects essential for LTD, one of which is the dampening of postsynaptic activation of ERK.

Overexpression of PYK2 is sufficient to depress basal synaptic strength, and like PYK2's role in LTD, this effect requires Y402 (Figure 3). There are a few mechanistic distinctions, however, between the basal and activity-dependent roles of PYK2. PYK2 kinase activity is required for LTD, but not for depression of basal synaptic strength (Figure 4), and PYK2 overexpression suppresses ERK phosphorylation following NMDAR stimulation, but not in the basal state (Figure 6). These mechanistic differences could explain how WT-PYK2 overexpression or WT-PYK2* "molecular replacement," both of which depress basal synaptic strength, failed to occlude LTD (Figure 3, 4). NMDAR-dependent recruitment of PYK2 through Y402-independent mechanisms (Figure S1) could additionally gate PYK2's role in LTD, much like how NMDAR stimulation gates phosphatase action in LTD (Morishita et al., 2001).

A Novel Role for PYK2 in LTD

Two properties of PYK2 make it an attractive component of LTD signaling. First, PYK2 is activated by a rise in intracellular calcium. One possible mechanism is that calcium-calmodulin complexes bind PYK2 directly, and induce dimerization and transphosphorylation at Y402 (Kohno et al., 2008). It has also been proposed that calcium-calmodulin binding to PSD-95 induces PYK2 association and clustering, which favors Y402 transphosphorylation in the protein complex (Bartos et al., 2010). In agreement with our findings, this study also reported that chemical activation of NMDARs leads to PYK2 Y402 phosphorylation and redistribution in cultured hippocampal neurons (Bartos et al., 2010). Another possibility is that PYK2 Y402 phosphorylation-activation occurs via the calcium-dependent serine/threonine phosphatase calcineurin (Faure et al., 2007). These authors reported that in PC12 cells, calcineurin enhances PYK2 activity and Y402 phosphorylation through serine/threonine dephosphorylation of multiple PYK2 residues (Faure et al., 2007). We found a similar shift in PYK2 mobility in neurons induced by chem-LTD (Figure 1B), which was blocked by calcineurin inhibitors (Figure S1A). The link between calcineurin and PYK2 is intriguing, because calcineurin is well-

established to be required for LTD (Mulkey et al., 1993, 1994). Forebrain-specific knockout of calcineurin function abolishes LTD, and causes schizophrenia-like behavioral deficits in working memory, prepulse inhibition, and social interaction (Zeng et al., 2001; Miyakawa et al., 2003). The behavioral effects of loss of function of PYK2 remain to be determined.

Second, PYK2 is known to bind PSD-95 (Seabold et al., 2003), which is required for LTD (Migaud et al., 1998). Furthermore, a study has shown that mutation of the SH3-GK domain in PSD-95 blocks LTD in hippocampal neurons (Xu et al., 2008); the SH3-GK region is where PYK2 appears to bind PSD-95 (Seabold et al., 2003). It is possible that PYK2 association with PSD-95 plays a role in LTD, and alteration of PYK2 signaling may be one explanation for the LTD defect observed in the presence of PSD-95 SH3-GK mutants. This is consistent with a recent study proposing that PYK2 binding to PSD-95 is required for PYK2 activation and phosphorylation at Y402 (Bartos et al., 2010).

PYK2-ERK signaling in LTD

There is much evidence linking ERK signaling to synaptic plasticity and learning and memory (reviewed in Thomas and Huganir, 2004). ERK pathway inhibitors reduce spatial learning and fear conditioning (Blum et al., 1999; Selcher et al., 1999; Atkins et al., 1998). These inhibitors also block LTP in acute hippocampal slices (English and Sweatt, 1997) and in vivo hippocampal LTD (Thiels et al., 2003), leading to the view that differences in the magnitude or duration of ERK activation between LTP and LTD could be important, with more modest elevations in ERK activity favoring LTD (Thiels et al., 2003; Coba et al., 2008). In fact, different ERK activation time-courses are known to couple to distinct processes in other cell types: modest, transient ERK activity induces proliferation in PC12 cells, whereas prolonged ERK activity induces differentiation (Marshall, 1995). Our data support the idea that alteration of ERK signaling dynamics could affect the recruitment of LTP versus LTD pathways, with PYK2 playing a crucial role in determining that balance.

What mechanisms might mediate PYK2's effect on ERK signaling in synapses? In some non-neuronal cell types, PYK2 has been linked to enhancement of ERK activity through the recruitment of Grb2 (adaptor) and Sos (guanine nucleotide exchange factor [GEF] for Ras) proteins (Lev et al., 1995; Dikic et al., 1996). In NIH3T3 cells, however, PYK2 has been

reported to inhibit ERK activity (Zhao et al., 2000). In neurons, ERK signaling is regulated by Ras GEFs and GTPase activating proteins (GAPs), several of which are represented in the PSD (Thomas and Huganir, 2004; Sheng and Hoogenraad, 2007). PYK2's presence in the PSD, and in particular the NMDAR complex (Seabold et al., 2003), could enable interactions with GTPase regulators in the PSD, and thus provide another coupling mechanism between calcium influx and MAPK activity.

Role of PYK2 in LTP

Our conclusion that PYK2 is important for LTD is in apparent contradiction to Huang et al (2001), who reported that micropipette infusion of recombinant PYK2 into CA1 cells induced Src-dependent NMDAR potentiation and occluded LTP. It is interesting to note that this blockade of LTP by PYK2 infusion is consistent with our finding that WT-PYK2 overexpression inhibits LTP (Figure 7). One explanation for why we did not see an increase in NMDAR strength with WT-PYK2 overexpression is that the post-translational modification, assembly, and trafficking of injected recombinant protein versus transfected cDNA of PYK2 could lead to different results in neurons. Injection of recombinant PYK2 could lead to abnormal PYK2 function at extrasynaptic sites, for example. It is also possible that acute versus chronic time courses of PYK2 manipulation have different effects.

PYK2 targets and clinical implications

We consider PYK2 to be a necessary component of the collective signaling network that underlies LTD induction. As a large scaffold protein, PYK2 could interact with multiple factors at the synapse. For example, PYK2 has been linked to the small GTPases RhoA and Rap2 (Lim et al., 2008; McLeod et al., 2004), which cause loss of spines, the dendritic protrusions containing synaptic sites (Nakayama et al., 2000; Ryu et al., 2008). PYK2 is also reported to destabilize the structural protein beta-catenin (Van Buul et al., 2005), which is activity-regulated by tyrosine phosphorylation in neurons (Murase et al., 2002). Consistent with these ideas, LTD is associated with spine shrinkage in hippocampal neurons (Okamoto et al., 2004; Zhou et al., 2004). While we did not find a significant difference in steady-state spine morphology with

PYK2 shRNA or WT-PYK2 expression in dissociated neurons (Figure S3), it would be interesting to see if PYK2 plays a role in activity-dependent spine shrinkage or stability.

PYK2 activation has been reported in pathological conditions of neurotoxicity, cerebral ischemia, and seizures (Cheung et al., 2000; Tian et al., 2000; Wright et al., 2007), raising the possibility that PYK2 could contribute to synapse failure during stroke or neurotoxic conditions via LTD-like mechanisms. Further studies on the signaling proteins involved in LTD may guide future therapeutic approaches for diseases of synapse loss or neurodegeneration.

Acknowledgements:

We thank Wen-Cheng Xiong and Huaye Zhang for reagents, and Kelly Foster and Daniel Seeburg for data acquisition and analysis programs. We thank Dieter Edbauer, Kenny Futai, Nelly Khidekel, and Baris Bingol for critical comments on the manuscript. MS was Investigator of the Howard Hughes Medical Institute.

Figure Legends and Figures

Figure 1. Chem-LTD induces PYK2 phosphorylation at Y402. (A) Detection of phospho-Y402-PYK2, PYK2, and PSD-95 in hippocampal subcellular fractions. Lanes: H (crude homogenate, 6 μg); S1 (supernatant after first spin removing nuclei and cellular debris, 6 μg); P1 (nuclei and cellular debris, 6 μg); S2 (cytosol and microsomal membranes, 6 μg); P2 (crude synaptosomes, 6 μg); LS1 (synaptosomal cytosolic fraction, 6 μg); LP1 (mitochondria and synaptosomal membranes; 6 μg); PSD I (Triton X-100-extracted postsynaptic densities, 2 μg); PSD II (Triton X 100-extracted postsynaptic densities from PSD I, 2 μg). (B) Time course of GluR1 S845 dephosphorylation after chem-LTD treatment in cultured hippocampal neurons. In this and all other experiments in this study, quantified phospho-protein signal in each lane was normalized to total protein signal, and the final ratio was normalized to untreated (0') control. Data are quantified in the graph at right, $n = 3$, $^{***}p < 0.001$ compared to untreated control, one-way ANOVA with Dunnett's post-test. (C) Time course of PYK2 Y402 phosphorylation after chem-LTD treatment. $n = 3$, $^{*}p < 0.05$ compared to untreated control, one-way ANOVA with Dunnett's post-test.

Figure 2. Knockdown of PYK2 blocks LTD. (A, B) PYK2 shRNA blocks LTD (A) but luciferase shRNA does not (B). Groups of four consecutive EPSC measurements were averaged, and then normalized to the average EPSC magnitude of the first 10 minutes of baseline recordings (pre-LTD induction). Bar graphs show the average normalized EPSC of the last 10 minutes of recording. PYK2 shRNA: $n = 12$ pairs; $^{*}p = 0.031$, paired Student's t-test. Luciferase shRNA: $n = 12$ pairs; $p = 0.56$, paired Student's t-test. Scale bars, 50 pA/25 msec. (C, D) Neither PYK2 shRNA (C) nor luciferase shRNA (D) affects LTP. Groups of six consecutive EPSC measurements were averaged, and then normalized to the average EPSC magnitude of the first 3 minutes of baseline recording (pre-LTP induction). Statistical significance was assessed by comparing the average normalized EPSC of the last 10 minutes of recording (bar graphs). PYK2 shRNA: $n = 9$ pairs; $p = 0.48$, paired Student's t-test. Scale bar, 30 pA/25 msec. Luciferase shRNA: $n = 7$ pairs; $p = 0.64$, paired Student's t-test. Scale bar, 50 pA/25 msec. (E) PYK2 shRNA and luciferase shRNA do not significantly alter baseline AMPAR transmission. PYK2 shRNA paired recordings (transfected cell versus untransfected

neighboring cell in the same slice): n = 12 pairs; p = 0.55 versus untransfected control, paired Student's t-test. Luciferase shRNA paired recordings: n = 19 pairs; p = 0.50 versus untransfected control, paired Student's t-test. Scale bars, 20 pA/100 msec. (F) PYK2 shRNA and luciferase shRNA have similar effects on NMDAR transmission. PYK2 shRNA paired recordings: n = 9 pairs, p = 0.024 versus untransfected control, paired Student's t-test. Luciferase shRNA paired recordings: n = 18 pairs, p = 0.015 versus untransfected control, paired Student's t-test. Scale bars, 50 pA/100 msec

Figure 3. PYK2 Y402 is required for LTD. (A) Overexpression of Y402F-PYK2 blocks LTD. n = 10 pairs; **p = 0.0057, paired Student's t-test. Scale bars, 50 pA/25 msec. (B) WT-PYK2 overexpression does not affect LTD. n = 9 pairs; p = 0.43, paired Student's t-test. Scale bars, 50 pA/25 msec. (C) Overexpression of WT-PYK2 inhibits AMPAR transmission, whereas expression of Y402F-PYK2 does not. WT-PYK2 paired recordings: n = 11 pairs; p = 0.049 versus untransfected control, paired Student's t-test. Y402F-PYK2 paired recordings: n = 11 pairs; p = 0.45 versus untransfected control, paired Student's t-test. Scale bars, 20 pA/100 msec. (D) Neither WT-PYK2 nor Y402F-PYK2 expression affects NMDAR transmission. WT-PYK2 paired recordings: n = 11 pairs; p = 0.52 versus untransfected control, paired Student's t-test. Y402F-PYK2 paired recordings: n = 11 pairs; p = 0.83 versus untransfected control, paired Student's t-test. Scale bars, 50 pA/100 msec.

Figure 4. PYK2 kinase activity is required for LTD. (A) Overexpression of K457A-PYK2 inhibits AMPAR transmission. WT-PYK2 overexpression data from Figure 3C is repeated here for comparison. K457A PYK2 paired recordings: n = 13 pairs; p = 0.036 versus untransfected control, paired Student's t-test. Scale bars, 20 pA/100 msec. (B) Both WT-PYK2* and K457A-PYK2*, in the presence of PYK2 shRNA, depress baseline AMPAR transmission. PYK2 shRNA and shRNA-resistant PYK2 constructs were mixed 1:1 for transfections. WT-PYK2* + shRNA paired recordings: n = 13 pairs; p = 0.036 versus untransfected control, paired Student's t-test. K457A-PYK2* + shRNA paired recordings: n = 12 pairs; p = 0.026 versus untransfected control, paired Student's t-test. Scale bars, 20 pA/100 msec. (C, D) WT-PYK2* fully restores LTD (C), whereas K457A-PYK2* only partially rescues LTD (D), in the presence of PYK2

shRNA. WT-PYK2* + shRNA: n = 10 pairs; p = 0.91, paired Student's t-test. K457A-PYK2* + shRNA: n = 11 pairs; *p = 0.031, paired Student's t-test. Scale bars, 50 pA/25 msec.

Figure 5. Effect of PYK2 shRNA on the activation of ERK and other signaling pathways. (A) Representative blots of phosphorylation time course of PYK2, ERK, Src, GSK3beta, Akt, and JNK following chem-LTD. (B) Quantification of data from (A). For each graph, 3-4 independent experiments were performed. All signal intensity ratios (phospho-protein level / total protein level) were normalized to untreated (0') luciferase shRNA-transfected samples. Normalized phospho-ERK signal represents the average of p42 and p44 intensity ratios; normalized phospho-JNK signal represents the p46 intensity ratio only (p54 intensity was barely detectable in experiments). **p < 0.01, two-way ANOVA with Bonferroni's post-test between time-matched samples (PYK2 shRNA vs. luciferase shRNA).

Figure 6. WT-PYK2 overexpression depresses NMDA-dependent ERK phosphorylation. (A) Representative images of transfected neurons (DIV16+3) immunostained for phospho-ERK (green) and beta-gal marker (red) untreated (0') or after chem-LTD treatment (2.5' and 5'). Scale bar, 30 μm. (B) Quantification of data from (A). Average fluorescence intensities of phospho-ERK signal in cell somas were all normalized to untreated empty-vector control. Each experimental group was compared to the corresponding empty-vector control for that time point. *p < 0.05, **p < 0.01, ***p < 0.001, unpaired Student's t-test.

Figure 7. WT-PYK2 overexpression inhibits LTP. (A, B) Overexpression of WT-PYK2 (A), but not Y402F-PYK2 (B) reduces LTP. WT-PYK2: n = 8 pairs; p = 0.011, paired Student's t-test. Scale bar, 20 pA/25 msec (WT-PYK2), 50 pA/25 msec (untransfected). Y402F-PYK2: n = 7 pairs; p = 0.64, paired Student's t-test. Scale bar, 20 pA/25 msec (Y402F-PYK2), 30 pA/25 msec (untransfected).

Supplemental Figure Legends

Figure S1. Chem-LTD affects SDS-PAGE mobility and biochemical distribution of PYK2. (A) Representative blots (out of 3-4 independent experiments performed) of the effect of 1 hour cyclosporine A (1 μM) or FK506 (1 μM) treatment on PYK2 mobility (control treatments with

the same volume of DMSO solvent were performed in parallel). (B) Cultured hippocampal neurons, untreated (0') or chem-LTD treated (5'), were homogenized and separated into crude Triton-soluble and Triton-insoluble fractions. Equal amounts of protein (10 μg) from homogenate (H), Triton-soluble (S), and Triton-insoluble (I) fractions were loaded per lane. A representative blot is shown, probed for phospho-Y402 PYK2 and subsequently for total PYK2. A control blot probed against total ERK is also shown. Quantification of total PYK2 in Triton-insoluble versus Triton-soluble fractions in each experiment is also shown. n = 3 experiments, *$p < 0.05$, unpaired Student's t-test.

Figure S2. PYK2 shRNA knocks down PYK2. (A) Lentiviral transduction of PYK2 shRNA decreases PYK2 expression in cultured hippocampal neurons (DIV 15+7), without affecting expression of NMDAR subunits NR2A and NR2B, PSD-95, or AMPAR GluR1 subunit. (B) Representative images of endogenous PYK2 staining in cultured hippocampal neurons (DIV 19+3) expressing luciferase shRNA or PYK2 shRNA. Scale bar, 30 μm.

Figure S3. PYK2 does not affect dendrite or dendritic spine morphology. (A) Transfected neurons (DIV19+3) are displayed in low-magnification images (scale bar, 30 μm); dendritic segments are shown in high-magnification images (scale bar, 3 μm). (B) Quantification (mean ± SEM) is shown for spine density (number of protrusions per 10 μm dendrite segment), spine length (μm), and spine width (μm). n = 15-20 per group; no statistically significant changes as assessed by one-way ANOVA with Dunnett's test. (C) Quantification of dendritic complexity by Scholl analysis, depicting number of dendritic crossings per 12.5 μm radial distance from the soma. n = 15-20 per group; no statistically significant changes as assessed by two-way ANOVA with Bonferroni's test.

Figure S4. WT-PYK2* and K457A-PYK2* are resistant to PYK2 shRNA. WT-PYK2 and K457A-PYK2 protein expression is suppressed by PYK2 shRNA, but not by luciferase shRNA or empty vector control (pSuper) in HEK 293 cells. WT-PYK2* and K457A-PYK2* contain silent mutations rendering them resistant to PYK2 shRNA.

Figure S5. PYK2 and calcineurin inhibitors delay GluR1 S845 dephosphorylation. (A) Representative blot of GluR1 S845 dephosphorylation following chem-LTD, in luciferase shRNA- and PYK2 shRNA-expressing neurons. Quantification of phospho-GluR1 signal intensity ratios (phospho-GluR1 level / total GluR1 level, normalized to the corresponding untreated samples) is shown on the right. $n = 4$; $^{*}p < 0.05$, $^{**}p < 0.01$, $^{***}p < 0.001$, one-way ANOVA with Dunnett's post-test. (B) Representative blot and quantification of phospho-GluR1 from neurons treated with the calcineurin inhibitor FK506 (1 μM), or an equivalent volume of vehicle (DMSO). $n = 6$; $^{*}p < 0.05$, $^{**}p < 0.01$, $^{***}p < 0.001$, one-way ANOVA with Dunnett's post-test. (C) Representative blot and quantification of phospho-GluR1 from neurons treated with the calcineurin inhibitor cyclosporine A (1 μM) or an equivalent volume of vehicle (DMSO). $n = 5$; $^{*}p < 0.05$, $^{**}p < 0.01$, $^{***}p < 0.001$, one-way ANOVA with Dunnett's post-test.

Figure 1

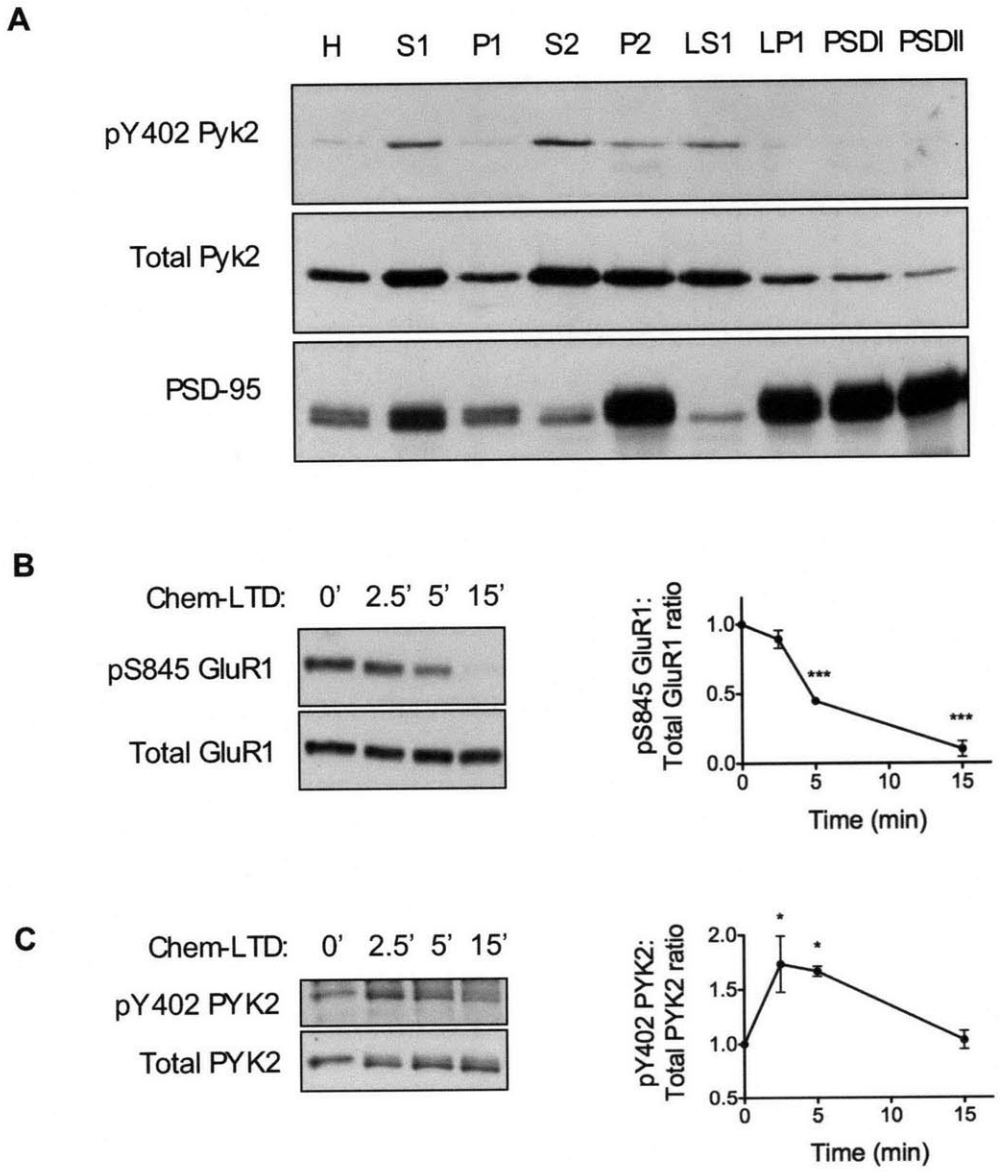
A
H
S1
P1
S2
P2
LS1
LP1
PSDI
PSDII
pY402 Pyk2
Total Pyk2
PSD-95
B
Chem-LTD:
0'
2.5'
5'
15'
pS845 GluR1
Total GluR1
pS845 GluR1: Total GluR1 ratio
1.0
0.5
0.0
***
***
0
5
10
15
Time (min)
C
Chem-LTD:
0'
2.5'
5'
15'
pY402 PYK2
Total PYK2
pY402 PYK2: Total PYK2 ratio
2.0
1.5
1.0
0.5
*
*
0
5
10
15
Time (min)

Figure 2

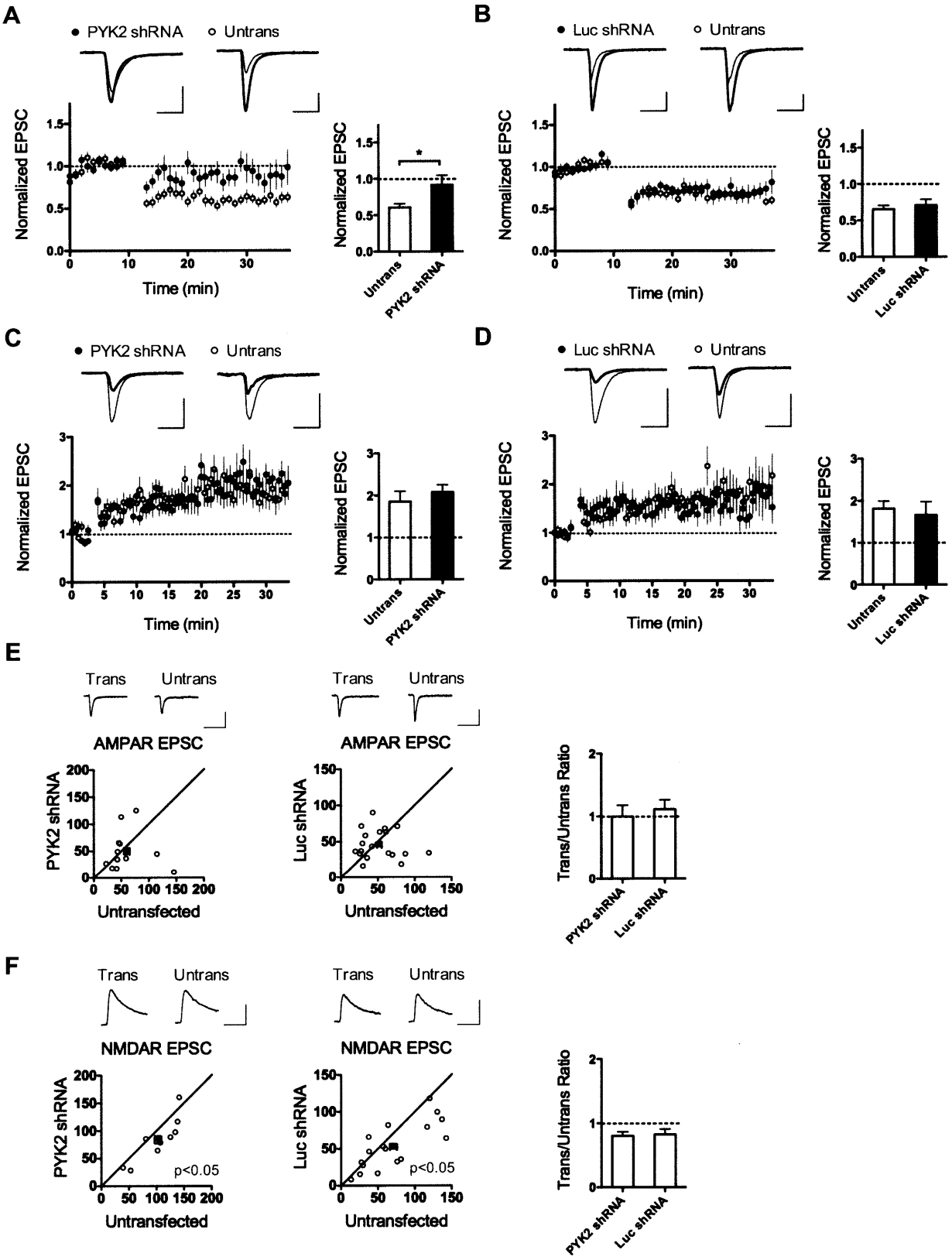
A
PYK2 shRNA
Untrans
Normalized EPSC
Time (min)
Untrans
PYK2 shRNA
B
Luc shRNA
Untrans
Normalized EPSC
Time (min)
Untrans
Luc shRNA
C
PYK2 shRNA
Untrans
Normalized EPSC
Time (min)
Untrans
PYK2 shRNA
D
Luc shRNA
Untrans
Normalized EPSC
Time (min)
Untrans
Luc shRNA
E
Trans
Untrans
AMPAR EPSC
PYK2 shRNA
Untransfected
Trans
Untrans
AMPAR EPSC
Luc shRNA
Untransfected
Trans/Untrans Ratio
PYK2 shRNA
Luc shRNA
F
Trans
Untrans
NMDAR EPSC
PYK2 shRNA
p<0.05
Untransfected
Trans
Untrans
NMDAR EPSC
Luc shRNA
p<0.05
Untransfected
Trans/Untrans Ratio
PYK2 shRNA
Luc shRNA

Figure 3

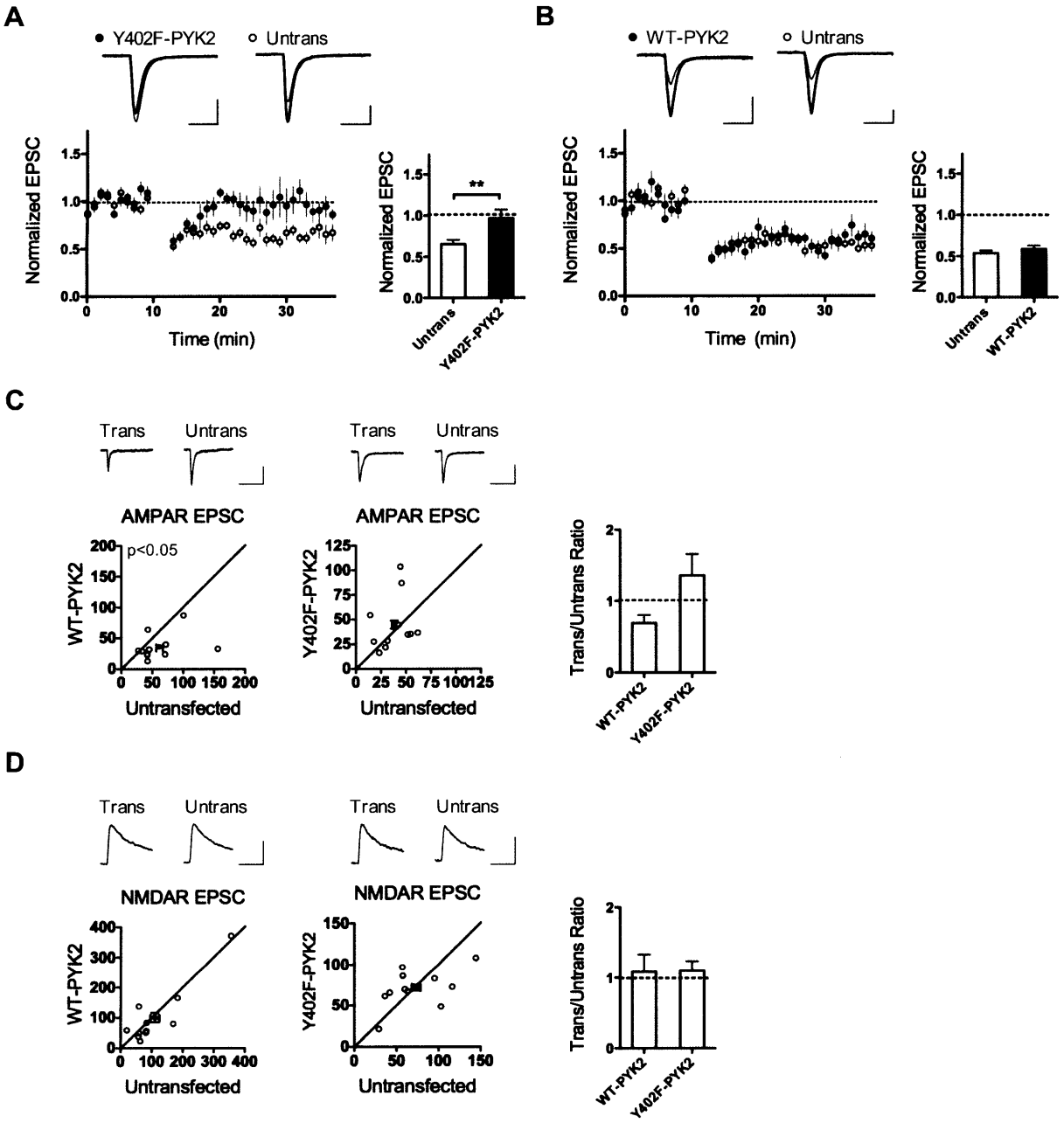
A
Y402F-PYK2
Untrans
Normalized EPSC
Time (min)
Untrans
Y402F-PYK2
B
WT-PYK2
Untrans
Normalized EPSC
Time (min)
Untrans
WT-PYK2
C
Trans
Untrans
AMPAR EPSC
p<0.05
WT-PYK2
Untransfected
Y402F-PYK2
Trans/Untrans Ratio
D
NMDAR EPSC

Figure 4

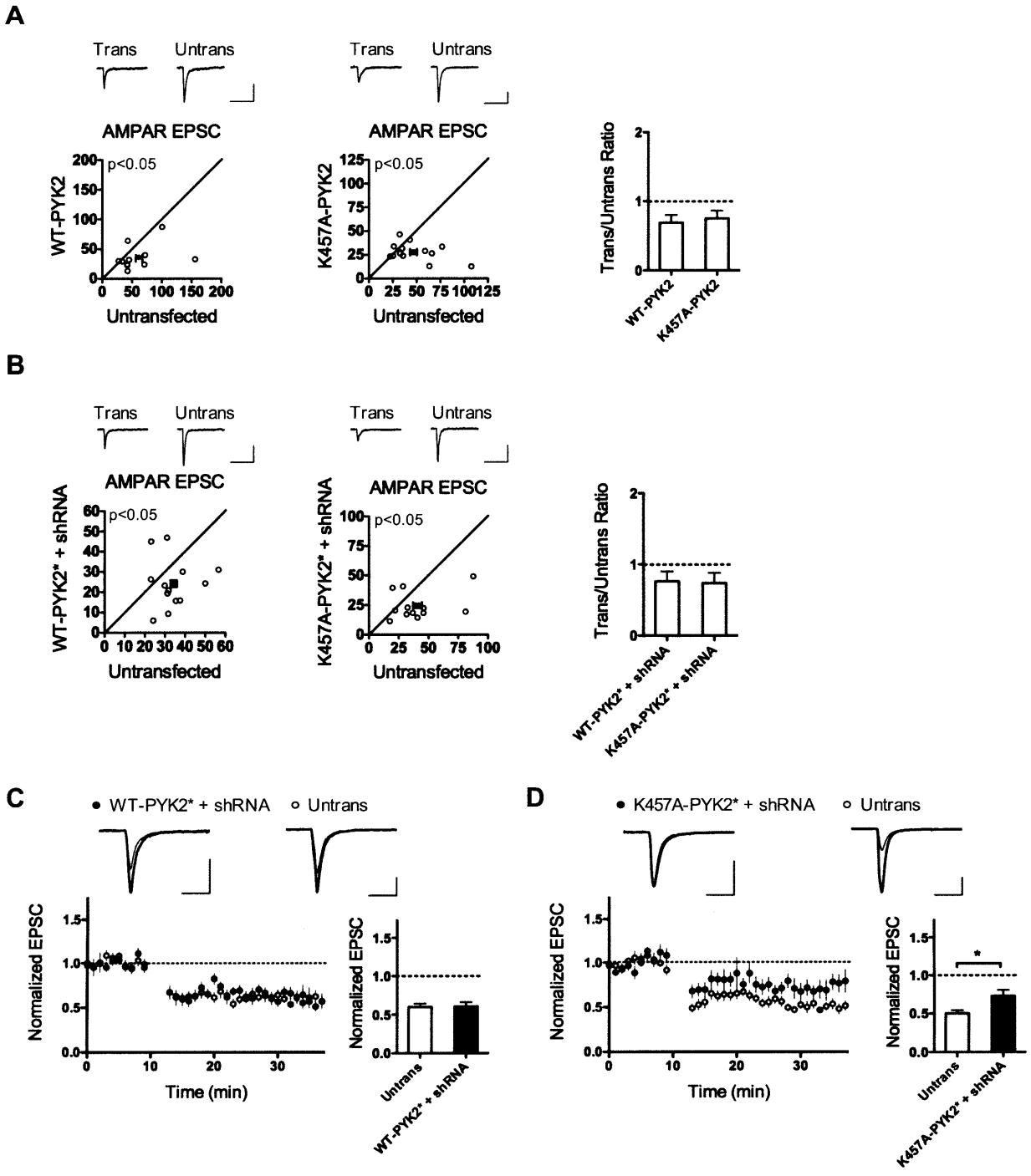
A
Trans
Untrans
AMPAR EPSC
WT-PYK2
p<0.05
Untransfected
K457A-PYK2
Trans/Untrans Ratio
B
WT-PYK2* + shRNA
K457A-PYK2* + shRNA
C
WT-PYK2* + shRNA
Untrans
Normalized EPSC
Time (min)
D
K457A-PYK2* + shRNA

Figure 5

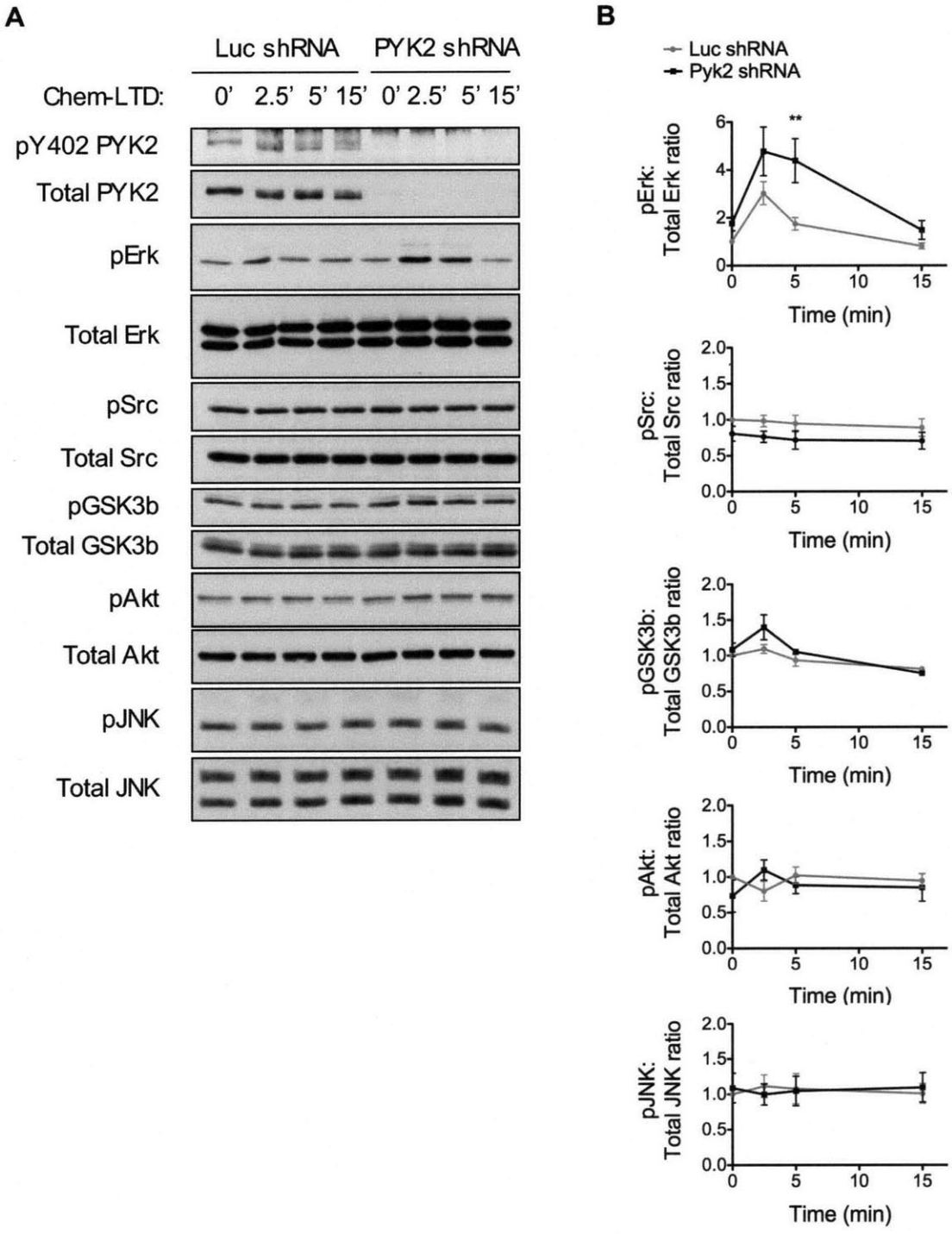
A
Luc shRNA
PYK2 shRNA
Chem-LTD:
0' 2.5' 5' 15' 0' 2.5' 5' 15'
pY402 PYK2
Total PYK2
pErk
Total Erk
pSrc
Total Src
pGSK3b
Total GSK3b
pAkt
Total Akt
pJNK
Total JNK
B
Luc shRNA
Pyk2 shRNA
pErk: Total Erk ratio
**
Time (min)
pSrc: Total Src ratio
Time (min)
pGSK3b: Total GSK3b ratio
Time (min)
pAkt: Total Akt ratio
Time (min)
pJNK: Total JNK ratio
Time (min)

Figure 6

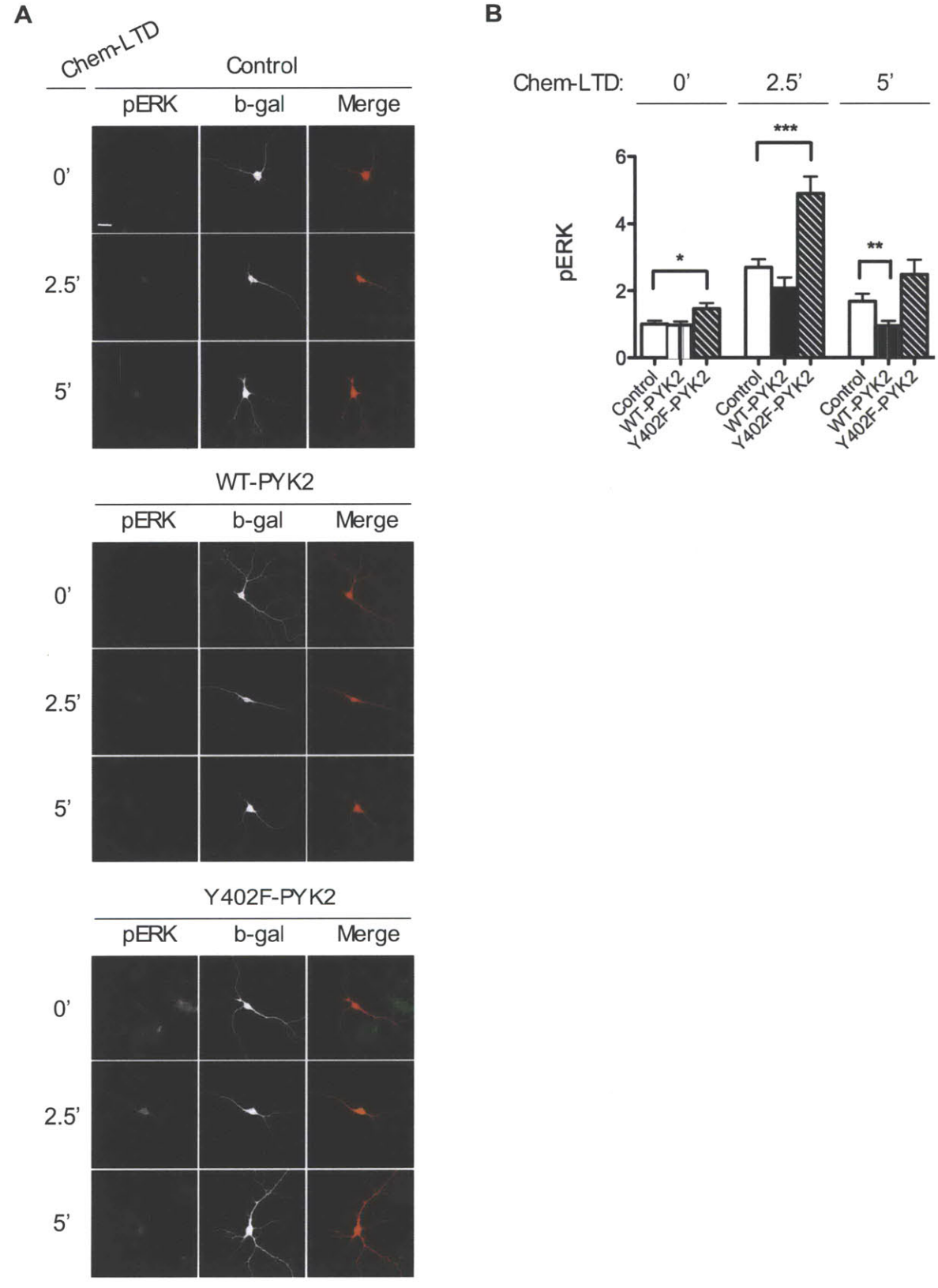
A
Chem-LTD
Control
pERK
b-gal
Merge
0'
2.5'
5'
WT-PYK2
pERK
b-gal
Merge
0'
2.5'
5'
Y402F-PYK2
pERK
b-gal
Merge
0'
2.5'
5'
B
Chem-LTD:
0'
2.5'
5'
pERK
6
4
2
0
*
***
**
Control
WT-PYK2
Y402F-PYK2
Control
WT-PYK2
Y402F-PYK2
Control
WT-PYK2
Y402F-PYK2

Figure 7

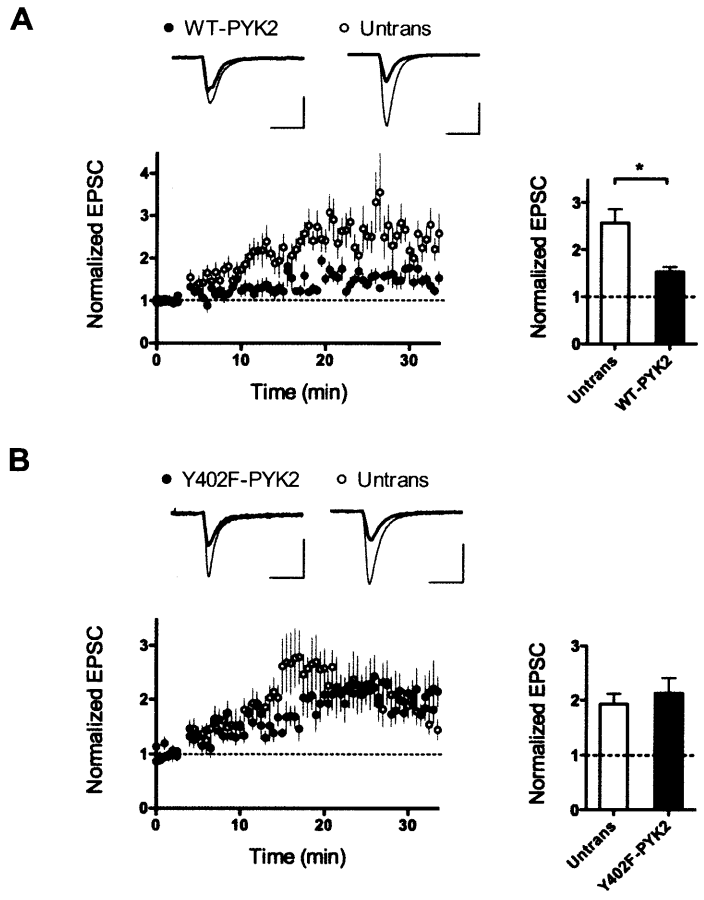
A
• WT-PYK2
○ Untrans
Normalized EPSC
Time (min)
Untrans
WT-PYK2
B
• Y402F-PYK2
○ Untrans
Normalized EPSC
Time (min)
Untrans
Y402F-PYK2

Figure S1

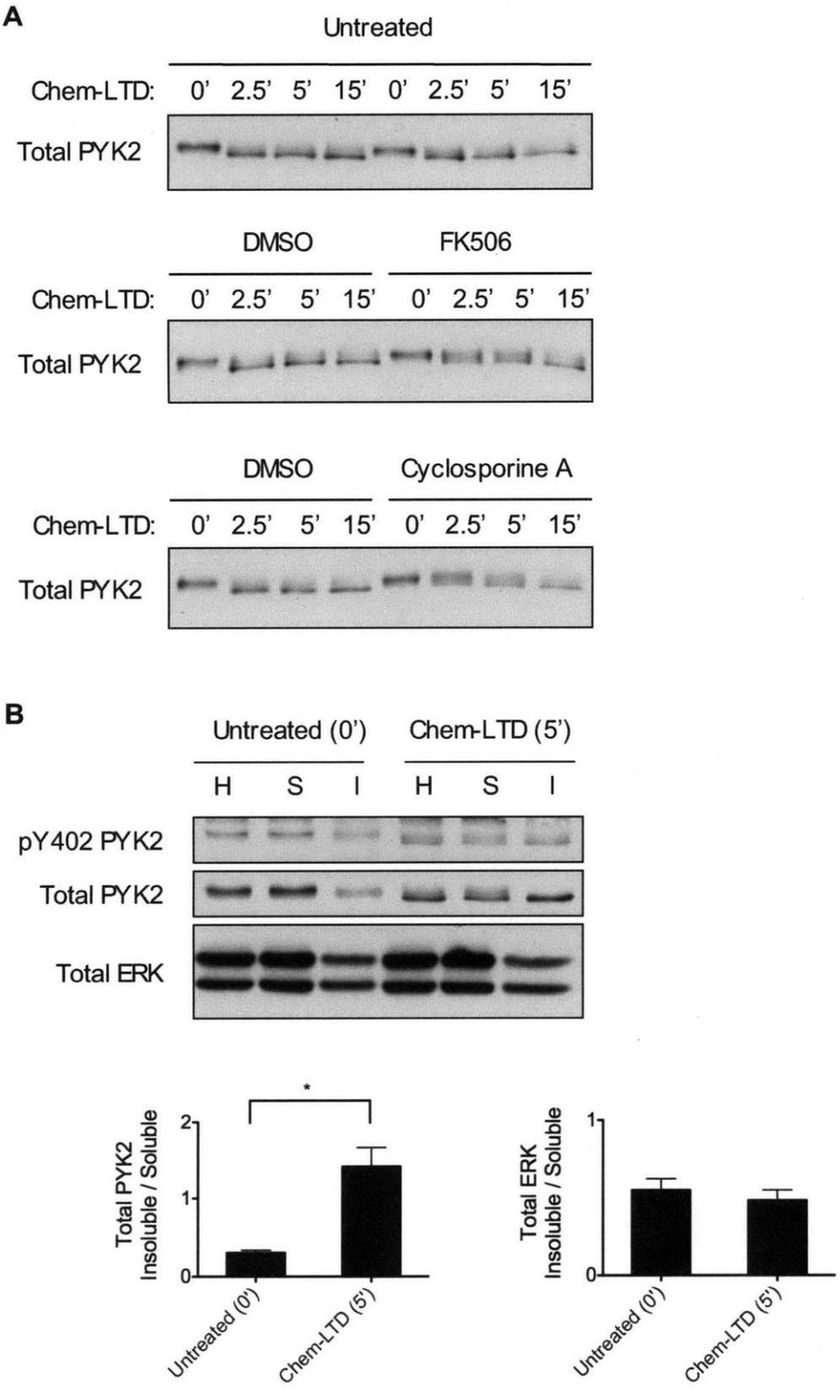
A
Untreated
Chem-LTD: 0' 2.5' 5' 15' 0' 2.5' 5' 15'
Total PYK2
DMSO
FK506
Chem-LTD: 0' 2.5' 5' 15' 0' 2.5' 5' 15'
Total PYK2
DMSO
Cyclosporine A
Chem-LTD: 0' 2.5' 5' 15' 0' 2.5' 5' 15'
Total PYK2
B
Untreated (0')
Chem-LTD (5')
H S I H S I
pY402 PYK2
Total PYK2
Total ERK
Total PYK2 Insoluble / Soluble
2
1
0
*
Untreated (0')
Chem-LTD (5')
Total ERK Insoluble / Soluble
1
0
Untreated (0')
Chem-LTD (5')

Figure S2

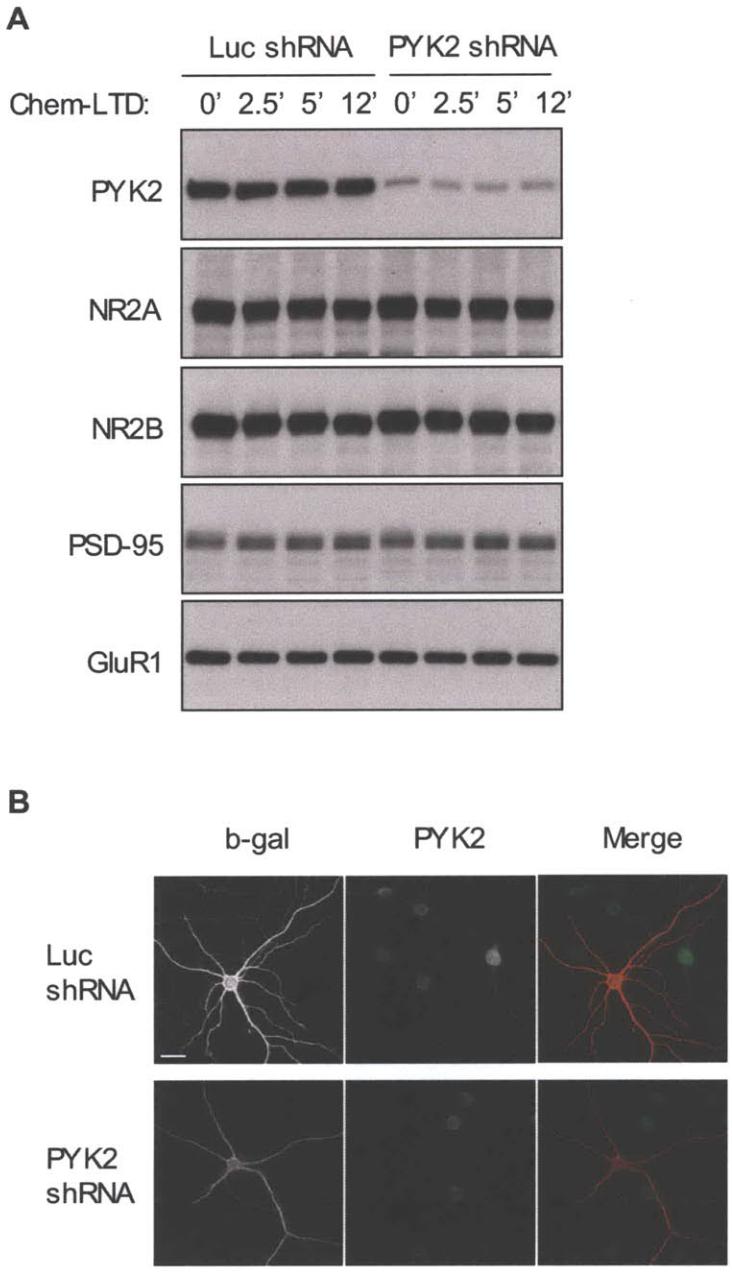
A
Luc shRNA
PYK2 shRNA
Chem-LTD:
0' 2.5' 5' 12' 0' 2.5' 5' 12'
PYK2
NR2A
NR2B
PSD-95
GluR1
B
b-gal
PYK2
Merge
Luc shRNA
PYK2 shRNA

Figure S3

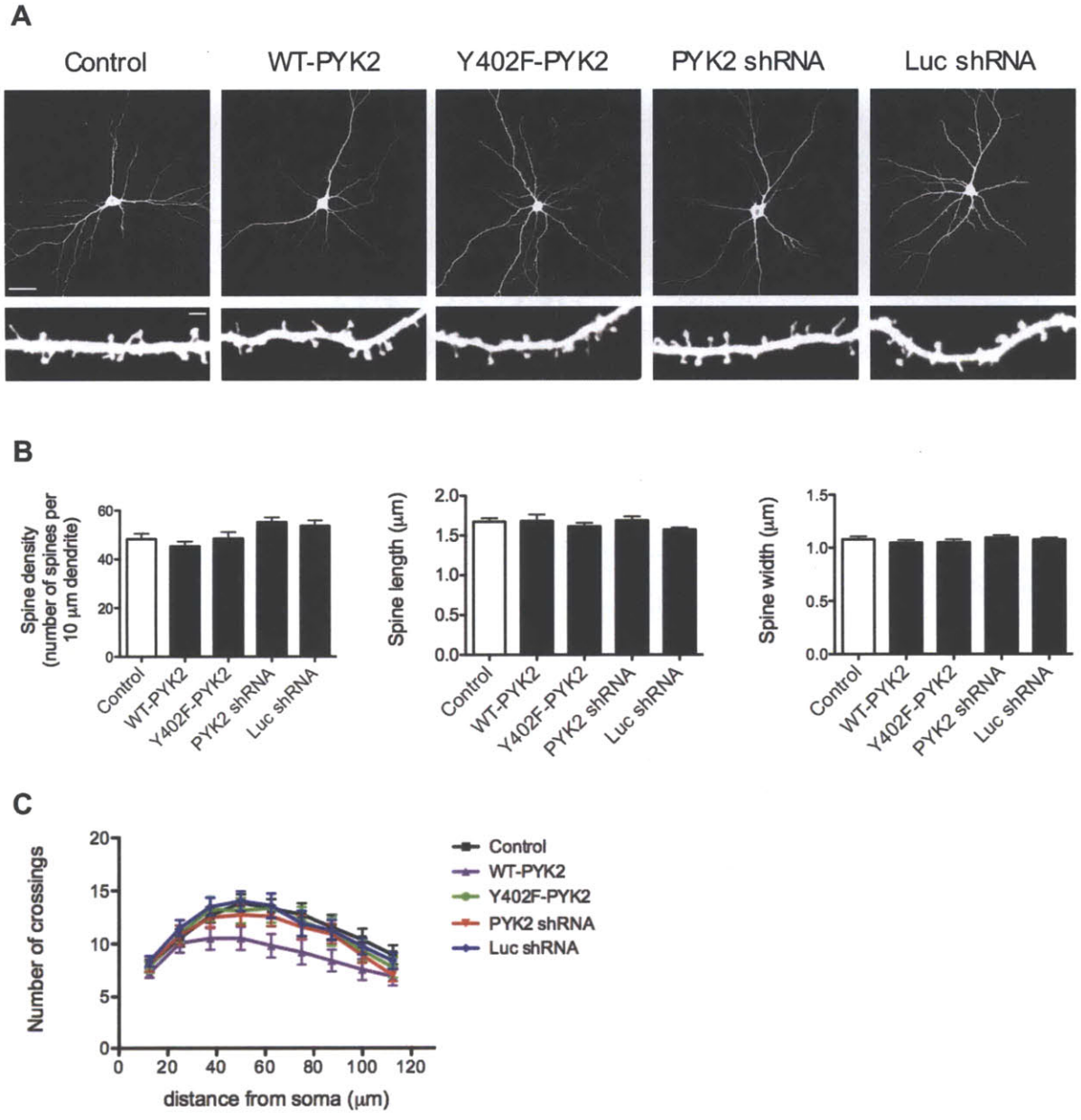
A
Control
WT-PYK2
Y402F-PYK2
PYK2 shRNA
Luc shRNA
B
Spine density (number of spines per 10 µm dendrite)
Spine length (µm)
Spine width (µm)
Control
WT-PYK2
Y402F-PYK2
PYK2 shRNA
Luc shRNA
C
Number of crossings
distance from soma (µm)
Control
WT-PYK2
Y402F-PYK2
PYK2 shRNA
Luc shRNA

Figure S4

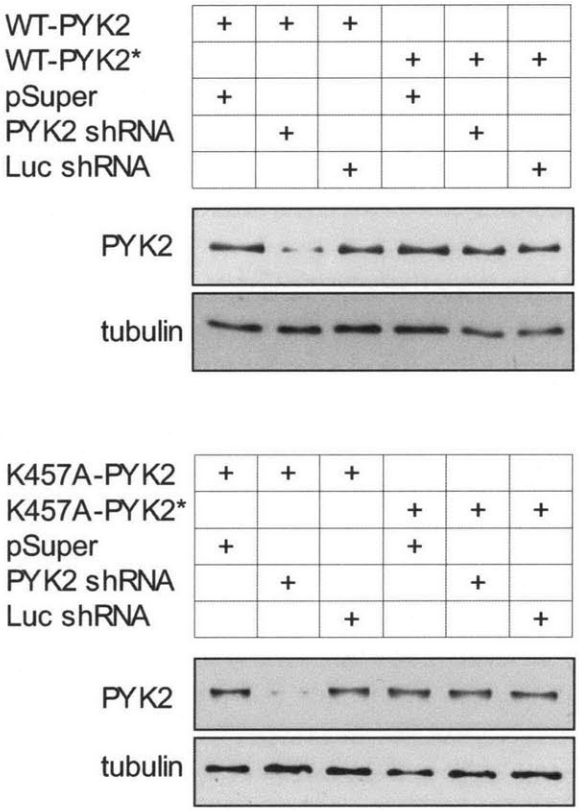
WT-PYK2
WT-PYK2*
pSuper
PYK2 shRNA
Luc shRNA
PYK2
tubulin
K457A-PYK2
K457A-PYK2*
pSuper
PYK2 shRNA
Luc shRNA
PYK2
tubulin

Figure S5

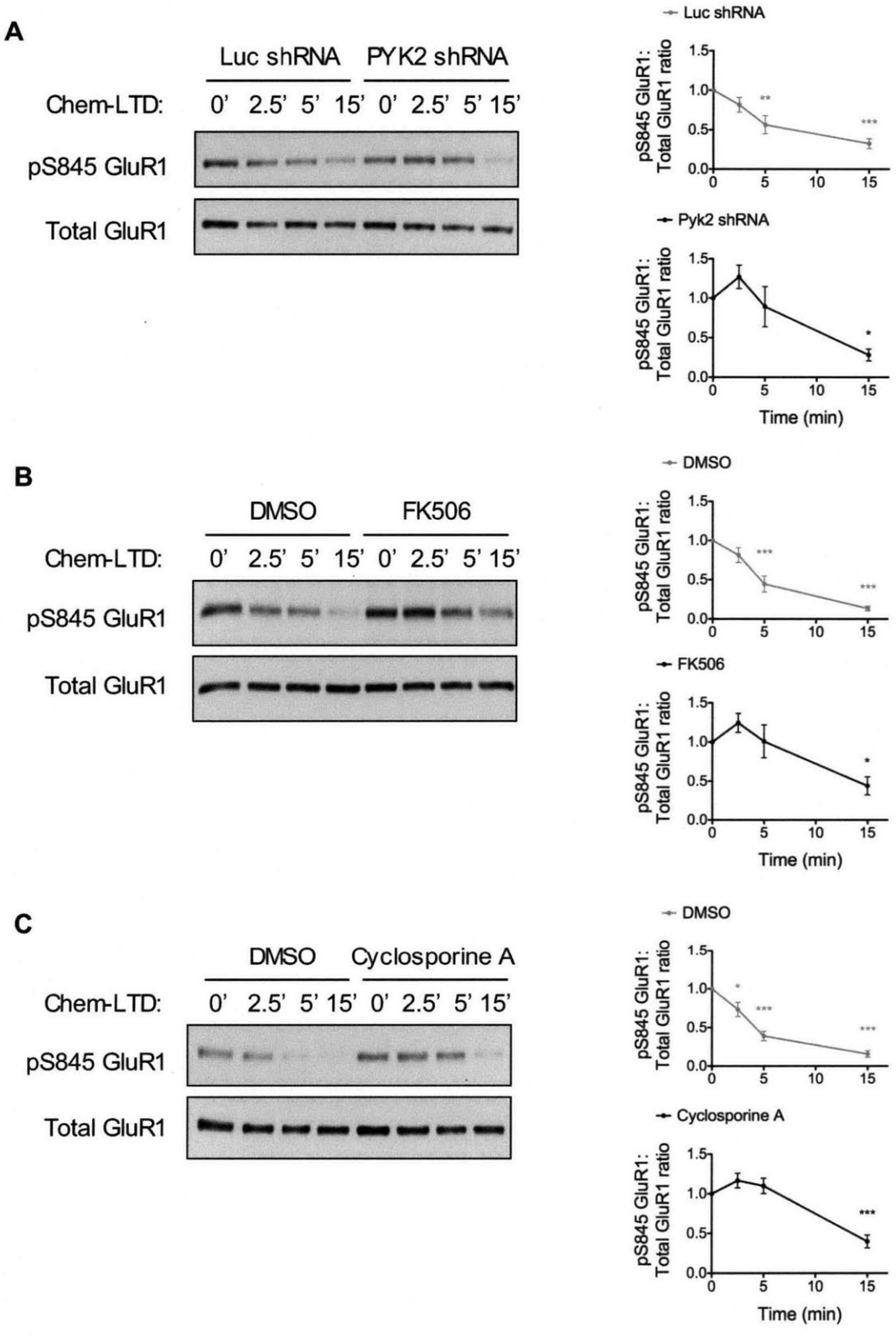
A
Luc shRNA
PYK2 shRNA
Chem-LTD:
0' 2.5' 5' 15' 0' 2.5' 5' 15'
pS845 GluR1
Total GluR1
Luc shRNA
pS845 GluR1: Total GluR1 ratio
Pyk2 shRNA
Time (min)
B
DMSO
FK506
Chem-LTD:
0' 2.5' 5' 15' 0' 2.5' 5' 15'
pS845 GluR1
Total GluR1
DMSO
FK506
pS845 GluR1: Total GluR1 ratio
Time (min)
C
DMSO
Cyclosporine A
Chem-LTD:
0' 2.5' 5' 15' 0' 2.5' 5' 15'
pS845 GluR1
Total GluR1
DMSO
Cyclosporine A
pS845 GluR1: Total GluR1 ratio
Time (min)

References

Ahmadian G, Ju W, Liu L, Wyszynski M, Lee S, Dunah A, Taghibiglou C, Wang Y, Lu J, Wong T, Sheng M, Wang Y (2004) Tyrosine phosphorylation of GluR2 is required for insulin-stimulated AMPA receptor endocytosis and LTD. EMBO J 23:1040-1050.

Alvarez V, Sabatini B (2007) Anatomical and physiological plasticity of dendritic spines. Ann Rev Neurosci 30:79-97.

Atkins C, Selcher J, Petraitis J, Trzaskos J, Sweatt, J (1998) The MAPK cascade is required for mammalian associative learning. Nat Neurosci 1:602-609.

Avraham H, Park S, Schinkmann K, Avraham S (2000) RAFTK/Pyk2-mediated cellular signaling. Cell Signal 12:123-133.

Bartos J, Ulrich J, Li H, Beazely M, Chen Y, MacDonald J, Hell J (2010) Postsynaptic clustering and activation of Pyk2 by PSD-95. J Neurosci 30:449-463.

Blum S, Moore A, Adams F, Dash P (1999) A mitogen-activated protein kinase cascade in the CA1/CA2 subfield of the dorsal hippocampus is essential for long-term spatial memory. J Neurosci 19:3535-3544.

Brummelkamp T, Bernards R, Agami R (2002) A system for stable expression of short interfering RNAs in mammalian cells. Science 296:550-553.

Cheung H, Takagi N, Teves L, Logan R, Wallace N, Gurd J (2000) Altered association of protein tyrosine kinases with postsynaptic densities after transient cerebral ischemia in the rat brain. J Cereb Blood Flow Metab 20:505-512.

Coba M, Valor L, Kopanitsa M, Afinowi N, Grant S (2008) Kinase networks integrate profiles of N-methyl-D-aspartate receptor-mediated gene expression in hippocampus. J Biol Chem 283:34101-34107.

Collins M, Husi H, Yu L, Brandon J, Anderson C, Blackstock W, Choudhary J, Grant S (2006) Molecular characterization and comparison of the components and multiprotein complexes in the postsynaptic proteome. J Neurochem 97 Supp 1:16-23.

Ehlers M (2000) Reinsertion of degradation of AMPA receptors determined by activity-dependent endocytic sorting. Neuron 28:511-525.

Ehrlich I, Malinow R (2004) Postsynaptic density 95 controls AMPA receptor incorporation during long-term potentiation and experience-driven synaptic plasticity. J Neurosci 24:916-927.

English J, Sweatt J (1997) A requirement for the mitogen-activated protein kinase cascade in hippocampal long term potentiation. J Biol Chem 272:19103-19106.

Faure C, Corvol J, Toutant M, Valjent E, Hvalby O, Jensen V, Messari S, Corsi J, Kadare G, Girault J (2007) Calcineurin is essential for depolarization-induced nuclear translocation and tyrosine phosphorylation of PYK2 in neurons. J Cell Sci 120:3034-3044.

Gil-Henn H, Destaing O, Sims N, Aoki K, Alles N, Neff L, Sanjay A, Bruzzaniti A, De Camili P, Baron R, Schlessinger J (2007) Defective microtubule-dependent podosome organization in osteoclasts lead to increased bone density in Pyk2 (-/-) mice. J Cell Biol 178:1053-1064.

Girault J, Costa A, Derkinderen P, Studler J, Toutant M (1999) FAK and PYK2/CAKbeta in the nervous system: a link between neuronal activity, plasticity, and survival? Trends Neurosci 22:257-263.

Grant S, O'Dell T, Karl K, Stein P, Soriano P, Kandel E (1992) Impaired long-term potentiation, spatial learning, and hippocampal development in fyn mutant mice. Science 258:1903-1910.

Han K, Kim M, Seeburg D, Seo J, Verpelli C, Han S, Chung H, Ko J, Lee H, Kim K, Heo W, Meyer T, Kim H, Sala C, Choi S, Sheng M, and Kim E (2009) Regulated RalBP1 binding to RalA and PSD-95 controls AMPA receptor endocytosis and LTD. PLoS Biol 7:e1000187.

Hashido M, Hayashi K, Hirose K, Iino M (2006) Ca2+ lightning conveys cell-cell contact information inside cells. EMBO Reports 7:1117-1123.

Hayashi T, Huganir R (2004) Tyrosine phosphorylation and regulation of the AMPA receptor by SRC family tyrosine kinases. J Neurosci 24:6152-6160.

Huang Y, Lu W, Ali D, Pelkey K, Pitcher G, Lu Y, Aoto H, Roder J, Sasaki T, Salter M, MacDonald J (2001) CAKbeta/Pyk2 kinase is a signaling link for induction of long-term potentiation in CA1 hippocampus. Neuron 29:485-496.

Kim M, Dunah A, Wang Y, Sheng M (2005) Differential roles of NR2A- and NR2B-containing NMDA receptors in Ras-ERK signaling and AMPA receptor trafficking. Neuron 46:745-760.

Kim M, Futai K, Jo J, Hayashi Y, Cho K, Sheng M (2007) Synaptic accumulation of PSD-95 and synaptic function regulated by phosphorylation of serine-295 of PSD-95. Neuron 56:488-502.

Kohno T, Matsuda E, Sasaki H, Sasaki T (2008) Protein-tyrosine kinase CAKbeta/PYK2 is activated by binding Ca2+/calmodulin to FERM F2 alpha2 helix and thus forming its dimer. Biochem J 410:513-523.

Lakkakorpi P, Bett A, Lipfert L, Rodan G, Duong L (2003) PYK2 autophosphorylation, but not kinase activity, is necessary for adhesion-induced association with c-Src, osteoclast spreading, and bone resorption. J Biol Chem 278:11502-11512.

Lee H, Kameyama K, Huganir R, and Bear M (1998) NMDA induces long-term synaptic depression and dephosphorylation of the GluR1 subunit of AMPA receptors in hippocampus. Neuron 21:1151-1162.

Lee H, Takamiya K, Han J, Man H, Kim C, Rumbaugh G, Yu S, Ding L, He C, Petralia R, Wenthold R, Gallagher M, Huganir R (2003) Phosphorylation of the AMPA receptor GluR1 subunit is required for synaptic plasticity and retention of spatial memory. Cell 112:631-643.

Lev S, Moreno H, Martinez R, Canoll P, Peles E, Musachhio J, Plowman G, Rudy B, and Schlessinger J (1995) Protein tyrosine kinase PYK2 involved in Ca2+-induced regulation of ion channel and MAP kinase functions. Nature 376:737-745.

Li X, Dy R, Cance W, Graves L, and Earp H (1999) Interactions between two cytoskeleton-associated tyrosine kinases: calcium-dependent tyrosine kinase and focal adhesion tyrosine kinase. J Biol Chem 274:8917-8924.

Lim Y, Lim S, Tomar A, Gardel M, Bernard-Trifilo J, Chen X, Uryu S, Canete-Soler R, Zhai J, Lin J, Schlaepfer W, Nalbant P, Bokock G, Ilic D, Waterman-Storer C, and Schlaepfer D (2008) Pyk2 and FAK connections to p190Rho guanine nucleotide exchange factor regulate RhoA activity, focal adhesion formation, and cell motility. J Cell Biol 180:187-203.

Lois C, Hong E, Pease S, Brown E, and Baltimore D (2002) Germline transmission and tissue-specific expression of transgenes delivered by lentiviral vectors. Science 295:868-872.

Lu Y, Roder J, Davidow J, and Salter M (1998) Src activation in the induction of long-term potentiation in CA1 hippocampal neurons. Science 279:1363-1367.
Malenka R, Kauer J, Perkel D, Mauk D, Kelly P, Nicoll R, and Waxham M (1989) An essential role for postsynaptic calmodulin and protein kinase activity in long-term potentiation. Nature 340:554-557.
Malinow R, Schulman H, and Tsien R (1989) Inhibition of postsynaptic PKC or CaMKII blocks induction but not expression of LTP. Science 245:862-866.
Marshall C (1995) Specificity of receptor tyrosine kinase signaling: transient versus sustained extracellular signal-regulated kinase activation. Cell 80:179-185.
McLeod S, Shum A, Lee R, Takei F, Gold M (2004) The Rap GTPases regulate integrin-mediated adhesion, cell spreading, actin polymerization, and Pyk2 tyrosine phosphorylation in B lymphocytes. J Biol Chem 279:12009-12019.
Migaud M, Charlesworth P, Dempster M, Webster L, Watabe A, Makhinson M, He Y, Ramsay M, Morris R, Morrison J, O'Dell T, and Grant S (1998) Enhanced long-term potentiation and impaired learning in mice with mutant postsynaptic density-95 protein. Nature 396:433-439.
Miyakawa T, Leiter L, Gerber D, Gainetdinov R, Sotnikova T, Zeng H, Caron M, Tonegawa S (2003) Conditional calcineurin knockout mice exhibit multiple abnormal behaviors related to schizophrenia. Proc Natl Acad Sci 100:8987-8992.
Morishita W, Connor J, Xia H, Quinlan E, Shenolikar S, and Malenka R (2001) Regulation of synaptic strength by protein phosphatase 1. Neuron 32:1133-1148.
Mulkey R, Herron C, Malenka R (1993) An essential role for protein phosphatases in hippocampal long-term depression. Science 261:1051-1055.
Mulkey R, Endo S, Shenolikar S, Malenka R (1994) Involvement of a calcineurin/inhibitor-1 phosphatase cascade in hippocampal long-term depression. Nature 369:486-488.
Murase S, Mosser E, Schuman E (2002) Depolarization drives beta-catenin into neuronal spines promoting changes in synaptic structure and function. Neuron 35:91-105.
Nakayama A, Harms M, Luo L (2000) Small GTPases Rac and Rho in the maintenance of dendritic spines and branches in hippocampal pyramidal neurons. J Neurosci 20:5329-5338.
Okamoto K, Nagai T, Miyawaki A, Hayashi Y (2004) Rapid and persistent modulation of actin dynamics regulates postsynaptic reorganization underlying bidirectional plasticity. Nat Neurosci 7:1104-1112.
Okigaki M, Davis C, Falasca M, Harroch S, Felsenfeld D, Sheetz M, Schlessinger J (2003) Pyk2 regulates multiple signaling events crucial for macrophage morphology and migration. Proc Natl Acad Sci 100:10740-10745.
Park S, Avraham H, Avraham S (2004) RAFTK/Pyk2 activation is mediated by trans-acting autophosphorylation in a Src-independent manner. J Biol Chem 279:33315-33322.
Qin Y, Zhu Y, Baumgart J, Stornetta R, Seidenman K, Mack V, van Aelst L, Zhu J (2005) State-dependent Ras signaling and AMPA receptor trafficking. Genes Dev 19:2000-2015.
Ryu K, Futai K, Feliu M, Weinberg R, Sheng M (2008) Constitutively active Rap2 transgenic mice display fewer dendritic spines, reduced extracellular signal-regulated kinase signaling, enhanced long-term depression, and impaired spatial learning and fear extinction. J Neurosci 28:8178-8188.

Sala C, Futai K, Yamamoto K, Worley P, Hayashi Y, Sheng M (2003) Inhibition of dendritic spine morphogenesis and synaptic transmission by activity-inducible protein Homer 1a. J Neurosci 23:6327-6337.

Seabold G, Burette A, Lim I, Weinberg R, Hell J (2003) Interaction of the tyrosine kinase Pyk2 with the N-methyl-D-aspartate receptor complex via the Src homology 3 domains of PSD-95 and SAP102. J Biol Chem 278:15040-15048.

Seeburg D, Sheng M (2008) Activity-induced Polo-Like Kinase 2 is required for homeostatic plasticity of hippocampal neurons during epileptiform activity. J Neurosci 28:6583-6591.

Selcher J, Atkins C, Trzaskos J, Paylor R, Sweatt J (1999) A necessity for MAP kinase activation in mammalian spatial learning. Learn Mem 6:478-490.

Sheng M, Hoogenraad C (2007) The postsynaptic architecture of excitatory synapses: a more quantitative view. Ann Rev Biochem 76:823-847.

Silva A, Paylor R, Wehner J, Tonegawa S (1992) Impaired spatial learning in alpha-calcium-calmodulin kinase II mutant mice. Science 257:206-211.

Stein V, House D, Bredt D, Nicoll R (2003) Postsynaptic density-95 mimics and occludes hippocampal long-term potentiation and enhances long-term depression. J Neurosci 23:5503-5506.

Tada T, Sheng M (2006) Molecular mechanisms of dendritic spine morphogenesis. Curr Opin Neurobiol 16:95-101.

Tada T, Simonetta A, Batterton M, Kinoshita M, Edbauer D, Sheng M (2007) Role of Septin cytoskeleton in spine morphogenesis and dendrite development in neurons. Curr Biol 17:1752-1758.

Thiels E, Kanterewicz B, Norman E, Trzaskos J, Klann E (2002) Long-term depression in the adult hippocampus *in vivo* involves activation of extracellular signal-regulated kinase and phosphorylation of Elk-1. J Neurosci 22:2054-2062.

Thomas G, Huganir R (2004) MAPK cascade signaling and synaptic plasticity. Nat Rev Neurosci 5:173-183.

Tian D, Litvak V, Lev S (2000) Cerebral ischemia and seizures induce tyrosine phosphorylation of PYK2 in neurons and microglial cells. J Neurosci 20:6478-6487.

Van Buul J, Anthony E, Fernandez-Borja M, Burridge K, and Hordijk P (2005) Proline-rich tyrosine kinase 2 (Pyk2) mediates vascular endothelial-cadherin-based cell-cell adhesion by regulating beta-catenin tyrosine phosphorylation. J Biol Chem 280:21129-21136.

Wright S, Malinin N, Powell K, Yednock T, Rydel R, Griswold-Prenner I (2007) Alpha2beta1 and alphaVbeta1 integrin signaling pathways mediate amyloid-beta-induced neurotoxicity. Neurobiol Aging 28:226-237.

Xiong W, Parsons J (1997) Induction of apoptosis after expression of PYK2, a tyrosine kinase structurally related to focal adhesion kinase. J Cell Biol 139:529-539.

Xu W, Schlüter O, Steiner P, Czervionke B, Sabatini B, Malenka R (2008) Molecular dissociation of the role of PSD-95 in regulating synaptic strength and LTD. Neuron 57:248-262.

Zeng H, Chattarji S, Barbarosie M, Rondi-Reig L, Philpot B, Miyakawa T, Bear M, Tonegawa S (2001) Forebrain-specific calcineurin knockout selectively impairs bidirectional synaptic plasticity and working/episodic-like memory. Cell 107:617-629.

Zhang H, Macara I (2006) The polarity protein PAR-3 and TIAM1 cooperate in dendritic spine morphogenesis. Nat Cell Biol 8:227-237.

Zhao J, Zheng C, Guan J (2000) Pyk2 and FAK differentially regulate progression of the cell cycle. J Cell Sci 113:3064-3072.

Zhou Q, Homma K, Poo M (2004) Shrinkage of dendritic spines associated with long-term depression of hippocampal synapses. Neuron 44:749-757.

Zhu J, Qin Y, Zhao M, Van Aelst L, Malinow R (2002) Ras and Rap control AMPA receptor trafficking during synaptic plasticity. Cell 110:443-455.

Zhu, Y., Pak, D., Qin, Y., McCormack, S., Kim, M., Baumgart, J., Velamoor, V., Auberson, Y., Osten, P., van Aelst, L., Sheng, M., and Zhu, J. (2005). Rap2-JNK removes synaptic AMPA receptors during depotentiation. Neuron *46*, 905-916.

CHAPTER 4:

Conclusions

Activity-dependent depression, or long term depression (LTD), of synaptic strength is critical for experience-dependent plasticity in the brain (see Malenka and Bear, 1994; Citri and Malenka, 2008). In neuropsychiatric disorders such as schizophrenia or Alzheimer's disease, LTD signaling pathways may be inhibited or exacerbated (Miyakawa et al., 2003; Hsieh et al., 2006; Peineau et al., 2007; Citri and Malenka, 2008; Li et al., 2009). In this thesis, we provide novel insights into the molecular mechanism of LTD at hippocampal synapses, which may guide future therapeutic approaches for diseases of synapse failure.

I. GSK-3beta phosphorylation of PSD-95 is required for LTD

GSK-3beta is a serine/threonine kinase implicated in schizophrenia, Alzheimer's disease, and mood disorders (Jope and Roh, 2006). At hippocampal synapses, GSK-3beta is essential for LTD, and is activated by NMDAR stimulation via Ser-9 dephosphorylation (Peineau et al., 2007). Here we identify the first known synaptic target of GSK-3beta, the scaffold protein PSD-95, and show that this phosphorylation is functionally important for LTD. GSK-3beta phosphorylates Thr-19 of PSD-95, and reduces N-terminal multimerization of PSD-95. Mutations in Thr-19 affect PSD-95 multimerization, synaptic clustering, and stability in spines, and GSK-3beta is required for NMDA-induced dispersal of synaptic PSD-95 clusters. We find that Thr-19 phosphorylation of PSD-95 increases with NMDAR stimulation, and is required for LTD. Thus GSK-3beta phosphorylation of PSD-95 at Thr-19 is a critical step in LTD.

One potential caveat of our study is that the effect of Thr-19 mutations on PSD-95 function in neurons were examined in the presence of endogenous PSD-95, which may or may not confound our results. "Molecular replacement" approaches were designed to overcome this potential problem, by expressing PSD-95 mutants while simultaneously knocking down endogenous PSD-95 (Xu et al., 2008). These types of experiments are useful for studying how PSD-95 molecules target to synapses devoid of a pre-existing PSD-95 lattice (Sturgill et al., 2009). We were more interested, however, in the molecular behavior of PSD-95 proteins already present at synapses, where the effects of PSD-95 multimerization and clustering become important (Hsueh et al., 1997; El-Husseini et al., 2002; Morabito et al., 2004). Additionally, our model predicted that T19A-PSD-95 molecules would act as "dominant negative" mutants in blocking PSD-95 multimerization and thus LTD. Expression of T19A-PSD-95 in the context of

endogenous PSD-95, therefore, was also an informative experiment as well as molecular replacement with T19A-PSD-95 mutants alone (an argument also made in Xu et al., 2008). Consistent with our results, Xu et al. (2008) found that N-terminal PSD-95 mutations blocked LTD in the presence or absence of endogenous PSD-95.

Implications for PSD-95 signaling

Several questions remain unanswered by our study. What is the molecular mechanism for Thr-19-mediated de-multimerization of PSD-95, and how does this translate to reduced PSD-95 stability and removal from synapses? Thr-19 resides near Cys-3/Cys-5 palmitoylation sites, and Thr-19 phosphorylation could affect PSD-95 palmitoylation. De-palmitoylation of PSD-95 is not required for LTD, however (Xu et al., 2008), so it is unlikely that de-palmitoylation is the only effect of Thr-19 phosphorylation on PSD-95 function. We find that Thr-19 phosphorylation blocks head-to-head multimerization of PSD-95, which could also be caused by electrostatic repulsion of N-terminal phosphate groups.

De-multimerization of PSD-95 may be an initial step toward destabilization of the synaptic PSD-95 lattice, and subsequent dispersal of PSD-95 molecules from the spine (Sturgill et al., 2009). PSD-95 dispersal, in turn, could decrease synaptic AMPAR content. In fact, AMPAR interactions with PSD-95 (through Stargazin) hinder AMPAR mobility at synaptic sites (Bats et al., 2007), so it is possible that PSD-95 dispersal disrupts the "corralling" effect of the PSD-95 lattice, thereby enabling diffusion of AMPAR complexes to extrasynaptic sites where endocytosis occurs (see Chapter 1). The relationship between PSD-95-AMPAR movements at synapses and the pathways of AMPAR internalization in LTD should be examined in further detail.

What signaling proteins mediate Thr-19 dephosphorylation? We found that Thr-19 PSD-95 is dephosphorylated upon chemical LTP treatment, which could be due to suppression of GSK-3beta kinase activity and/or elevated activity of an unknown phosphatase. Components of this Thr-19 dephosphorylation pathway may also be important in the homeostatic regulation of PSD-95 function after LTD, or after periods of chronic activity manipulation.

Several other PSD-95 residues undergo activity-dependent regulation by phosphorylation, and it is unknown how Thr-19 phosphorylation relates to these other pathways.

Dephosphorylation of Ser-295 in PSD-95 is required for LTD, and causes a reduction in synaptic accumulation of PSD-95 (Kim et al., 2007). It is possible that PSD-95 must be properly modified at both Thr-19 and Ser-295 residues in order to undergo de-stabilization at synapses during LTD, since expression of the phospho-mimic S295D-PSD-95 mutant, which can still be phosphorylated at T19, blocks LTD (additionally, the phospho-mimic T19D-PSD-95 mutant is not sufficient to occlude LTD, although the presence of endogenous PSD-95 in our experiment may be masking the effect of this mutation). Ser-73 phosphorylation is also important for PSD-95 destabilization, consistent with reports that N-terminal PDZ domains are required for PSD-95 incorporation into the synaptic lattice (Steiner et al., 2008; Sturgill et al., 2009). Whether Ser-73 phosphorylation is regulated during LTD, and whether this step (or PDZ domain-dependent PSD-95 incorporation) is affected by Thr-19 phosphorylation, remains to be examined.

Implications for GSK-3beta signaling

Our study defines one critical target of GSK-3beta in LTD, but there are likely many more to uncover. It also remains a mystery whether the Akt and Wnt signaling pathways of GSK-3beta intersect at the synapse, given that components of both pathways have been identified in the PSD. Beta-catenin, for example, controls synaptic strength, structure, and scaling (Okuda et al., 2007; Tai et al., 2007; Peng et al., 2009), and it is unknown whether expression of S9A-GSK-3beta also affects beta-catenin function in neurons. Additionally, it would be interesting to examine whether NMDAR activation regulates GSK-3beta recruitment to synapses, thereby favoring contact with PSD-95 molecules. If so, what are the factors involved in this recruitment?

Our findings may shed light on the pathophysiology of neuropsychiatric diseases tied to GSK-3beta function. Overexpression of GSK-3beta causes neurodegeneration (Lucas et al., 2001), whereas a reduction in GSK-3beta activity reverses depression- and schizophrenia-like behaviors in mice (O'Brien et al., 2004; Mao et al., 2009). It would be interesting to test whether PSD-95 clustering or stability at synapses is affected in these animal models, and if so, whether rescuing this function of PSD-95 (perhaps through genetic means; e.g., construction of T19A-PSD-95 or T19D-PSD-95 knockin strains) can influence behavioral phenotypes. Additionally, neuropsychiatric behaviors and synaptic plasticity should be examined in S9A-GSK-3beta

knockin mice, which we would expect to show perturbations in the molecular properties of synaptic PSD-95.

II. PYK2 is required for LTD

PYK2, a calcium-dependent tyrosine kinase involved in cell migration, is found in the PSD of neurons (Avraham et al., 2000; Huang et al., 2001; Collins et al., 2006), but its function in neurons is poorly understood. Here we report a novel role for PYK2 in LTD. NMDAR stimulation induces PYK2 phosphorylation at Tyr-402. We find that PYK2 is necessary for LTD but not LTP in hippocampal neurons, and identify both kinase- and scaffold (Y402)-dependent roles for PYK2 in LTD. We further show that PYK2 is required to suppress NMDA-induced ERK phosphorylation in neurons. Overexpression of PYK2 depresses NMDA-dependent ERK phosphorylation and inhibits LTP, but not LTD. Our studies support a mechanism whereby PYK2 antagonizes ERK signaling to promote LTD at the expense of LTP.

One potential caveat of our study is that the results we obtained with chemical LTD (bath NMDAR stimulation) may not fully explain the effects we observed with electrophysiological LTD or LTP (which presumably depends on synaptic NMDAR activation; see Chapter 1). Although chemical LTD in dissociated cultures allows for unbiased time-course analysis (on a ~2.5-minute scale) of biochemical signaling events within a population of mature neurons, it is possible that the PYK2 signaling pathways recruited by this protocol of NMDAR stimulation are not recruited (or recruited differently) by electrophysiological induction of LTD in slice cultures. Further experiments will be needed to address this possibility, such as imaging the molecular activation of ERK and other putative signaling events in slice-cultured neurons before and after electrophysiological LTD induction (see *Implications for ERK signaling in LTD* below).

Our model suggests that alterations in PYK2 activity could shift the postsynaptic activity threshold (Θ_m) of the Bienenstock, Cooper, and Munro model (see Chapter 1; Bienenstock et al., 1982). Thus PYK2 knockdown or Y402F-PYK2 overexpression blocks LTD without affecting LTP, whereas WT-PYK2 overexpression blocks LTP without affecting LTD. The reason why we didn't observe LTP enhancement with PYK2 knockdown (or LTD enhancement with WT-PYK2 overexpression) could be because our pairing protocols induced LTP (or LTD) too robustly for these effects to be parsed. We would predict that at intermediate stimulation

frequencies, it may be possible to see enhanced LTP with PYK2 knockdown; in fact, when we tried inducing LTP at a lower frequency of presynaptic stimulation (2Hz, 200 pulses, holding at 0 mV), neurons expressing PYK2 shRNA exhibited LTP while neurons expressing luciferase shRNA did not (Hsin and Sheng, unpublished data). If PYK2 activity does indeed influence the cellular LTP/LTD threshold within neurons, it would be intriguing to see whether chronic regulation of PYK2 levels contributes to mechanisms of metaplasticity.

Implications for PYK2-ERK signaling

A key question raised by our study is the identity of the signaling factor(s) that links PYK2 activity to ERK phosphorylation. As discussed in Chapter 1, activity of the small GTPases Ras and Rap influence ERK activity in neurons, and multiple GTPase regulators (activating GEFs and inactivating GAPs) have been identified in the PSD. The most abundant of these is SynGAP, a RasGAP that inhibits ERK signaling and has been implicated in LTP and chemical LTD (Kim et al., 2003; Rumbaugh et al., 2006; Kim et al., 2005; Carlisle et al., 2008; see Chapter 1). Both SynGAP and PYK2 associate with PSD-95 (Kim and Sheng, 2004), suggesting that PYK2 could potentially modulate SynGAP function within the PSD-95 complex. In fact, we find that PYK2 expression, but not expression of kinase-dead or Y402F-PYK2, causes tyrosine phosphorylation of SynGAP in human embryonic kidney (HEK) cells (Hsin, Wang, and Sheng, unpublished data), and SynGAP is reportedly tyrosine-phosphorylated in the forebrain (Collins et al., 2005). The signaling circuitry in HEK cells, unfortunately, complicates further study of this functional interaction, since PYK2 expression independently enhances ERK activity in HEK cells through recruitment of the RasGEF, Sos (Lev et al., 1995). Additionally, SynGAP's involvement in LTP argues against a straightforward mechanism for contributing to PYK2 signaling in LTD (Kim et al., 2003). Further studies will be needed to dissect the precise role of SynGAP in synaptic plasticity, and to examine whether PYK2 affects SynGAP function (or the function of other GAPs and GEFs) in neurons.

PYK2 could also regulate dephosphorylation of ERK. In cortical neurons, ERK is dephosphorylated by the striatal-enriched tyrosine phosphatase (STEP; Paul et al., 2003). STEP is activated by calcineurin, and can limit the duration of glutamate-induced ERK phosphorylation in neurons (Paul et al., 2003). Infusion of recombinant STEP into hippocampal

slices blocks LTP like PYK2 (Pelkey et al., 2002), and the role of STEP in LTD is unknown. PYK2 could modulate ERK signaling by activation of STEP; however, STEP is not predicted to be regulated by tyrosine phosphorylation, and does not contain any protein motifs expected to interact with PYK2's domains (Braithwaite et al., 2006). Nonetheless, a systematic examination of other spatial or temporal regulators of ERK signaling in neurons (for example, ERK pathway scaffolds) could prove fruitful.

Implications for ERK signaling in LTD

How do PYK2's effects on ERK phosphorylation modulate synaptic plasticity? The hypothesis that varying levels and/or temporal characteristics of ERK activity could affect the induction of LTP versus LTD (see Chapter 1) has never been directly tested. A methodical analysis, similar to experiments investigating the role of intracellular calcium levels in LTP/LTD, is needed (Chapter 1). For example, live-imaging of an ERK activity sensor in neurons after LTP or LTD stimulation can reveal the precise spatiotemporal dynamics of active ERK. A fluorescence resonance energy transfer (FRET)-based probe for ERK activity, in fact, has recently been described, and would be useful for such a study (Harvey et al., 2008). To examine whether varying levels of ERK are actually required for LTP or LTD, one possible experiment is to use partial blockade of ERK activity to try converting an LTP-inducing stimulus to an LTD-inducing one, much like how partial blockade of NMDAR function was found to convert LTP to LTD in hippocampal neurons (Cummings et al., 1996; Nishiyama et al., 2000).

ERK activity is required for the Ras pathway of AMPAR insertion during LTP (Zhu et al., 2002). Inhibition of ERK, therefore, could promote LTD by countering the effect of Ras on AMPAR trafficking. The question then remains, which AMPAR subunit is affected by PYK2 signaling? Although it has been reported that tyrosine phosphorylation of the GluR2 subunit promotes AMPAR endocytosis during LTD (Ahmadian et al., 2004; Hayashi and Huganir, 2004), we did not detect GluR2 tyrosine phosphorylation in our chemical LTD experiments (Hsin, Wang, and Sheng, unpublished data), so we were unable to test if PYK2 is involved in tyrosine phosphorylation of GluR2 in neurons. In HEK cells, PYK2 expression does not increase tyrosine phosphorylation of GluR2 (Hayashi and Huganir, 2004; Hsin and Sheng, unpublished data). GluR1, on the other hand, is regulated during LTD and AMPAR

internalization by dephosphorylation of Ser-845, and mutations in GluR1 Ser-845 block LTD (Lee et al., 2000; Lee et al., 2010). Indeed, we found that PYK2 knockdown affected the time course of GluR1 Ser-845 dephosphorylation, similar to the effects of calcineurin inhibitors, which are known to block LTD. This is in agreement with previous reports linking Ras-ERK signaling to the regulation of GluR1 phosphorylation at this site (Qin et al., 2005). Thus it is likely that PYK2's effect on LTD at the AMPA receptor level is mediated through GluR1 Ser-845 dephosphorylation.

Implications for other aspects of PYK2 signaling

PYK2 binds PSD-95 at the SH3-GK region (Seabold et al., 2003), and mutations in this region block LTD (Xu et al., 2008). PYK2 association with PSD-95 is required for activity-dependent activation of PYK2 (Bartos et al., 2010), and it would be interesting to test whether any of the PSD-95 mutants identified above (e.g., multimerization-deficient PSD-95 molecules) also affect PYK2 activity. Conversely, PYK2 may promote LTD by regulating PSD-95 function, and it remains unknown whether PYK2 association affects PSD-95 multimerization, phosphorylation, or stability in spines.

PSD-95 knockouts exhibit increased LTP and reduced LTD (Migaud et al., 1998), suggesting that like PYK2, PSD-95 promotes LTD at the expense of LTP. Calcineurin knockouts also display enhanced LTP and impaired LTD (Zeng et al., 2001), and calcineurin inhibition leads to elevated glutamate-induced ERK phosphorylation (Paul et al., 2003), similar to the effects of PYK2 knockdown. We found that calcineurin inhibitors affected PYK2 mobility in SDS-PAGE, consistent with reports that calcineurin regulates PYK2 function (Faure et al., 2007). A common pathway of calcineurin-PYK2-PSD-95 signaling, therefore, may play a central role in LTD (and in blocking LTP), and the precise sequence of molecular steps between these three proteins during LTD induction should be explored in further detail.

There are probably additional targets of PYK2 signaling at synapses, and these can be identified by a screen for PYK2's binding partners in neurons (e.g., mass spectrometry analysis of purified wild type PYK2 protein complexes, compared to Y402F-PYK2 complexes that cannot signal LTD). Another important question raised by our findings is the molecular significance of NMDA-induced changes in PYK2 biochemical distribution, and how this step

relates to Y402 phosphorylation and kinase activity requirements. To examine whether NMDAR stimulation affects the molecular stability of PYK2, we attempted to investigate the dynamics of PYK2 tagged with photoactivatable GFP (PA-GFP) in neurons; however, these proteins did not respond to photoactivation in spines or dendrites (Hsin, Wang, and Sheng, unpublished data). Other techniques for molecular tagging should be used to address the question of whether PYK2 stability is regulated by synaptic activity.

PYK2 inhibition of LTP raises the interesting possibility that PYK2 is regulated by LTP stimuli. We found that chemical LTP (rolipram/forskolin treatment in the absence of magnesium) also increased PYK2 Y402 phosphorylation (Hsin, Wang, and Sheng, unpublished data), and it would be intriguing to see if the duration or magnitude of PYK2 activation under these conditions differs from what is observed during chemical LTD. We found that PYK2 knockdown also enhanced chemical LTP-dependent ERK phosphorylation (Hsin, Wang, and Sheng, unpublished data), a finding consistent with the idea that PYK2 inhibits LTP.

PYK2 is reportedly activated in cerebral ischemia and seizures (Cheung et al., 2000; Tian et al., 2000), but a role for PYK2 in the pathogenesis of stroke has never been examined. Our studies suggest the interesting possibility that PYK2 activation in ischemia may recruit LTD mechanisms in neurons to precipitate synapse failure in stroke. Additional tools for inhibiting PYK2 function are needed to examine this idea experimentally, including genetic knockout models and chemical blockers of PYK2. Can these reagents reduce LTD, and prevent synaptic depression or cell damage from cerebral ischemia? PYK2 knockouts appear grossly normal, although nervous system function and behaviors were not examined (Okigaki et al., 2003). The caveat of the knockout is that chronic loss of PYK2 could trigger compensation effects (e.g., upregulation of FAK activity) or cause developmental defects (e.g., reduced synapse elimination) that may complicate findings in mature neurons. Acute administration of chemical PYK2 inhibitors, on the other hand, could circumvent these issues. By specifically blocking PYK2 enzymatic activity, these inhibitors can also help distinguish between kinase and scaffold roles of PYK2. In fact, one inhibitor compound we examined (PF-431396; Buckbinder et al., 2007) blocked only the NMDA-induced increase in PYK2 Tyr-402 phosphorylation, but had no effect on basal PYK2 Tyr-402 levels (Hsin and Sheng, unpublished data), consistent with our result that PYK2 kinase activity is important for LTD, but not for basal synaptic depression (Chapter 3). A severe lack of kinase selectivity of this compound, however, precluded us from pursuing

further studies with this inhibitor (Han et al., 2009; Hsin and Sheng, unpublished data). The development of more selective PYK2 inhibitors will be useful for future studies.

III. Possible interactions between GSK-3beta and PYK2 pathways

As more molecules become implicated in LTP and LTD, the field of synaptic plasticity has understandably developed a level of molecular cacophony to outsiders (Sanes and Lichtman, 1999). The findings in this thesis merit a consideration of how two novel LTD pathways, GSK-3beta-PSD-95 and PYK2-ERK, can signal the same phenomenon. Three possible points of cross-over between these pathways should be further examined.

PSD-95

Both GSK-3beta and PYK2 interact with PSD-95. It is possible that these LTD mechanisms intersect at PSD-95: for example, GSK-3beta-dependent phosphorylation and de-multimerization of PSD-95 could promote PSD-95 loss from synapses, thus reducing PYK2 association with the PSD and diminishing its interaction with synaptic signaling partners. Experiments examining PYK2 function in the presence of multimerization-deficient PSD-95 molecules could help test this hypothesis.

Interestingly, Xu et al. (2008) found that expression of PSD-95 with simultaneous mutations in both the N-terminal and SH3-GK regions rescued LTD. They propose that the N-terminal mutations increased proteolysis of PSD-95 at the synapse, thereby generating a C-terminal fragment that acts as a dominant negative truncation to block LTD (except that expression of this C-terminal fragment alone does not block LTD; Xu et al., 2008). Double-mutant PSD-95 (Q15A-L460P or Q15A with an SH3-GK deletion), they found, rescued LTD because the C-terminal mutations abolish function of the truncated product.

At first glance, this finding is difficult to reconcile with our model outlined above, which predicts that expression of double-mutant PSD-95 would block LTD, much like expression of T19A-PSD-95. However, we believe that the data of Xu et al. (2008) do not completely rule out this interpretation. LTD experiments with Q15A-L460P or Q15A-delta-SH3-GK mutants were all performed in the presence of endogenous PSD-95, and it is unclear whether these mutants could target properly to synapses (Xu et al., 2008). If the double mutants did not express well,

for example, then the observed rescue in LTD could be due to LTD mediated by endogenous PSD-95. Thus it remains possible that N- and C-terminal mutations in PSD-95 have functionally distinct effects on LTD.

GSK-3beta Tyr-216 phosphorylation

Phosphorylation of Tyr-216 within the catalytic domain of GSK-3beta enhances GSK-3beta kinase activity, although it is not required for kinase function (Kockeritz et al., 2006). The precise role of Tyr-216 is unclear, however, since its phosphorylation is constitutive in most cell types (Doble and Woodgett, 2003). The kinase responsible for Tyr-216 phosphorylation also remains a mystery. Studies claiming that GSK-3beta auto-phosphorylates itself at this site, for example, have not been reproduced in all cell types (Doble and Woodgett, 2003; Forde and Dale, 2007). Interestingly, PYK2 has been reported to phosphorylate Tyr-216 of GSK-3beta in pheochromocytoma (PC12) and Chinese hamster ovary (CHO) cells (Hartigan et al., 2001; Sayas et al., 2006), suggesting another possible mechanism for cross-talk between PYK2 and GSK-3beta pathways. In hippocampal neurons, however, PYK2 knockdown does not affect GSK-3beta phosphorylation at this site, and phospho-Y216 levels of GSK-3beta are unaltered by NMDAR stimulation (Hsin, Kim, Wang, and Sheng, unpublished data). Thus PYK2 is unlikely to regulate GSK-3beta in neurons by direct phosphorylation.

Phosphatases

Although GSK-3beta may not be a direct target of PYK2, there are a few striking similarities between the functional roles of GSK-3beta and PYK2 in hippocampal neurons. Both signaling pathways affect synaptic strength under activity conditions (NMDAR stimulation) more than under basal conditions (Chapter 3; Peineau et al., 2007), and overexpression of PYK2 or GSK-3beta can inhibit LTP (Chapter 3; Hooper et al., 2007; Zhu et al., 2007). These properties are reminiscent of the effects of calcineurin/PP1 signaling in synaptic plasticity (Chapter 1; although calcineurin overexpression inhibits "intermediate-phase" LTP, Winder et al., 1998). Indeed, both PYK2 and GSK-3beta appear to be activated by Ser/Thr dephosphorylation (Chapter 1), suggesting that phosphatase activity may be a shared upstream component of both signaling pathways. NMDAR-dependent activation of calcineurin/PP1 in

hippocampal neurons, therefore, could be a key step in recruiting most major players in LTD signaling. Further investigation of this and other possible links between PYK2 and GSK-3beta can help formulate our understanding of a core, integrated mechanism for LTD.

IV. References

Ahmadian G, Ju W, Liu L, Wyszynski M, Lee S, Dunah A, Taghibiglou C, Wang Y, Lu J, Wong T, Sheng M, and Wang Y (2004) Tyrosine phosphorylation of GluR2 is required for insulin-stimulated AMPA receptor endocytosis and LTD. EMBO J 23:1040-1050.

Avraham H, Park S, Schinkmann K, and Avraham S (2000) RAFTK/Pyk2-mediated cellular signaling. Cell Signal 12:123-133.

Bartos J, Ulrich J, Li H, Beazely M, Chen Y, MacDonald J, and Hell J (2010) Postsynaptic clustering and activation of Pyk2 by PSD-95. J Neurosci 30:449-463.

Bats C, Groc L, Choquet D (2007) The interaction between Stargazin and PSD-95 regulates AMPA receptor surface trafficking. Neuron 53:719-734.

Bienenstock EL, Cooper LN, and Munro PW (1982) Theory for the development of neuron selectivity: orientation specificity and binocular interaction in visual cortex. J Neurosci 2:32-48.

Braithwaite S, Paul S, Nairn A, and Lombroso P (2006) Synaptic plasticity: one STEP at a time. Trends Neurosci 29:452-458.

Buckbinder L, Crawford D, Qi H, Ke H, Olson L, Long K, Bonnette P, Baumann A, Hambor J, Grasser W, Pan L, Owen T, Luzzio M, Hulford C, Gebhard D, Paralkar V, Simmons H, Kath J, Roberts W, Smock S, Guzman-Perez A, Brown T, and Li M (2007) Proline-rich tyrosine kinase 2 regulates osteoprogenitor cells and bone formation, and offers an anabolic treatment approach for osteoporosis. Proc Natl Acad Sci USA 104:10619-10624.

Carlisle H, Manzerra P, Marcora E, and Kennedy M (2008) SynGAP regulates steady-state and activity-dependent phosphorylation of cofilin. J Neurosci 28:13673-13683.

Cheung H, Takagi N, Teves L, Logan R, Wallace N, and Gurd J (2000) Altered association of protein tyrosine kinases with postsynaptic densities after transient cerebral ischemia in the rat brain. J Cereb Blood Flow Metab 20:505-512.

Citri A and Malenka RC (2008) Synaptic plasticity: multiple forms, functions, and mechanisms. Neuropsychopharm 33:18-41.

Collins M, Yu L, Coba M, Husi H, Campuzano I, Blackstock W, Choudhary J, and Grant S (2005) Proteomic analysis of in vivo phosphorylated synaptic proteins. J Biol Chem 280:5972-5982.

Collins M, Husi H, Yu L, Brandon J, Anderson C, Blackstock W, Choudhary J, and Grant S (2006) Molecular characterization and comparison of the components and multiprotein complexes in the postsynaptic proteome. J Neurochem 97 Supp 1:16-23.

Cummings J, Mulkey R, Nicoll R, and Malenka R (1996) Ca2+ signaling requirements for long-term depression in the hippocampus. Neuron 16:825-833.

Doble B and Woodgett J (2003) GSK-3: tricks of the trade for a multi-tasking kinase. J Cell Sci 116:1175-1186.

El-Husseini A, Schnell E, Dakoji S, Sweeney N, Zhou Q, Prange O, Gauthier-Campbell C, Aguilera-Moreno A, Nicoll R, and Bredt D (2002) Synaptic strength regulated by palmitate cycling on PSD-95. Cell 108:849-863.

Faure C, Corvol J, Toutant M, Valjent E, Hvalby O, Jensen V, Messari S, Corsi J, Kadare G, and Girault J (2007) Calcineurin is essential for depolarization-induced nuclear translocation and tyrosine phosphorylation of PYK2 in neurons. J Cell Sci 120:3034-3044.

Forde J and Dale T (2007) Glycogen synthase kinase 3: a key regulator of cellular fate. Cell Mol Life Sci 64:1930-1944.

Han S, Mistry A, Chang J, Cunningham D, Griffor M, Bonnette P, Wang H, Chrunyk B, Aspnes G, Walker D, Brosius A, and Buckbinder L (2009) Structural characterization of proline-rich tyrosine kinase 2 (PYK2) reveals a unique (DFG-out) conformation and enables inhibitor design. J Biol Chem 284:13193-13201.

Hartigan J, Xiong W, and Johnson G (2001) Glycogen synthase kinase 3beta is tyrosine phosphorylated by PYK2. Biochem Biophys Res Commun 284:485-489.

Harvey C, Ehrhardt A, Cellurale C, Zhong H, Yasuda R, Davis R, and Svoboda K (2008) A genetically encoded fluorescent sensor of ERK activity. Proc Natl Acad Sci USA 105:19264-19269.

Hayashi T and Huganir R (2004) Tyrosine phosphorylation and regulation of the AMPA receptor by SRC family tyrosine kinases. J Neurosci 24:6152-6160.

Hooper C, Markevich V, Plattner F, Killick R, Schofield E, Engel T, Hernandez F, Anderton B, Rosenblum K, Bliss T, Cooke S, Avila J, Lucas J, Giese K, Stephenson J, and Lovestone S (2007) Glycogen synthase kinase-3 inhibition is integral to long-term potentiation. Eur J Neurosci 25:81-86.

Hsieh H, Boehm J, Sato C, Iwatsubo T, Tomita T, Sisodia S, and Malinow, R (2006) AMPAR removal underlies Abeta-induced synaptic depression and dendritic spine loss. Neuron 52:831-843.

Hsueh Y, Kim E, and Sheng M (1997) Disulfide-linked head-to-head multimerization in the mechanism of ion channel clustering by PSD-95. Neuron 18:803-814.

Huang Y, Lu W, Ali D, Pelkey K, Pitcher G, Lu Y, Aoto H, Roder J, Sasaki T, Salter M, and MacDonald J (2001) CAKbeta/Pyk2 kinase is a signaling link for induction of long-term potentiation in CA1 hippocampus. Neuron 29:485-496.

Jope R and Roh M (2006) Glycogen synthase kinase-3 (GSK3) in psychiatric diseases and therapeutic interventions. Curr Drug Targets 7:1421-1434.

Kim E and Sheng M (2004) PDZ domain proteins of synapses. Nat Rev Neurosci 5:771-781.

Kim J, Lee H, Takamiya K, and Huganir R (2003) The role of synaptic GTPase-activating protein in neuronal development and synaptic plasticity. J Neurosci 23:1119-1124.

Kim M, Dunah A, Wang Y, and Sheng M (2005) Differential roles of NR2A- and NR2B-containing NMDA receptors in Ras-ERK signaling and AMPA receptor trafficking. Neuron 46:745-760.

Kim M, Futai K, Jo J, Hayashi Y, Cho K, and Sheng M (2007) Synaptic accumulation of PSD-95 and synaptic function regulated by phosphorylation of serine-295 of PSD-95. Neuron 56:488-502.

Kockeritz L, Doble B, Patel S, and Woodgett J (2006) Glycogen synthase kinase-3 – an overview of an over-achieving protein kinase. Curr Drug Targets 7:1377-1388.

Lee H, Kameyama K, Huganir R, and Bear M (1998) NMDA induces long-term synaptic depression and dephosphorylation of the GluR1 subunit of AMPA receptors in hippocampus. Neuron 21:1151-1162.

Lee H, Takamiya K, He K, Song L, and Huganir R (2010) Specific roles of AMPA receptor subunit GluR1 (GluA1) phosphorylation sites in regulating synaptic plasticity in the CA1 region of hippocampus. J Neurophysiol 103:479-489.

Lev S, Moreno H, Martinez R, Canoll P, Peles E, Musachhio J, Plowman G, Rudy B, and Schlessinger J (1995) Protein tyrosine kinase PYK2 involved in Ca2+-induced regulation of ion channel and MAP kinase functions. Nature 376:737-745.

Li S, Hong S, Shepardson N, Walsh D, Shankar G, and Selkoe D (2009) Soluble oligomers of amyloid beta protein facilitate hippocampal long-term depression by disrupting neuronal glutamate uptake. Neuron 62:788-801.

Lucas J, Hernandez F, Gomez-Ramos P, Morgan M, Hen R, and Avila J (2001) Decreased nuclear beta-catenin, tau hyperphosphorylation and neurodegeneration in GSK-3beta conditional transgenic mice. EMBO J 20:27-39.

Malenka RC and Bear MF (2004) LTP and LTD: an embarrassment of riches. Neuron 44:5-21.

Mao Y, Ge X, Frank C, Madison J, Koehler A, Doud M, Tassa C, Berry E, Soda T, Singh K, Biechele T, Petryshen T, Moon R, Haggarty S, and Tsai L (2009) Disrupted in schizophrenia 1 regulates neuronal progenitor proliferation via modulation of GSK3beta/beta-catenin signaling. Cell 136:1017-1031.

Migaud M, Charlesworth P, Dempster M, Webster L, Watabe A, Makhinson M, He Y, Ramsay M, Morris R, Morrison J, O'Dell T, and Grant S (1998) Enhanced long-term potentiation and impaired learning in mice with mutant postsynaptic density-95 protein. Nature 396:433-439.

Miyakawa T, Leiter L, Gerber D, Gainetdinov R, Sotnikova T, Zeng H, Caron M, and Tonegawa S (2003) Conditional calcineurin knockout mice exhibit multiple abnormal behaviors related to schizophrenia. Proc Natl Acad Sci USA 100:8987-8992.

Morabito M, Sheng M, and Tsai L (2004) Cyclin-dependent kinase 5 phosphorylates the N-terminal domain of the postsynaptic density protein PSD-95 in neurons. J Neurosci 24:865-876.

Nishiyama M, Hong K, Mikoshiba K, Poo M, Kato K (2000) Calcium stores regulate the polarity and input specificity of synaptic modification. Nature 408:584-588.

O'Brien W, Harper A, Jove F, Woodgett J, Maretto S, Piccolo S, and Klein P (2004) Glycogen synthase kinase-3beta haploinsufficiency mimics the behavioral and molecular effects of lithium. J Neurosci 24:6791-6798.

Okigaki M, Davis C, Falasca M, Harroch S, Felsenfeld D, Sheetz M, and Schlessinger J (2003) Pyk2 regulates multiple signaling events crucial for macrophage morphology and migration. Proc Natl Acad Sci USA 100:10740-10745.

Okuda T, Yu L, Cingolani L, Kemler R, and Goda Y (2007) Beta-catenin regulates excitatory postsynaptic strength at hippocampal synapses. Proc Natl Acad Sci USA 104:13479-13484.

Paul S, Nairn A, Wang P, and Lombroso P (2003) NMDA-mediated activation of the tyrosine phosphatase STEP regulates the duration of ERK signaling. Nat Neurosci 6:34-42.

Peineau S, Taghibiglou C, Bradley C, Wong TP, Liu L, Lu J, Lo E, Wu D, Saule E, Bouschet T, Matthews P, Isaac JT, Bortolotto ZA, Wang YT, and Collingridge GL (2007) LTP inhibits LTD in the hippocampus via regulation of GSK3beta. Neuron 53:703-717.

Pelkey K, Askalan R, Paul S, Kalia L, Nguyen T, Pitcher G, Salter M, and Lombroso P (2002) Tyrosine phosphatase STEP is a tonic brake on induction of long-term potentiation. Neuron 34:127-138.

Peng Y, He S, Marie H, Zeng S, Ma J, Tan Z, Lee S, Malenka R, and Yu X (2009) Coordinated changes in dendritic arborization and synaptic strength during neural circuit development. Neuron 61:71-84.

Qin Y, Zhu Y, Baumgart J, Stornetta R, Seidenman K, Mack V, Van Aelst L, and Zhu J (2005) State-dependent Ras signaling and AMPA receptor trafficking. Genes Dev 19:2000-2015.

Rumbaugh G, Adams J, Kim J, and Huganir R (2006) SynGAP regulates synaptic strength and mitogen-activated protein kinases in cultured neurons. Proc Natl Acad Sci USA 103:4344-4351.

Sanes J and Lichtman J (1999) Can molecules explain long-term potentiation? Nat Neurosci 2:597-604.

Sayas C, Ariaens A, Ponsioen B, Moolenaar W (2006) GSK-3 is activated by the tyrosine kinase Pyk2 during LPA1-mediated neurite retraction. Mol Biol Cell 17:1834-1844.

Seabold G, Burette A, Lim I, Weinberg R, and Hell J (2003) Interaction of the tyrosine kinase Pyk2 with the N-methyl-D-aspartate receptor complex via the Src homology 3 domains of PSD-95 and SAP102. J Biol Chem 278:15040-15048.

Steiner P, Higley M, Xu W, Czervionke B, Malenka R, and Sabatini B (2008) Destabilization of the postsynaptic density by PSD-95 serine 73 phosphorylation inhibits spine growth and synaptic plasticity. Neuron 60:788-802.

Sturgill J, Steiner P, Czervionke B, and Sabatini B (2009) Distinct domains within PSD-95 mediate synaptic incorporation, stabilization, and activity-dependent trafficking. J Neurosci 29:12845-12854.

Tai C, Mysore S, Chiu C, and Schuman E (2007) Activity-regulated N-cadherin endocytosis. Neuron 54:771-785.

Tian D, Litvak V, and Lev S (2000) Cerebral ischemia and seizures induce tyrosine phosphorylation of PYK2 in neurons and microglial cells. J Neurosci 20:6478-6487.

Winder D, Mansuy I, Osman M, Moallem T, Kandel E (1998) Genetic and pharmacological evidence for a novel, intermediate phase of long-term potentiation suppressed by calcineurin. Cell 92:25-37.

Xu W, Schluter O, Steiner P, Czervionke B, Sabatini B, and Malenka R (2008) Molecular dissociation of the role of PSD-95 in regulating synaptic strength and LTD. Neuron 57:248-262.

Zeng H, Chatterji S, Barbarosie M, Rondi-Reig L, Philpot B, Miyakawa T, Bear M, and Tonegawa S (2001) Forebrain-specific calcineurin knockout selectively impairs bidirectional synaptic plasticity and working/episodic-like memory. Cell 107:617-629.

Zhu J, Qin Y, Zhao M, Van Aelst L, and Malinow R (2002) Ras and Rap control AMPA receptor trafficking during synaptic plasticity. Cell 110:443-455.

Zhu L, Wang S, Liu D, Yin Y, Tian Q, Wang X, Wang Q, Chen J, and Wang J (2007) Activation of glycogen synthase kinase-3 inhibits long-term potentiation with synapse-associated impairments. J Neurosci 27:12211-12220.

APPENDIX:

Assessing molecular correlates of environmental enrichment in hippocampal synapses

Honor Hsin, Jianying Zhou*, Junmin Peng*, and Morgan Sheng

HH performed environmental enrichment, biochemical purification, and western blot validation experiments in Figures 1, 2, 3, 5. JZ performed mass spectrometry experiments and technical analyses in Figure 4, Table 1, and Table S1. *Dept of Human Genetics, Emory University School of Medicine, GA.

Abstract

Laboratory animals – rats, mice – are usually bred and housed in clean but impoverished environments. Exposure of rodents to enriched environments improves cognitive function and delays the progression of neurological diseases. In hippocampal neurons, environmental enrichment (EE) significantly enhances synaptogenesis and synaptic function. Here we investigated whether EE alters the molecular composition of the hippocampal postsynaptic density (PSD) by liquid chromatography-tandem mass spectrometry (LC-MS/MS) analysis of the PSD proteome with label-free quantification. Although EE slightly increased the amount of total protein in PSD fractions, the vast majority of identified proteins showed no change in relative abundance between EE and control samples. For six proteins predicted to exhibit significant abundance changes by mass spectrometry analysis, Western blot experiments failed to validate these effects. Our results suggest that either PSD composition is not affected by EE, or that EE-induced changes at the PSD cannot be determined solely by our methods of purification, LC-MS/MS, and/or label-free quantification. Other approaches, such as stable isotope labeling in mass spectrometry-based quantification of the PSD proteome, may begin to address these issues.

Introduction

In the mammalian brain, excitatory synapses are defined by a postsynaptic density (PSD), a segment of thickened postsynaptic membrane (~200-800 nm wide and ~30-50 nm thick) containing receptors, channels, adhesion molecules, signaling enzymes, scaffolds, cytoskeletal elements, and other proteins (Sheng and Hoogenraad, 2007). The molecular composition of the PSD is dynamically regulated by synaptic activity, a process involving mechanisms of protein phosphorylation, translocation, palmitoylation, ubiquitination, degradation, and synthesis, among others. Due to its relative ease of biochemical purification, the PSD has been the subject of intense proteomic analysis by mass spectrometry over the last decade (Sheng and Hoogenraad, 2007; Bayes and Grant, 2009). These studies have revealed much about the number of proteins in the PSD and their quantitative stoichiometry (Walikonis et al., 2000; Jordan et al., 2004; Li et al., 2004; Peng et al., 2004; Yoshimura et al., 2004; Collins et al., 2006), as well as the differences in PSD composition across anatomical sub-regions of the brain (Cheng et al., 2006) or evolutionary boundaries between species (Emes et al., 2008).

Environmental enrichment (EE) is a behavioral paradigm where animals are exposed to surroundings that are *complex* and *novel*, often involving voluntary exercise and a combination of social, visual, and tactile stimuli (Van Praag et al., 2000; Nithianantharajah and Hannan, 2006). Objects and toys in these environments are moved or changed frequently, which provides cognitive stimulation in the form of spatial re-orientation (Nithianantharajah and Hannan, 2006). This is in contrast to conventional housing of rodents, which typically consists of smaller cages, with a deprived and socially-isolated environment. EE has been documented to have drastic effects on brain function and structure, from behavioral to cellular and molecular levels. Rodents exposed to EE, for example, exhibit enhanced learning and memory, decreased anxiety, and increased exploratory behavior (Roy et al., 2001; Schrijver et al., 2002; Benaroya-Milshtein et al., 2004; Leggio et al., 2005; Bennett et al., 2006). EE housing also partially rescues (or delays the onset of) behavioral phenotypes in a variety of neurological disease models, including Fragile X mental retardation (Restivo et al., 2005), Huntington's disease (Van Dellen et al., 2000), Parkinson's disease (Bezard et al., 2003), Alzheimer's disease (Jankowsky et al., 2005), epilepsy (Young et al., 1999), and stroke (Ohlsson and Johansson, 1995).

EE increases neurogenesis, synaptogenesis, and dendritic branching in the brain, and also enhances hippocampal LTP at CA1 synapses (Greenough et al., 1985; Van Praag et al., 1999; Rampon et al., 2000a; Duffy et al., 2001; Leggio et al., 2005; Gogolla et al., 2009). In cortical neurons, EE increases the average length of the PSD (Diamond et al., 1975). In the hippocampus, EE gates the functional contribution of various signaling pathways to synaptic plasticity: whereas LTP in conventionally-housed mice requires Ras-GRF1 and Ras-GRF2 function, LTP in EE-exposed mice is independent of Ras-GRF activity and requires a novel cAMP/p38-dependent pathway (Li et al., 2006). The degree of PKA-dependence in LTP signaling also differs between EE and conventionally-housed animals (Duffy et al., 2001). We thus wondered whether EE, as a behavioral paradigm that influences synaptic plasticity and signaling, could affect the molecular composition of the PSD.

Microarray expression studies in EE-exposed mice have revealed significant changes in the cortical levels of gene products associated with transcription, translation, neuronal signaling (e.g. PSD-95, calmodulin), neuronal structure (e.g. N-cadherin), and protein degradation (Rampon et al., 2000b). At the protein level, two-dimensional gel electrophoresis (2DE) analysis showed that a tiny fraction (1-2%) of the somatic and dendritic proteomes of hippocampal CA1

neurons was significantly affected by EE exposure (>1.5-fold across 4 replicate runs; McNair et al., 2007). Matrix-assisted laser desorption/ionization and time-of-flight (MALDI-TOF) mass analysis of these altered protein spots revealed little overlap in the identities of these proteins between somatic and dendritic proteomes, and between proteomic and transcriptomic studies (Rampon et al., 2000b; McNair et al., 2007). Although it appears that most proteins are unaffected by EE exposure, 2DE experiments are generally biased against membrane proteins and proteins of low abundance (Ong and Mann, 2005).

To circumvent these issues, we employed a liquid chromatography-tandem mass spectrometry approach (LC-MS/MS) that has been used heavily to study the PSD proteome (Jordan et al., 2004; Li et al., 2004; Peng et al., 2004; Yoshimura et al., 2004; Cheng et al., 2006; Collins et al., 2006; Edbauer et al., 2009). We purified hippocampal PSDs from conventionally- and EE-housed adult male rats, and found that total protein was slightly (~25%) increased in the EE PSD preparation, consistent with increased synapse number after EE exposure (Greenough et al., 1985; Rampon et al., 2000a). Two replicates of EE and control PSD samples were analyzed by LC-MS/MS, and we examined peptide differences by extracted ion current (EIC) analysis, a label-free method for quantifying relative protein abundances (Liao et al., 2004; Ong and Mann, 2005; Edbauer et al., 2009). Of a total ~1000 distinct proteins identified by tandem MS scans, only ~30 qualified proteins showed >1.5-fold change in all pair-wise comparisons of EE and control replicates. Six of these proteins could be analyzed by western blotting; however, none of the predicted changes in protein abundance could be verified. This suggests that our PSD purification, LC-MS/MS, and/or EIC-quantification protocols are unsuitable for identifying EE-induced changes in the PSD proteome, or that EE does not affect the molecular composition of the hippocampal PSD. Further studies are needed to investigate the effects of EE at the synapse, and techniques such as stable isotope labeling in MS quantification may prove useful for this purpose.

Materials and Methods

Environmental enrichment protocol

Considerable variability exists in the EE paradigms used by previous groups, particularly with respect to (1) age of animals at onset of EE exposure, (2) sex of animals, (3) daily length of

EE exposure (e.g., 1-3 hours per day versus continuously throughout the day), (4) presence or absence of voluntary exercise in EE, (5) duration of EE exposure, and (6) social conditions of conventionally-housed controls (Van Praag et al., 2000; Nithianantharajah and Hannan, 2006). In selecting an appropriate protocol, we surveyed the literature and chose the most commonly represented conditions for each of these categories to use in our EE paradigm. Five adult male rats (8 weeks of age) were continuously housed together in a large cage (20 inches x 30 inches x 16 inches) containing brightly-colored and textured plastic toys, PVC tube tunnels, and two treadmills (Figure 1A) for 16 days. Objects were rearranged daily within the cage, and replaced every 2-3 days. Control rats (same age and sex) were single-housed in conventional cages in the same room (Figure 1A) for 16 days. Food and water were provided ad libitum, and all cages were changed every 4 days.

PSD preparation

After 16 days of enriched or conventional housing, all rats were sacrificed by light carbon dioxide euthanasia, and dissected on the same day. Intact hippocampi were quickly collected from each animal and snap frozen in liquid nitrogen. PSD purification was performed as described (Cheng et al., 2006; Edbauer et al., 2009). For each condition (EE and control), all 10 hippocampi were pooled and homogenized in buffer A (5 mM HEPES pH 7.4, 1 mM MgCl2, 0.5 mM CaCl2, 20 mM beta-glycerophosphate, 10 mM pyrophosphate) with a Teflon homogenizer. After the first spin at 1,400 x g for 10 minutes, the pellet (P1) was homogenized again in buffer A and spun at 700 x g for 10 minutes. Supernatants from both spins (S1 and S1') were pooled and then separated into three equal parts (labeled C1, C2, C3 for control samples, and EE4, EE5, EE6 for EE samples). These parts remained separate for all subsequent purification steps, although the steps continued to be performed in parallel. After a spin at 13,800 x g for 10 minutes, the membrane pellet (P2) fractions were homogenized in buffer B (0.32 M sucrose, 6 mM Tris pH 8.0, 1 mM beta-glycerophosphate), loaded onto a discontinuous sucrose gradient (0.85 M/1 M/1.15 M sucrose in 8 mM Tris pH 8.0), and spun at 82,500 x g for 2 hours (SW41 rotor). Synaptosome fractions (Syn) were collected at the 1 M/1.15 M sucrose interface and lysed by mixing with an equal volume of buffer C (6 mM Tris pH 8.0, 1% Triton X-100). Samples were then spun at 33,000 x g for 1 hr (Ti70.1 rotor) to yield PSD pellets (PSD I). All steps were performed at 4 degrees, and all buffers contained cocktail protease and phosphatase

inhibitors (Sigma). Two PSD isolates from each condition (C2, C3, EE5, EE6) were used for LC-MS/MS analysis, and the remaining isolates were used for validation purposes (silver staining and western blot experiments; C1 and EE4). Approximately 10% of S1, S2, P2, and Syn fractions from the purification of C1 and EE4 isolates were saved for further biochemical analysis. Protein concentration was quantified by Bradford assay.

For silver staining, samples were run on an 8% SDS-PAGE gel, and fixed with formaldehyde fixing solution (1.85% paraformaldehyde, 40% methanol) for 10 minutes at room temperature. After washing in water, the gel was submerged in 0.02% sodium thiosulfate for ~ 1 minute, washed, and submerged in 0.1% silver nitrate solution for 10 minutes. The gel was developed in fresh thiosulfate developing solution (3% sodium carbonate, 0.0004% sodium thiosulfate, 1.85% paraformaldehyde) and slowly agitated for under a minute. Citric acid solution (2.3 M) was added 1:20 to the developing solution, and the gel was agitated for 10 minutes before scanning.

Mass spectrometry analysis

PSD isolates (C2, C3, EE5, EE6) were dissolved in 50 mM Tris pH 8.5 with 1% SDS at 95 degrees for 5 minutes, reduced with 10 mM dithiothrietol at 37 degrees for 30 minutes, and Cys-alkylated with 50 mM iodoacetamide at room temperature for 30 minutes. Total protein in each isolate was estimated on a silver-stained SDS-PAGE gel with known concentration standards. For mass spectrometry analysis, samples were separated on 10% SDS-PAGE gels, which were cut into two pieces (high molecular weight: >50 Kd; low molecular weight: <50 Kd). In-gel digestion with trypsin was performed on all eight gel samples, and the peptides were analyzed by LC-MS/MS as described (Liao et al., 2004; Edbauer et al, 2009). Briefly, equal amounts of total protein from each sample was loaded onto LC columns as described, and LC elution profiles (for each molecular weight group) appeared highly similar across all four control and EE samples. Eluted peptides underwent electrospray ionization, and were detected in MS survey and MS/MS scans (total: ~120,000) on an ion trap mass spectrometer. Acquired MS/MS spectra were searched against a rat protein database (National Center for Biotechnology Information; Eng et al., 1994). Common contaminants, such as trypsin and keratins, were included in the database, and modifications were added to account for possible phosphorylated Ser/Thr/Tyr residues, as described (Edbauer et al., 2009). A total of 3,154 peptides were

identified, which translated to a total of 1033 proteins. Proteins that shared peptides were grouped together; 538 groups were detected.

EIC quantification

The signal intensity of each peptide in an MS survey scan can be measured over time, as the peptide elutes from the chromatographic column (Ong and Mann, 2005). EIC is the integrated area under this curve of signal intensity versus time, and when compared between two different experiments for any given peptide, EIC can be used to estimate the peptide's relative abundance between the two states (Ong and Mann, 2005). The criteria for ion extraction have been described previously (Liao et al., 2004; Edbauer et al., 2009). For each peptide, an EIC abundance ratio was calculated between each EE-control comparison (C2-EE5, C2-EE6, C3-EE5, C3-EE6), and transformed into $\log_2$ values (to convert multiplicative error to additive error; Cheng et al., 2006). For proteins identified by more than one peptide, these $\log_2$ values were averaged to yield the overall protein abundance ratio.

To arrive at the list of proteins in Table 1, all 1033 proteins identified by mass spectrometry were filtered by $\log_2$ abundance ratios, with a cutoff of ≥ 0.6 or ≤ -0.6 ($\geq$1.5-fold or $\leq$-1.5-fold) for each EE-control comparison. Common contaminants (e.g. keratins) were removed. The remaining proteins (65) were manually examined for match quality (whether peptide ion peaks can be adequately matched between EE and control scans, according to *m/z* and retention time criteria) and EIC quality (whether EIC peaks can be adequately discerned from the noise intensity), as described (Edbauer et al., 2009). Those proteins with poor matches or weak EIC peaks were discarded, as described previously (Edbauer et al., 2009).

Antibodies

For fourteen of the proteins in Table 1, primary antibodies were unavailable. Of the remaining proteins, eight could not be detected by western blot with commercial antibodies in any biochemical fraction examined: rabbit anti-Pax6, Chemicon; mouse anti-Pax6, R&D Systems; goal anti-Septin10, Santa Cruz Biotechnology; mouse anti-neurocan (chondroitin sulfate proteoglycan 3), Developmental Studies Hybridoma Bank; goat anti-hyaluronan and proteoglycan link protein, Santa Cruz Biotechnology; mouse anti-myelin proteolipid protein, Chemicon; mouse anti-PP2A A subunit, Cell Signaling Technology; goat anti-ARPc1a, Novus

Biologicals; rabbit anti-ARP2, Cell Signaling Technology. The following antibodies were used to detect the remaining six proteins: guinea pig anti-Septin7, gift of Dr. Tomoko Tada; mouse anti-HDJ2, Novus Biologicals; mouse anti-MAP1A, Sigma; mouse anti-gephyrin, Synaptic Systems; mouse anti-Flotillin, BD Transduction Labs; rabbit anti-MEK2, Santa Cruz Biotechnology. Other antibodies used in this study were mouse anti-PSD-95, Neuromab; mouse anti-tubulin, Sigma; rabbit anti-NR2A and rabbit anti-NR2B, gift of Dr. Kelly Foster.

Western blot

Protein samples were separated on 10% SDS-PAGE gels in running buffer (25 mM Tris, 200 mM glycine, 0.1% SDS). Gels were transferred to nitrocellulose membranes in transfer buffer (48 mM Tris, 39 mM glycine, 0.04% SDS, 20% methanol). Membranes were blocked with 5% skim milk powder in Tris-buffered saline (TBS, pH 7.6) with 0.1% Tween-20 (blocking solution lacking Tween-20 was used for infrared fluorescence detection of antibody signal) and probed overnight at 4 degrees with primary antibodies in blocking solution. For chemiluminescence quantification, membranes were probed with sheep anti-mouse or donkey anti-rabbit HRP-linked secondary antibodies (GE Healthcare), exposed to ECL chemiluminescence substrate (Perkin-Elmer), and developed on an X-OMAT processor (Kodak). For infrared fluorescence quantification, membranes were probed with goat anti-rabbit (800 nm) or donkey anti-mouse (700 nm) infrared dye-conjugated secondary antibodies (LI-COR), and scanned on an Odyssey imager (LI-COR).

Results

To investigate whether environmental enrichment affects the molecular composition of the hippocampal PSD, we exposed five adult male rats (aged 8 weeks) to an enriched environment consisting of a large cage with toys, tunnels, and running wheels (see Methods; Figure 1A). Five control males of the same age were kept in separate conventional cages (Figure 1A). EE and control animals were housed for 16 days, a duration considered sufficient for the emergence of neurogenesis, plasticity, and behavioral differences (Bruel-Jungerman et al., 2005; Nithianantharajah and Hannan, 2006; Li et al., 2006). As early as one day after EE exposure, rats in enriched environments displayed noticeably increased locomotion and exploratory activity

within their cage, compared to control animals. After environmental exposure, all animals were sacrificed and bilateral hippocampi were removed. Total hippocampal weights were similar between EE and control groups (EE: 131 ± 0.004 mg; control: 140 ± 0.006 mg; $p = 0.23$, unpaired Student's t-test), indicating that dissection procedures were relatively consistent. For each group, all hippocampi were pooled into a single homogenate, which was then divided into three equal parts that were purified in parallel (see Methods; Figure 1B). Two replicates each of EE and control PSD samples were used for LC-MS/MS analysis, to enable quantification of relative protein abundances from both inter-sample (EE versus control) and intra-sample (EE versus EE) comparisons. The remaining PSD samples were used for silver stain and western blot analyses ("quality tests").

Interestingly, the amount of total protein in purified PSD fractions was elevated in EE samples relative to control (144 μg and 168 μg in EE vs. 120 μg and 132 μg in control fractions for LC-MS/MS, as quantified by SDS-PAGE; 90 μg in EE vs. 72 μg in control fractions for quality tests, as quantified by Bradford assay). This slight (~25%) increase, despite comparable total hippocampal weights, is consistent with an EE-induced increase in overall synapse number noted by other groups (Greenough et al., 1985; Rampon et al., 2000a). When visualized by silver stain, however, protein band patterns and intensities from EE and control PSD fractions appeared very similar, suggesting that protein composition and abundances were mostly unchanged by EE exposure (Figure 2). Western blot experiments also showed similar biochemical distribution of the known PSD proteins postsynaptic density-95 (PSD-95) and N-methyl-D-aspartate receptor (NMDAR) subunits 2A and 2B (Figure 3A). Tubulin alpha subunit, which is not highly enriched in the PSD, was also distributed in a similar manner between EE and control fractions (Figure 3B). Thus EE exposure does not appear to affect the relative abundance of most PSD proteins.

For PSD fractions that underwent LC-MS/MS, thousands (15,144) of MS/MS spectra were acquired and analyzed, amounting to 3,154 total peptides identified. Some peptides were shared between proteins, so proteins with a shared peptide were clustered into one group. We identified a total of 1,033 proteins, spread across 538 groups (Table S1). EIC quantification (see Methods) was used to estimate relative abundance of these proteins between pairs of PSD samples. The distribution of $\log_2$ abundance ratios is shown for one inter-sample (EE-control) and one intra-sample (EE-EE) comparison (Figure 4). Both curves fit normal distributions very

well, and the fitted distributions were highly similar (EE-control comparison: $\mu = -0.01$, $\sigma = \sim 0.35$; EE-EE comparison: $\mu = -0.01$, $\sigma = \sim 0.33$; Figure 4), implying that biological differences between EE and control PSDs cannot be easily discerned from experimental variability in this study.

Nonetheless, we generated a list of candidate proteins predicted by mass spectrometry analysis to exhibit significant changes between EE and control samples, and asked whether these changes could be verified by Western blot analysis. Approximately 30 qualified candidates were identified based on fold-change (>1.5-fold in all possible EE-control comparisons) and quality of EIC data (see Methods; Table 1). Antibodies were available for fourteen of the proteins in Table 1, but only six could be detected by Western blot of biochemical fractions; these are shown in Figure 5. None of the proteins expected to be more abundant in EE PSD fractions (Septin 7, DnaJ homolog protein 2 [HDJ2], microtubule-associated protein 1A [MAP1A], mitogen activated protein kinase kinase 2 [MEK2]) or more abundant in control PSD fractions (flotillin 2, gephyrin) showed significant differences between EE and control samples when analyzed by Western blotting (Figure 5). Thus several predicted changes in protein abundance from our study could not be validated by a different approach.

Discussion

Our results suggest that EIC quantification of LC-MS/MS data obtained from our PSD preparations cannot be solely used to quantify relative protein abundances after EE exposure. EIC quantification has been performed widely in other MS studies (Andersen et al., 2003; Liao et al., 2004; Steen et al., 2005; Edbauer et al., 2009), and has the advantage of not requiring an additional labeling step in the MS procedure. By comparing signal intensities of the *same* peptide (between different MS runs), EIC quantification need not address sources of error that plague comparisons between *different* peptides (e.g., variable electrospray ionization efficiencies; Ong and Mann, 2005). The possibility still exists, however, that some peptides are never detected or analyzed by LC-MS/MS (e.g., are not well-retained on the LC column). Additionally, nonsystematic errors can accrue from PSD purification to mass spectrometry steps, and these errors increase the variability of calculated protein abundances. If EE affects PSD composition in only a small proportion of hippocampal synapses, for example, then it could be

difficult to distinguish EE-induced changes from experimental noise. We note that EIC quantification of PSD fractions has never been successfully demonstrated before, so it is possible that the numerous purification steps required for extracting PSDs complicate use of this quantification method.

We consider the candidate proteins in Table 1 to be statistical outliers, and probably not genuine substrates of a biological effect. Many of these proteins were identified by only one peptide (Table 1), and we would expect these results to be less accurate than data obtained from proteins identified by multiple peptides.

Recent advances in stable isotope labeling methods have proven useful for MS-based quantification of protein abundances (Ong and Mann, 2005). For example, isotope-containing peptides can be synthesized and used as internal standards for absolute quantification of proteins within a sample (AQUA method; Gerber et al., 2003). Heavy and light isotope protein-labeling reagents can be used to analyze two different proteomes simultaneously (ICAT method, for isotope-coded affinity tag; Gygi et al., 1999). Both strategies have been employed successfully in analyzing the PSD proteome (Peng et al., 2004; Cheng et al., 2006). Metabolic incorporation of stable isotopes within proteins has also garnered considerable interest, although there are barriers to using this technique in mammalian animals (Wu et al., 2004). Nonetheless, these stable isotope methods could be helpful in future studies of EE-induced effects on the PSD proteome. Additionally, it could be interesting to analyze the effect of EE on the composition of stable PSD protein complexes, such as membrane-associated guanylate kinase signaling complexes (MASCs) or NMDAR complexes, both of which have been well-studied in the brain (Sheng and Hoogenraad, 2007; Bayes and Grant, 2009).

The possibility remains that EE has no effect on PSD composition in hippocampal neurons. Total synapse number may be increased by EE, but all synapses may possess PSDs identical to those found in conventionally-housed animals. The effects of EE on synaptic physiology could be due to changes on epigenetic rather than proteomic levels (Fischer et al., 2007), which in turn could influence the function of specific signaling pathways at the synapse. Further studies on the precise molecular changes induced by EE (and dissociated components of EE, such as social interaction alone, or exercise alone) can help unravel the mysteries of complex animal-environment interactions.

Figure Legends and Figures

Figure 1. Environmental enrichment and PSD preparation. (A) Image of conventional (right) and enriched (left) environments used in this study. (B) Simplified diagram of preparation steps for conventionally-housed control samples (right) and EE samples (left). For each condition, hippocampal tissue from 5 rats was pooled and homogenized, and the total homogenate was divided into three equal parts for PSD purification. Two PSD isolates for each condition were used for LC-MS/MS studies, and the remaining isolates were used for silver staining and western blot analyses ("quality tests"). All PSD purification steps were performed in parallel.

Figure 2. Comparison of EE and control PSD fractions by silver staining. Varying amounts of EE and control PSD (quality test fractions) were run on an SDS-PAGE gel, and protein bands were silver stained. Molecular mass markers are shown on the left (kDa).

Figure 3. Biochemical distribution of some PSD proteins in EE and control samples. (A) Enrichment of PSD-95, NR2A, and NR2B by subcellular fractionation in EE and control hippocampus. The following fractions are shown: S1 (first supernatant after spinning to remove nuclei and cellular debris, 5 μg); S2 (cytosol and microsomal membranes, 5 μg); P2 (crude synaptosomal fraction, 5 μg); Syn (synaptosomal fraction after sucrose gradient, 1 μg); PSD (triton-extracted PSD fraction, 5 μg). The final two lanes are 1:10 dilutions of the original PSD fractions. (B) Distribution of tubulin alpha subunit across EE and control subcellular fractions. All labeled fractions are the same as in (A). The first two lanes are 1:5 dilutions of the original S1 fractions.

Figure 4. Distribution of relative protein abundances. Relative protein abundances were obtained by EIC quantification, and converted into $\log_2$ ratios (C/EE and EE/EE). Proteins were binned into 0.25-unit intervals, and each curve was fit to a normal distribution (with mean, μ; standard deviation, σ) as described in Cheng et al. (2006).

Figure 5. Biochemical distribution of proteins predicted to be enriched in EE or control PSD samples. Western blots are shown for four proteins (Septin 7, HDJ2, MAP1A, MEK2) expected to be more abundant in EE PSD fractions, and two proteins (Flotillin 2, Gephyrin) expected to be more abundant in control PSD fractions. A control for PSD-95 distribution is also shown. All subcellular fractions are the same as in Figure 3.

Table 1. List of PSD proteins predicted by EIC quantification to be affected by EE. Each protein is indicated by its NCBI protein reference number (at time of mass analysis experiment, 2/18/07) and official description and gene name (as of March 29, 2010). Predicted proteins that have since been removed from the database as a result of standard genome annotation processing are indicated by asterisks (*) in the description. "Mean log2 (EE/C)" is the mean of all four log2 (EE/C) values from each pair-wise comparison between EE and control PSD isolates. "# peptides" signifies the total number of peptides analyzed for that protein.

Table S1. List of all PSD proteins identified by LC-MS/MS. Proteins sharing a peptide were clustered into groups, and groups were numbered based on the largest extracted ion current intensity of a peptide within the group. All other parameters are as defined in Table 1.
Weblink: http://sites.google.com/site/honorhsin/home-1

Figure 1

A

B

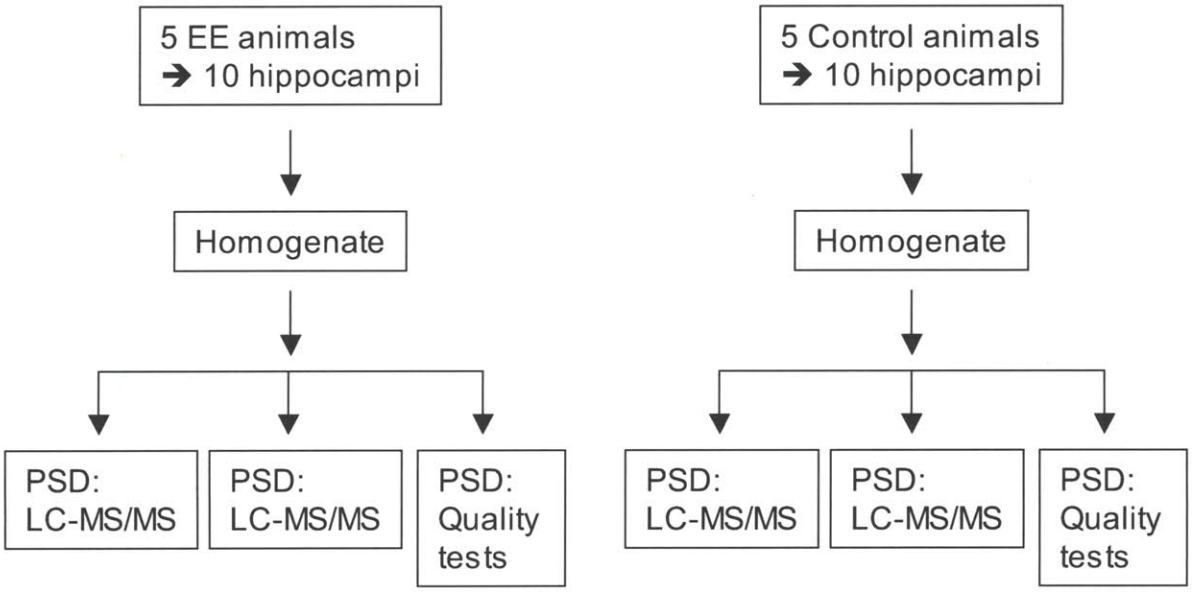
5 EE animals
➔ 10 hippocampi
Homogenate
PSD:
LC-MS/MS
PSD:
LC-MS/MS
PSD:
Quality
tests
5 Control animals
➔ 10 hippocampi
Homogenate
PSD:
LC-MS/MS
PSD:
LC-MS/MS
PSD:
Quality
tests

Figure 2

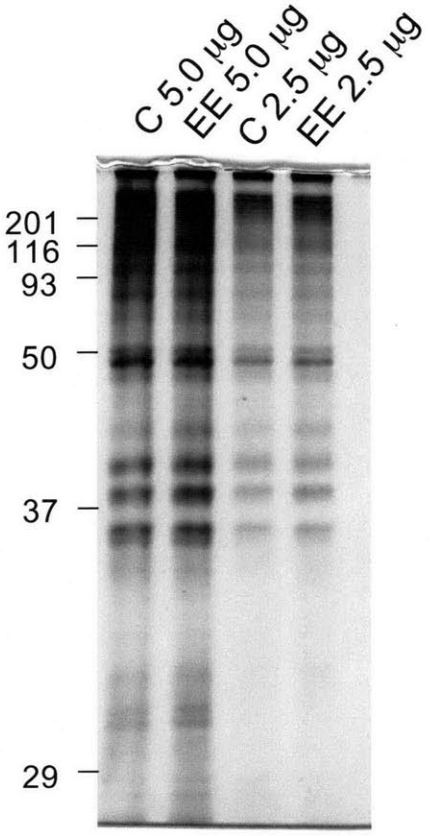

Figure 3

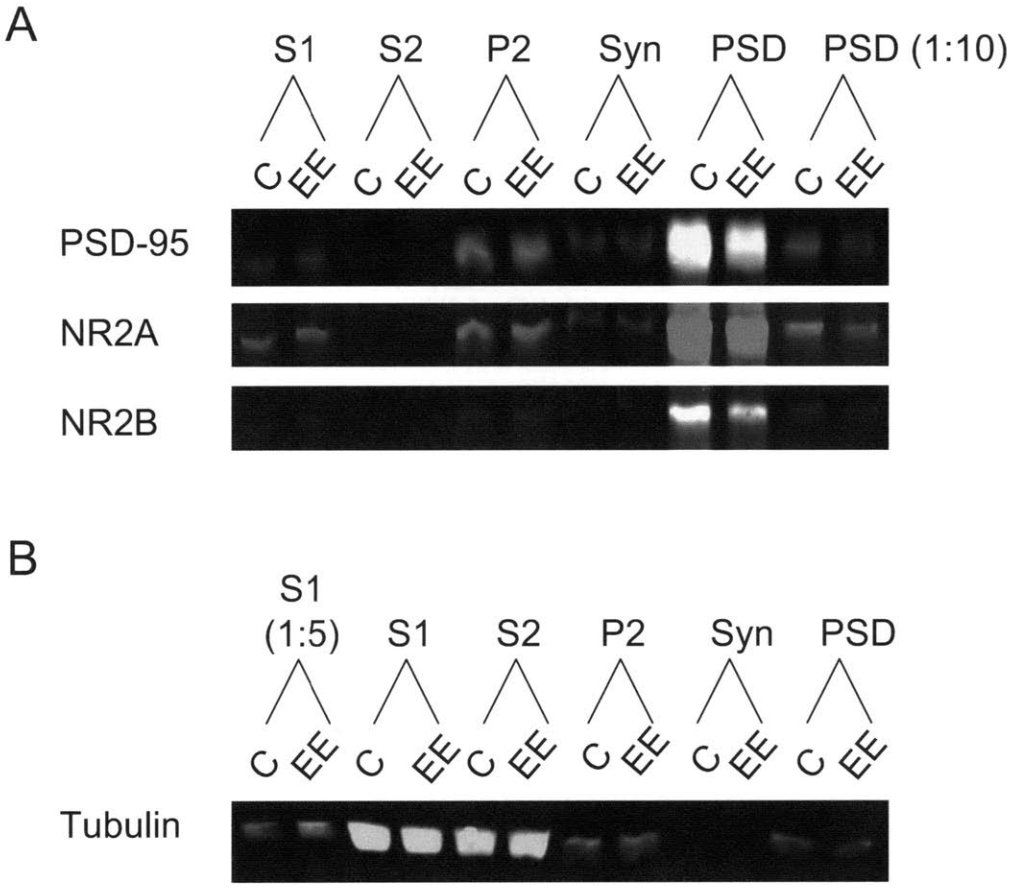
A
S1
S2
P2
Syn
PSD
PSD (1:10)
C
EE
PSD-95
NR2A
NR2B
B
S1
(1:5)
S1
S2
P2
Syn
PSD
C
EE
Tubulin

Figure 4

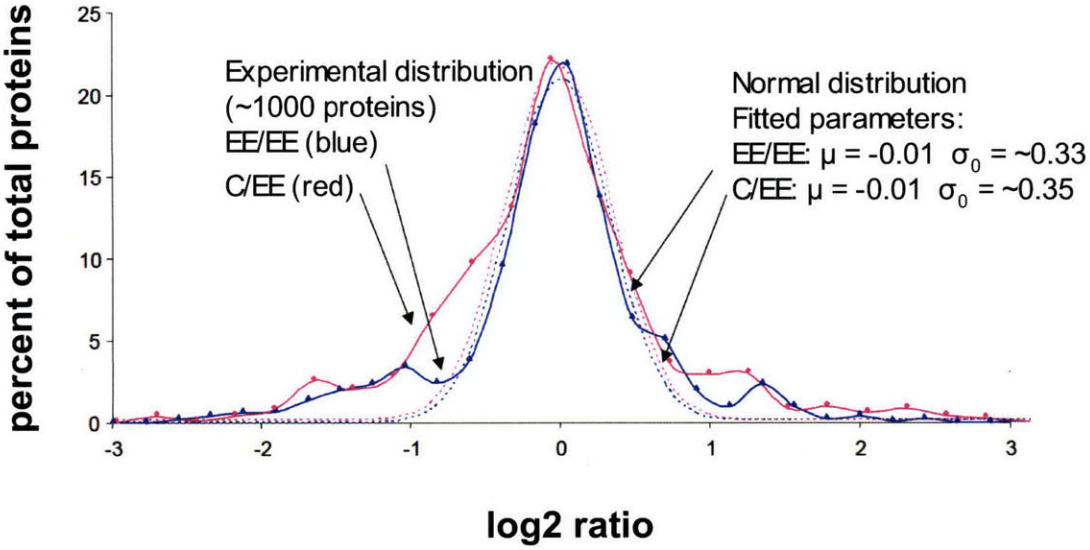
percent of total proteins
25
20
15
10
5
0
-3
-2
-1
0
1
2
3
Experimental distribution
(~1000 proteins)
EE/EE (blue)
C/EE (red)
Normal distribution
Fitted parameters:
EE/EE: μ = -0.01 σ0 = ~0.33
C/EE: μ = -0.01 σ0 = ~0.35
log2 ratio

Table 1

Reference	Description	Gene Name	mean log2 (EE/C)	# peptides
NP_037133.1	paired box 6	Pax6	3.44	1
XP_225887.3	*Predicted:* SH3 domain and tetratricopeptide repeats-containing protein 2	Sh3tc2	3.10	1
NP_075223.1	dnaJ homolog subfamily A member 1	Dnaja1	2.48	1
XP_344781.2	*Predicted:* zinc finger, CCHC domain containing protein 14	Zcchc14	2.33	1
XP_233955.3	kelch-like 29	Klhl29	2.33	1
XP_219716.3	PDZ domain containing 4	Pdzd4	2.01	1
NP_001014055.1	septin 10	Sept10	1.71	1
XP_237064.3	*Predicted:* Y59A8B.19	RGD1310819	1.50	3
NP_579817.1	mitogen activated protein kinase kinase 2	Map2k2	1.50	1
NP_112257.1	microtubule-associated protein 1A	Map1a	1.48	2
NP_072138.1	septin 7	Sept7	1.44	3
XP_224759.4	*Predicted:* Pleckstrin and Sec7 domain containing protein 3 (Arf6GEF)	Psd3	1.24	1
NP_113841.1	Neurocan	Ncan	1.19	1
XP_579521.1	*Predicted:* hypothetical protein XP_579521*		1.19	1
NP_062062.1	hyaluronan and proteoglycan link protein 1	Hapln1	0.95	3
XP_233308.3	*Predicted:* NF-kappaB repressing factor	Nkrf	0.83	1
XP_220423.3	septin 8	Sept8	0.83	1
NP_112252.1	myelin proteolipid protein	Plp1	-1.20	1
NP_114018.1	flotillin 2	Flot2	-1.24	1
NP_001020589.1	protein phosphatase 2A 65 kDa regulatory subunit A beta isoform	Ppp2r1b	-1.41	2
NP_074056.1	gephyrin	Gphn	-1.50	1
NP_073197.1	GABA (A) receptor-associated protein-like 2	Gabarapl2	-1.70	1
XP_344238.2	potassium channel tetramerisation domain containing 8	Kctd8	-1.83	1
NP_112408.1	actin-related protein 2/3 complex subunit 1A	Arpc1a	-1.88	1
XP_576587.1	*Predicted:* peptidylprolyl isomerase A*		-2.38	1
XP_575932.1	*Predicted:* peptidylprolyl isomerase A*		-2.38	1
NP_001009268.1	actin-related protein 2	Actr2	-2.58	2
NP_077368.1	hydroxysteroid (17-beta) dehydrogenase 4	Hsd17b4	-3.11	1

Figure 5

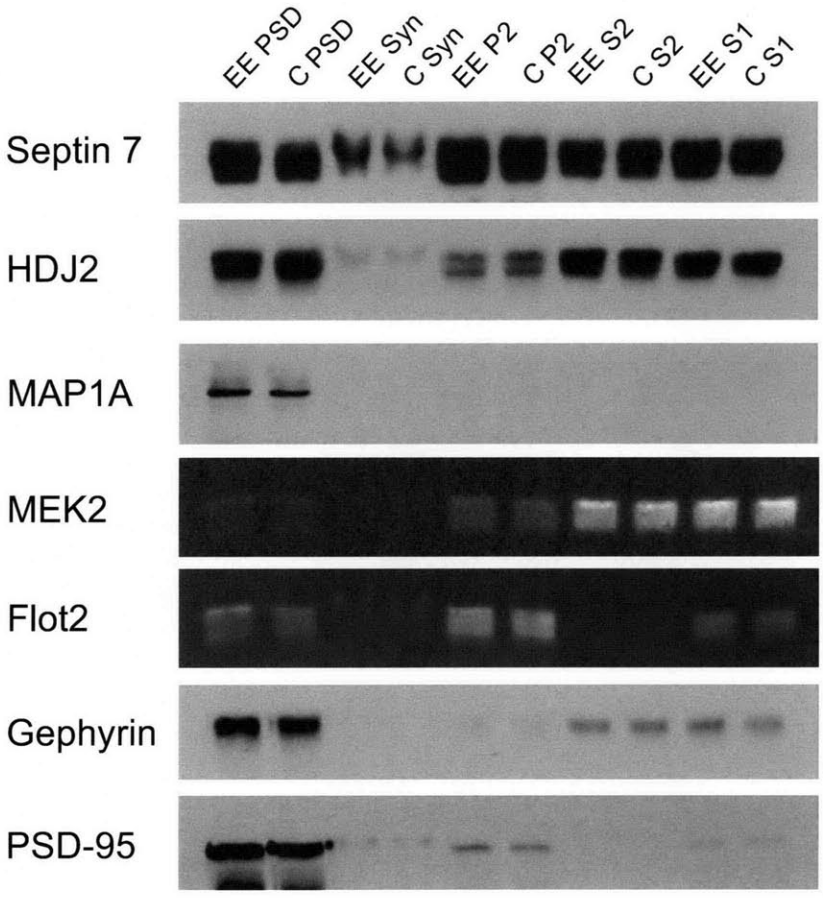
EE PSD
C PSD
EE Syn
C Syn
EE P2
C P2
EE S2
C S2
EE S1
C S1
Septin 7
HDJ2
MAP1A
MEK2
Flot2
Gephyrin
PSD-95

References

Andersen J, Wilkinson C, Mayor T, Mortensen P, Nigg E, and Mann M (2003) Proteomic characterization of the human centrosome by protein correlation profiling. Nature 426:570-574.

Bayes A, and Grant S (2009) Neuroproteomics: understanding the molecular organization and complexity of the brain. Nat Rev Neurosci 10:635-646.

Benaroya-Milshtein N, Hollander N, Apter A, Kukulansky T, Raz N, Wilf A, Yaniv I, and Pick C (2004) Environmental enrichment in mice decreases anxiety, attenuates stress responses and enhances natural killer cell activity. Eur J Neurosci 20:1341-1347.

Bennett J, McRae P, Levy L, and Frick K (2006) Long-term continuous, but not daily, environmental enrichment reduces spatial memory decline in aged male mice. Neurobiol Learn Mem 85:139-152.

Bezard E, Dovero S, Belin D, Duconger S, Jackson-Lewis V, Przedborski S, Piazza P, Gross C, and Jaber M (2003) Enriched environment confers resistance to 1-methyl-4-phenyl-1,2,3,6-tetrahydropyridine and cocaine: involvement of dopamine transporter and trophic factors. J Neurosci 23:10999-11007.

Bruel-Jungerman E, Laroche S, and Rampon C (2005) New neurons in the dentate gyrus are involved in the expression of enhanced long-term memory following environmental enrichment. Eur J Neurosci 21:513-521.

Cheng D, Hoogenraad C, Rush J, Ramm E, Schlager M, Duong D, Xu P, Wijayawardana S, Hanfelt J, Nakagawa T, Sheng M, and Peng J (2006) Relative and absolute quantification of postsynaptic density proteome isolated from rat forebrain and cerebellum. Mol Cell Proteomics 5:1158-1170.

Collins M, Husi H, Yu L, Brandon J, Anderson C, Blackstock W, Choudhary J, and Grant S (2006) Molecular characterization and comparison of the components and multiprotein complexes in the postsynaptic proteome. J Neurochem 97 Supp 1:16-23.

Diamond M, Lindner B, Johnson R, Bennett E, and Rosenzweig M (1975) Differences in occipital cortical synapses from environmentally enriched, impoverished, and standard colony rats. J Neurosci Res 1:109-119.

Duffy S, Craddock K, Abel T, and Nguyen P (2001) Environmental enrichment modifies the PKA-dependence of hippocampal LTP and improves hippocampus-dependent memory. Learn Mem 8:26-34.

Edbauer D, Cheng D, Batterton M, Wang C, Duong D, Yaffe M, Peng J, and Sheng M (2009) Identification and characterization of neuronal mitogen-activated protein kinase substrates using a specific phosphomotif antibody. Mol Cell Proteomics 8:681-695.

Emes R, Pocklington A, Anderson C, Bayes A, Collins M, Vickers C, Croning M, Malik B, Choudhary J, Armstrong J, and Grant S (2008) Evolutionary expansion and anatomical specialization of synapse proteome complexity. Nat Neurosci 11:799-806.

Eng J, McCormack A, and Yates J (1994) An approach to correlate tandem mass spectral data of peptides with amino acid sequences in a protein database. J Am Soc Mass Spectrom 5:976-989.

Fischer A, Sananbenesi F, Wang X, Dobbin M, and Tsai L (2007) Recovery of learning and memory is associated with chromatin remodeling. Nature 447:178-182.

Gerber S, Rush J, Stemman O, Kirschner M, and Gygi S (2003) Absolute quantification of proteins and phosphoproteins from cell lysates by tandem MS. Proc Natl Acad Sci USA 100:6940-6945.

Gogolla N, Galimberti I, Deguchi Y, and Caroni P (2009) Wnt signaling mediates experience-related regulation of synapse numbers and mossy fiber connectivities in the adult hippocampus. Neuron 62:510-525.

Greenough W, Hwang H, and Gorman C (1985) Evidence for active synapse formation or altered postsynaptic metabolism in visual cortex of rats reared in complex environments. Proc Natl Acad Sci USA 82:4549-4552.

Gygi S, Rist B, Gerber S, Turecek F, Gelb M, and Aebersold R (1999) Quantitative analysis of complex protein mixtures using isotope-coded affinity tags. Nat Biotechnol 17:994-999.

Jankowsky J, Melnikova T, Fadale D, Xu G, Slunt H, Gonzales V, Younkin L, Younkin S, Borchelt D, and Savonenko A (2005) Environmental enrichment mitigates cognitive deficits in a mouse model of Alzheimer's disease. J Neurosci 25:5217-5224.

Jordan B, Fernholz B, Boussac M, Xu C, Grigorean G, Ziff E, and Neubert T (2004) Identification and verification of novel rodent postsynaptic density proteins. Mol Cell Proteomics 3:857-871.

Leggio M, Mandolesi L, Federico F, Spirito F, Ricci B, Gelfo F, and Petrosini L (2005) Environmental enrichment promotes improved spatial abilities and enhanced dendritic growth in the rat. Behav Brain Res 163:78-90.

Li K, Hornshaw M, Van Der Schors R, Watson R, Tate S, Casetta B, Jimenez C, Gouwenberg Y, Gundelfinger E, Smalla K, Smit A (2004) Proteomics analysis of rat brain postsynaptic density: implications of the diverse protein functional groups for the integration of synaptic physiology. J Biol Chem 279:987-1002.

Li S, Tian X, Hartley D, and Feig L (2006) The environmental versus genetics in controlling the contribution of MAP kinases to synaptic plasticity. Curr Biol 16:2303-2313.

Liao L, Cheng D, Wang J, Duong D, Losik T, Gearing M, Rees H, Lah J, Levey A, and Peng J (2004) Proteomic characterization of postmortem amyloid plaques isolated by laser capture dissection. J Biol Chem 279:37061-37068.

McNair K, Broad J, Riedel G, Davies C, and Cobb S (2007) Global changes in the hippocampal proteome following exposure to an enriched environment. Neurosci 145:413-422.

Nithianantharajah J and Hannan A (2006) Enriched environments, experience-dependent plasticity and disorders of the nervous system. Nat Rev Neurosci 7:697-709.

Ohlsson A and Johansson B (1995) Environment influences functional outcome of cerebral infarction in rats. Stroke 26:644-649.

Ong S and Mann M (2005) Mass spectrometry-based proteomics turns quantitative. Nat Chem Biol 1:252-262.

Peng J, Kim M, Cheng D, Duong D, Gygi S, and Sheng M (2004) Semiquantitative proteomic analysis of rat forebrain postsynaptic density fractions by mass spectrometry. J Biol Chem 279:21003-21011.

Rampon C, Tang Y, Goodhouse J, Shimizu E, Kyin M, and Tsien J (2000a) Enrichment induces structural changes and recovery from nonspatial memory deficits in CA1 NMDAR1-knockout mice. Nat Neurosci 3:238-244.

Rampon C, Jiang C, Dong H, Tang Y, Lockhart D, Schultz P, Tsien J, and Hu Y (2000b) Effects of environmental enrichment on gene expression in the brain. Proc Natl Acad Sci USA 97:12880-12884.

Restivo L, Ferrari F, Passino E, Sgobio C, Bock J, Oostra B, Bagni C, Ammassari-Teule M (2005) Enriched environment promotes behavioral and morphological recovery in a mouse model for the fragile X syndrome. Proc Natl Acad Sci USA 102:11557-11562.

Roy V, Belzung C, Delarue C, and Chapillon P (2001) Environmental enrichment in BALB/c mice: effects in classical tests of anxiety and exposure to a predatory odor. Physiol Behav 74:313-320.

Schrijver N, Bahr N, Weiss I, and Wurbel H (2002) Dissociable effects of isolation rearing and environmental enrichment on exploration, spatial learning, and HPA activity in adult rats. Pharmacol Biochem Behav 73:209-224.

Sheng M and Hoogenraad CC (2007) The postsynaptic architecture of excitatory synapses: a more quantitative view. Ann. Rev. Biochem. 76:823-847.

Steen H, Jebanathirajah J, Springer M, and Kirschner M (2005) Stable isotope-free relative and absolute quantitation of protein phosphorylation stoichiometry by MS. Proc Natl Acad Sci USA 102:3948-3953.

Van Dellen A, Blakemore C, Deacon R, York D, and Hannan A (2000) Delaying the onset of Huntington's in mice. Nature 404:721-722.

Van Praag H, Christie B, Sejnowski T, and Gage F (1999) Running enhances neurogenesis, learning, and long-term potentiation in mice. Proc Natl Acad Sci USA 96:13427-13431.

Van Praag H, Kempermann G, and Gage F (2000) Neural consequences of environmental enrichment. Nat Rev Neurosci 1:191-198.

Walikonis R, Jensen O, Mann M, Provance D, Mercer J, and Kennedy M (2000) Identification of proteins in the postsynaptic density fraction by mass spectrometry. J Neurosci 20:4069-4080.

Wu C, MacCoss M, Howell K, Matthews D, and Yates J (2004) Metabolic labeling of mammalian organisms with stable isotopes for quantitative proteomic analysis. Anal Chem 76:4951-4959.

Yoshimura Y, Yamauchi Y, Shinkawa T, Taoka M, Donai H, Takahashi N, Isobe T, and Yamauchi T (2004) Molecular constituents of the postsynaptic density fraction revealed by proteomic analysis using multidimensional liquid chromatography-tandem mass spectrometry. J Neurochem 88:759-768.

Young D, Lawlor P, Leone P, Dragunow M, and During M (1999) Environmental enrichment inhibits spontaneous apoptosis, prevents seizures and is neuroprotective. Nature Med 5:448-453.